Epigenetic Regulation of Cytokine Production in Endotoxin Tolerance

DISSERTATION

zur Erlangung des akademischen Grades
d o c t o r r e r u m n a t u r a l i u m
(Dr. rer. nat.)
im Fach Biologie

eingereicht an der
Lebenswissenschaftlichen Fakultät
der Humboldt-Universität zu Berlin

von

CLAUDIA RESCHKE
Master of Science in Molekulare Lebenswissenschaften

Präsident der Humboldt-Universität zu Berlin
Prof. Dr. Jan-Hendrik Olbertz

Dekan der Lebenswissenschaftlichen Fakultät
Prof. Dr. Richard Lucius

Gutachter: 1. Prof. Dr. Hans-Dieter Volk

2. Prof. Dr. Alf Hamann

3. Prof. Dr. Robert Jack

Tag der mündlichen Prüfung: 22. Februar 2016

“Everything is going to be fine in the end.
If it’s not fine it’s not the end.”

Oscar Wilde

Zusammenfassung

Unter Endotoxintoleranz versteht man die Toleranzentwicklung in Monozyten und anderen Immunzellen gegenüber Lipopolysaccharid (LPS) aufgrund einer vorangegangenen Endotoxin-Stimulation, welche *in vivo* als auch *in vitro* beobachtet werden kann. Dabei zeichnen sich Endotoxin-tolerante Monozyten und Makrophagen durch eine verminderte Induktion pro-inflammatorischer Zytokine aus, während Gene, welche für die Phagozytose und Wundheilung verantwortlich sind, weiterhin exprimiert werden. LPS-induzierte Toleranz kann bis zu mehrere Tage andauern, selbst wenn der auslösende Stimulus nicht mehr vorhanden ist. Eine mögliche Erklärung für die vorübergehende Inhibierung pro-inflammatorischer Gene könnten demnach epigenetische Veränderungen sein. Um diese Frage zu beantworten, wurden humane LPS-tolerante Monozyten mittels eines *in vitro* Endotoxintoleranz-Modells auf epigenetische Veränderungen untersucht.

Der erste Teil der Arbeit konzentrierte sich auf die Analyse individueller, immunrelevanter Gene. Die Promotorregionen der pro-inflammatorischen Gene *TNF* und *CXCL10* zeigten in toleranten Monozyten eine Verringerung der Transkription einhergehend mit einer verminderten Induktion der aktivierenden Histonmodifikationen H3K27ac und H4ac auf. Die Expression dieser Gene war in den toleranten Monozyten zudem sehr stark inhibiert, was auf eine hohe LPS-Toleranzwirkung schließen lässt (*highly tolerizable genes).* Demgegenüber wiesen Gene wie *IL6* und *IL1B* eine Zunahme an H4ac und H3K27ac auf, während ihre Genexpression in widersprüchlicher Weise reduziert war. Die Genexpression von *IL6* und *IL1B* war allerdings noch gut nachweisbar, selbst in toleranten Monozyten (*intermediately tolerizable genes*). Darüber hinaus war insbesondere die *IL6*-Genexpression im Vergleich zu den Veränderungen der Histonmodifikationen verstärkt von der Signaltransduktionskapazität toleranter Monozyten abhängig, wohingegen die stark tolerisierbaren Gene *TNF* und *CXCL10* eine verminderte Induktion aktivierender Histonmarker unabhängig von der Signalstärke aufwiesen. Weitere Untersuchungen der DNA-Methylierung und der Histonmodifikationen H3K9me2, H3K27me3 und H4K20me3 zeigten, dass diese repressiven epigenetischen Marker in pro-inflammatorischen Genen toleranter Monozyten nicht erhöht waren. Lediglich konnte in toleranten, re-stimulierten Monozyten vereinzelt eine Zunahme an H3K9me2 und H4K20me3 in genomischen Regionen *upstream* von *IL1*-verwandten Genen (*IL1B*, *IL1A* und *IL1R1*) identifiziert werden, während *IL6* – widersprüchlich zur Genexpression – eine Verringerung an repressiven H3K27me3 aufzeigte.

Der zweite Teil befasste sich mit der Analyse globaler epigenetischer Veränderungen von Histonmodifikationen und DNA Methylierung im Vergleich zur Gesamt-mRNA-Expression unter zur Hilfenahme von *Next Generation* Sequenzierungen. Hier konnte man eine starke Verschiebung von aktivierenden Histonmodifikationen (H4ac, H3K27ac) in naïven Monozyten zu repressiven Histonmarkern (H3K9me2, H3K27me3, H4K20me3) in toleranten,

re-stimulierten Zellen beobachten. Insbesondere zeigten intergenische Genomregionen einen verstärkten Anstieg an repressiven Histonmodifikationen, was auf eine mögliche regulatorische Funktion dieser Bereiche in der Endotoxintoleranz schließen lässt. Weiterhin wurden die differentiell regulierten Regionen auf Transkriptionsfaktor-Bindestellen untersucht. Genomische Bereiche, die eine Anreicherung an repressiven H3K9me2 und H4K20me3 in toleranten Monozyten zeigten, wiesen verstärkt das Bindungsmotiv für SMAD3 auf. Zudem ergaben funktionale *Gene Ontology* (GO)-Analysen dieser Regionen eine Überrepräsentation von Genen, welche an Signalwegen und der Transkription beteiligt sind. Dies impliziert eine mögliche Rolle von TGFβ in der SMAD3-vermittelten Induktion repressiver Histonmodifikationen in intergenischen Regionen und Genen, welche für die Signalkaskade/Transktiptionsmaschinerie wichtig sind. Im Gegensatz dazu zeigten tolerante Monozyten eine Reduzierung in der DNA Methylierung auf, welche auch nicht mit den beschriebenen Veränderungen der Histonmodifikationen korrelierte. Auffallend war, dass mehrere tausend genomische Regionen (> 10 000) Veränderungen in den untersuchten Histonmodifkationen und der DNA-Methylierung aufwiesen, allerdings insgesamt nur 3638 Gene differentiell exprimiert waren. Korrelationsuntersuchungen der identifizierten epigenetischen Veränderungen mit der globalen mRNA Expression in toleranten Monozyten zeigten, dass etwa 27 % der differentiell exprimierten Gene eine epigenetische Signatur aufwiesen, welche im Einklang mit dem Histon-Code steht, während Veränderungen der DNA-Methylierung keinen Einfluss auf die Genexpression zu haben schien.

Die vorliegenden Daten zeigen, dass die epigenetische Umgebung von Monozyten stark von der Endotoxintoleranz beeinträchtigt wird. Es existiert jedoch kein gemeinsames epigenetisches Muster, welches die Toleranzinduktion einzelner pro-inflammatorischer Zytokine erklären könnte. Vielmehr scheint es, dass verschiedene Mechanismen direkt oder indirekt zusammenwirken und somit zur veränderten Genexpression der Monozyten beitragen, die schlussendlich charakteristisch für Endotoxintoleranz sind. Ein tiefgreifendes Verständnis der globalen epigenetischen Veränderungen in der Endotoxintoleranz kann zudem die Grundlage für neue Behandlungsstrategien von Sepsispatienten liefern. Hier führt eine systemische Immuntoleranz (auch als *‚Immunparalyse‘* bezeichnet) gegenüber eindringender Erreger und deren Bestandteile zu einer erhöhten Sterblichkeitsrate.

Schlagwörter:

Epigenetik, Endotoxintoleranz, Monozyten

Summary

The phenomenon by which monocytes and other immune cells become tolerant *in vivo* as well as *in vivo* after repetitive exposure to lipopolysaccharide (LPS) is known as endotoxin tolerance. Endotoxin-tolerant monocytes and macrophages are characterized by a diminished induction capacity of pro-inflammatory cytokines, whereas genes involved in phagocytosis and wound healing are basically unaffected. As LPS tolerance lasts for several days, even after the stimulus is cleared, a transient silencing of immune response genes by epigenetic changes is very likely. To answer this question, an *in vitro* endotoxin tolerance model with human monocytes was used to analyze alterations in the epigenetic landscape of LPS-tolerant cells.

The first part of the study focused on the analysis of individual immune response genes. The promoter regions of the pro-inflammatory genes *TNF* and *CXCL10* showed a reduction in transcription-linked histone marks, in particular H4ac and H3K27ac, in tolerant monocytes. These genes were also characterized by a high tolerization effect indicated by an abolished gene expression in endotoxin tolerance (*highly tolerizable genes*). In contrast, genes like *IL6* and *IL1B* showed an increase in H4ac and H3K27ac, while their gene expression was paradoxically reduced. Notably, gene expression of *IL6* and *IL1B* was still detectable even in tolerant monocytes (*intermediately tolerizable genes*). Moreover, particularly the *IL6* gene expression was dependent on signaling strength in tolerant monocytes rather than changes in histone modifications, whereas the highly tolerizable genes *TNF* and *CXCL10* possessed diminished induction in activating histone modifications independent of signaling transduction. Further analysis of H3K9me2, H3K27me3, H4K20me3 and DNA methylation indicated that these repressive epigenetic marks were not enhanced in pro-inflammatory genes in tolerant monocytes. Solely, enrichment in H3K9me2 and H4K20me3 in the upstream regions of *IL1*-related genomic loci (*IL1B*, *IL1A* and *IL1R1*) could be identified, whereas *IL6* – conversely to its gene expression – showed a reduction in repressive H3K27me3 in tolerant monocytes treated with LPS.

The second part focused on the analysis of global epigenetic changes in histone marks and DNA methylation in comparison to total mRNA expression using next generation sequencing approaches. A drastic shift was observed from activating histone modifications (H4ac, H3K27ac) in naïve monocytes to repressive ones (H3K9me2, H3K27me3, H4K20me3) in tolerant cells treated with LPS. In particular intergenic regions gained repressive histone modifications implying a regulatory function in endotoxin tolerance. Analysis of transcription factor binding sites within differentially regulated regions identified a significant enrichment for the binding motif of SMAD3 in genomic regions enriched for repressive H3K9me2 and H4K20me3 in tolerant monocytes. Functional GO enrichment analysis of these regions further revealed overrepresentation of genes involved in signaling and transcription.

This implies a role of TGFβ in SMAD3-mediated induction of repressive histone modifications in intergenic regions and genes important for the signaling transduction/transcription machinery. By contrast, DNA methylation was reduced in tolerant monocytes, which did not correlate with alterations in histone marks. Strikingly, several thousand genomic regions (> 10 000) were differentially regulated by histone modifications and DNA methylation, though only 3638 genes in total were differentially expressed. Correlation of the identified epigenetic changes with global mRNA expression analysis in tolerant monocytes revealed that approximately 27 % of differentially expressed genes showed an epigenetic signature consistent with the histone code, while DNA methylation had no impact on gene expression.
The present data indicate that the epigenetic environment of monocytes is highly affected by endotoxin tolerance; however, no common epigenetic pattern exists, which might explain the tolerization of specific pro-inflammatory cytokines. It rather demonstrates that different mechanisms directly or indirectly act together to downregulate the expression capacity of monocytes, which results in the characteristics known for endotoxin tolerance. Hence, molecular understanding of these global epigenetic changes in endotoxin tolerance will provide the basis for finding novel treatment strategies for sepsis patients, where a systemic tolerization of the immune system (so-called *'immunoparalysis'*) to invading pathogens and their components increases the patient mortality rate.

Keywords:

Epigenetics, endotoxin tolerance, monocytes

Table of Contents

Zusammenfassung **V**
Summary **VII**
Table of Contents **IX**
List of Abbreviations **XIII**
1. Introduction **1**
1.1 The Immune System – An Overview 1
1.2 The Innate Immune Response and Pattern Recognition Receptors 2
1.3 LPS Signaling by Toll-like Receptor 4 (TLR4) 3
1.4 Cytokines and Chemokines – Mediators of Inflammation 6
1.5 Sepsis: A Disorder of the Immune System 7
1.6 Endotoxin Tolerance: A Model for Analyzing *'Immunoparalysis'* in Sepsis Patients 9
1.7 Epigenetics 11
1.7.1 DNA Methylation 12
1.7.2 Histone Modifications 13
1.8 Aims and Objectives 16
2. Results **19**
2.1 The Impact of LPS Tolerization on Specific Immune Response Genes 19
2.1.1 Analysis of Cytokine Profile in Naïve and Tolerant Human Monocytes 19
2.1.2 Potential Role of Histone Modifications in Tolerant Human Monocytes 22
2.1.3 Analysis of Tolerant Murine Macrophages by Histone Modifications 26
2.1.4 Analysis of Signaling Strength on Histone Modifications 27
2.1.5 Analysis of Endotoxin Tolerance in High-Dose Tolerized Human Monocytes 29
2.1.6 Analysis of Repressive Histone Marks in Endotoxin Tolerance 33
2.1.7 DNA Methylation Analyses within the Promoter Regions of *IL6* and *TNF* 35
2.2 Genome-Wide Analysis of Epigenetic Changes in Endotoxin Tolerance 38
2.2.1 Global Analyses of Histone Modifications by ChIP-Seq 38
2.2.1.a Characterization of Enriched Regions (Peaks) 38
2.2.1.b Analysis of Genomic Regions Differentially Regulated by Histone Modifications in LPS-Tolerant Monocytes 41
2.2.2 Global Analysis of DNA Methylation by MethylCap-Seq 50
2.2.3 Validation of Epigenetic Changes by Global mRNA Expression 53
3. Discussion **57**
3.1 Individual Class T Genes are Differentially Affected by Epigenetic Changes and Signaling Events in Endotoxin Tolerance 58
3.1.1 The Role of Activating Events in Individual Genes 58
3.1.2 The Role of Repressive Events in Individual Genes 61
3.1.3 Summary 64
3.2 Endotoxin Tolerance Alters Genome-Wide the Epigenetic Signature of Human Monocytes 66
3.2.1 Global Analysis of Histone Modifications 67
3.2.2 Global Analysis of DNA Methylation 70
3.2.3 Epigenetic Changes Partially Correlate with Gene Expression 71
3.2.4 Summary 74

3.3 Impact of Epigenetic Changes in Endotoxin Tolerance and Sepsis 76
3.4 Outlook 77

4. Materials & Methods 79
4.1 Software & Programs 79
4.2 Materials 80
4.3 Methods 80
4.3.1 Cell Culture 80
4.3.1.a Human Peripheral Blood Mononuclear Cell (PBMC) Isolation 80
4.3.1.b Human Monocyte Isolation by Magnetic Cell Separation 80
4.3.1.c Human Monocyte Cultures and the Endotoxin Tolerance Model 81
4.3.1.d Optimization of Culture Conditions for Cultivation of Human Monocytes 81
4.3.1.e Isolation and Cultivation of Murine Bone Marrow-Derived Macrophages 84
4.3.2 Flow Cytometry 84
4.3.2.a Determination of Purity and Cell Viability with 7AAD 85
4.3.2.b Live/Dead Discrimination with a Fixable Dye 85
4.3.2.c Extracellular Staining of Cell Surface Molecules 85
4.3.2.d Intracellular Signaling Analysis of p38 MAP Kinase (MAPK) 85
4.3.2.e Intracellular Cytokine Staining 85
4.3.3 ELISA and Multiplex 86
4.3.4 RNA Isolation, cDNA Synthesis and Quantitative Real Time PCR (qRT-PCR) 86
4.3.5 Chromatin Immunoprecipitation (ChIP) 87
4.3.5.a Sample Preparation (ChIP) 88
4.3.5.b Detection of DNA Fragments by Agarose Gel Electrophoresis 90
4.3.5.c Quantitative Real Time PCR (qRT-PCR) of ChIP DNA 90
4.3.5.d Optimization of ChIP 91
4.3.6 ChIP-Sequencing (ChIP-Seq) 92
4.3.6.a Next Generation Sequencing (NGS) of ChIP DNA 92
4.3.6.b Pre-Processing: Quality Filtering and Read Mapping of ChIP-Seq Data 94
4.3.6.c Visualization of Binding Profiles 95
4.3.6.d Peak Calling 96
4.3.6.e Spatial Clustering Approach for the Identification of ChIP-Enriched Regions (SICER) 97
4.3.6.f Determining the Final Peak Lists 98
4.3.7 Bioinformatical Downstream Analyses of ChIP-Seq Data 99
4.3.7.a Gene Annotation and Gene Body Distribution 99
4.3.7.b Binding Profiles around the Transcription Start Site (TSS) 99
4.3.7.c Cluster Analysis of Chromatin Signatures (Heat map) 100
4.3.7.d Analysis of Gene Overlap between Gene Lists 100
4.3.7.e Gene Ontology (GO) Enrichment Analysis of ChIP-Seq Data 100
4.3.7.f Identification of Transcription Factor Binding Sites (TFBSs) 100
4.3.8 Specific DNA Methylation Analysis of the Human *IL6* and *TNF* Promoter Using Short Bisulfite Sequencing (BS-Seq) 100
4.3.8.a DNA Preparation and Bisulfite Conversion 101
4.3.8.b PCR of Target Promoter 101
4.3.8.c Purification of PCR Products 102

4.3.8.d Detection of PCR Products by Gel Electrophoresis 102
4.3.8.e Restriction Enzyme Digestion for Specificity Analysis of PCR Products 102
4.3.8.f Sequencing of PCR Products 102
4.3.8.g Pre-processing and Computational Analysis 103
4.3.9 DNA Methylation Analysis by MethylCap-Sequencing (MethylCap-Seq) 103
4.3.9.a Sample Preparation (MethylCap) 103
4.3.9.b Pre-Processing and Visualization of MethylCap-Seq Data 104
4.3.9.c Identification of Genome-Wide DNA-Methylated Regions 104
4.3.9.d Gene Ontology (GO) Enrichment Analysis of MethylCap-Seq Data 105
4.3.10 Expression Profiling by mRNA Sequencing (mRNA-Seq) 105
4.3.10.a Sample Preparation (mRNA) 105
4.3.10.b Data Processing and Determining of Differentially Expressed Genes 105
4.3.10.c Heat map of Differentially Expressed Genes 106
4.3.10.d GO Enrichment Analysis of mRNA-Seq Data 106
4.3.10.e Analysis of Gene Overlap between Gene Lists 106
4.4 Statistical Analysis 106

5. Appendix 107
5.1 Cytokines and Chemokines – An Overview 107
5.2 Binding Sites of Primer Pairs for ChIP-qPCR Analysis of Human Monocytes and Murine Macrophages 110
5.3 Cytometer Settings 112
5.4 DNA Methylation Analysis by BS-Seq 113
5.5 MethylCap-Seq Binding Profiles within the *FPR1*, *IL8*, *IL1B* & *CXCL10* Genes 116
5.6 Transcription Factor Binding Sites (TFBSs) Identified by HOMER 117
5.7 Gene Ontology (GO) Enrichment Analysis by DAVID 121

6. References 129
7. Contributions of Third Parties to the Present Work 145
Curriculum Vitae XV
Danksagung XVII
Eidesstattliche Erklärung XIX

List of Abbreviations

° C	degree Celsius
%	percent
≥ / >	greater or equal / greater
≤ / <	less or equal / less
α	alpha
β	beta
γ	gamma
7AAD	7-aminoactinomycin D
AP1	activating protein-1
APC	allophycocyanin
ATP	adenosine triphosphate
BAM	binary version of the sequence alignment/map (SAM) file
BED	browser extensible data
BCRT	Berlin-Brandenburg center for regenerative therapies
bp	base pairs
BSA	bovine serum albumin
cAMP	cyclic adenosine 3',5'-monophosphate
Cat. No.	catalog number
CCL	CC chemokine ligand with two adjacent cysteines
CD	cluster of differentiation
cDNA	complementary desoxyribonucleic acid
CDS	coding DNA sequence
ChIP	chromatin immunoprecipitation
CO_2	carbon dioxide
CpG	cytosine and guanine separated by phosphate
CREB	cAMP response element-binding protein
CXCL	CXC chemokine ligand with two cysteines seperated by amino acid X
DAVID	Database for Annotation, Visualization and Integrated Discovery
DNA	deoxyribonucleic acid
DraI	restriction endonuclease from *Deinococcus radiophilus*
EDTA	ethylene diamine tetraacetic acid
EGTA	ethylene glycol tetraacetic acid
e.g.	latin *exempli gratia* (for example)
ELISA	enzyme-linked immunosorbent assay
ERK1/2	extracellular signal-regulated kinases 1 and 2
FAM	6-carboxyfluorescein
FASTQ	text-based storing file for sequences
FCS	fetal calf serum
FDR	false discovery rate
FITC	fluorescein isothiocyanate
FPR1	formyl peptide receptor 1
FSC	forward scatter
g	gram
g (in x g)	gravity
Geom. Mean	geometric mean fluorescence intensity
G(M)-CSF	granulocyte(-monocyte) colony stimulating factor
GREAT	Genomic Regions Enrichment of Annotations Tool
GO	gene ontology
GRO	growth-regulated oncogene
h	hour(s)
H_2O	chemical formula for water
HCl	hydrochloric acid
HOMER	Hypergeometric Optimization of Motif EnRichment
HPRT	hypoxanthine guanine phosphoribosyl transferase
IFN	interferon
IκB	inhibitor of kappa B
IgG	Immunoglobulin G
IKK	IκB kinase
IL	interleukin
IP-10	Interferon gamma-induced protein 10
IL-1RA	Interleukin-1 receptor antagonist
IRAK	IL-1 receptor-associated kinase
IRF	interferon regulatory factor
JNK	c-Jun N-terminal kinase

K	lysine
kDA	kilo Dalton
kb	kilo base pairs
l	liter
LiCl	lithium chloride
m	milli
M	molar
µ	micro
MACS	magnetic activated cell sorting
MAP(K)	mitogen-activated protein (kinase)
MCP	monocyte chemoattractant protein
M-CSF	macrophage colony-stimulating factor
MD2	myeloid differentiation factor 2
MHC	major histocompatibility complex
min	minute(s)
MIP	macrophage inflammatory proteins
MPC	2-methacryroyloxy-ethylphosphorylcholine
MPI	Max Planck Institute
mRNA	messenger ribonucleic acid
MyD88	myeloid differentiation primary response gene 88
NaCl	chemical formula for sodium chloride
NEMO	NFκB essential modulator
NFκB	nuclear factor 'kappa-light-chain-enhancer' of activated B-cells
NGS	next generation sequencing
No.	number
NOD	nucleotide-binding oligomerization domain
p38	p38 mitogen-activated protein
p.adj	adjusted *P* value
PAMP	pathogen-associated molecular pattern
PBMC	peripheral blood mononuclear cell
PBS	phosphate buffered saline
PCR	polymerase chain reaction
PE	phycoerythrin
PRR	pattern recognition receptors
pVal	*P* value
qRT-PCR	quantitative real-time PCR
RIG	retinoic acid inducible gene
RPKM	reads per kilobase of transcripts per million mapped reads
rpm	rounds per minute
RT	room temperature
SAM	sequence alignment/map format
sec	second(s)
SICER	spatial clustering for identification of ChIP-enriched regions
SSC	sideward scatter
SsPI	restriction endonuclease from *Sphaerotilus species*
TAE	tris base-acetic acid-EDTA buffer
TAK1	TGFβ-activated kinase 1
TAMRA	Tetramethylrhodamine
TANK	TRAF family member-associated NFκB activator
TF	transcription factor
TFBS	transcription factor binding site
TGF	tumor growth factor
TIR	Toll-interleukin-1 receptor
TIRAP	TIR domain-containing adapter protein
TLR	Toll-like receptor
TNF	tumor necrosis factor
TRAF	TNF receptor-associated factor
TRAM	TRIF-related adaptor molecule
TRIF	TIR domain-containing adapter-inducing IFNβ
Tris	tris(hydroxymethyl)aminomethane
TSS	transcription start site
TTS	transcription termination site
UCSC	University of California, Santa Cruz
UTR	untranslated region
V	voltage
VEGF	vascular endothelial growth factor

1. Introduction

1.1 The Immune System – An Overview

The immune system is composed of many specialized cell types and soluble factors that use a complex array of protective mechanisms to control and eliminate a huge range of potential pathogenic organisms and toxic substances. Moreover, it is involved in the anti-tumor responses and the regulation of tissue homeostasis, repair and regeneration (Medzhitov 2008).

In general, the immune system is didactically divided into two parts: The innate and the adaptive immune systems. Innate immunity is an evolutionarily ancient part of host immunity and exists in diverse forms in all multicellular organisms – including vertebrates, invertebrates and plants. As a first line of host defense against infectious agents and dangerous materials, the innate immune response is immediately generated. By contrast, the adaptive immune system presumably developed in the jawed fish 500 million years ago and is found in the descending vertebrates (Cooper & Alder 2006, Flajnik & Kasahara 2010, Murphy *et al.* 2012b). With a latency of four to seven days, it allows great variability and provides the host with a highly specific and individualized immunological memory for infections, but also mediates autoimmunity, allergy and allograft rejection (Iwasaki & Medzhitov 2010, Janeway 2001, Janeway & Medzhitov 2002, Medzhitov & Janeway 2000).

Both systems detect structural features of pathogens that mark them as different (non-self) from the host (self), and thereby induce a protective immune response to eliminate the danger (Medzhitov & Janeway 2002). However, the mechanisms and receptors for host defense are distinct: Whereas the innate immune response relies on a limited number of germline-encoded receptors that recognize conserved molecular structures shared by many pathogens – but not by self-tissues; the adaptive immunity is based on antigen-specific receptors, which are assembled by somatic rearrangement of germline gene segments, passing a diversification process and providing unique specificity for foreign structures (Iwasaki & Medzhitov 2010, Janeway & Medzhitov 2002).

Initially, invading pathogens are sensed by members of the innate immune system *e.g.* macrophages and dendritic cells, which trigger a fast and robust inflammatory response to protect the host (Delves & Roitt 2000, Parkin & Cohen 2001). Inflammation is a complex pathophysiological condition that leads to the recruitment of immune cells and clearance of infectious agents, but also guides tissue repair and wound healing processes to sites of infection (Medzhitov 2008, Takeuchi & Akira 2010).

Hallmarks of inflammation are pain (*dolor*), heat (*calor*), redness (*rubor*), swelling (*tumor*) and loss of function (*functio laesa*) (Celsus circa 30 AD, Majno 1975, Nathan 2002, Rather 1971, Rock *et al.* 2010). They result from the increase of blood flow and blood vessel permeability,

release of liquid and inflammatory mediators into the tissue and recruitment of immune cells to sites of infection. Inflammation is important as it supports killing of the invading pathogen, prevents spreading of infectious agents and promotes tissue repair (Medzhitov 2008, Murphy *et al.* 2012a).

Additionally, innate immunity plays an essential role in induction and regulation of the subsequent adaptive immune response composed of T and B lymphocytes (Iwasaki & Medzhitov 2010, Janeway 2001). Activation of dendritic cells by infectious agents results in their maturation, induction of co-stimulatory molecules and increased antigen-presentation capacity via major histocompatibility complexes (MHCs). Following activation, dendritic cells migrate to secondary lymphoid organs *e.g.* lymph nodes, where they encounter naïve T lymphocytes. Within secondary lymphoid organs, dendritic cells function as specialized antigen-presenting cells and the interaction of these cells with T lymphocytes mediates selection, activation and clonal expansion of T lymphocytes highly specific to antigens derived from microbial pathogens. T lymphocytes mediate cell-mediated toxicity of infected cells and help to establish humoral immunity by activating specific antibody-producing B lymphocytes (Chaplin 2010, Forster *et al.* 2008, Iwasaki & Medzhitov 2010, Medzhitov & Janeway 2002).
After removal of the inflammatory agent, termination of inflammation and cellular homeostasis is achieved by anti-inflammatory mediators and induction of apoptosis in immune cells (Foster & Medzhitov 2009, Glass & Saijo 2010, Liew *et al.* 2005, Serhan 2007, Serhan & Savill 2005).

1.2 The Innate Immune Response and Pattern Recognition Receptors

Initial sensing of invading pathogens like bacteria, viruses or fungi is mediated by non-professional immune cells, such as epithelial cells and fibroblasts located at host-environment boundaries, as well as by professional cells of the innate immune system. Monocytes and macrophages, natural killer (NK) cells and other innate lymphoid cells (Artis & Spits 2015), dendritic cells, polymorphonuclear leukocytes like neutrophils, and mast cells are implicated as primary effectors during initial inflammation and activation of innate immunity (Muralidharan & Mandrekar 2013). The innate immune specificity is genetically programmed to detect invariant features of invading microbes. The best-characterized microbial sensors of the innate immune system are the so-called *pattern recognition receptors* (PRRs), which detect relatively invariant molecular patterns found in most microorganisms. These foreign structures – present only in microbial pathogens among entire classes – are referred to as *pathogen-associated molecular patterns* (PAMPs) (Beutler 2004, Janeway 1989, Medzhitov & Janeway 2000).

Best-known examples of PAMPs include microbial unmethylated DNA, viral double stranded RNA and cell wall components of bacteria *e.g.* lipopolysaccharides (LPS) from gram-negative bacteria, peptidoglycans and lipoteichoic acids (Beutler 2004, Medzhitov & Janeway 2000). Moreover, endogenous molecules released from damaged cells by necrosis such as high mobility group box 1 (HMGB1), monosodium urate crystals and adenosine triphosphate (ATP) can be sensed by PRRs. These immunogenic molecules are termed as *damage- or danger-associated molecular patterns* (DAMPs) (Kaczmarek *et al.* 2013, Rock *et al.* 2010, Rosin & Okusa 2011).

The main tasks of PRRs include opsonization, activation of complement and coagulation cascades, phagocytosis, induction of apoptosis and activation of inflammatory signaling pathways (Janeway & Medzhitov 2002, Medzhitov 2001). PRRs can be broadly categorized into three functional classes: Secreted, endocytic and signaling.

Secreted PRRs (opsonins) bind to microbial cell surfaces and mark pathogens for phagocytosis by macrophages and neutrophils. Moreover, some opsonins *e.g.* C-reactive protein (CRP) and mannan-binding lectin (MBL) function as activators of the complement system (classical and lectin pathways). *Endocytic* PRRs such as scavenger receptor and mannose receptor are expressed on cell surfaces and mediate recognition and subsequent phagocytosis of pathogens without inducing inflammatory mediators (Janeway & Medzhitov 2002, Jeannin *et al.* 2008, Medzhitov & Janeway 2000).

The biggest class of PRRs, including Toll-like receptors (TLRs), RIG-I-like receptors (RLRs) and NOD-like receptors (NLRs), activates signaling events. *Signaling* PRRs are localized in membranes – either on cell surfaces or in endosomal/lysosomal organelles (TLRs) – or in the cytosol (RLPs, NLPs). After binding to PAMPs or DAMPs, they induce signaling transduction cascades leading to activation of different master transcription factors and subsequent expression of a variety of immune response genes encoding for pro-inflammatory cytokines, type I interferons (IFNs), chemokines, anti-microbial proteins, MHCs and co-stimulatory molecules. The transcription factors nuclear factor kappa B (NFκB) and activator protein 1 (AP1) trigger gene expression of pro-inflammatory cytokines, whereas interferon regulatory factors (IRFs) induce production of type I IFNs (Akira *et al.* 2006, Kawai & Akira 2010, Takeuch & Akira 2011).

1.3 LPS Signaling by Toll-like Receptor 4 (TLR4)

The family of TLRs is among the best-characterized PRRs and plays a key role in pathogen recognition and initiation of acute inflammation. In 1996, these PRRs identified in *Drosophila* were discovered to be involved in anti-fungal responses (Lemaitre *et al.* 1996). One year later, the first human homolog for the *Toll* protein was described (Medzhitov *et al.* 1997). So far, 13 mammalian TLR homologs have been identified, which differ from each other in ligand

specificities and localization within the host cell – including 12 in mice (TLR1-9 and TLR11-13) and 10 in humans (TLR1-10) (Akira *et al.* 2006, Beutler 2004, Kawai & Akira 2010, Murad 2014, Oldenburg *et al.* 2012, Takeuchi & Akira 2010).

The host innate immune system recognizes several bacterial virulence factors. Among them belong endotoxins from gram-negative bacteria (*e.g.* LPS, Lipid A) to the most potent inflammatory stimulus (Pfeiffer 1892). The glycolipid LPS is the major component of the outer membrane of gram-negative bacteria. It consists of a hydrophobic lipid A domain, a core polysaccharide, and an O-polysaccharide chain of variable length (Kelly *et al.* 1991, Nikaido 1962, Osborn 1963, Raetz & Whitfield 2002).
The key pattern recognition receptor for detection of gram-negative bacteria and their associated endotoxins is TLR4 (Poltorak *et al.* 1998a, Poltorak *et al.* 1998b). Together with the TLR4 co-receptor cluster of differentiation 14 (CD14) (Wright *et al.* 1990), endotoxin signaling leads to activation of signaling cascades promoting the production of pro-inflammatory cytokines and IFNs. CD14 is an extrinsic glycosylphosphatidylinositol (GPI)-anchored membrane protein and was first identified as a marker for monocytes (Goyert *et al.* 1986). The 55 kDa glycoprotein CD14 is expressed on the surface of myelomonocytic cells or can be secreted in a soluble form (Ulevitch & Tobias 1995). Thus, monocytes and macrophages are crucial mediators of inflammation (Zanoni & Granucci 2013).
The exact signaling pathway of LPS is not completely understood. It is known that a complex interaction of several molecules is involved (**Fig. 1-1**). TLR4 forms a homodimer at the cell surface. The LPS-binding protein (LBP) mediates transport of LPS molecules to TLR4 (Schumann *et al.* 1990, Tobias *et al.* 1986). At the plasma membrane, LBP is thought to transfer LPS to CD14. For initiation of the transduction pathway, CD14 transfers LPS to the myeloid differentiation factor 2 (MD2) that lacks a transmembrane anchor, but is associated with TLR4. Once the LPS-TLR4-MD2 complex is formed, the entire complex consisting of two blocks of LPS-TLR4-MD2 dimerizes and recruits several cytoplasmic adapter molecules through the interaction with the Toll-interleukin-1 receptor (TIR) domain of TLR4. TLR4 is unique as it is the only TLR that engages all four adaptors – TIR domain-containing adapter protein (TIRAP), myeloid differentiation primary response gene 88 (MyD88), TRIF-related adaptor molecule (TRAM) and TIR domain-containing adapter-inducing IFNβ (TRIF). Therefore, it is capable of activating both: (1) the TIRAP-MyD88-dependent pathway and (2) the TRAM-TRIF-dependent pathway (Akira & Hoshino 2003, Kawai & Akira 2011, Medzhitov & Janeway 2000, Murad 2014, Zanoni & Granucci 2013). Notably, CD14 is important for the LPS-induced internalization of TLR4 leading to the activation of the MyD88-independent (TRIF-dependent) signaling pathway (Zanoni *et al.* 2011).
Functionally, MyD88-dependent signaling triggers induction of NFκB and mitogen-activated protein (MAP) kinase cascades leading to synergistic production of variable pro-inflammatory

genes including tumor necrosis factor (TNF, also known as TNFα[1]), interleukin-1β (IL-1β), IL-6 and CXCL8/IL-8, whereas the MyD88-independent transduction cascade is primary involved in expression of type I IFNs *e.g.* IFNα and IFNβ (Kawai & Akira 2010) (for more details see **Fig. 1-1**).

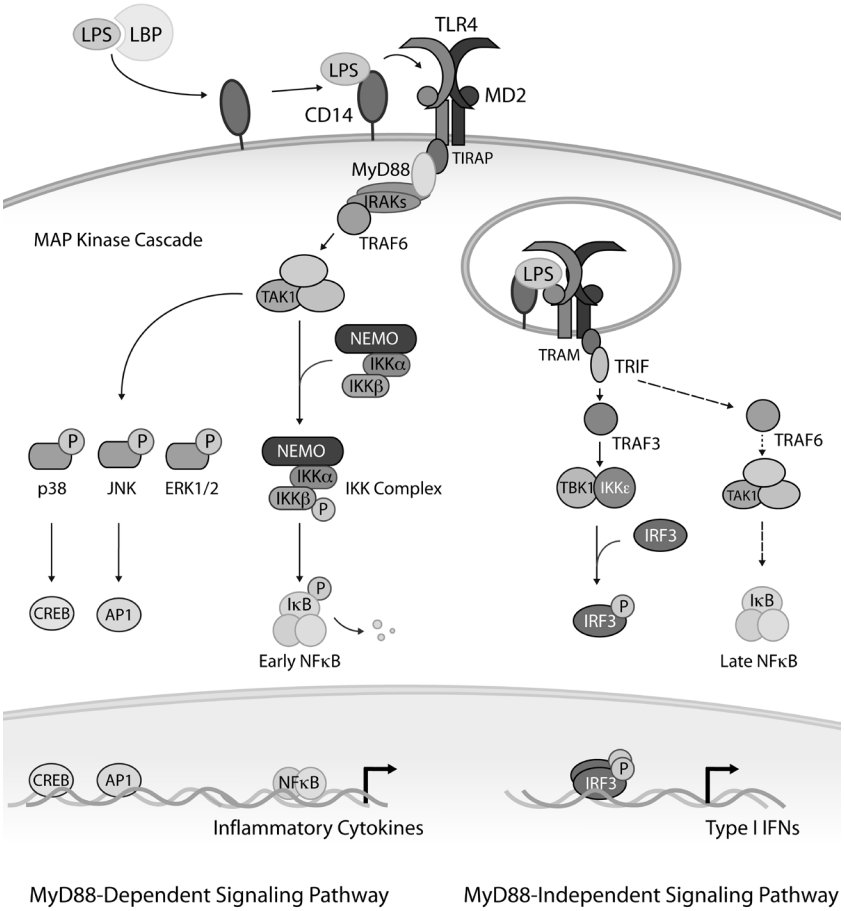

Fig. 1-1: Simplified diagram of LPS signaling through TLR4 (adapted from Akira *et al.* 2006, Kawai & Akira 2010 and Kawai & Akira 2011). LBP coveys LPS to CD14 on the cell surface of monocytes and macrophages. CD14 then transfers LPS to MD2 and TLR4, which form a complex (homodimer, here simplified). TLR4 is capable of activating two signaling branches by recruitment of different adapter combinations. (1) TLR4 signaling on the cell surface through the TIRAP-MyD88 signaling pathway (MyD88-dependent) leads to the first wave of NFκB activation (early NFκB) and the production of pro-inflammatory cytokines. Upon TLR4 activation, MyD88 recruits several members of the IRAK family and TRAF6. Following activation, TRAF6 recruits and interacts with the TAK1 complex, activating it to phosphorylate the IκB kinase (IKK) complex. Once activated, the IKK complex can directly phosphorylate IκB, targeting it for degradation and releasing NFκB, which translocates into the nucleus and activates the expression of target genes encoding for pro-inflammatory cytokines *e.g.* IL-1β, IL-6 and TNF. Simultaneously, TAK1 initiates the MAP kinase cascade. The MAP kinases p38, JNK and ERK1/2 activate CREB and AP1, which target cytokine genes. When IRF5 is activated by TAK1 (not shown), it translocates into the nucleus and binds to IFN-stimulated response element (ISRE) motifs in the promoter regions of cytokines. (2) The ensuing internalization of the entire receptor complex into late endosomes initiates the TRAM-TRIF signaling pathway (MyD88-independent), which is hallmarked by late NFκB activation and production of type I IFNs. TRIF signaling leads to TRAF3 and TBK1/IKKε activation, both of which are required for IRF3 phosphorylation. Dimerized IRF3 molecules translocate into the nucleus and induce type I IFN production. Simultaneous activation of TRAF6 by TRIF induces late NFκB activation and MAP kinase cascade signaling. Abbreviations: CREB = cAMP response element-binding protein, ERK = extracellular-signal-regulated kinase, IκB = inhibitor of kappa B, IRAK = IL-1 receptor-associated kinase, JNK = c-Jun N-terminal kinase, NEMO = NFκB essential modifier, p38 = p38 mitogen-activated protein kinase, TAK1 = TGFβ-activated kinase 1, TBK1 = TANK-binding kinase 1, TRAF = TNF receptor-associated factor.

[1] http://www.uniprot.org/uniprot/P01375 (as of October 2015)

1.4 Cytokines and Chemokines – Mediators of Inflammation

Cytokines, which include interleukins, interferons, colony-stimulating factors, chemokines, and many growth factors, play an essential role in induction and regulation of immune responses. Cytokines are produced by many different cell types and often show features of functional pleiotropy and redundancy. They act as communication molecules between cells. Receptor binding leads to activation of signaling cascades resulting in expression of immune relevant genes, changes in metabolism, proliferation or differentiation, migration and apoptosis depending on the type and developmental state of the target cells. Moreover, extensive crosstalk by cytokines shapes the adaptive immune response (reviewed in Mosser & Edwards (2008), Ramnath *et al.* (2006), Schulte *et al.* (2013), Striz *et al.* (2014) and Turner *et al.* (2014)).

Cytokines can act as activating and pro-inflammatory molecules in immune responses *e.g.* TNF, IL-6, IL-1β and IFNγ; or mediate inhibiting and anti-inflammatory cell functions *e.g.* IL-10 and transforming growth factor β (TGFβ). Additionally, specific types of cytokines named chemokines are important for recruitment of immune cells to sites of infection and injured tissues *e.g.* CXCL8/IL-8, CCL3/MIP-1α (macrophage inflammatory protein 1α) and CXCL10/IP-10 (IFNγ inducible protein 10). The controlled orchestration of these and other cytokines leads to activation of the immune system and clearance of the infectious agents.

Briefly, at the beginning of an inflammation, the primary master regulators of the immune response are TNF and IL-1β, which are produced mainly by monocytes and macrophages. Both cytokines act synergistically to activate further immune cells and produce *"later"* cytokines such as IL-6 and CXCL8/IL-8 that potentiate the inflammatory process. IL-6, for instance, activates lymphocytes and stimulates production of components of the complement system. Moreover, TNF and IL-1β activate the coagulation system and increase the vascular permeability of endothelial cells. The latter one facilitates infiltration of leucocytes *e.g.* neutrophils, lymphocytes and monocytes to the inflammatory site, which are attracted by chemokines *e.g.* CXCL8/IL-8 and CXCL10/IP-10. Once the inflammatory agent is removed, anti-inflammatory cytokines like IL-10 and TGFβ are important terminators of inflammatory processes. They restore the immunological homeostasis by inhibiting the production of pro-inflammatory cytokines and promoting tissue repair (reviewed in Ramnath *et al.* (2006) and Schulte *et al.* (2013)). For a more comprehensive overview about each cytokine, see *Appendix* **5.1**.

Although cytokines are critical for host defense, uncontrolled cytokine release – either pro- or anti-inflammatory – can have detrimental effects to the host by promoting hyperinflammation or immunosuppression. An example for this is sepsis, where systemic activation of the host immune system leads to an imbalance in cytokine production affecting the whole body by damaging body tissues and organs (Biswas & Lopez-Collazo 2009).

1.5 Sepsis: A Disorder of the Immune System

In the early 1990s, sepsis was defined as a clinical syndrome that is characterized by a systemic inflammatory immune response (SIRS) of a host to a (suspected) severe infection, typically of bacterial origin (Bone *et al.* 1992, Vincent *et al.* 2013). Criteria for SIRS are based on four categories including body temperature, respiratory rate, white blood cell count and heart rate (Iskander *et al.* 2013).
Development of sepsis arises when local inflammatory processes fail to prevent spreading of pathogens via the blood stream and induce a systemic activation of the entire immune system (Rittirsch *et al.* 2008). Sepsis can further develop into severe sepsis characterized by acute organ dysfunction of *e.g.* liver and kidneys, and septic shock with hypotension (low blood pressure not responding to any treatment) (Angus & van der Poll 2013). The clinical manifestations of sepsis were already known at the time of Hippocrates (Majno 1991, Rittirsch *et al.* 2008) and – still today – sepsis remains a serious public health issue in the intensive care units, with about six million deaths worldwide per year. The mortality rate ranges from 20 % for sepsis to more than 50 % for septic shock (Angus *et al.* 2006, Monneret *et al.* 2008). Although the risk of dying from sepsis has declined over the past decades, the incidence of sepsis still increases, thus, the number of patients dying each year is similar to the number of people dying with acute myocardial infarction (Martin 2012).

Sepsis was thought to be hallmarked by a biphasic nature, which is characterized by an initial phase of overt inflammation (SIRS) that leads to a later immunocompromised phase to counterbalance the initial inflammatory response (CARS, compensatory anti-inflammatory response syndrome) (Hutchins *et al.* 2014). Nowadays, it is questioned whether the inflammatory amplitude of SIRS controls the extent of CARS or if they start independently with the same trigger. Moreover, a mixed antagonist response syndrome (MARS) is described, where both conditions – SIRS and CARS – co-exist, either as temporary homeostasis during the transition from SIRS to CARS or over the complete course of infection (Adib-Conquy & Cavaillon 2009, Bone 1996, Hoflich & Volk 2002, Tang *et al.* 2010). Nevertheless, sepsis basically consists of two distinct but not mutually exclusive phases; imbalance of either response can result in host damage caused directly by excessive inflammation or indirectly through immune dysfunction (Hotchkiss *et al.* 2013, Rittirsch *et al.* 2008).

The amplitude of the hyperinflammatory phase (SIRS) can persist for a variable period of time depending on patient's age (Martin *et al.* 2006), comorbidities, organism virulence and other factors including genetic polymorphisms in cytokine genes and PRRs (Cook *et al.* 2004, Kumpf & Schumann 2010), affecting both the innate and adaptive immune systems (**Fig. 1-2**) (Hotchkiss & Karl 2003, Hotchkiss *et al.* 2013, Iskander *et al.* 2013).

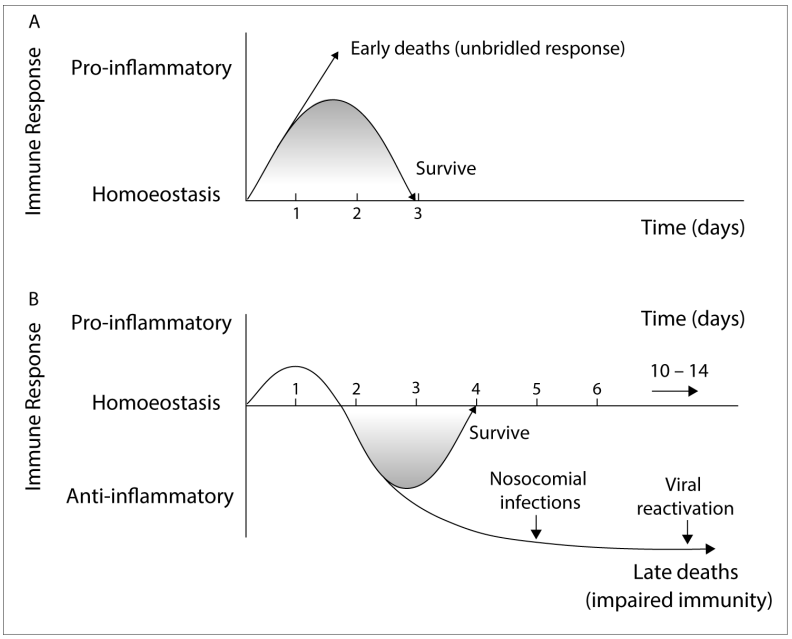

Fig. 1-2: The immune response in sepsis (adapted from Hotchkiss *et al.* 2013). The course and outcome of sepsis are determined by many factors including pathogen virulence, comorbidities and genetic pre-determinants. (A) Although both pro-inflammatory (SIRS) and anti-inflammatory responses (CARS) develop rapidly after sepsis, the initial response in previously healthy young patients who now develop severe sepsis is dominated by a cytokine-driven hyper-inflammation. Mortality in this early phase of sepsis is mainly mediated by cardiovascular collapse and multiple organ dysfunctions. (B) However, most of the patients who develop sepsis are elderly with several comorbidities, which impair proper immune responses. These patients show a reduced hyperinflammatory phase and rapidly enter a state of chronic morbidity and profound severe immunosuppression lasting for days or weeks. The longer the predominantly anti-inflammatory phase lasts, the higher the risk for the patient to develop secondary infections such as nosocomial infections resulting in high mortality. However, appropriate biomarkers are still limited to distinguish the two phases. So far, persistent decrease in human leukocyte antigen DR (HLA-DR) expression on monocytes is a common feature of the immunedepressive state (Docke *et al.* 1997a). The usage of biomarkers increases the efficacy of treatment, either with anti-inflammatory therapies within the first hyperinflammatory phase or boosting treatments for immunity reactivation within the immunocompromised phase (Eichacker *et al.* 2002).

Previously healthy young adults who develop sepsis often show a cytokine-driven hyperinflammation indicated by shock, high fever and multiple organ failure. Full-blown, systemic activation of immune responses occurs due to releases of PAMPs and DAMPs from invading microorganisms and damaged host tissue, resulting in an overstimulation of immune cells and an imbalanced cytokine response known as *'cytokine storm'* (Hotchkiss *et al.* 2013, Thomas 1972). High production of pro-inflammatory cytokines *e.g.* TNF, IL-1β and IL-6 – normally beneficial for fighting against pathogens – now converts into an excessive damaging inflammation mediating a severe dysregulation of various body systems. An unbalanced network of pro-inflammatory mediators leads to vascular leakage of fluid into tissues by TNF and IL-1β, and cardiac dysfunction by IL-6. Moreover, activation of coagulation cascades results in microvascular thromboses throughout the body and impaired perfusion of critical organs, which lead to multi-organ failure and often death due to *cytokine storm*-mediated responses (see **Fig. 1-2** A) (reviewed in Hotchkiss & Karl (2003), Hotchkiss *et al.* (2013), Hutchins *et al.* (2014), Rittirsch *et al.* (2008) and Sriskandan & Altmann (2008)).

In contrast, elderly people have a reduced or absent hyperinflammation phase and rapidly develop impaired immunity (see **Fig. 1-2** B). Sepsis is now increasingly a disease of elderly

people older than 65 years (Hotchkiss *et al.* 2013, Martin *et al.* 2006). Here, the imbalance of a favored immunocompromised status increases the risk of secondary or nosocomial infections with weakly virulent or opportunistic organisms followed by a high mortality (Otto *et al.* 2011). Nosocomial or hospital-acquired infections are defined as infections occurring during treatment in a healthcare unit which are secondary to the patient's original condition (Rittirsch *et al.* 2008). Immunosuppression (also known as *'immunoparalysis'*; Docke *et al.* (1997b) and Volk HD *et al.* (1989)) is mediated by a shift towards anti-inflammatory cytokines and unresponsiveness of immune cells. One hallmark of sepsis is the reduced ability of monocytes to produce pro-inflammatory cytokines, such as TNF, IL-1β and IL-6, in response to bacterial challenges (Ertel *et al.* 1995, Manjuck *et al.* 2000, Munoz *et al.* 1991, Volk *et al.* 1991). Moreover, the reduced ability to fight and eliminate the causative agents is due to a loss of lymphocytes, dendritic cells and gastrointestinal epithelial cells by apoptosis (Hotchkiss *et al.* 1999, Hotchkiss *et al.* 2002, Hotchkiss *et al.* 2001).

As anti-inflammatory therapeutic strategies were not successful, sepsis and its pathophysiological events are now thought to be mainly driven by immune suppression resulting in secondary infections. Thus, understanding immunological defects that impair host immunity is crucial for treatment of sepsis patients since careful boosting of immune system improves survival (Hotchkiss *et al.* 2013, Hutchins *et al.* 2014, Marshall 2014).

1.6 Endotoxin Tolerance: A Model for Analyzing *'Immunoparalysis'* in Sepsis Patients

Some of the unbalanced features of sepsis with gram-negative bacteria have been linked to endotoxin tolerance (Biswas & Lopez-Collazo 2009, Lopez-Collazo & Del Fresno 2013). Endotoxin tolerance is a phenomenon observed in animals and humans, in which immune cells become transiently unresponsive to endotoxin treatment (*e.g.* LPS) after a first exposure to LPS (Beeson 1946, Michalek *et al.* 1980, Virca *et al.* 1989, Ziegler-Heitbrock *et al.* 1994). Monocytes and macrophages are the principal cells responsible for the induction of endotoxin tolerance *in vivo* (Freudenberg & Galanos 1988). As tolerance minimizes damage caused by a given level of excessive inflammation and immunopathology (Medzhitov *et al.* 2012), endotoxin tolerance can be assumed to be a mechanism of host protection (Biswas & Lopez-Collazo 2009).

To analyze the systemic mechanisms occurring during sepsis and endotoxin tolerance, several *in vivo* and *in vitro* models were established. They are based on the tolerization effect of two consecutive treatments of animals or immune cells, in particular monocytes and macrophages, with endotoxin mimicking a primary (pro-inflammatory phase) and a secondary infection (anti-inflammatory phase) in sepsis (Lopez-Collazo & Del Fresno 2013).

An *in vitro* endotoxin model with monocytes demonstrated that a first exposure to endotoxin for only one hour is sufficient to develop tolerance. However, exposure with LPS for six to eight hours is more effective in inducing a tolerant status in monocytes lasting for up to five days (del Fresno *et al.* 2009).
Characteristically, LPS tolerant cells are refractory to induce inflammatory cytokine and chemokine expression, such as TNF, IL-6, IL-1β, CCL3/MIP-1α, and CXCL10/IP-10 (the encoding genes are referred to as *'tolerizable genes'*), and show impaired antigen presentation capacity. By contrast, secretion of anti-inflammatory cytokines like the IL-1 receptor antagonist (IL-1RA), IL-10 and TGFβ, and production of anti-microbial PRRs like the macrophage receptor with collagenous structure (MARCO) and the formyl peptide receptor 1 (FPR1) are unaltered or even enhanced (referred to as *'non-tolerizable genes'*) (Allantaz-Frager *et al.* 2013, Biswas & Shalova 2012, Cavaillon & Adib-Conquy 2006, Foster *et al.* 2007, McCall *et al.* 1993, McCall & Yoza 2007, Yoza *et al.* 2000). Thus, endotoxin tolerance is not only a simple downregulation of pro-inflammatory molecules, but rather a *'reprogramming'* of monocytes and macrophages.
Physiologically, this poorly inflammatory, tolerant phenotype is protective in hyperinflammation conditions including sepsis as this phenomenon allows for high phagocytic activity and bacterial clearance while avoiding the excessive toxicity associated with high cytokine production contributing to protection against septic shock (Biswas & Lopez-Collazo 2009, Biswas & Shalova 2012, Lopez-Collazo & Del Fresno 2013, Medzhitov *et al.* 2012). However, secondary infections in sepsis-like conditions lead to a high patient mortality as the tolerant immune system does not initiate further immune responses against new invading pathogens.

The molecular basis of endotoxin tolerance is still not fully understood. LPS-tolerant cells show downregulation of many inflammatory signaling proteins (reviewed in Fan & Cook (2004)). However, a loss of LPS signaling can only partly explain the phenomenon of endotoxin tolerance. In tolerant cells, LPS stimulation can still induce the expression of genes that encode for anti-inflammatory cytokines and anti-microbial mediators, but activation of pro-inflammatory genes is refractory. Thus, the differential tolerization effect of LPS on monocytes and macrophages rather favors the concept of gene reprogramming than an overall downregulation of LPS-induced gene expression (Cavaillon & Adib-Conquy 2006).
Epigenetic modifications in the chromatin structure of tolerant cells including selective changes in histone modifications and nucleosomal rearrangement are emerging as an explanation for reprogramming of monocytes and macrophages (Carson *et al.* 2011, Chan *et al.* 2005, El Gazzar *et al.* 2009, McCall & Yoza 2007, Medzhitov & Horng 2009, Yoza *et al.* 2000). Thus, understanding chromatin modifications in *tolerizable* and *non-tolerizable genes*

could elucidate the accessibility of gene loci in tolerant monocytes and macrophages leading to a better understanding of the progression of endotoxin tolerance and sepsis.

1.7 Epigenetics

The epigenetic landscape refers to all mechanisms that modulate gene expression without changing the underlying DNA sequence. An overview is depicted in **Fig. 1-3**.

Traditionally, epigenetic modifications were seen as stable, heritable changes in gene expression that are transferred from one cell or organism to their progeny and underlie stable differentiation into various cell types and tissues (Kouzarides 2007).
Moreover, epigenetic changes are now considered to be dynamically regulated and reversible to allow chromatin flexibility in response to environmental stimulation. Thus, epigenetics are not only important in the development of cell types and organisms, but also in immune responses and disease establishment including cancer (Bernstein *et al.* 2007, Carson *et al.* 2011, Falkenberg & Johnstone 2014, Shakespear *et al.* 2011).

Chromatin consists of DNA with associated proteins, mainly histones, which are important for packaging and organizing of DNA but also dictate gene transcription. The epigenetic landscape, including DNA methylation, histone modifications, nucleosome positioning and non-coding RNA, influences gene expression. Chromatin flexibility is mediated mainly by two principal mechanisms: DNA methylation and chromatin modifications (see **Fig. 1-3**). Coordinated modifications of DNA and/or associated proteins result in changes within the physical accessibility of DNA to transcription factors. These multiple mechanisms lead to regulated organization of gene loci into transcriptionally active or silent states (Berger 2007, Bernstein *et al.* 2007). Open or transcriptionally active chromatin (euchromatin) is accessible to transcription factors and polymerases, whereas transcriptionally silent chromatin (heterochromatin) is densely packed (Bernstein *et al.* 2007, Carson *et al.* 2011, Falkenberg & Johnstone 2014, Shakespear *et al.* 2011).

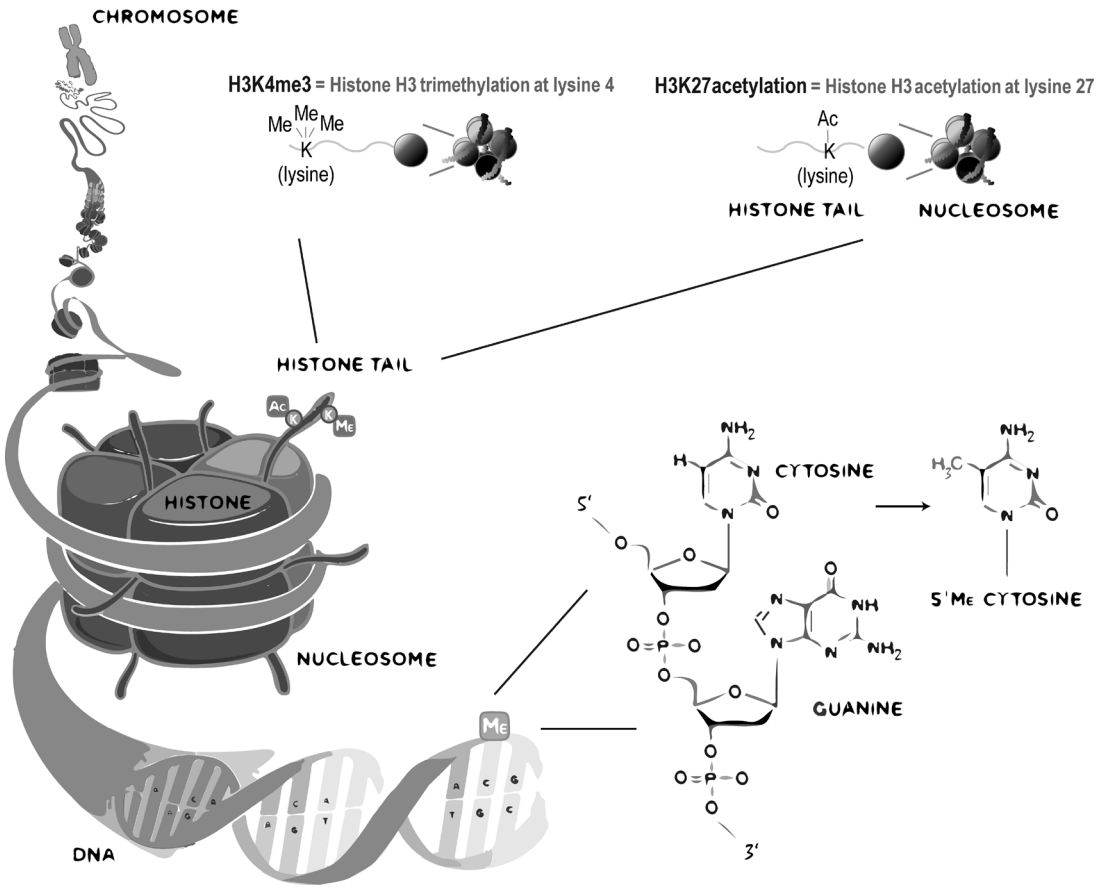

Fig. 1-3: Organization of DNA and epigenetic modifications of chromatin (adapted from Bernstein *et al.* (2007)). DNA is hierarchically organized in the eukaryotic nucleus with DNA-associated proteins into higher structural units. This structural organization allows it to fit within the small nucleus, but also provides rapid and precise access for transcription, replication and repair. A nucleosome is the first structural unit, which consists of 147 bp DNA wrapped around a histone core containing two copies each of the histone proteins H2A, H2B, H3 and H4 (Luger *et al.* 1997). The nucleosomes are connected by the linker histone H1 forming a *'beads on a string'*-like structure. Nucleosomes are higher ordered and packaged to a secondary structure referred to as the 30 nm chromatin fiber (Depken & Schiessel 2009). During mitosis, the chromatin fiber is further packaged into dense chromosomal structures (metaphase chromosome). Besides packaging, chromatin plays an important role in gene expression. The N-terminal tails of histones can be modified and, thereby, dictate the expression pattern of the underlying DNA sequence by influencing the contact between nucleosomes or recruiting other DNA- and histone-binding proteins including non-histone proteins like transcription factors. In addition, the DNA molecule itself can be modified. DNA methylation occurring at position five of the cytosine ring within 5'-cytosine-guanine-3' dinucleotides (CpGs) is considered to have a repressed chromatin status and shows inhibition of gene expression.

1.7.1 DNA Methylation

Mammalian DNA methylation of cytosine bases within 5'-cytosine-guanine-3' dinucleotides (CpGs) is associated with a repressed chromatin structure and inhibition of gene expression (Bird & Wolffe 1999).

Several DNA (cytosine-5)-methyltransferases (DNMTs) are known: The *de novo* methyltransferases DNMT3a and DNMT3b are responsible for introducing cytosine methylation at previously unmethylated CpG sites, whereas in maintenance the

methyltransferase DNMT1 copies pre-existing methylation patterns onto the new DNA strand during DNA replication (Klose & Bird 2006). However, there is evidence that this classification is too simplistic as DNMT1 also displays *de novo* activity (Brenner & Fuks 2007, Jair *et al.* 2006). Another enzyme closely related to DNMT3a and DNMT3b is the DNTM3-like protein (DNMT3L) that does not contain intrinsic DNA methyltransferase activity, but physically associates with DNMT3a and DNMT3b and stimulates their methylation activity (Goll & Bestor 2005, Klose & Bird 2006).

Repression of gene expression by DNA modifications is mediated by two possible mechanisms: (1) DNA methylation inhibits the association of some DNA-binding factors to their DNA loci *e.g.* transcription factors, or, (2) proteins that recognize methylated CpGs bind and recruit co-repressors to form a chromatin remodeling co-repressor complex to silence gene expression directly. These DNA-binding proteins are called methyl-CpG-binding proteins (MBPs). Moreover, the co-repressor complex can interact with histone deacetylases (HDACs) and histone methyltransferases (HMTs), which indirectly induce repression through other epigenetic changes like histone modifications (Klose & Bird 2006).

1.7.2 Histone Modifications

DNA is associated with histone proteins for packaging eukaryotic DNA within the nucleus. The basic structure of DNA storage is called a nucleosome, which consists of 147 bp of DNA wrapped around an octamer of histone proteins containing of two copies each of the histones H2A, H2B, H3 and H4 (Luger *et al.* 1997).

Besides their important role in dynamic packaging of genetic material, histones can undergo covalent modifications: Post-translational modifications of N-terminal histone tails include lysine (K) and arginine (R) methylation, lysine acetylation, serine phosphorylation, lysine ubiquiylation and SUMOylation among others (Peterson & Laniel 2004). These modifications can direct winding or unwinding of the associated DNA and provide a binding platform for transcription factors and chromatin-associated proteins that initiate or repress gene transcription (Clapier & Cairns 2009, Smale 2010a). It is believed that the coordinated modifications of a given histone, also known as *histone code hypothesis* or *histone code theory*, can dictate the transcription state of the nearby gene locus (Iizuka & Smith 2003, Jenuwein & Allis 2001, Strahl & Allis 2000). The activating or repressing feature of these modifications is dependent on the modification itself, but also on the location of the modification within the histone tail (see **Fig. 1-4**) (Carson *et al.* 2011).

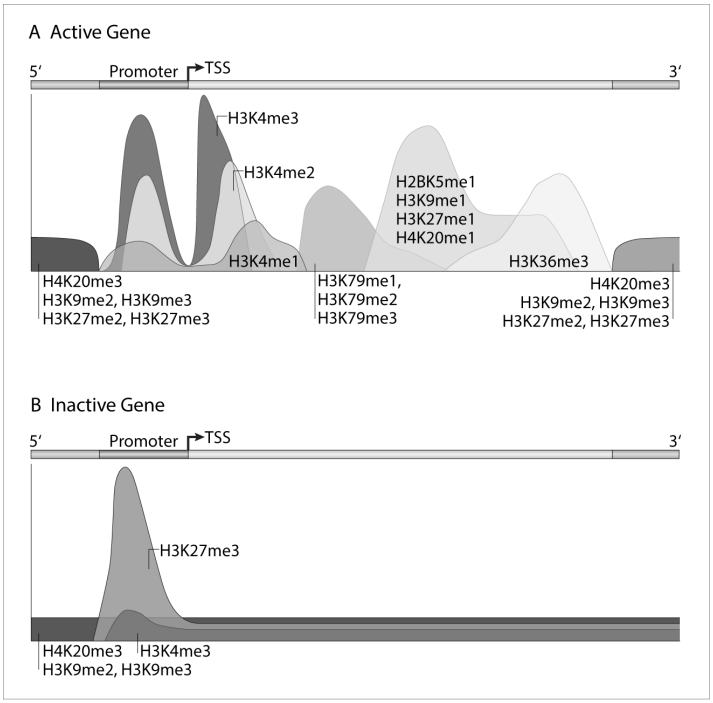

Fig. 1-4: Methylations of histone residues (adapted from Kooistra & Helin (2012), with contributions from Kouzarides (2007) and Northrup & Zhao (2011)). Genes and gene-associated elements need to be accessible for different genomic functions like cell replication, DNA repair and to respond to external stimuli. Histone proteins are not only important for packaging and fitting of DNA into the nucleus, but modifications of these proteins can also orchestrate gene expression. Acetylation of lysine within the histone tail mediates unfolding of chromatin since it neutralizes the basic charge of the lysine and thereby is associated with active transcription (acetylation is not depicted in figure). (A) Methylation at lysines (K) and arginines (R) of histone proteins can appear in one of three different forms: mono-, di-, or trimethyl for lysines and mono- or di- for arginines. Methylation of lysine at position 4 on histone 3 (H3K4), H3K36 and H3K79 is associated with actively transcribed genes. In particular, mono-, di- and trimethylation of H3K4 is highly localized to a few nucleosomes around the promoter region and at the transcription start site (TSS). Within the transcribed region of active genes, the following modifications are localized: monomethylation of H2BK5, H3K9, H3K27, H4K20 and mono-, di- or trimethylation of H3K79, whereas H3K36me3 peaks at the 3′end of transcribed genes. (B) On repressed genes, the methylation marks H3K9me2, H3K9me3 and H4K20me3 are relatively homogeneously distributed, whereas H3K27me3 peaks at promoters.

Actively transcribed genes tend to be associated with multiple *'activating'* modifications, whereas silent genes are associated with only a few *'repressive'* modifications or are not associated with any modifications (Northrup & Zhao 2011). Generally speaking, histone acetylation and many methylation events are positively correlated with gene activation, whereas histone H3 di- and trimethylation on lysine 27 (H3K27me2, H3K27me3) and lysine 9 (H3K9me2, H3K9me3), as well as histone H4 trimethylation on lysine 20 (H4K20me3) are exceptions that are negatively correlated with gene expression (Barski *et al.* 2007, Kooistra & Helin 2012, Northrup & Zhao 2011, Strahl & Allis 2000). The association of histone modifications as activating or repressive is based on their correlation with gene expression. For instance, trimethylation of H3K4 (H3K4me3) is found around the transcription start site (TSS) of active genes, whereas H3K9me3 indicates heterochromatin and H3K27me3 is critical for repression of developmental genes (Bernstein *et al.* 2007, Kouzarides 2007). For an overview about histone modifications and their impact on gene expression see **Table 1-1**.

Table 1-1: Overview of important post-translational modifications of histones at promoters and enhancers and their impact on gene expression. A promoter is a genomic region located near the transcription start site (TSS), which mediates gene transcription (Northrup & Zhao 2011). Regions of DNA that activate transcription but are not located at the TSS are referred to as enhancers. Bivalent modifications of activating and silencing (repressive) marks in promoters and enhancers indicate a so-called poised status to keep the underlying gene sequence silent but inducible, which allows plasticity in processes including cell differentiation (Kouzarides 2007, Shlyueva *et al.* 2014, Voigt *et al.* 2013).

Transcription Status	Kind of Modification at Promoter/Gene	Enhancer
Silent / Repressive	H3K27me3 (me = methylation)	H3K27me3
	H3K9me2	
	H3K9me3	
	H4K20me3	
Poised	H3K27me3	H3K27me3
	H3K4me3	H3K4me1 or H3K4me2
Active	H3K4me3	H3K4me1, H3K4me2
	H3K9ac (ac = acetylation)	H3K9ac
	H3K27ac	H3K27ac
	H3K18ac	H3K18ac
	H4ac (K5, K8, K13, K16)	H4ac (K5, K8, K13, K16)

Note: The table does not provide a complete overview. The information included is based on Barski *et al.* (2007), Berger (2007), Northrup & Zhao (2011), Strahl & Allis (2000) and Wang *et al.* (2008).

Generally, epigenetic regulations are very dynamic: *'Epigenetic writers'* such as histone acetyltransferases (HATs), histone methyltransferases (HMTs) and DNA methyltransferases (DNMTs) lay down epigenetic marks on DNA molecules or histones. These marks are recognized by *'epigenetic readers'*, which recruit other chromatin modifiers and remodeling proteins to alter chromatin function and structure. *'Epigenetic erasers'* such as histone deacetylases (HDACs) catalyze the removal of epigenetic marks. Addition and removal of these post-translational modifications lead to the addition and/or removal of other marks in a highly complicated manner. Together, histone and DNA modifications regulate various DNA-dependent processes, including transcription, DNA replication and DNA repair (reviewed in Berger (2007), Black *et al.* (2012), Falkenberg & Johnstone (2014) and Shakespear *et al.* (2011)). Moreover, there is a deep cross talk between DNA methylation and histone modifications. As already mentioned above (see DNA methylation in *Introduction* section, **1.7.1**), DNA methylation signals histone modification, but also vice versa (Kooistra & Helin 2012, Kouzarides 2007). For instance, trichostatin A treatment (an HDAC inhibitor) causes impaired CpG methylation. Moreover, the histone modification H3K9me3 directly affects chromatin silencing and heterochromatin formation by recruiting the heterochromatin protein 1 (HP1), which can interact with DNMTs (Brenner & Fuks 2007, Dormann *et al.* 2006, Fuks 2005, Smallwood *et al.* 2007).

1.8 Aims and Objectives

Epigenetic changes play an important role in regulating inflammatory immune responses. Sensing pathogens and danger signals transmits signals to transcription factors and other chromatin-modifying proteins, and recruits them to inflammatory gene loci (Stender & Glass 2013). Thus, inflammatory gene expression is associated with a diversity of additional chromatin modifications such as histone acetylation and methylation that open gene loci and facilitate transcription (Carson *et al.* 2011, Ivashkiv 2011).

In sepsis and endotoxin tolerance, tolerant cells exhibit a selective defect in the induction of a subset of genes, encoding pro-inflammatory cytokines (*tolerizable*, also referred to as class T genes), while the expression of other genes encoding for instance for anti-microbial mediators is still active (*non-tolerizable*, also referred to as class NT genes). There is evidence that inflammatory processes in sepsis and endotoxin tolerance resulting in increases or decreases of gene expression are mediated by epigenetic changes including DNA methylation, histone modifications and chromatin remodeling. For instance, Foster and her colleagues analyzed murine macrophages in an *in vitro* endotoxin tolerance model and could show that the differential expression patterns of *tolerizable* and *non-tolerizable genes* were due to different patterns of histone modifications (Foster *et al.* 2007). Other studies indicated that the *IL1B* and *TNF* genes displayed an enrichment of the repressive histone mark H3K9me2 within their promoter regions in tolerant THP1 cells, a monocytic cell line (Chan *et al.* 2005, El Gazzar *et al.* 2007). Moreover, the same group showed an increase in DNA methylation within the *TNF* promoter of tolerant THP1 cells (El Gazzar *et al.* 2008).

These and other results indicate that epigenetic changes happen in hyperinflammatory immune responses such as sepsis and endotoxin tolerance, resulting in an impaired expression of genes that regulate key immune activation responses: Therefore, what is intended to provide host protection from immunopathology now renders the host more susceptible to further infections. However, many of the mentioned studies analyzed epigenetic changes in endotoxin tolerance with a focus on murine macrophages, monocytic cell lines, or only a limited number of genes. Thus, further understanding and detection of these hyperinflammatory-induced epigenetic modifications especially in a human setting could lead to early identification of immunocompromised patients allowing more timely immune-boosting therapies (Hotchkiss *et al.* 2013).

This study aimed to clarify the understanding of epigenetic changes in endotoxin tolerance experimentally in the human model. The main question was whether stable non-permissive epigenetic changes take place to selectively modify the pro-inflammatory response responsible for inflammation-associated pathology, while allowing expression of anti-inflammatory and anti-microbial mediators in human monocytes during LPS tolerization.

Therefore, human primary monocytes were analyzed in an *in vitro* endotoxin tolerance model. The focus included the analysis of particular immune response genes and also the identification of genome-wide alterations in the monocytic epigenetic landscape.

The following specific questions were addressed in the first part of the present study:

- Do changes in activating histone modifications allow a discrimination of *tolerizable* (class T) and *non-tolerizable genes* (class NT) in LPS-tolerant human CD14-positive monocytes?
- Are there species-related differences in the positive, transcription-linked histone patterns of human monocytes and murine macrophages in endotoxin tolerance?
- Besides activating events, do changes in repressive histone modifications allow a classification in *tolerizable* (class T) and *non-tolerizable genes* (class NT)?
- Does DNA methylation have an impact on repression of *tolerizable genes*, in particular, the genes encoding for the pro-inflammatory cytokines TNF and IL-6?

The following specific issues were addressed in the second part:

- Are there global changes in histone modifications that affect the whole monocytic genome? What might be the underlying mechanism?
- Does endotoxin tolerance have a genome-wide impact on DNA methylation?
- If so, do these global changes in epigenetic modifications have an influence on gene expression?

2. Results

2.1 The Impact of LPS Tolerization on Specific Immune Response Genes

2.1.1 Analysis of Cytokine Profile in Naïve and Tolerant Human Monocytes

Initially, culture conditions for cultivation of human monocytes were optimized to increase the viability of monocytes *in vitro* for several days, thus ruling out differences in downstream assays coming from a high proportion of dead cells. For a detailed overview of the optimization process, please go to the *Materials & Methods* section (**4.3.1.d**).
For all following experiments, human $CD14^+$ monocytes were cultured in MPC-treated plates with IMDM medium supplemented with human AB serum from PAN-Biotech (*Cat. No.:* P30-2901M, *Lot No.:* P073305).

To verify the hypothesis that LPS tolerization differentially affects gene expression of immune response genes, human monocytes were subjected to the *in vitro* endotoxin tolerance model (see **Fig. 2-1** for a general overview), and cytokine and chemokine secretion patterns of naïve and tolerant human monocytes were characterized using the Luminex system from Millipore. The Luminex technology is a bead-based multi-analyte panel and provides simultaneous measurement of multiple protein targets in a single sample (Multiplex)[2].

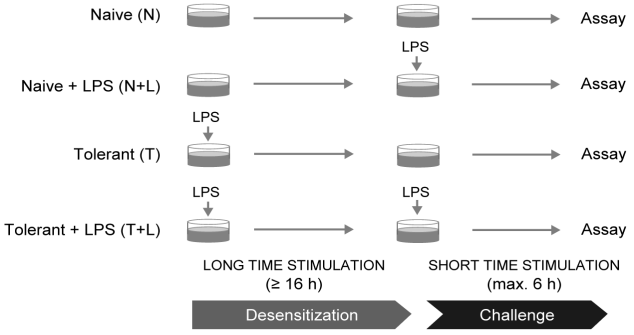

Fig. 2-1: General experimental design for induction of endotoxin tolerance. Human $CD14^+$ monocytes were left untreated (Naïve) or treated with LPS overnight (Tolerant) for a minimum of 16 h, washed, given fresh media and stimulated with LPS where indicated (Naïve + LPS, Tolerant + LPS).

The supernatants of unstimulated naïve monocytes (N), naïve cells treated with LPS for a maximum of 4 h (N+L), monocytes rendered tolerant with LPS treatment overnight (T) and tolerant cells re-stimulated with LPS (T+L) were compared for cytokine secretion. In parallel, the induction of intracellular signaling events by LPS stimulation was exemplarily analyzed by flow cytometric analysis of the MAP kinase p38 phosphorylation (see **Fig. 2-2** for gating strategy and **Fig. 2-3 A** for experimental design). Naïve monocytes stimulated with LPS (N+L) showed an increase in p38 signaling, which was abolished in tolerant monocytes re-stimulated with LPS (T+L, **Fig. 2-3** B). Although the signaling was diminished in tolerant cells, the production and secretion of cytokines and chemokines showed a heterogeneous secretion pattern (**Fig. 2-3** D).

[2] https://www.lifetechnologies.com/de/de/home/life-science/protein-biology/protein-assays-analysis/luminex-assays.html (as of October 2015)

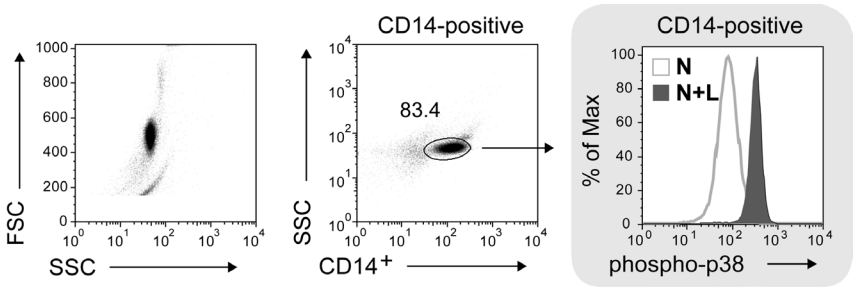

Fig. 2-2: Signaling analysis in monocytes. Gating strategy for analysis of p38 phosphorylation by flow cytometry. Cells were stimulated with LPS for 15 min and stained intracellularly for p38 activation with the BD Phosflow System.

Consistent with previous studies (Allantaz-Frager *et al.* 2013, Foster *et al.* 2007), the cytokines and chemokines analyzed in tolerant monocytes could be broadly categorized according to their induction capacity into two gene classes: *Tolerizable* (class T) and *non-tolerizable genes* (class NT, **Fig. 2-3** D and E). *Tolerizable genes* showed a diminished expression upon re-exposure to LPS (T+L/N+L ratio < 1), whereas *non-tolerizable genes* were even more highly expressed in tolerant cells (T+L/N+L ratio > 1; see **Fig. 2-3** E).

Several secreted proteins, including pro-inflammatory cytokines like TNF, IL-6 and IL-1β showed decreased induction after re-stimulation with LPS in tolerant human monocytes and, thus, were classified into class T genes (**Fig. 2-3** D and E). Notably, the experiment was performed without additional ATP stimulus; therefore, the expression of IL-1α and IL-1β was almost indetectable in the supernatant. The supplementation of ATP is, however, necessary as a second signaling stimulus that mediates cleavage and secretion of the mature forms of IL-1α and IL-1β (Schroder & Tschopp 2010). A detailed look at the expression pattern of these cytokines revealed that the broad classification might be too simplistic. Especially within the class T genes, the LPS tolerization effect on individual cytokines was highly heterogeneous. One subgroup including TNF, CCL3/MIP-1α, CCL4/MIP-1β and CXCL10/ IP-10 was highly produced in naïve monocytes challenged with LPS (N+L), but their expression was almost completely lost in tolerant cells (T+L, **Fig. 2-3** D, upper panel). Another subgroup containing IL-6 and IL-1β showed basic cytokine secretion even in tolerant monocytes (**Fig. 2-3** D, middle panel). Moreover, CXCL8/IL-8 and probably CXCL1/GRO and IL-10 were re-inducible in tolerant cells, although the expression did not completely reach the same levels as in naïve cells challenged with LPS (**Fig. 2-3** D, middle panel).

In contrast, G-CSF, CCL2/MCP-1 and CCL7/MCP-3 categorized into class NT genes remained inducible despite reduced signaling and were produced in tolerant cells in even higher levels compared to naïve monocytes challenged with LPS (**Fig. 2-3** D, lower panel). Another well-known example for a class NT gene encodes for the receptor FPR1 (Foster *et al.* 2007). Analysis of *FPR1* mRNA clearly showed a higher expression profile in tolerant monocytes treated with LPS compared to naïve ones (**Fig. 2-3** C). Interestingly, IL-1RA, which is also considered to belong to the class NT genes, showed only low levels of re-challenge dependent induction (**Fig. 2-3** D, middle panel).

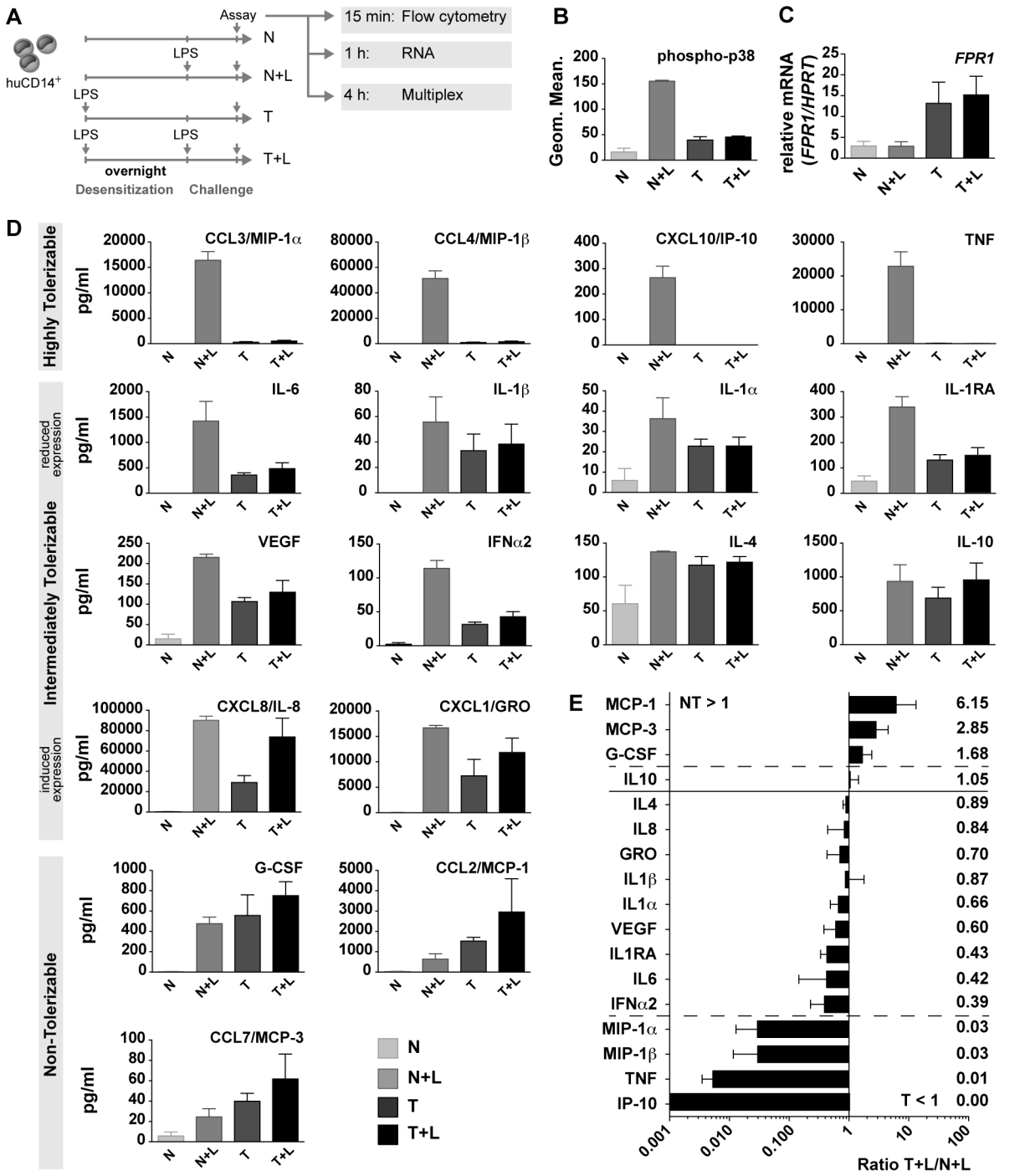

Fig. 2-3 Differential gene expression pattern in endotoxin-tolerant human monocytes. (A) Experimental design: Human CD14$^+$ monocytes were tolerized overnight with 100 ng/ml LPS (T) or left untreated (N), washed and given fresh media the following day and stimulated with 100 ng/ml LPS for the indicated time points (N+L, T+L). (B) Summary of p38 signaling in tolerized and naïve human monocytes after 15 min stimulation with 100 ng/ml LPS. (C) Naïve and tolerized cells were treated for 1 h with 100 ng/ml LPS or left untreated. Cell pellets were lysed and mRNA expression of *FPR1* was determined from isolated total RNA. (D) Naïve or tolerized monocytes were treated with LPS (N+L, T+L) or left untreated (N, T) for 4 h. Supernatants from cell cultures were analyzed by Luminex bead-based multiplex analysis panel. (E) The ratios *T+L/N+L* of the analyzed cytokines and chemokines from D are represented as horizontal bar plot: A ratio above 1 (solid line) is considered as *non-tolerizable* (NT) *gene* and below 1 as *tolerizable* (T) *gene*, whereas the dashed lines indicate a potential transition zone. Data are shown for 3 independent experiments (mean ± SEM).

In summary, despite reduced signaling capacity in tolerant monocytes, the secretion of individual cytokines and chemokines was differentially affected and could be roughly categorized into class T and NT genes. However, detailed multiplex analyses indicated that this broad classification might be too simplistic and that a sub-grouping in a total of three to four classes would better describe the expression patterns of immune response genes in endotoxin tolerance. For instance, LPS tolerization had a high effect on *e.g.* TNF and CXCL10/IP-10 production in tolerant monocytes (*'highly tolerizable'*), whereas pro-inflammatory cytokines and chemokines like IL-1β, IL-6 and CXCL8/IL-8 were only moderately affected (*'intermediately tolerizable'*). The latter group could be further sub-divided into (a) cytokines that showed reduced expression in tolerant monocytes with only limited additional induction capacity after LPS re-stimulation (*e.g.* IL-1β and IL-6) and (b) cytokines that could be re-induced in tolerant cells (*e.g.* CXCL8/IL-8 and CXCL1/GRO). By contrast, other chemokines like CCL7/MCP-3 showed an accumulation of expression over time and were produced even higher in tolerant monocytes treated with LPS. They showed a similar expression profile as the receptor FPR1, which belongs to the class NT genes (*non-tolerizable*).

2.1.2 Potential Role of Histone Modifications in Tolerant Human Monocytes

LPS tolerization seemed to differentially affect the expression of immune response genes in human monocytes. Changes at the chromatin level can have an impact on gene expression (Jenuwein & Allis 2001, Strahl & Allis 2000) and Foster *et al.* (2007), for instance, showed that class T and NT genes were differentially regulated by alterations in histone modifications in murine macrophages. Therefore, the potential role of histone marks in endotoxin tolerance in human monocytes was analyzed by chromatin-immunoprecipitation (ChIP) assays.

ChIP is a very powerful tool that allows the study of transcriptional regulation by enabling the localization of transcription factors and modified histones to specific DNA loci (Gilmour & Lis 1985, Jackson 1978, Solomon *et al.* 1988, Solomon & Varshavsky 1985). It is based on the preservation of proteins bound to the DNA *in vivo* by a fixation agent, normally formaldehyde. Following chromatin purification and shearing of DNA-protein complexes into short stretches, fragmented chromatin is subjected to immunoprecipitation using an antibody directed towards a protein of interest, *e.g.* histone protein bearing a specific modification. After specific enrichment of chromatin fragments, the co-captured DNA is purified and subsequently analyzed (Caretti *et al.* 2003, Kuo & Allis 1999, Weinmann & Farnham 2002). An overview about the ChIP technique is schematically depicted in **Fig. 2-4**.
The enriched DNA can be analyzed by quantitative real-time PCR (ChIP-qPCR). Here, primer pairs specific to a genomic region, *e.g.* promoter region of the *TNF* gene, are used to

detect co-localized DNA fragments. This approach, however, only focuses on specific gene regions of interest. A genome-wide analysis of DNA-protein-interactions is achieved by sequencing all enriched DNA fragments (ChIP-Seq). Aligning the sequenced reads to the human genome generates a binding profile, where high enrichment of DNA sequences (titled as *'peaks'*) represents the location of the analyzed DNA-protein interaction. For more details see the *Materials & Methods* section (**4.3.5** and **4.3.6**). Various bioinformatic tools involving peak calling for identification of significant enriched regions (representing interaction sites), gene annotations and searching for transcription factor binding sites can be applied for down-stream investigations (see below in **2.2.1** in *Results* section, and also **4.3.7** in *Materials & Methods* section).

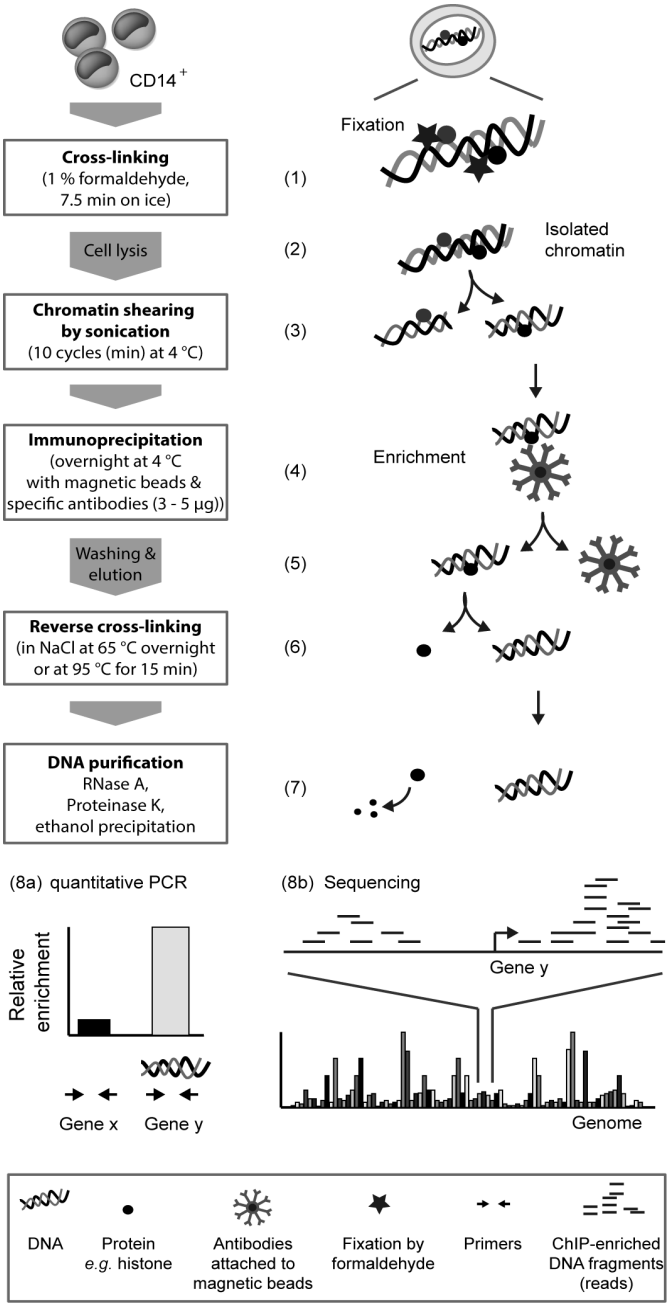

Fig. 2-4: Schematic overview of ChIP assays used in this study to analyze histone modifications in human monocytes. (1) $CD14^+$ human monocytes were fixed with 1 % formaldehyde for 7.5 min on ice. Here, formaldehyde fixation is schematically represented by a star. (2) After lysis of cell and nucleic membranes, (3) freed chromatin was sheared by sonication for 10 cycles at 4 °C (Bioruptor from Diagenode, high power, 30 sec on/off). A small aliquot of input DNA representing total DNA (not shown in figure) was stored until further use and was processed from step 6 on along with the ChIP-enriched DNA. Input DNA further served as an internal control for the ChIP assay (for more details see *Materials & Methods*, **4.3.5)**. (4) Magnetic Dynabeads were attached to ChIP-validated antibodies directed to histone modifications and subsequently incubated with sheared chromatin. Control immunoprecipitation was performed with a non-specific IgG. (5) After magnetic sort and washing, specifically enriched DNA-protein-complexes were eluted. (6) Reversal of cross-linking from formaldehyde fixation was performed and (7) DNA was purified by RNA and protein digestion following ethanol precipitation. (8a) ChIP-enriched DNA was either analyzed by quantitative PCR and SYBR Green with primer pairs specifically designed to detect genes of interest or (8b) directed to sequencing for genome-wide analysis of DNA-protein interactions.

To apply ChIP assays for analyses of epigenetic changes in human monocytes, the technique was first established and further optimized empirically according to DNA cross-linking and shearing. For more details, please go to *Materials & Methods* section **4.3.5.d**. Best fragmentation results were achieved by fixation of human monocytes on ice for 7.5 min followed by shearing of isolated chromatin for 10 cycles. These conditions were used for all subsequent ChIP assays.

First, changes of gene expression with combined ChIP-qPCR analyses were performed with a specific focus on genes involved in endotoxin tolerance. In particular, the histone patterns of *TNF*, *IL6* and *IL1B* (class T genes) were compared to that of *FPR1* (class NT gene). The promoter regions (transcription start site, TSS ± 1 kb) of these genes were analyzed for enrichment of H3K4me3, acetylation of H3K27 (H3K27ac) and global H4 acetylation (H4ac). These histone marks are considered to indicate open, transcriptionally active chromatin (Bernstein *et al.* 2005, Santos-Rosa *et al.* 2002, Schneider *et al.* 2004). For specific localization of primer pairs used, please go to *Appendix* section **5.2**. H3K4me3 and H4ac were already analyzed in murine macrophages and showed distinct patterns in LPS-induced chromatin modifications (Foster *et al.* 2007, Yan *et al.* 2012). Besides, H3K27ac is an additional marker for active promoters and enhancers (Creyghton *et al.* 2010, Hawkins *et al.* 2011, Rada-Iglesias *et al.* 2011).
The induction of *TNF*, *IL6* and *IL1B* mRNA expression was diminished in tolerant human monocytes stimulated with LPS (T+L), whereas *FPR1* showed an even higher mRNA expression compared to naïve monocytes treated with LPS (N+L, **Fig. 2-5** B). Consistent with the expression pattern, the *FPR1* gene showed re-acetylation of H4 and an increase in H3K4me3 and H3K27ac in tolerant cells re-stimulated with LPS (T+L). Interestingly, the histone pattern of the *IL6* and *IL1B* genes resembled that of *FPR1*. However, the induction of activating histone marks in the promoter/TSS regions of *IL6* and *IL1B* did not correlate with their reduced gene expression in tolerant cells (**Fig. 2-5** C). By contrast, *TNF* showed a different histone pattern in endotoxin tolerance. Most strikingly, *TNF* showed a reduced re-acetylation of H4 and H3K27 in tolerant cells re-treated with LPS (in **Fig. 2-5** C), which mirrored its reduced expression capacity in human tolerant monocytes (in **Fig. 2-5** B).

Additionally to ChIP-qPCR analyses, ChIP-Seq was performed. This approach allowed an objective analysis of histone marks without focusing on specific gene regions (*e.g.* promoter/TSS region). Representative binding profiles of H3K27ac and H4ac within the *FPR1*, *IL6*, *IL1B* and *TNF* genes are depicted in **Fig. 2-5** D. Analyses by ChIP-Seq confirmed that the *FPR1* gene showed higher enrichment of particularly H3K27ac in tolerant monocytes re-stimulated with LPS (T+L) compared to naïve ones (N). But again, and in contrast to the publication of Foster *et al.* (2007) that demonstrated a distinct chromatin pattern associated

with gene silencing in class T genes, the *IL6* and *IL1B* genes were linked with activating histone marks even in tolerant monocytes which was best observed by comparison of N with T+L. The genomic region of *TNF* in tolerant cells treated with LPS (T+L), however, was associated with restricted acetylation of H3K27 and H4 comparable to naïve monocytes (N).

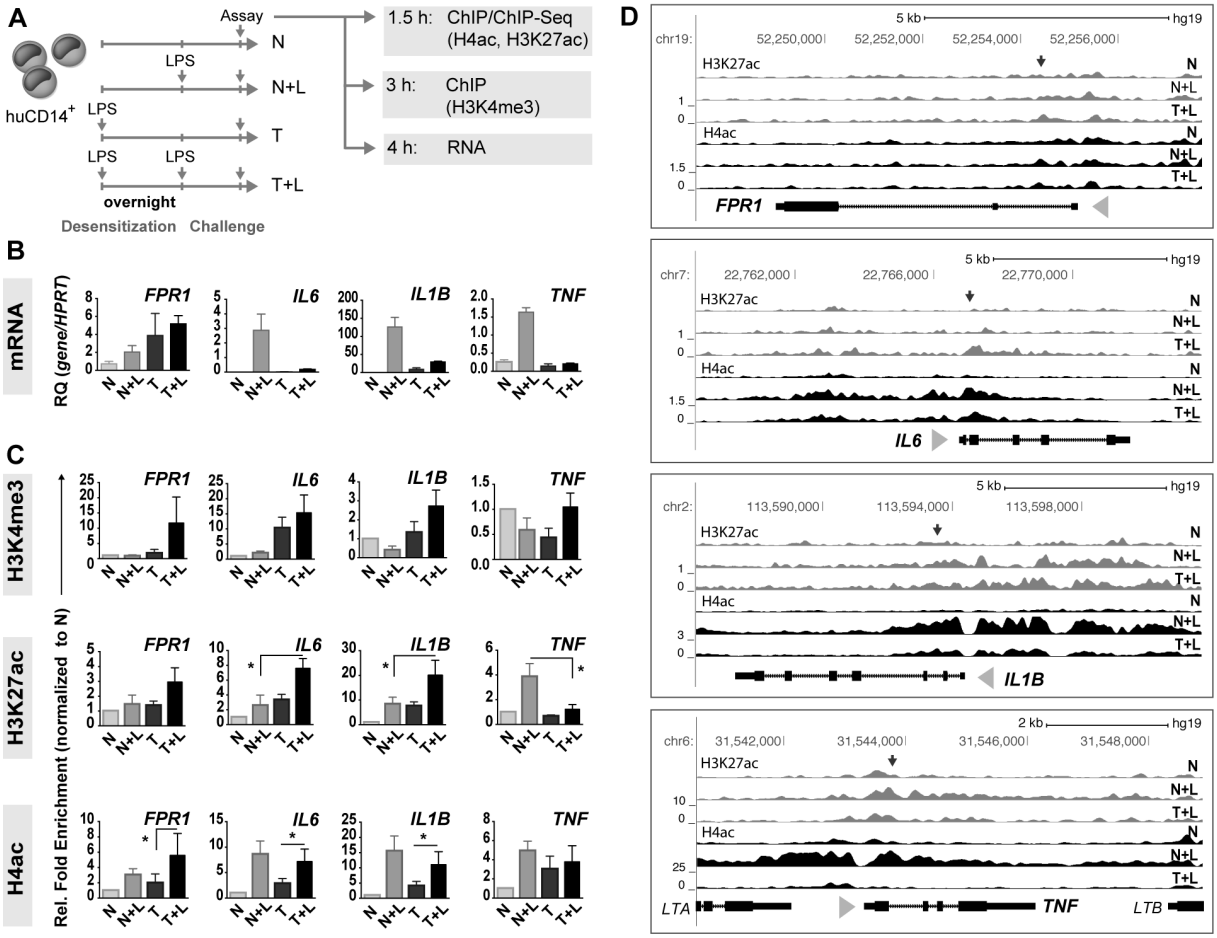

Fig. 2-5: The class T genes *IL6* and *IL1B* possess similar histone patterns like the class NT gene *FPR1*. (A) Human naïve and tolerant monocytes (tolerized with 100 ng/ml LPS) were stimulated with 100 ng/ml LPS for the indicated time points. (B) Cells were subjected to mRNA expression analysis. Depicted are mean values ± SEM of 3 independent experiments as relative quantification (RQ). (C) ChIP-qPCR analyses were performed at 3 h (H3K4me3) or 1.5 h (H4ac and H3K27ac). Results are shown as mean ± SEM of ≥ 5 independent experiments (statistical analysis between two samples was performed by Wilcoxon matched-pairs signed-rank test, *p ≤ 0.05). (D) ChIP-Seq analysis: H3K27ac and H4ac binding profiles within the *FPR1*, *IL6*, *IL1B* and *TNF* genomic regions are displayed in the UCSC Genome Browser. Arrows indicate positions of primer pairs for ChIP-qPCR analysis and triangles show transcription direction.

Taken together, the analyses of the transcription-linked histone modifications H3K4me3, H3K27ac and H4ac demonstrated that the reduced mRNA expression capacity of the class T genes *IL1B*, *IL6* and *TNF* were only partially reflected by their histone pattern indicating that other mechanisms might be involved in LPS tolerization.

2.1.3 Analysis of Tolerant Murine Macrophages by Histone Modifications

Many endotoxin tolerance studies were investigated in mice. To rule out species-specific differences between humans and mice regarding histone modifications, murine macrophages were generated from bone marrow cells of C57BL/6 mice and subjected to endotoxin tolerance followed by ChIP-qPCR analysis using antibodies directed towards the activating histone marks H4ac and H3K4me3 (**Fig. 2-6** A).

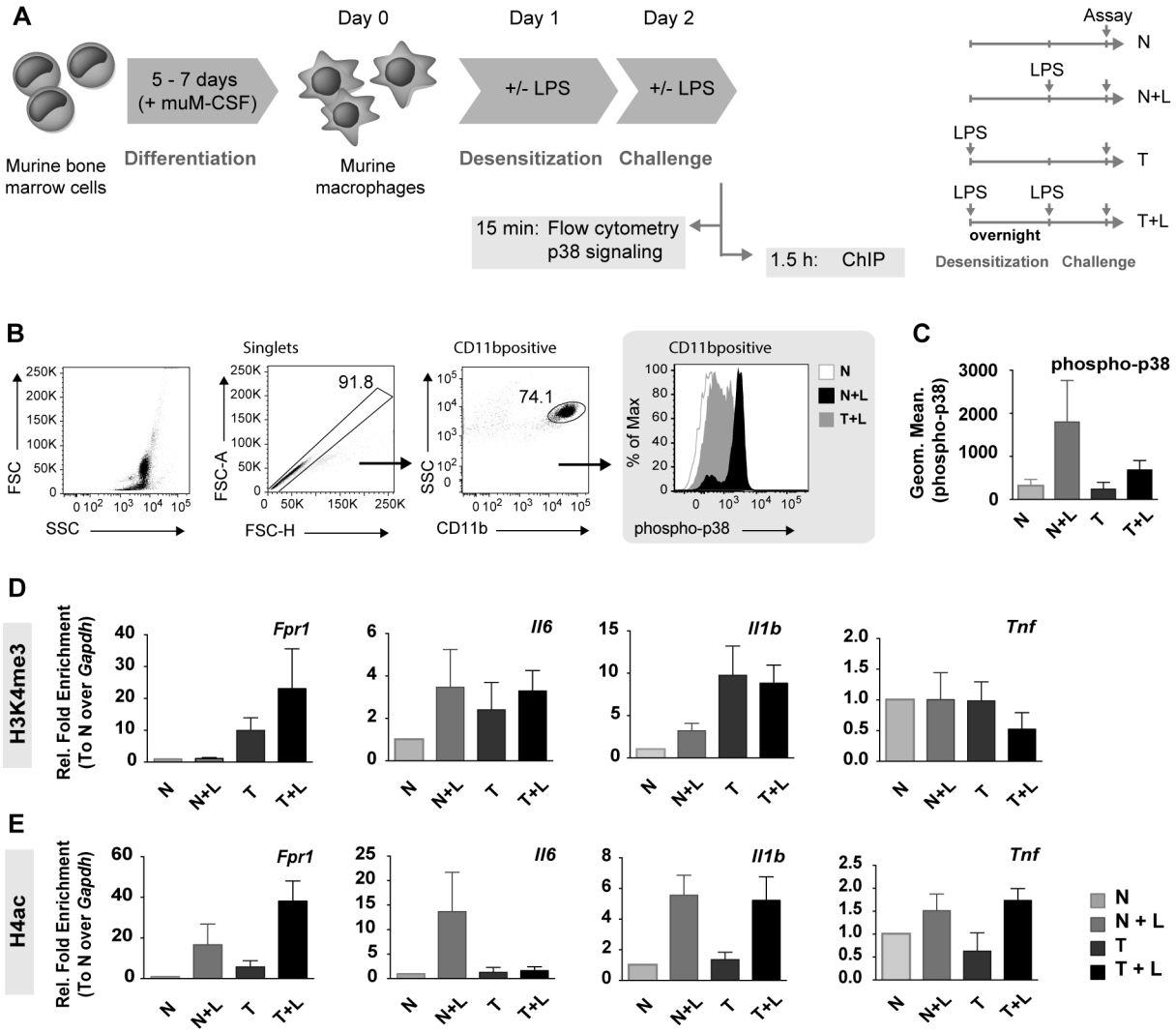

Fig. 2-6: The murine *Il6* and *Tnf* genes possess different histone patterns in endotoxin tolerance compared to the human *IL6* and *TNF* genes. (A) Murine macrophages were generated from bone marrow cells of C57BL/6 mice by cultivation of cells with murine M-CSF (muM-CSF) for 5 to 7 days. Differentiated macrophages were subjected to endotoxin tolerance. Cells were either tolerized with 100 ng/ml LPS overnight or left untreated. Subsequently, naïve and tolerant murine macrophages were stimulated with 100 ng/ml LPS for the indicated time points. (B) Gating strategy for signaling analysis of p38 activation: Naïve and tolerant macrophages were stimulated with 100 ng/ml LPS for 15 min and p38 phosphorylation was analyzed by BD PhosFlow following flow cytometric analysis. (C) Summary of p38 signaling in murine macrophages. (D and E) ChIP-qPCR analyses of H3K4me3 (D) and H4ac (E). Due to high variation, a general normalization to *Gapdh* was performed. Data represent 3 (H4ac) or 4 (H3K4me3) independent experiments with mean values ± SEM shown.

Similar to human monocytes, the signaling capacity was diminished in tolerant murine macrophages (**Fig. 2-6** B and C). However, the dynamic of histone modifications of murine macrophages and human monocytes were partially conflicting between these two species. The class T gene *Il1b* and the class NT gene *Fpr1* showed enrichment of H3K4me3 and H4ac in tolerant murine macrophages (**Fig. 2-6** D and E). In contrast to human monocytes, the re-acetylation of H4 within the *Il6* promoter in tolerant murine macrophages re-stimulated with LPS was diminished. Strikingly, acetylation of the *Tnf* gene was still inducible in murine macrophages (**Fig. 2-6** E), which was not observed in human monocytes (**Fig. 2-5** C).

The analyses of human and murine cells by changes in histone modifications indicated that differences in the regulation of histone marks exist between the species. This would imply that endotoxin tolerance might be partially mediated by different mechanisms in humans versus mice.

2.1.4 Analysis of Signaling Strength on Histone Modifications

The histone pattern observed in human monocytes did not correlate with the expression of the analyzed genes. Whereas the *TNF* gene showed diminished re-acetylation of H4 and H3K27 which mirrored its reduced gene expression in tolerant human monocytes, the class T genes *IL6* and *IL1B* contradictorily showed an increase in activating histone modifications (as seen in **Fig. 2-5**).

To investigate the effect of signaling strength on the induction of activating histone modifications in endotoxin tolerance, the magnitude of signaling and capability of tolerant cells to activate p38 phosphorylation was analyzed in a more defined experimental setup. Therefore, human primary monocytes were tolerized overnight by two different dosages of LPS before re-stimulation (**Fig. 2-7** A). Compared to the naïve control group, tolerization of monocytes with low-dose LPS (T1, 1 ng/ml) led only to a slightly reduced, but clearly detectable, signaling capacity of tolerant cells, whereas p38 phosphorylation was nearly abolished in monocytes tolerized with high-dose LPS (T100, 100 ng/ml; **Fig. 2-7** B).

Monocytes tolerized with different dosages of LPS were subjected to ChIP-qPCR assays for analyses of H3K27ac and H4ac in endotoxin tolerance. Parallel gene expression analyses showed that the mRNA expression of the class NT gene *FPR1* was higher in low- and high-dose tolerized monocytes (**Fig. 2-7** C), whereas the cytokine production of the class T genes encoding for IL-6, IL-1β (*intermediately tolerizable*), TNF and CXCL10/IP-10 (*highly tolerizable*) was reduced (**Fig. 2-7** D). In particular, IL-6 followed a signaling-dependent expression, whereas TNF and CXCL10/IP-10 production was basically already tolerized in low-dose treated monocytes. Besides, CXCL8/IL-8 was again highly inducible even in high-dose tolerized monocytes reaching an expression level similar to naïve cells stimulated with LPS (**Fig. 2-7** D).

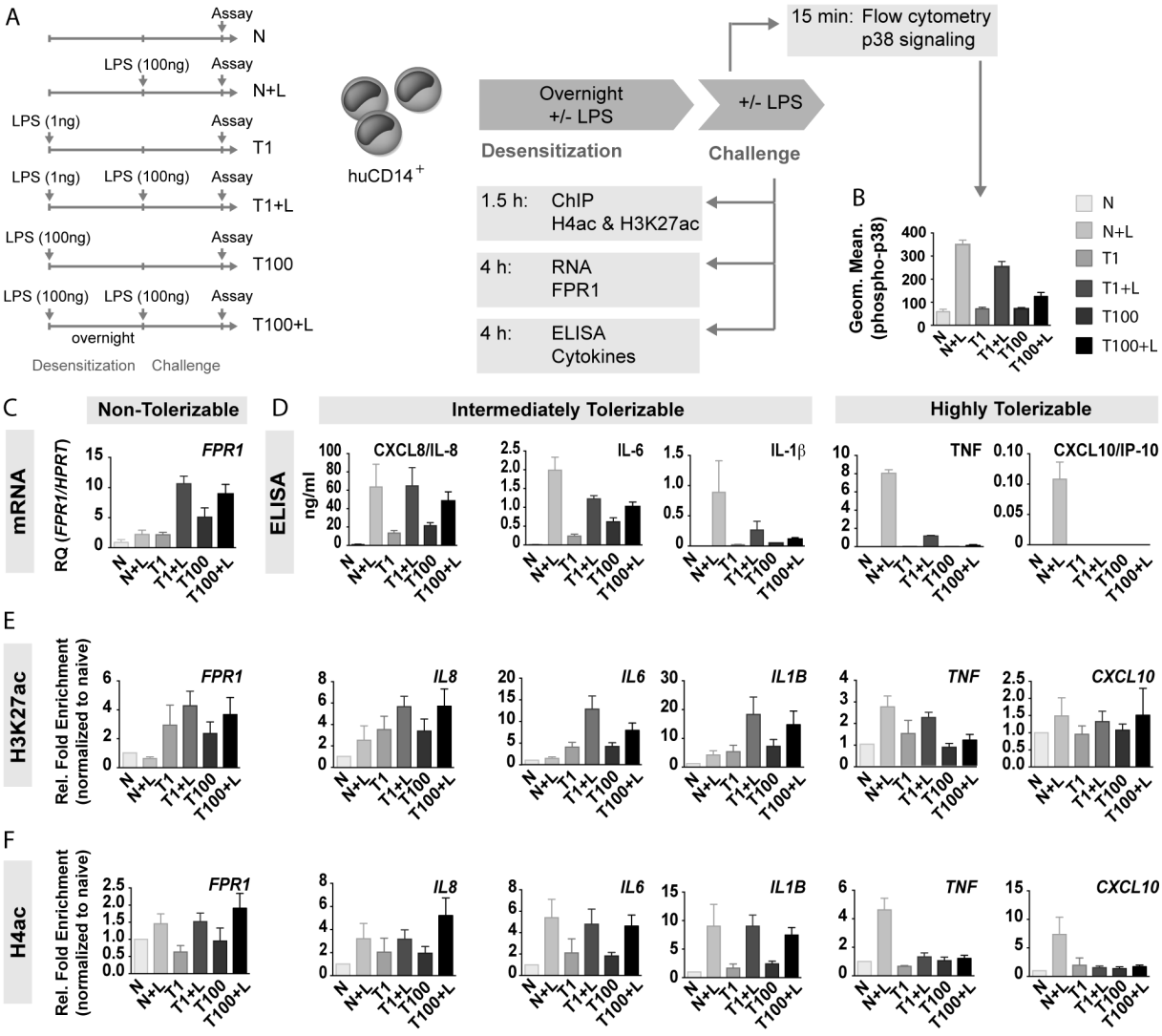

Fig. 2-7: Tolerization of human monocytes with two different LPS dosages distinctly induces activating histone modifications in *intermediately tolerizable* and *highly tolerizable genes*. (A) Experimental setup: Human monocytes were tolerized overnight with 1 ng/ml LPS (T1) or 100 ng/ml LPS (T100). Untreated cells served as naïve (N) control. Naïve (N) and tolerant cells (T1, T100) were washed, given fresh media and stimulated with 100 ng/ml LPS for the indicated time points. (B) Signaling in monocytes was analyzed by flow cytometric analysis of p38 phosphorylation after 15 min stimulation with LPS. Results are shown for 5 independent experiments. (C) Cells were lysed and mRNA expression of *FPR1* was determined from total RNA. Data are shown for 3 independent experiments (mean ± SEM). (D) Monocytes (N, T1, T100) were stimulated with LPS for 4 h. For analysis of IL-1β secretion, ATP was added 15 min before the end of stimulation. Supernatants were collected and analyzed for cytokine secretion by ELISA. (E, F) Cells were subjected to ChIP-qPCR for analyses of H3K27ac (E) and H4ac (F). Results are depicted as mean values ± SEM of 4-5 independent experiments.

In comparison to the naïve control group, LPS treatment of low- and high-dose tolerized monocytes induced acetylation of H3K27 in the *FPR1* gene (class NT gene), but also in *IL8*, *IL6* and *IL1B* (class T genes), with the highest induction in the lower LPS dosage (**Fig. 2-7** E). Moreover, these genes showed re-acetylation of H4 even in tolerant monocytes (**Fig. 2-7** F). By contrast, H3K27ac was reduced in *TNF* and *CXCL10* (class T genes) in

tolerant monocytes (**Fig. 2-7** E). Most strikingly, re-acetylation of H4 in the *TNF* and *CXCL10* genes was basically lost in high-dose, but also low-dose, tolerized monocytes (**Fig. 2-7** F), implying either a signaling-independent mechanism or a different sensitivity towards signaling strength, where already minimally reduced p38 activation leads to inhibition of TNF and CXCL10/IP-10 production.

The examination of signaling strength and comparative analyses of inductions of activating histone modifications in endotoxin tolerance provided a deeper insight into the regulation of class T genes. CXCL8/IL-8, which is considered to belong to the class T genes (Allantaz-Frager *et al.* 2013), was again highly re-inducible in tolerant monocytes and the encoding gene displayed a similar histone pattern compared to the class NT gene *FPR1*. Moreover, IL-6 and presumably IL-1β were signaling-dependently produced and the encoding genes showed high enrichment of positive histone modifications even in tolerant monocytes. The data indicates a more signaling-mediated tolerization of these genes. The *TNF* and *CXCL10* genes, however, showed an absence in their re-induction of activating histone marks which was mostly independent of p38 signaling strength in tolerant monocytes. The data further confirmed the results obtained by multiplexed quantification of cytokines in **Fig. 2-3** and the sub-grouping of class T genes in endotoxin tolerance. Inhibition of gene expression of *highly tolerizable genes* like *TNF* and *CXCL10* might presumably be driven by epigenetic modifications, whereas tolerization of *intermediately tolerizable genes* like *IL6* and probably *IL1B* is signaling-dependent. Notably, as CXCL8/IL-8 production possessed high induction capacity even in tolerant monocytes, the question arises as to whether the encoding gene might be a sub-group of class NT genes.
Finally, previous work from a former PhD student showed that tolerization with low-dose LPS was mainly mediated by IL-10, as blocking of IL-10 during endotoxin tolerance induction could reverse LPS-tolerization. In contrast, tolerization with a high dose of LPS was basically mediated by reduction in signaling transduction (Krüger 2009). This implies that tolerization of *intermediately tolerizable genes* might be potentially mediated by signaling events that involve IL-10.

2.1.5 Analysis of Endotoxin Tolerance in High-Dose Tolerized Human Monocytes

Comparative analyses of signaling strength implicated a discriminative role of signaling in the tolerization of specific class T genes (**Fig. 2-7)**. To further investigate the possible impact of signaling on the limited expression of the class T genes encoding for TNF, IL-6 and IL-1β, the capability of LPS to induce p38 phosphorylation in tolerant monocytes was further analyzed in detail in high-dose tolerized cells (100 ng/ml LPS). Expression of these pro-inflammatory cytokines in comparison to FPR1 was analyzed by flow cytometry.

Gating strategies for extracellular analysis of FPR1 and intracellular cytokine production of TNF, IL-6 and IL-1β are depicted in **Fig. 2-8** A and B, respectively.

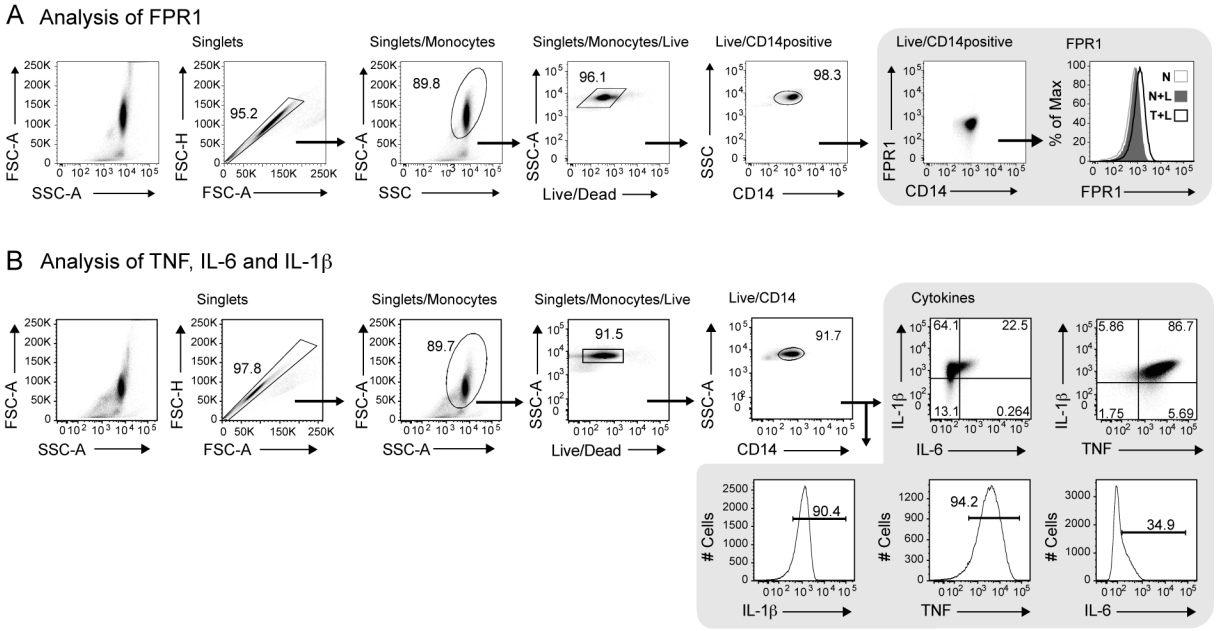

Fig. 2-8: Gating strategies for analyses of the receptor FPR1 and the cytokines TNF, IL-6 and IL1β by flow cytometry. Cells were first gated for singlets (FSC-H vs. FSC-A) followed by the discrimination of live cells from dead ones. CD14-positive monocytes were further investigated for (A) FPR1 expression on the cell surface or (B) intracellular cytokine production of TNF, IL-6 and IL-1β.

Human monocytes were subjected to endotoxin tolerance (**Fig. 2-9** A) and the samples were separated according to their p38 induction in tolerant cells (**Fig. 2-9** B-E and **Fig. 2-9** F-I, respectively). Dependent on the blood donor, high-dose tolerized monocytes (100 ng/ml LPS) showed either a complete loss (**Fig. 2-9** B) or a diminished induction of p38 phosphorylation compared to naïve monocytes treated with LPS (**Fig. 2-9** F). In parallel, production of TNF, IL-6 and IL-1β (class T genes) in relation to FPR1 (class NT gene) was analyzed by flow cytometry for the same samples (**Fig. 2-9** C-E and **Fig. 2-9** G-I, respectively).

Differences in signaling had no effect on FPR1 surface expression (**Fig. 2-9** C and G). Tolerant monocytes, which were completely incapable of induction of p38 phosphorylation (**Fig. 2-9** B), showed diminished IL-6 and IL-1β production (**Fig. 2-9** D). In contrast, normal expression of IL-6 and IL-1β was observed in tolerant cells treated with LPS (**Fig. 2-9** H) that were able to generate reduced, but detectable, p38 signaling (**Fig. 2-9** F). TNF expression, however, was almost not inducible in tolerant monocytes independent of signaling strength (**Fig. 2-9** D and H). Representative dot plots of flow cytometric analysis for each signaling condition are depicted in **Fig. 2-9** E and I, respectively.

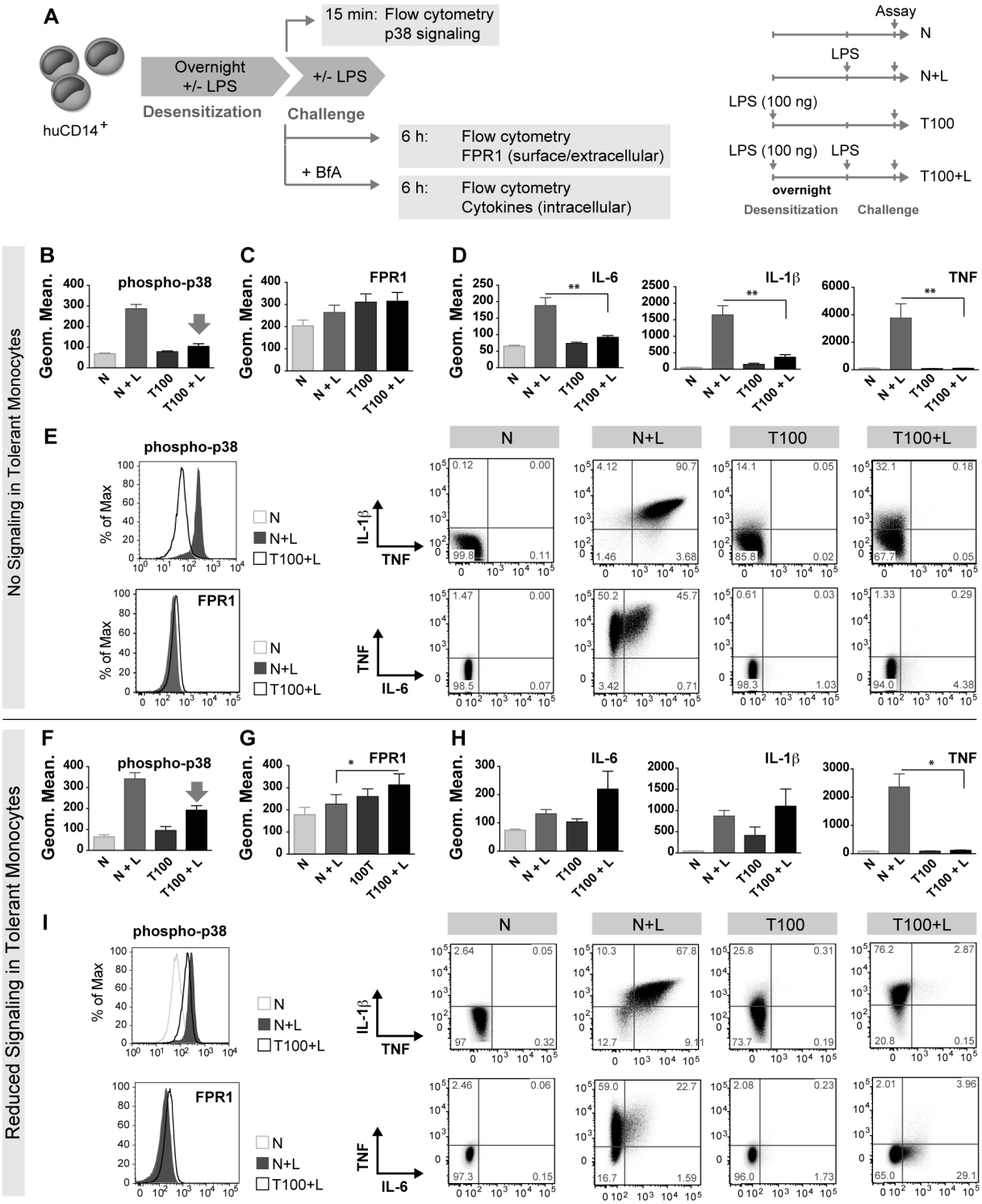

Fig. 2-9: Production of IL-6 and IL-1β is dependent on signaling strength in high-dose tolerized human monocytes. (A) Human naïve and tolerant monocytes (tolerized with 100 ng/ml LPS overnight) were stimulated with LPS for the indicated time points and subjected to parallel investigation of p38 signaling (B and F), FPR1 surface expression (C and G) and cytokine production (D and H) by flow cytometry. For analysis of intracellular cytokine production of TNF, IL-6 and IL-1β, monocytes were treated in the presence of Brefeldin A (BfA). Analyses of FPR1, TNF, IL-6 and IL-1β are depicted whether the tolerant monocytes showed either abolished (B to E) or reduced signaling in tolerant human monocytes (F to I). (E & I) Representative dot plots for both signaling conditions are shown. Depicted are mean values ± SEM of 6 (reduced signaling) or 8 (no signaling) independent experiments. Statistical analysis between two groups was performed by Wilcoxon matched-pairs signed-rank test (*p ≤ 0.05, **p ≤ 0.01).

Signaling dependent expression of IL-6 in high-dose tolerized human monocytes was also validated by ELISA (**Fig. 2-10** A), as detection by flow cytometry was not optimal (see **Fig. 2-9**). Again, reduced production of IL-6 was only observed in LPS tolerant cells, as long as p38 signaling was abolished (**Fig. 2-10** B and C), whereas detectable signaling in tolerant monocytes (**Fig. 2-10** D) had no impact on tolerization of IL-6 production (**Fig. 2-10** E). By contrast, TNF tolerization was independent of signaling (**Fig. 2-10** C and E).

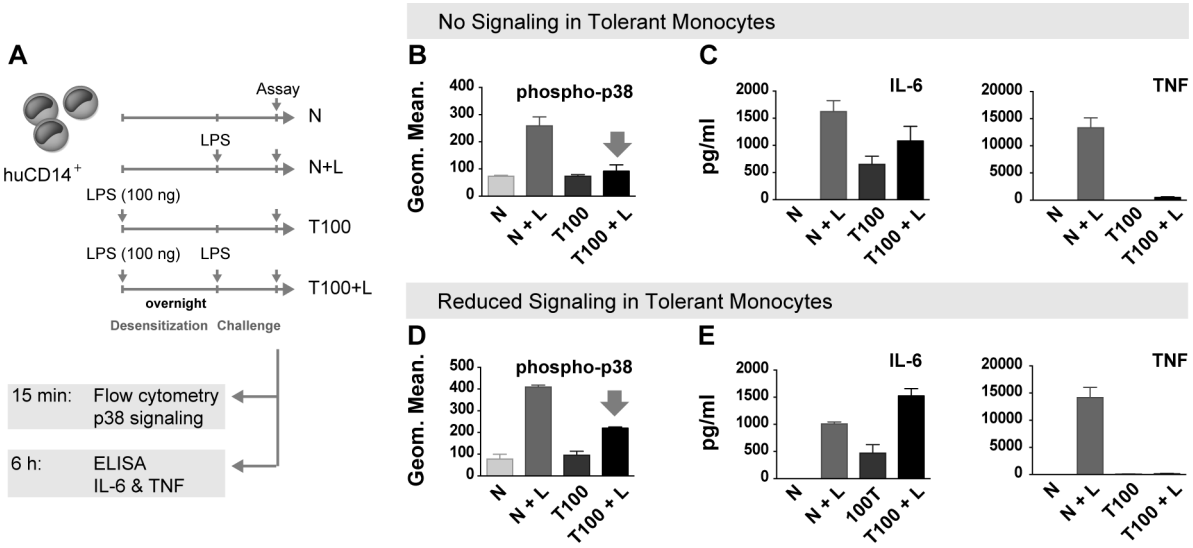

Fig. 2-10: Analysis of IL-6 and TNF production in high-dose tolerized human monocytes depending on signaling strength. (A) Human naïve and tolerant monocytes (tolerized with 100 ng/ml LPS overnight) were stimulated with LPS (100 ng/ml) for the indicated time points. (B, D) Signaling of p38 was investigated by flow cytometry. (C, E) In parallel, cell supernatant was subjected to ELISA for analysis of IL-6 and TNF production. Depicted are mean values ± SEM of 3 (reduced signaling) or 4 (no signaling) independent experiments.

In summary, analyses of high-dose LPS tolerization on TNF, IL-6 and IL-1β expression dependent on signaling strength further implicated that the encoding genes might potentially be regulated by different tolerance mechanisms. Whereas *TNF* tolerization might be more strongly regulated by epigenetic changes *e.g.* differences in activating histone modifications, tolerance induction of the *IL6* and *IL1B* genes seemed to be mainly mediated by reduced signaling strength in endotoxin tolerance, which is also reflected by their *'positive'* histone pattern (see **Fig. 2-5** and **Fig. 2-7**).

2.1.6 Analysis of Repressive Histone Marks in Endotoxin Tolerance

In the experiments described thus far, epigenetic changes were analyzed by modifications in activating histone marks. However, tolerization of class T genes might be instead regulated by enrichment in repressive histone marks than by suppressing activating marks. Therefore, ChIP assays with a focus on the repressive histone modifications H3K9me2, H3K27me3 and H4K20me3 followed by sequencing (ChIP-Seq) were performed (**Fig. 2-11** A). This approach was chosen as repressive histone marks cover repressed genes relatively homogeneously (Kooistra & Helin 2012).
H3K9me2 was already shown to be enriched in the promoter regions of *IL1B* and *TNF* in endotoxin-tolerant THP-1 cells (El Gazzar *et al.* 2009, El Gazzar *et al.* 2008) and H4K20me3 seemed to be involved as a repression checkpoint in LPS/TLR4-mediated signaling (Stender *et al.* 2012). Additionally, H3K27me3 is a well characterized repressive mark for down regulation of gene transcription and has an important role in cell development and differentiation (Barski *et al.* 2007, Boyer *et al.* 2006, Bracken *et al.* 2006).

Analyses of the histone marks H3K9me2, H3K27me3 and H4K20me3 by ChIP-Seq indicated that a general enrichment of these repressive marks in genes of pro-inflammatory cytokines was not detected in endotoxin-tolerant human monocytes (**Fig. 2-11**), which could have explained their reduced expression capacity. No significant differences in repressive histone marks could be observed for the *TNF*, *IL8* and *CXCL10* genes in human monocytes. Strikingly, *IL6* even displayed a reduction of the repressive mark H3K27me3 in tolerant cells (T+L) compared to naïve monocytes treated with LPS (N+L) (**Fig. 2-11** B), which is inversely correlated with its gene repression. Thus, it has to be further investigated how these modifications really affect expression of the analyzed genes or whether other, yet unidentified, repressive histone marks play a role *e.g.* SUMOylation (Berger 2007, Nathan *et al.* 2006, Shiio & Eisenman 2003).
By contrast, *IL1B* showed an increase in H3K9me2 circa 7 kb upstream from its TSS in tolerant monocytes. Moreover, ChIP-seq analyses revealed an increase in H4K20me3 near the TSS of *IL1A* and *IIL1R1* (encodes for the IL-1 receptor type I), which is involved in IL-1α and IL-1β signaling (**Fig. 2-11** C) (Weber *et al.* 2010). The induction of these repressive marks might have a specific impact on gene silencing of *IL1*-related genomic regions.

Again, analyses of repressive histone modifications could not identify a general, inhibiting histone pattern that might clarify the phenomenon by which endotoxin tolerance selectively tolerizes a specific set of genes (class T), whereas others are still inducible (class NT). Genome-wide analyses of ChIP-Seq data are illustrated in the *Results section* **2.2.1**, see below.

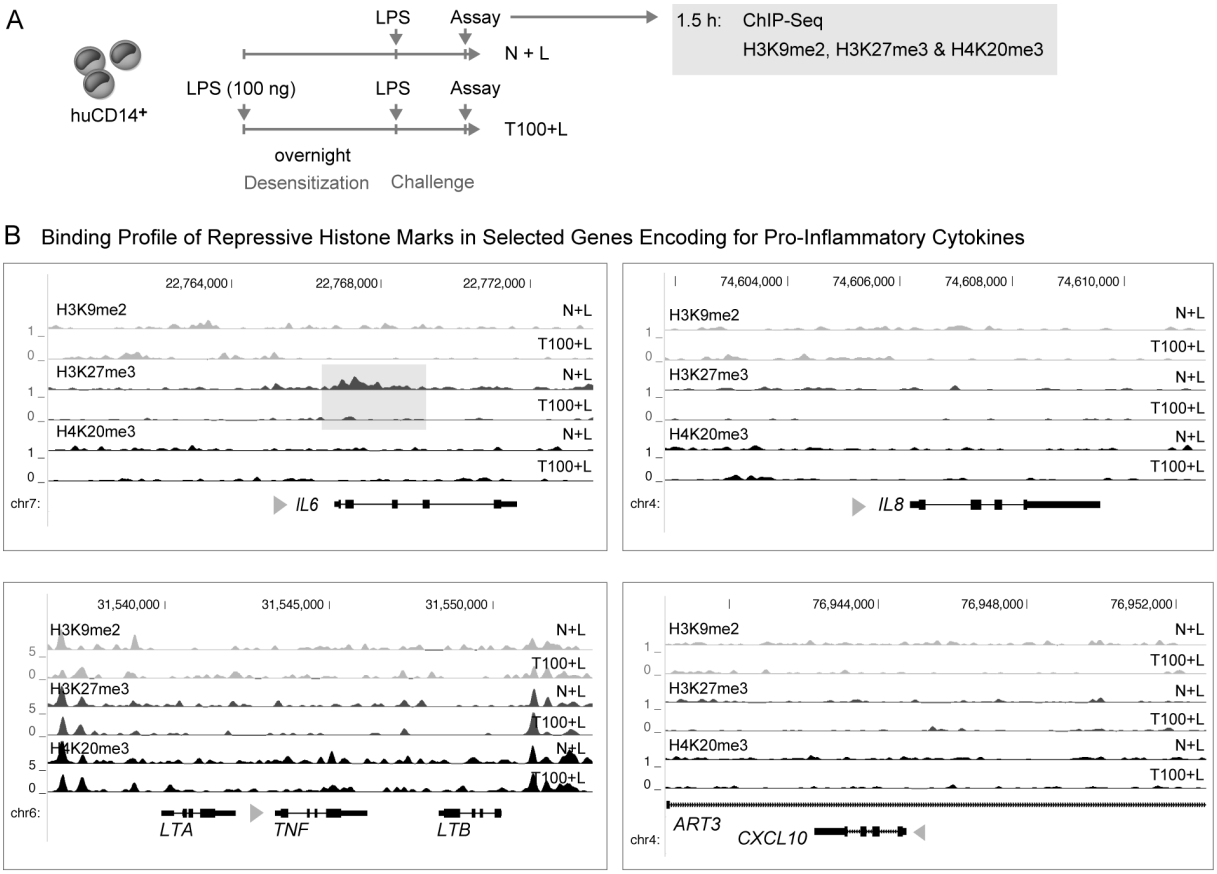

Fig. 2-11: Endotoxin-tolerant monocytes showed no common enrichment in the repressive histone modifications H3K9me2, H4K20me3 and H3K27me3 in selected genes. (A) Experimental setup: Human monocytes were tolerized overnight with 100 ng/ml LPS (T100). Untreated cells served as the naïve (N) control. Naïve (N) and tolerant cells (T100) were washed, given fresh media and stimulated with 100 ng/ml LPS for 1.5 h. (B and C) Cells were subjected to ChIP-Seq using antibodies directed towards H3K9me2, H3K27me3 and H4K20me3 to identify enrichment in repressive histone marks. Binding profiles of ChIP-Seq data within pro-inflammatory gene loci are displayed in the UCSC Genome Browser. Grey shaded boxes indicate significant changes in enrichment of repressive histone modifications identified by the peak caller SICER (for more details, see the *Results section* **2.2.1** below). Triangles indicate transcription direction.

2.1.7 DNA Methylation Analyses within the Promoter Regions of *IL6* and *TNF*

Finally, epigenetic repression of gene expression can also occur by methylation of cytosine bases at CpGs (Bird & Wolffe 1999). To elucidate a potential role of DNA methylation in tolerization of the pro-inflammatory cytokines IL-6 and TNF, the promoter regions of the encoding genes were analyzed by bisulfite conversion. Therefore, human monocytes were subjected to endotoxin tolerance and genomic DNA was isolated. Subsequent bisulfite conversion mediated deamination of unmethylated cytosine to uracil, whereas methylated cytosine remained unchanged. Following promoter-specific PCR, uracil was exchanged with tyrosine and PCR products were subjected to sequencing. Resulting sequences were compared to the original unconverted DNA to reveal the methylation status of the respective CpG sites.

The promoter region of the human *IL6* gene from -1200 bp to +27 bp contained 22 CpG motifs (Nile *et al.* 2008) and the *TNF* promoter region from -360 to +50 bp covered 12 CpGs (Campion *et al.* 2009) (**Fig. 2-12**).

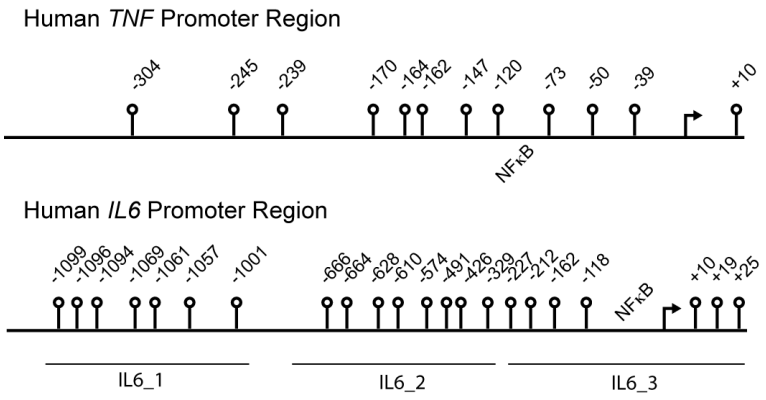

Fig. 2-12: Schematic representation of CpG motifs within the proximal promoter regions of the human *TNF* and *IL6* genes analyzed by bisulfite sequencing (adapted from Campion *et al.* (2009) and Nile *et al.* (2008)). The CpG dinucleotides that can be potentially methylated are represented by vertical lines with open circles, and their location relative to the transcription start site is indicated. Bisulfite-modified DNA was amplified by PCR following direct sequencing. The upstream region of the *IL6* gene was split into three amplicon sections of ca. 400 bp that are indicated as IL6_1, IL6_2 and IL6_3.

The DNA methylation status of the *TNF* and *IL6* promoter regions was compared in human monocytes subjected to endotoxin tolerance (**Fig. 2-13** A). As illustrated in **Fig. 2-13** B and C, naïve and tolerant primary monocytes treated with LPS showed no significant changes in *de novo* DNA methylation. Furthermore, no alterations in percentages of total DNA methylation could be identified between the different amplicons and conditions (**Fig. 2-13** D).

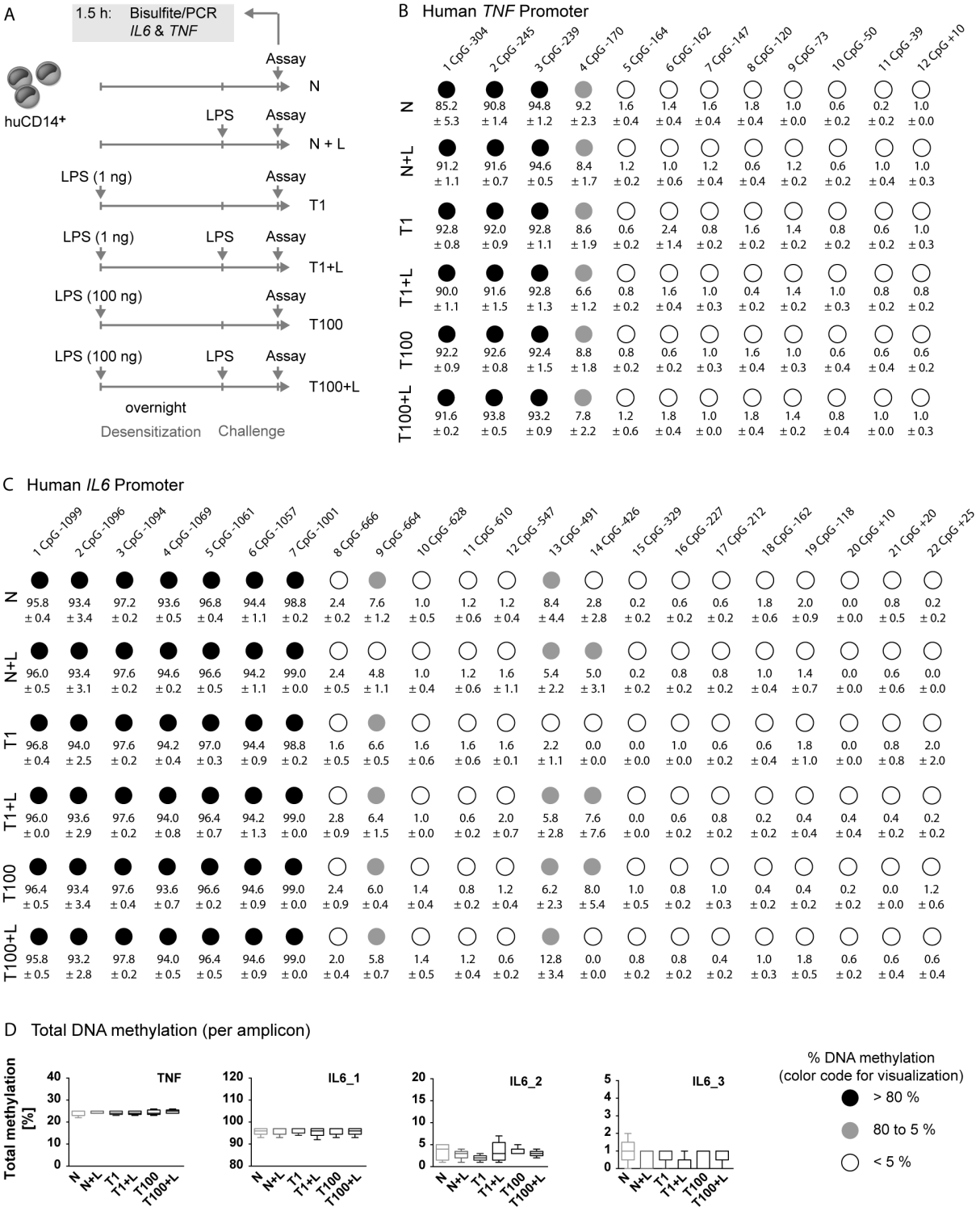

Fig. 2-13: The DNA methylation status in the *TNF* and *IL6* promoter regions is not altered by endotoxin tolerance. (A) Experimental setup: Human monocytes were tolerized overnight with 1 ng/ml LPS (T1) or 100 ng/ml LPS (T100). Untreated cells served as a naïve (N) control. Naïve (N) and tolerant cells (T1, T100) were washed, given fresh media and stimulated with 100 ng/ml LPS for 1.5 h. Isolated genomic DNA was bisulfite-treated, promoter-specifically amplified and subjected to direct sequencing. (B and C) Percentage of DNA methylation at each CpG position within the human *TNF* (B) and *IL6* (C) promoter regions is depicted as mean ± SEM of 5 independent experiments. The circle colors depict distinctly methylated regions: Black shows that more than 80 % of analyzed CpGs at that position was methylated, grey indicates methylation status between 80 to 5 % and white represents rarely methylated CpGs (below 5 %). (D) Comparison of total DNA methylation between the different samples and amplicons. The analysis was performed using the BiQ Analyzer HiMod (Becker *et al.* 2014).

The DNA methylation status was further validated by Methyl-Capture Sequencing (MethylCap-Seq). MethylCap-Seq is an approach that works similar to ChIP-Seq (Brinkman *et al.* 2010, Serre *et al.* 2010). Here, fragmented DNA is incubated with the methyl-binding domain (MBD) of proteins that can recognize methylated DNA (for more details see **4.3.9** in the *Materials & Methods* section). Enriched DNA is sequenced and binding profiles indicating methylated genomic regions can be visualized in a genome browser. MethylCap-Seq allows analysis of DNA methylation on a genome-wide scale, but potentially forfeits resolution of single methylated CpGs compared to promoter-specific bisulfite-sequencing.

As shown in **Fig. 2-14**, gene regions of *IL6* and *TNF* in naïve and tolerant human monocytes did not show a specific change in DNA methylation, which could explain the reduced expression of these pro-inflammatory cytokines in endotoxin tolerance. Binding profiles indicating localization of DNA methylation in the *FPR1*, *IL1B*, *IL8* and *CXCL10* genes can be found in the *Appendix* **5.5**. Detailed genome-wide analysis of MethylCap-Seq data is performed in **2.2.2** (see *Results* section below).

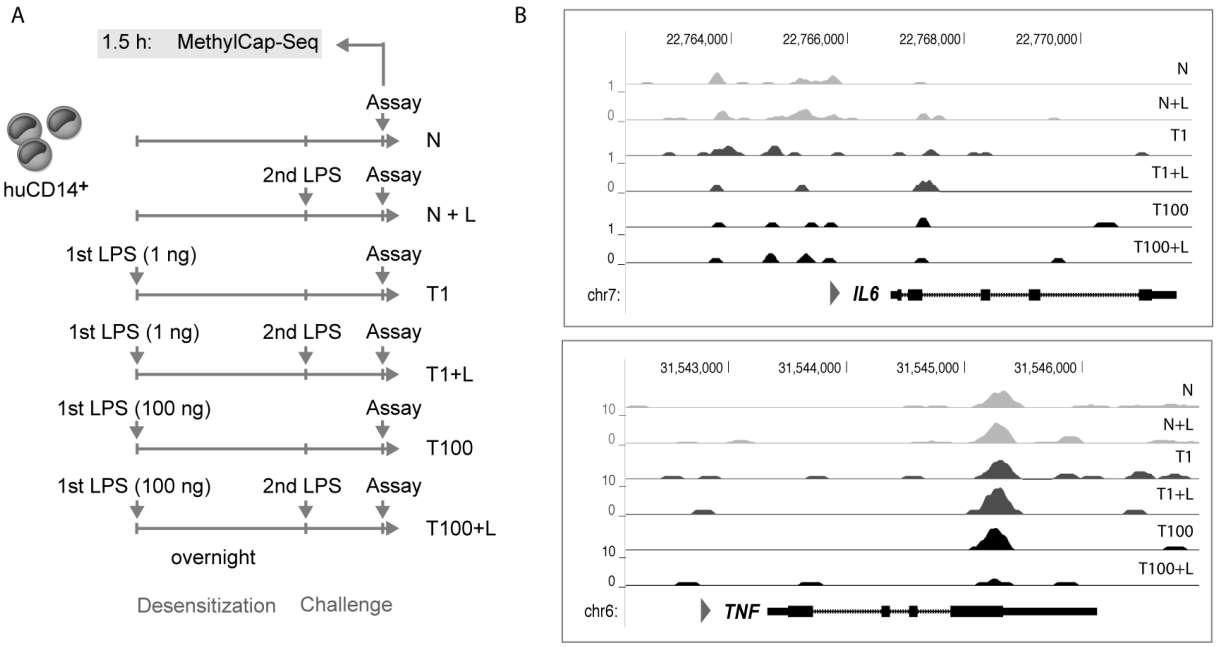

Fig. 2-14 Analysis of the *IL6* and *TNF* gene regions by MethylCap-Seq shows no change in DNA methylation. (A) Experimental setup: Human monocytes were tolerized overnight with 1 ng/ml LPS (T1) or 100 ng/ml LPS (T100). Untreated cells served as a naïve (N) control. Naïve (N) and tolerant cells (T1, T100) were washed, given fresh media and stimulated with 100 ng/ml LPS for 1.5 h. (B) Cells were subjected to MethylCap-Seq to identify enrichment in DNA methylation. Binding profiles of MBD-protein indicating methylated DNA within the *IL6* and *TNF* gene loci are displayed in the UCSC Genome Browser.

Taken together, the results obtained by promoter-specific analysis of the *IL6* and *TNF* genes demonstrated that repression by DNA methylation might not play a role in endotoxin tolerance, which could be further confirmed by MethylCap-Seq.

To summarize the first section, analyses of single LPS-induced genes in endotoxin tolerance indicated that alterations at the chromatin level by histone modifications played a role in regulation of specific genes. However, the impact of these epigenetic changes might be different for every individual gene as the histone pattern did not always correlate with gene expression. Moreover, analysis of DNA methylation within the *IL6* and *TNF* gene loci could not implicate this modification in repression of these genes. Thus, other mechanisms involving signaling strength might play a role in endotoxin tolerance.

2.2 Genome-Wide Analysis of Epigenetic Changes in Endotoxin Tolerance

2.2.1 Global Analyses of Histone Modifications by ChIP-Seq

2.2.1.a Characterization of Enriched Regions (Peaks)

ChIP-qPCR provides a limited picture of the regulation of histone modification during LPS tolerization as it focuses only on single immune-relevant genes. Therefore, ChIP combined with next generation sequencing (ChIP-seq) was performed to provide a global overview of changes in histone modifications in endotoxin tolerance throughout the genome allowing the identification of histone modifications within other genes such as transcriptional regulators, and other mechanisms responsible for endotoxin tolerization.

Addressing the assumption that tolerant genes remain repressed, ChIP-Seq experiments focused on the comparison of the following two conditions: (1) Naïve human monocytes treated with LPS (N+L) and (2) high-dose tolerized cells re-stimulated with LPS (T100+L). ChIP assays were performed using antibodies directed to the activating histone marks H4ac and H3K27ac, and the repressive marks H3K9me2, H3K27me3 and H4K20me3.

To identify significant peaks, ChIP-Seq assays were analyzed by the peak calling algorithm SICER, which was developed to specifically identify enriched genomic regions generated by ChIP-seq experiments analyzing histone modifications (Zang *et al.* 2009). A general overview about the significant peaks called by SICER for each histone mark in the two experimental conditions (N+L, T100+L) is demonstrated in **Fig. 2-15**. Enriched regions individually identified within the two conditions were termed *SinglePeaks* (**Fig. 2-15** B). Moreover, SICER provides an analysis script to identify distinct enriched genome regions by comparing one condition with another (here called *DiffPeaks*), thereby indicating differentially regulated genes or regions (**Fig. 2-15** C). Of note, both peak classes (*SinglePeaks* and *DiffPeaks*) can be identified by two separate analysis methods, thus, each peak list can be considered separately and used individually for downstream analyses.

In naïve monocytes treated with LPS (N+L), the majority of genomic regions were associated with activating histone marks, whereas tolerant cells re-stimulated with LPS (T100+L) showed enrichment in repressive histone marks (*SinglePeaks,* **Fig. 2-15** B). This effect was

even more dramatic when considering differentially enriched genomic regions. Most of the activating histone modifications, which showed at least a 2-fold change increase between the N+L versus T100+L conditions, were counted in naïve cells stimulated with LPS (N+L). This indicates that in tolerant cells, the majority of H4ac and/or H3K27ac in these genomic regions were reduced or even lost during LPS tolerization. Here, the lack of re-induction in the transcription-linked acetylation marks at H4 and H3K27 might be due to the reduced signaling capacity in high-dose tolerized human monocytes. Simultaneously, repressive histone modifications, in particular H3K9me2 and H4K20me3, were significantly enriched in tolerant cells challenged with LPS, indicating a global endotoxin tolerance-induced repression of genomic regions (T100+L, **Fig. 2-15** C). Notably, the histone mark H3K27me3 showed the lowest dynamic change in endotoxin tolerance.

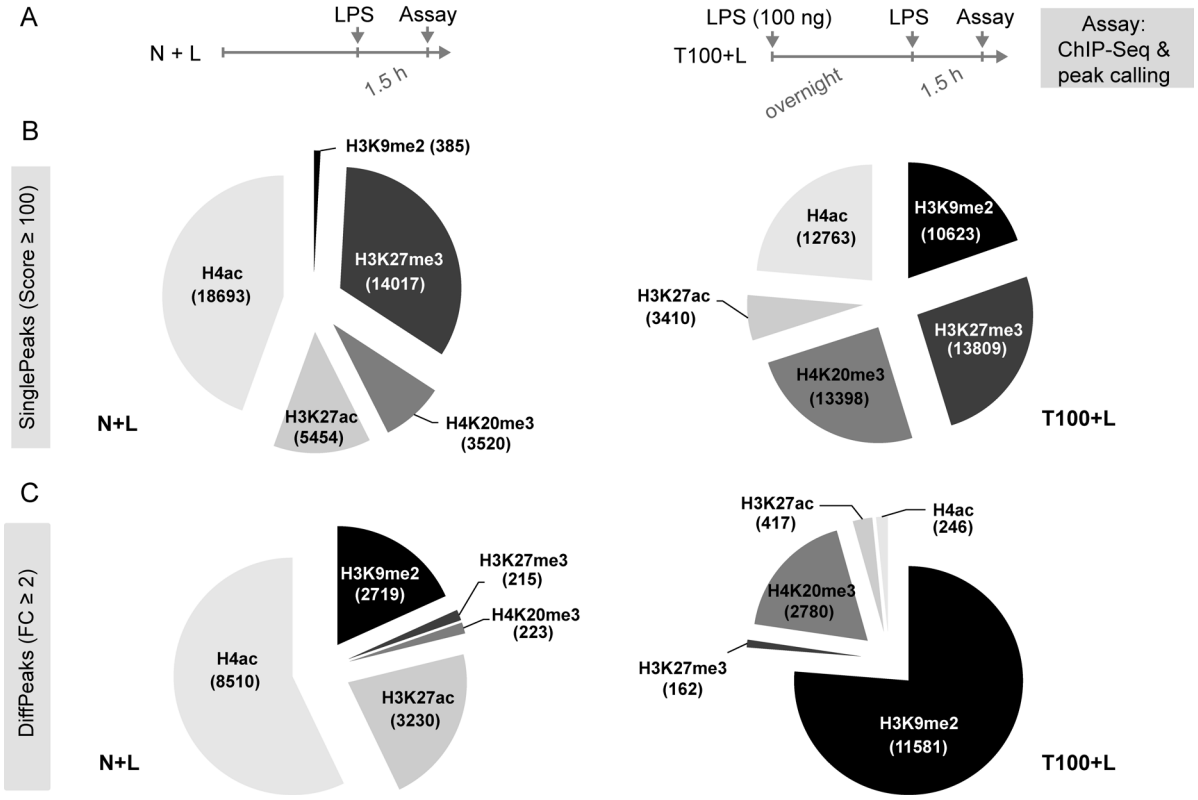

Fig. 2-15: Overview of global, histone mark-enriched genomic regions: Endotoxin tolerance induces a shift from activating to repressive histone marks. (A) Experimental setup: Naïve and tolerant human monocytes (tolerized with a high dose of LPS, 100 ng/ml) were stimulated with LPS (100 ng/ml) for 1.5 h (N+L, T+L) and subjected to ChIP-Seq analyses followed by peak calling using SICER. (B) The number of peaks with a minimum SICER score of 100 is depicted as pie charts for the activating histone modifications H3K27ac and H4ac, and for the repressive histone marks H3K9me2, H3K27me3 and H4K20me3. (C) Total numbers of differentially enriched regions (*DiffPeaks*) with a minimum fold change (FC) of 2 (*P* value of minimum 1e-6) were identified by the comparison of N+L and T100+L. Here, enriched genomic regions (peaks) were counted for one of the two conditions. It should be noted that the figure provides an overview of the number of significant peaks (enriched regions) identified by SICER independently whether peaks were potentially co-localized by different histone modifications. Moreover, the scripts for identification of *SinglePeaks* and *DiffPeaks* are distinct from each other, thus, peaks identified in one peak list do not necessarily appear in the other peak set.

Next, the localization and distribution of identified enriched regions within the given peak sets were determined. As an example, the gene body distribution of every histone mark analyzed for the condition N+L (*SinglePeaks*) is shown in **Fig. 2-16**. The histone modifications H3K27ac, H4ac and H3K27me3 were primarily localized in promoter and gene coding regions, whereas the repressive marks H3K9me2 and H4K20me3 were highly localized to intergenic regions, allowing only limited mapping to a specific gene (**Fig. 2-16** A and B).

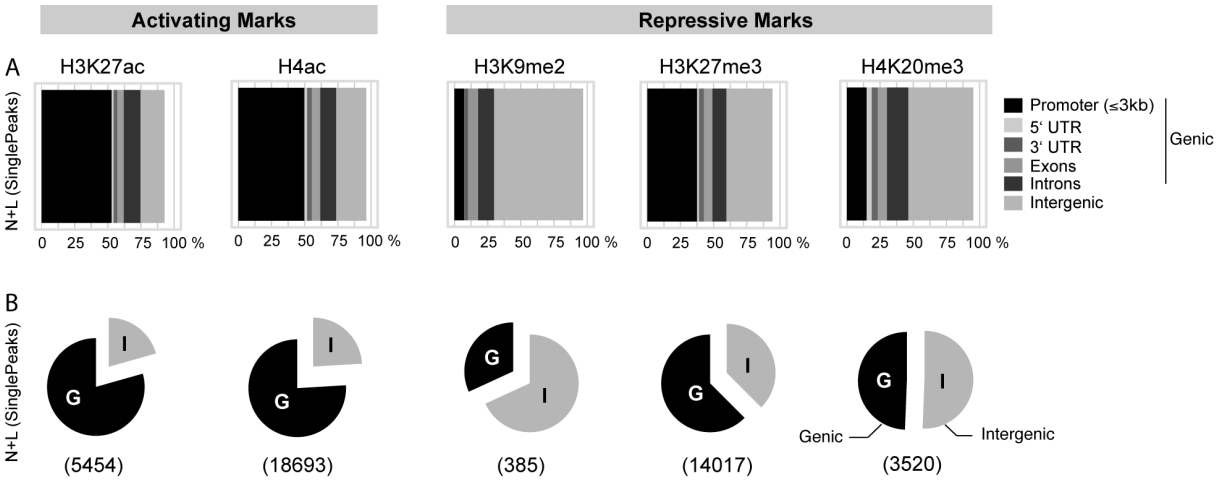

Fig. 2-16: Gene body distribution of analyzed histone modifications in N+L (*SinglePeaks*): H3K27ac, H4ac and H3K27me3 are located within gene-linked regions. (A) Bar plot representing location of peaks within the specified genomic regions. Genomic regions were divided into promoter, 5' UTR, 3' UTR, exon, intron or intergenic sections. (B) Overview of peak locations divided into genic (G) and intergenic regions (I) presented as VennPie plots, with the number in brackets representing the total count of identified regions (from **Fig. 2-15** B). Peak annotation and location were analyzed by the Bioconductor package ChIPseeker.

The binding profile of identified ChIP peaks around the transcription start site (TSS) was further investigated for the *SinglePeak* data set (**Fig. 2-17**). Peaks were mapped to the TSS region (± 10 kb) to obtain a binding matrix. The read count frequency around the TSS region in **Fig. 2-17** A is generated by the binding profile in **Fig. 2-17** B. The binding profile represents a gene (TSS region) in every line, and only peaks that aligned within the given genomic region are displayed.

Consistent with the gene body distribution, H3K27ac, H4ac and H3K27me3 were mainly distributed near the TSS of genes. In particular, H3K27ac and H4ac showed a sharp peak around the TSS region. Generally, the frequency of peak binding near the TSS was higher in activating histone marks compared to repressive ones (**Fig. 2-17** A and B).

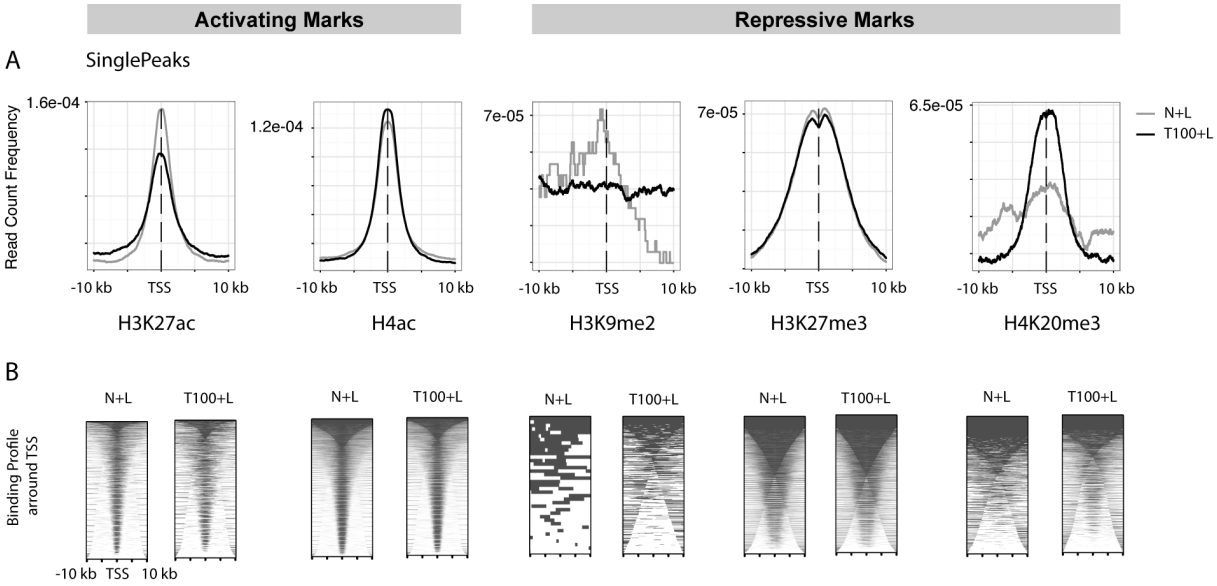

Fig. 2-17 ChIP peak binding profile of *SinglePeaks* around the TSS region (± 10 kb) in naïve (N+L) and tolerant monocytes stimulated with LPS (T+L): H3K27ac, H4ac and H3K27me3 are localized near to TSS regions. (A) Average profile plot. (B) Heat map of ChIP peaks binding to TSS regions. Plots are generated with the Bioconductor package ChIPseeker.

In summary, a general characterization of peaks identified by ChIP-Seq revealed that the activating histone marks H3K27ac and H4ac were highly enriched in naïve monocytes stimulated with LPS (N+L). The lack of re-enrichment of these histone modifications in tolerant monocytes might be due to an overall loss in signaling transduction. By contrast, repressive histone modifications, in particular H3K9me2 and H4K20me3, showed enrichment in tolerant monocytes re-stimulated with LPS (T100+L). Generally, localization of analyzed histone modifications was consistent with the literature (Barski *et al.* 2007, Bernstein *et al.* 2007, Kouzarides 2007). In particular, H3K27ac, H4ac and H3K27me3 were over-represented near gene-associated regions.

2.2.1.b Analysis of Genomic Regions Differentially Regulated by Histone Modifications in LPS-Tolerant Monocytes

The subsequent analyses focused on the characterization of genomic regions that either gained activating or repressive histone marks by a minimum fold change of 2 in tolerant monocytes (*DiffPeaks*, T100+L) compared to naïve cells treated with LPS (*DiffPeaks*, N+L). This approach allowed the identification of differentially regulated regions potentially mediated by endotoxin tolerance.

First, a general overview of the gene body distribution of *DiffPeaks* in naïve and tolerant monocytes clearly showed that LPS tolerization induced enrichment of histone marks mainly located within intergenic regions (**Fig. 2-18**).

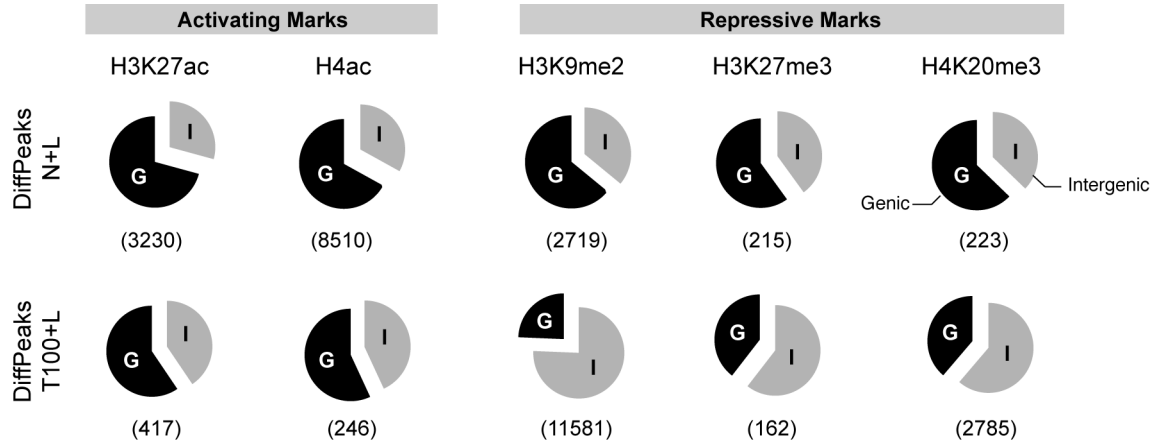

Fig. 2-18: Gene body distribution of *DiffPeaks* in naïve (N+L) and tolerant human monocytes treated with LPS (T100+L): Endotoxin tolerance induces enrichment of histone marks in intergenic regions. Genomic regions were broadly classified in genic (G) and intergenic regions (I) presented as VennPie plots, with the numbers representing the total peak counts identified by SICER shown in brackets (from **Fig. 2-15** C). Peak annotation and locations were analyzed by the Bioconductor package ChIPseeker.

Next, a hierarchical clustering was performed to get a global overview of the nature of differentially regulated peaks and to identify potential gene clusters that were regulated either by activating or repressive histone modifications in endotoxin tolerance. As a clustering of identified peaks over the complete human genome was not feasible due to limitations in computational power, a more simplified approach was used. Therefore, the identified peak sets for every histone modification were annotated by HOMER (Hypergeometric Optimization of Motif EnRichment, Heinz *et al.* (2010)) allowing mapping of peaks to the nearest TSS of a gene. This resulted in a list of annotated genes with specification of identified peaks and the distance to the specific TSS. Subsequently, all genes that belonged to differentially enriched regions (*DiffPeaks*, minimum fold change of 2, *P* value ≤ 1e-6) identified by comparing naïve (N+L) and tolerant monocytes treated with LPS (T100+L) were unified to one gene list. As *DiffPeaks* were counted either for one of the two conditions, the given gene list was compared to the *SinglePeak* data set (with a minimum SICER score of 100) to obtain values for both conditions. If multiple regions were associated with a single gene, the region with the highest SICER score was used. *DiffPeaks* showing a minimum fold change of 2, but a SICER Score below 100 in the *SinglePeak* data set, were counted as zero.

The final gene list indicating differentially bound regions by histone modifications was visualized as a heat map representing individual SICER scores of *SinglePeaks* of the annotated genes using unsupervised hierarchical clustering. Notably, the heat map shown in **Fig. 2-19** A only indicated a broad, simplified overview. It did not take into account that peaks called especially in tolerant cells were mainly located intergenically, which might lead to partially less specific correlations. However, a heat map generated focusing only on peaks localized within the TSS region (± 10 kb) identified similar gene clusters (not shown).

The global overview of differentially bound regions in endotoxin tolerance indicated that each of the analyzed histone modifications was basically exclusively associated with specific genes. Only small sets of genes showed co-localization in histone modifications. Moreover, histone modifications in tolerant and naïve monocytes did not cluster together indicating that the peaks were strongly diverse (**Fig. 2-19** A). Many genes in naïve monocytes stimulated with LPS (N+L) were associated with activating histone marks. Here, functional gene ontology (GO) enrichment analysis of *e.g.* H4ac-associated genes by GREAT (Genomic Regions Enrichment of Annotations Tool, McLean *et al.* (2010)) indicated that these genes mainly regulate TLR4-mediated immune responses (**Fig. 2-19** B). In tolerant cells, however, few gene clusters showed specific enrichment in acetylated histone marks and these clusters were different to the ones in naïve monocytes stimulated with LPS.

By contrast, H4K20me3 and H3K9me2 were enriched and partially co-localized in tolerant monocytes. Finally, a huge gene cluster in naïve and tolerant monocytes treated with LPS was associated with H3K27me3, which potentially regulates cell differentiation and development (Bernstein *et al.* 2007). However, only a small set of genes showed differences in H3K27me3, which is already indicated in **Fig. 2-15** C.

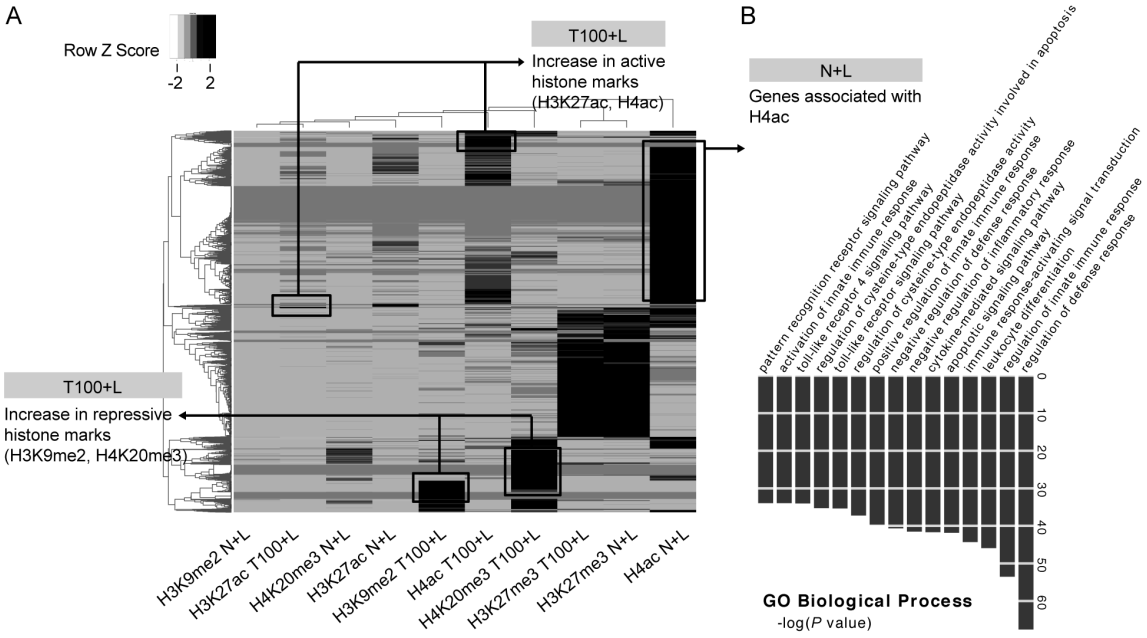

Fig. 2-19: Different gene clusters are affected by changes in histone modifications in endotoxin tolerance. (A) Heat map indicating genes that were differentially modified by histone modifications, with peak regions annotated to the nearest gene. Genes belonging to differentially regulated regions indicated by a minimum fold change of 2 (*P* value ≤ 1e-6) in *DiffPeaks* were unified to one gene list, and the given SICER Score of the corresponding genes identified as *SinglePeaks* were clustered using unsupervised hierarchical clustering (Euclidean). The heat map shows the SICER scores of differentially modified genomic regions (generated by R). (B) Gene Ontology (GO) enrichment analysis of genomic regions (peaks), which showed an increase in the activating histone mark H4ac in naïve monocytes treated with LPS (N+L), was performed by GREAT (Genomic Regions Enrichment of Annotations Tool). The scores for *'Biological Process'* (top 15) are expressed as -log(*P* value).

LPS tolerization induced global changes in histone modifications ranging from activating histone marks in naïve monocytes to adding repressive ones in tolerant cells. Of particular interest was the dynamic change in these epigenetic marks occurring in tolerant monocytes. Concerning the *histone code hypothesis* that genes possessing active or transcription-linked histone marks are likely expressed, whereas genes associated with repressive histone modifications show reduced gene expression (Strahl & Allis 2000), genomic regions that were significantly enriched in LPS tolerized monocytes for either activating or repressive histone marks were analyzed in detail. Thus, all downstream analyses focused mainly on the condition T100+L. This approach allowed for the identification of potential genes that were likely expressed in tolerant monocytes contributing to tolerance induction, *e.g.* transcriptional repressors, and parallel detection of gene groups which were repressed. A further goal was to identify the potential nature of epigenetic regulation occurring in endotoxin tolerance contributing to gene expression on the one hand and mediating gene repression on the other hand.

Generated peak lists that indicated a minimum 2-fold enrichment in at least one of the analyzed histone modifications in genomic regions of tolerant monocytes treated with LPS compared to naïve cells (*DiffPeaks* counted for T100+L) were further 'narrowed' to *histone-limited DiffPeak data sets*. A description of these peak sets can be found in **Table 2-1**. In detail, the *DiffPeak* lists were filtered for genomic regions, which possessed no parallel enrichment in the opposite activating or repressive histone modifications to rule out poised (bivalent) statuses in histone marks. A schematic outline of filtering is illustrated in **Fig. 2-20** A. For instance, *DiffPeaks* indicating enrichment in the activating histone mark H4ac in tolerant monocytes and showing induction (co-enrichment) in one of the repressive histone modifications H3K9me2, H3K27me3 or H4K20me3 were excluded in downstream analysis (**Fig. 2-20** A). In the opposite case, *DiffPeaks* enriched for example for the repressive mark H4K20me3 in tolerant monocytes lacking parallel enrichment in the activating histone marks H3K27ac and H4ac were maintained.

Table 2-1: Detailed description of *histone-limited DiffPeak data sets*

	Name of data set	Description
Activating	**H3K27ac_T_no_RepX** **H4ac_T_no_RepX**	*'T'* indicates enrichment in tolerant monocytes treated with LPS (T100+L) (*DiffPeaks*, fold change of minimum 2, *P* value ≤ 1e-6) *'no_RepX'* indicates no co-enrichment in repressive histone marks
Repressive	**H3K9me2_T_no_AcX** **H3K27me3_T_no_AcX** **H4K20me3_T_no_AcX**	*'T'* indicates enrichment in tolerant monocytes treated with LPS (T100+L) (*DiffPeaks*, fold change of minimum 2, *P* value ≤ 1e-6) *'no_AcX'* indicates no co-enrichment in activating histone marks

A Filtering of H4ac-Enriched Peaks in T100+L (H4ac_T) and No Co-Enrichment in Repressive Methylation Marks (no_RepX)

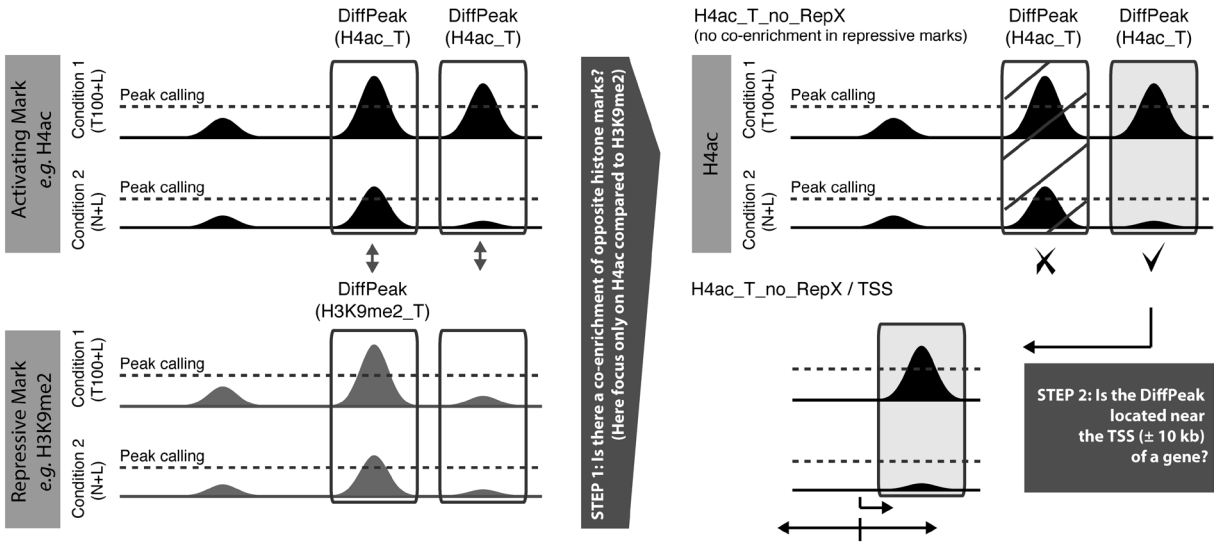

B Regions Differentially Modified in T100+L

H3K27ac_T	Total	417	
	no_RepX	377	90.4 %
	no_RepX / TSS (± 10 kb)	114	27.3 %
H4ac_T	Total	246	
	no_RepX	236	95.9 %
	no_RepX / TSS (± 10 kb)	48	19.5 %
H3K9me2_T	Total	11581	
	no_AcX	11551	99.7 %
	no_AcX / TSS (± 10 kb)	563	4.8 %
H3K27me3_T	Total	162	
	no_AcX	161	99.4 %
	no_AcX / TSS (± 10 kb)	34	21.0 %
H4K20me3_T	Total	2785	
	no_AcX	2759	99.1 %
	no_AcX / TSS (± 10 kb)	323	11.6 %

C Annotated Genes in T100+L (Overlap)

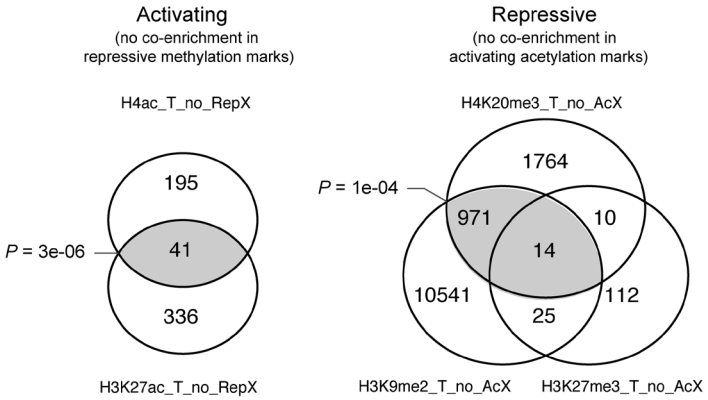

Fig. 2-20: Summary of differentially enriched regions (*DiffPeaks*) showing enrichment exclusively for either activating or repressive histone patterns in tolerant monocytes treated with LPS (T100+L). (A) Representative schematic overview for the generation of *histone-limited DiffPeak data sets* depicted for H4ac: Only *DiffPeaks* identified in the condition T100+L, which showed enrichment in an activating histone mark (here H4ac), but no co-enrichment in a repressive histone mark (here H3K9me2), were used for downstream analyses. (B) Total numbers of differentially enriched regions (*DiffPeaks*) in tolerant monocytes stimulated with LPS (T100+L, short indicated as 'T') are presented for each histone mark. *DiffPeaks* were further filtered for enriched regions that were exclusively regulated by differences in either activating (no co-enrichment in repressive marks, 'no_RepX') or repressive histone modifications (no co-enrichment in activating marks, 'no_AcX'). Moreover, the number of peaks located near the gene transcription start site (TSS ± 10 kb) is depicted. (C) Peaks were annotated to the nearest gene and the overlap of genes showing co-regulation of either positive or repressive histone modification patterns is represented as a VennPie plot using the Bioconductor package ChIPseeker. Significant gene overlap was calculated by the Bioconductor package GeneOverlap using the Fisher's exact test.

In **Fig. 2-20** B, an overview of the generated *histone-limited DiffPeak data sets* in tolerant monocytes treated with LPS is shown. Generally, most of the *DiffPeaks* (> 90 %) did not co-localize with the opposite histone signature (active or repressive, respectively). Moreover, the *histone-limited DiffPeak data sets* were annotated to the nearest gene and potential

co-enrichment of either activating (H3K27ac, H4ac) or repressive histone modifications (H3K9me2, H3K27me3 and H4K20me3) were represented as VennPlots (**Fig. 2-20** C). Only a restricted number of annotated genes seemed to be co-regulated by activating or repressive histone patterns in tolerant monocytes re-stimulated with LPS. Significant co-regulation could be identified for H4ac/H3K27ac and H3K9me2/H4K20me3 (**Fig. 2-20** C).
Additionally, only a limited number of the identified *histone-limited DiffPeaks* in tolerant monocytes stimulated with LPS (T100+L) was restricted to the TSS of genes (approximately 5 to 30 %, as can be seen in **Fig. 2-20** B), indicating that most of the peaks were basically located intergenically. This implies that in particular regulatory genomic elements like enhancers might be modified during endotoxin tolerance. Enhancers are distinct genomic regions that contain binding sites for transcription factors and co-repressors, thus influencing the expression of its target genes (Banerji *et al.* 1981). However, these regulatory elements seem to act independently of orientation and the distance to their target genes, and may function at large distances of several hundred kilobases or even megabases by looping (Shlyueva *et al.* 2014). The properties of enhancers make it difficult to determine their direct impact. Therefore, this thesis focused on the characterization of epigenetic events near promoter/TSS regions.

To identify biologically relevant differences, genes that showed a significant enrichment near the TSS (± 10 kb) in either activating (H4ac, H3K27ac) or repressive histone marks (H3K9me2, H3K27me3 or H4K20me3) in tolerant monocytes treated with LPS were considered for functional GO enrichment analyses using DAVID (Database for Annotation, Visualization and Integrated Discovery) (Huang *et al.* 2009a, b). This approach allows to identify genes which are significantly over-represented in a given gene set. An overview of GO clusters found is presented in **Fig. 2-21**. A complete list of over-represented genes found by DAVID is provided in the *Appendix* section **5.7**.
Genes associated with enrichment in the activating histone marks H4ac and H3K27ac in tolerant monocytes were preferentially involved in ion binding (**Fig. 2-21**, upper panel). A detailed look at the gene lists provided by DAVID indicates that H4ac and H3K27ac were found, for instance, in genes encoding for metallothioneins (MTs), which are important for regulation of oxidative stress responses (Kumari *et al.* 1998).
Genomic sites linked to an increase in the repressive histone mark H3K9me2 were also involved in ion binding. Moreover, most of the genes belonged to DNA binding proteins like zinc-finger transcription factors. Enrichment of H4K20me3 in tolerant monocytes was associated with genes involved in apoptosis. Furthermore, H3K27me3 was mainly enhanced in genes that mediate cell shape and movements dependent on actin filaments (**Fig. 2-21**, lower panel). DAVID analyses of genes associated with H3K9me2 and H4K20me3 also displayed hits in cell/organism developmental stages like reproduction, which partially makes

sense as these histone modifications are repressive marks indicating a developmental repression of these genes in monocytes. As, however, the focus of the analyses was narrowed to differentially regulated regions, these false positive results were excluded from further considerations.

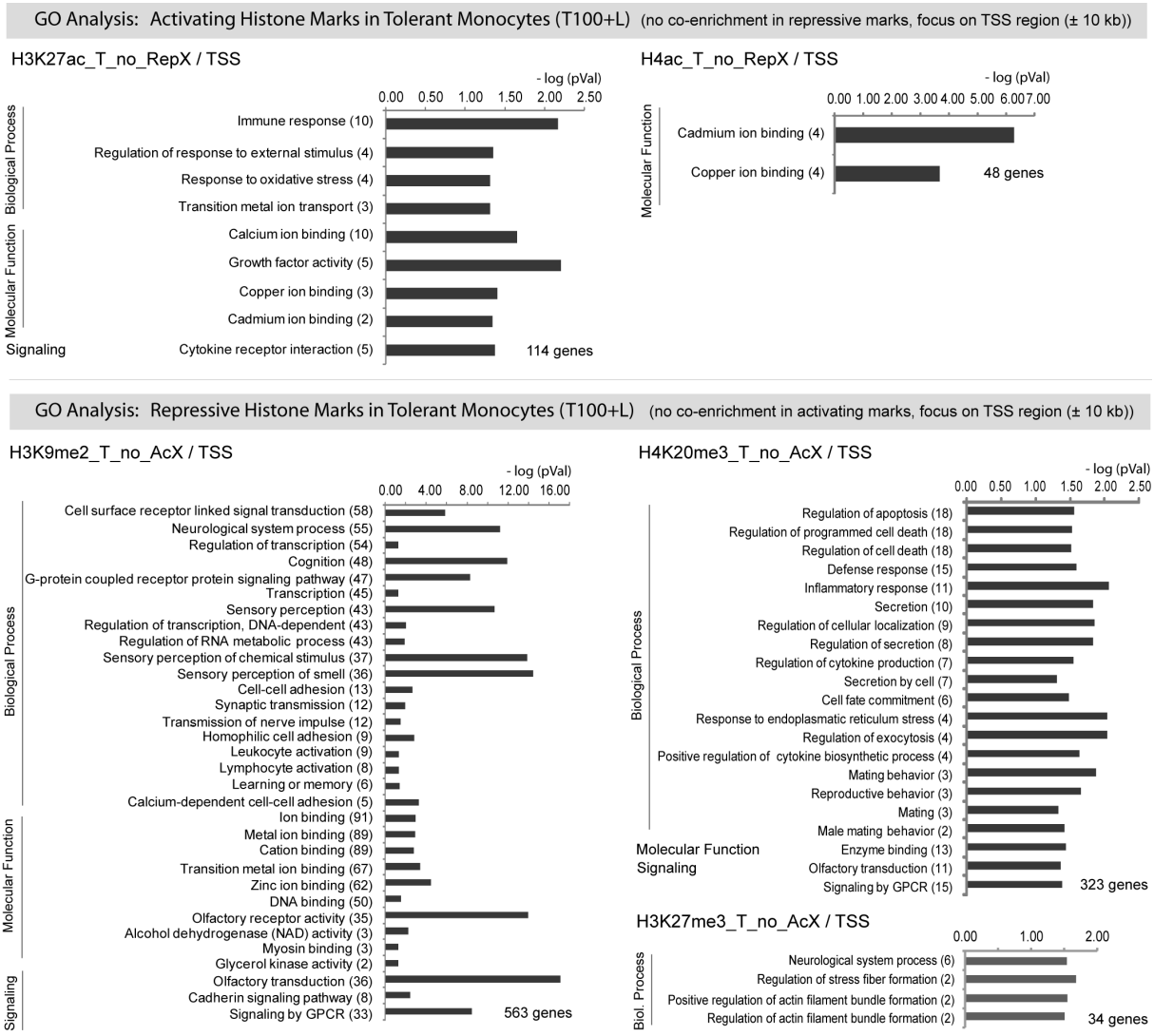

Fig. 2-21: Genes linked to activating histone marks in LPS-tolerant cells are involved in ion binding, whereas genes associated with repressive marks are implicated in transcription, apoptosis and filament formation. Annotated genes obtained from *histone-limited DiffPeak data sets* (TSS ± 10 kb) were used for functional gene ontology (GO) enrichment analysis using Database for Annotation, Visualization and Integrated Discovery (DAVID). The numbers of genes found significantly over-represented in the given gene set is shown in brackets. Only GO enrichment scores with a *P* value (pVal) below 0.05 were considered and are expressed as -log(*P* value).

Examples of differentially enriched regions for either activating or repressive histone modifications in tolerant human monocytes treated with LPS (T100+L) identified by SICER are depicted in **Fig. 2-22** A and B.

Gene expression of selected genes was further analyzed by qRT-PCR to determine whether the observed histone pattern identified by SICER was responsible for regulating the gene expression changes associated with endotoxin tolerance. Consistent with the *histone code hypothesis*, *MT1F* and *MT1L* mRNA expression (increase in activating histone modifications) were enhanced in tolerant monocytes (**Fig. 2-22** C). The zinc finger transcription factors *ZSCAN18* and *ZNF316* (increase in repressive histone modifications), however, showed LPS signaling-dependent expression and exhibited higher expression in T100+L compared to N+L. Notably, the mRNAs of these transcription factors were generally expressed in very low concentrations (**Fig. 2-22** D).

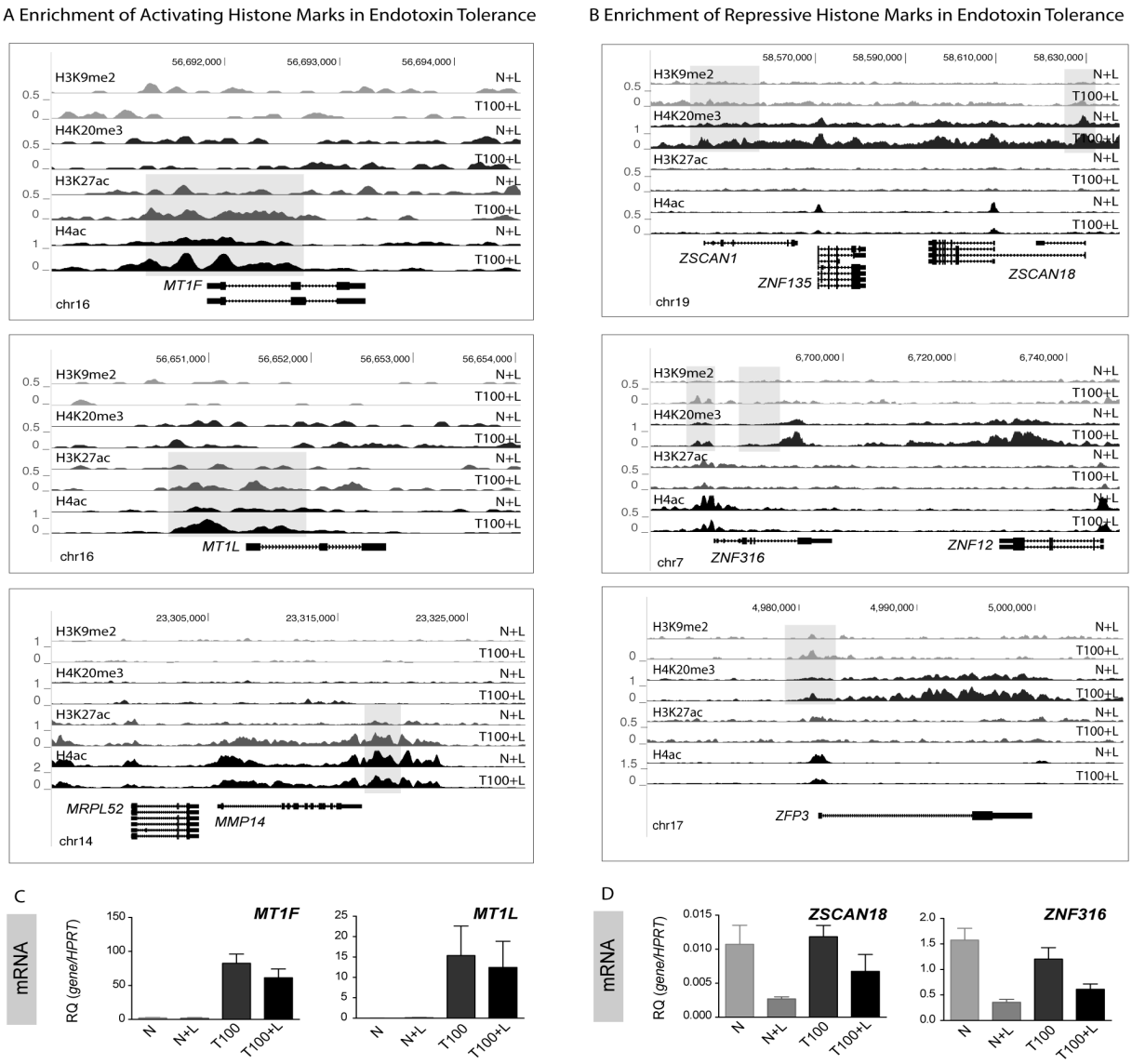

Fig. 2-22: Examples of differentially histone mark-enriched genomic regions in endotoxin tolerance identified by SICER. (A & B) Binding profiles indicating interactions of histone modifications within the genome are displayed in the UCSC Genome Browser. Significant peaks (fold change ≥ 2, *P* value ≤ 1e-6) identified by the peak caller SICER are shaded in grey. (A) Enrichment of activating histone marks. (B) Enrichment of repressive histone marks. (C & D) Expression analysis (mRNA) of selected genes showing enrichment in either activating (C) or repressive histone modifications (D) in T100+L (mean ± SEM of 3 independent experiments).

Next, the *histone-limited DiffPeak sets* were analyzed for transcription factor binding sites (TFBSs) to identify the transcription network within the genomic regions that showed either enrichment in activating or repressive histone modifications in endotoxin-tolerant monocytes treated with LPS. Here, all identified peaks without limitation in TSS regions were used to allow a genome-wide analysis.

TFBS analysis of DNA regions enriched for repressive H3K9me2 and H4K20me3 revealed a significant increase in the binding site for the transcription factor YY1 (ying-yang 1) (**Fig. 2-23**, left panel). However, most of the regions were potentially associated with SCL (stem cell leukemia) and SMAD3 (mothers against decapentaplegic homolog 3) binding motifs (**Fig. 2-23**, right panel). A combinational analysis of genomic regions co-localized by H3K9me2 and H4K20me3 indicated again an enrichment in SMAD binding sites (**Fig. 2-23**, lower part). Because of the low number of peak regions (*DiffPeaks*, see **Fig. 2-20** B) identified for enrichment of H4ac, H3K27ac and H3K27me3 in tolerant monocytes, no reliable assumptions for these marks could be assumed. A complete list of TFBSs found is provided in *Appendix* **5.6**.

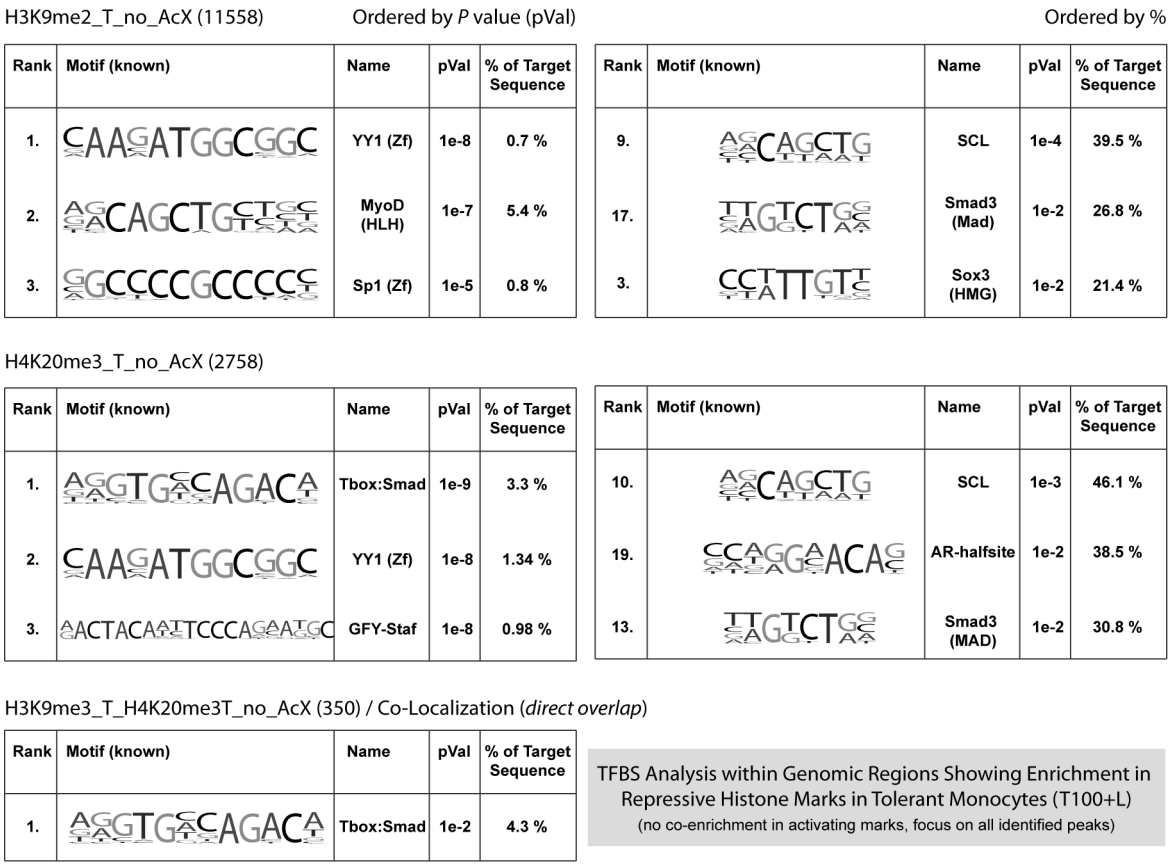

Fig. 2-23: Genomic regions linked to repressive H3K9me2 and H4K20me3 are enriched for YY1 and SMAD binding sites. *Histone-limited DiffPeak data sets* identified in tolerant monocytes treated with LPS (T100+L) were analyzed for transcription factor binding sites (TFBSs) by HOMER. Motifs identified in genomic regions showing significant enrichment in the repressive histone marks H3K9me2 and H4K20me3 (no co-enrichment in activating histone marks) are depicted either by *P* value (left hand side) or by percentage (right hand side).

Taken together, TFBSs for *e.g.* SMAD and YY1 were potentially enriched in genomic regions, which showed parallel increases in the repressive histone marks H3K9me2 and H4K20me3 in LPS-tolerant monocytes. This implies that these transcription factors might partially be the basis for the repressive histone pattern observed in endotoxin tolerance.

2.2.2 Global Analysis of DNA Methylation by MethylCap-Seq

Besides histone modifications, endotoxin-induced tolerization could be regulated by epigenetic changes in DNA methylation, which indicates repression (Bird & Wolffe 1999).

Global changes in DNA methylation induced by endotoxin tolerance were analyzed by Methyl-Capture Sequencing (MethylCap-Seq). MethylCap-Seq is based on the *in vitro* enrichment of methylated DNA fragments by the methyl-CpG binding domains (MBD) and subsequent massively parallel sequencing. This technique was already introduced in **2.1.7** (for more details see **4.3.9** in *Materials & Methods*). Of note, only preliminary data are presented here as replication of this approach is currently in process.

For better comparison between analyses of histone modifications by ChIP-Seq and DNA methylation by MethylCap-Seq, naïve monocytes stimulated with LPS (N+L) were compared with high-dose LPS-tolerized monocytes re-treated with LPS (T100+L) (**Fig. 2-24** A). Differentially methylated genomic regions were identified using the Bioconductor package MEDIPS (Lienhard *et al.* 2014) and significant changes were indicated by a minimum fold change of 2 (P value ≤ 0.01). Subsequently, genomic regions were annotated to the nearest gene. In total, 13 807 differentially methylated regions could be identified, from which 3756 regions were linked to TSS regions (± 10 kb, **Fig. 2-24** B).
LPS-tolerant human monocytes (T100+L) compared to naïve cells treated with LPS (N+L) showed an overall reduction in DNA methylation (**Fig. 2-24** C). Only 577 unique genes could be identified showing significant enrichments of DNA methylation by a minimum 2-fold change in tolerant monocytes (T100+L). Functional GO enrichment analysis of this gene data set revealed that most of the genes were mapped to phosphate metabolism and RNA binding (**Fig. 2-24** C, for a complete overview of GO results please go to *Appendix* section **5.7**). Selected examples of genes or gene regions, which showed significant enrichment in DNA methylation in tolerant monocytes treated with LPS, are depicted in **Fig. 2-24** D.

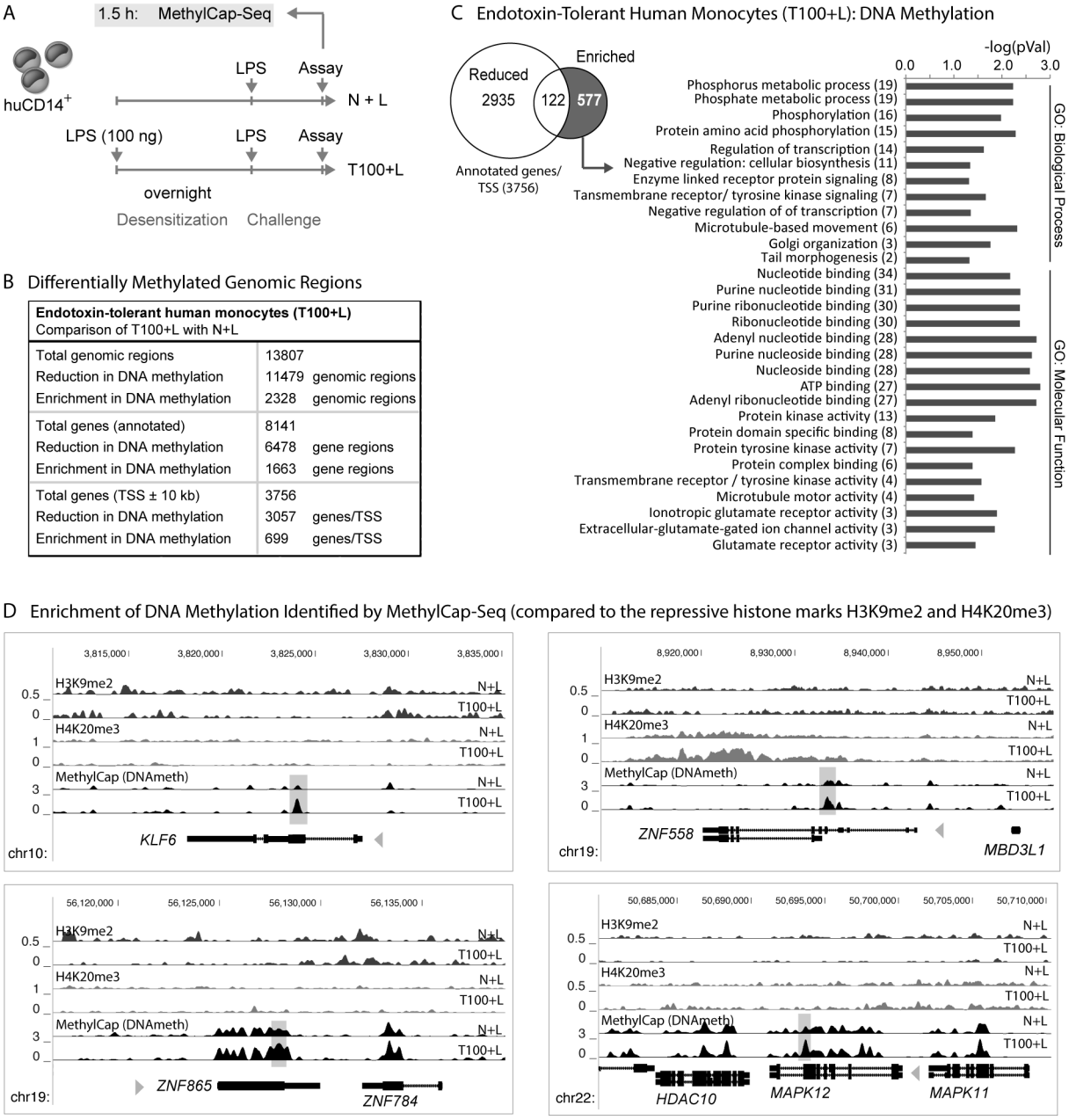

B Differentially Methylated Genomic Regions

Endotoxin-tolerant human monocytes (T100+L) Comparison of T100+L with N+L		
Total genomic regions	13807	
Reduction in DNA methylation	11479	genomic regions
Enrichment in DNA methylation	2328	genomic regions
Total genes (annotated)	8141	
Reduction in DNA methylation	6478	gene regions
Enrichment in DNA methylation	1663	gene regions
Total genes (TSS ± 10 kb)	3756	
Reduction in DNA methylation	3057	genes/TSS
Enrichment in DNA methylation	699	genes/TSS

Fig. 2-24: Endotoxin tolerance induces a global loss in DNA methylation. (A) Naïve and tolerant human monocytes were subjected to MethylCap-Seq. (B) Overview of significant differentially methylated genomic regions identified by comparison of N+L with T100+L. Genes were annotated by the Bioconductor package MEDIPS. (C) Genes showing enrichment in DNA methylation in tolerant monocytes treated with LPS (T100+L) were analyzed for functional GO enrichment using DAVID. The numbers of genes found significantly over-represented in the given gene set is shown in brackets. (D) Representative binding profiles indicating enrichment in DNA methylation in T100+L for selected genes are displayed in the UCSC Genome Browser. Differentially methylated regions (fold change ≥ 2, *P* value ≤ 0.01) identified by the Bioconductor package MEDIPS are shaded in grey.

Moreover, DNA methylation and histone marks can *"communicate"* with each other as both modifications provide binding platforms for various DNA- and histone-modifying proteins (Reviewed in Fuks (2005) and Brenner & Fuks (2007)). Therefore, identified genes showing enrichment in DNA methylation (near TSS up to 10 kb) in endotoxin-tolerant monocytes

treated with LPS (T100+L) were compared to the gene lists obtained by ChIP-Seq/SICER analysis, which indicated an increase in the repressive histone marks H3K9me2 and H4K20me3 but no co-enrichment in activating marks near the TSS of genes (**Fig. 2-25**).

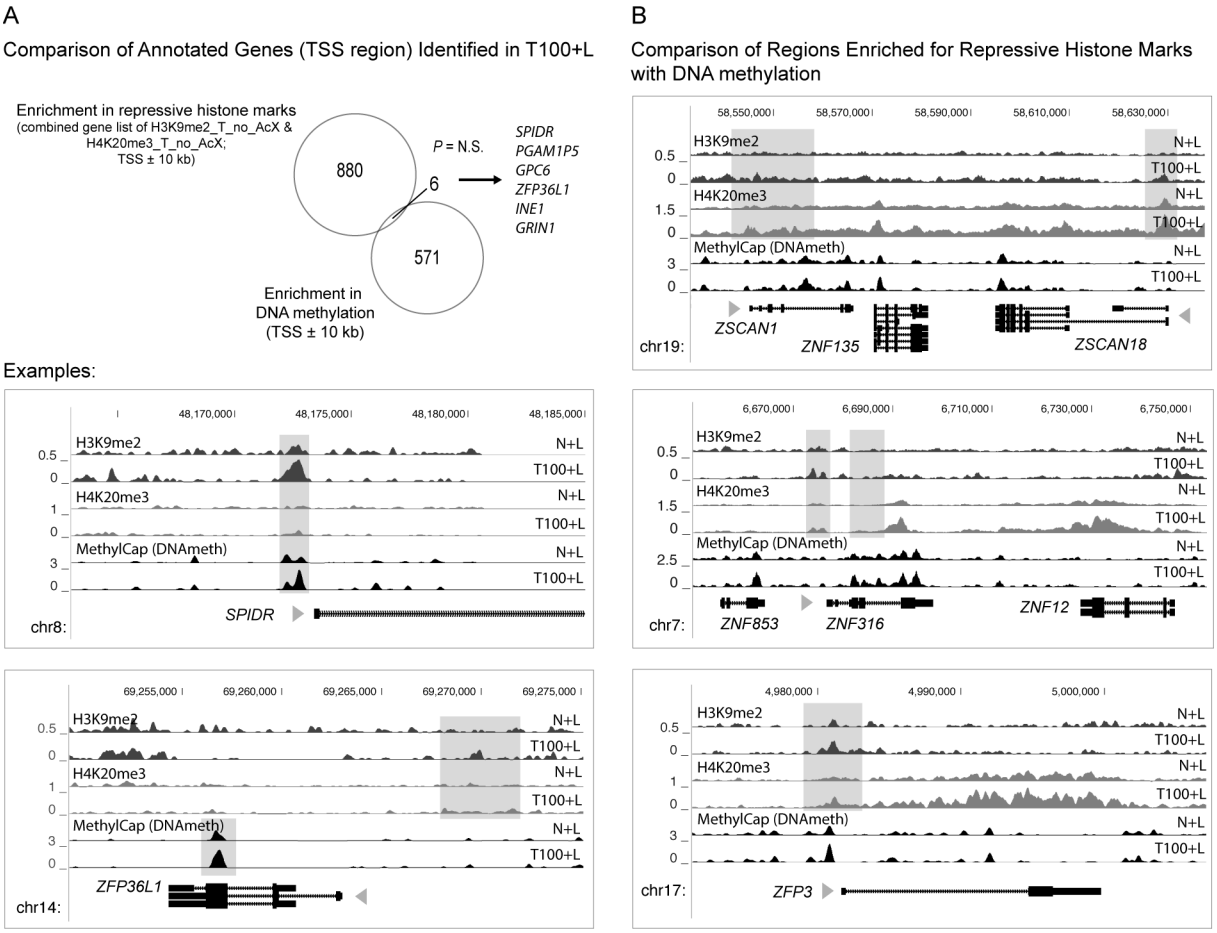

Fig. 2-25: Genomic regions showing enrichment in repressive histone modifications do not co-localize with DNA methylation. (A) Comparison of gene lists obtained by MethylCap-Seq/MEDIPS with ChIP-Seq/SICER data: Genes showing enrichment in DNA methylation in tolerant monocytes treated with LPS were compared to genes with significant enrichment in H3K9me2 and H4K20me3, but no co-enrichment in activating histone marks (*histone-limited DiffPeak data sets*, **Fig. 2-20** B). Only gene regions up to 10 kb from TSS were considered for analysis. (B) Binding profiles indicating enrichment in DNA methylation are compared to genes showing enrichment in the repressive histone modifications H3K9me2 and H4K20me3 in tolerant monocytes treated with LPS (T100+L) identified by SICER (from **Fig. 2-22** B). Binding profiles are depicted in the UCSC Genome Browser. Grey shaded boxes indicate significant differentially regulated regions identified by SICER or MEDIPS, respectively.

As indicated in **Fig. 2-25** A, no direct association could be found between DNA methylation and repressive histone modifications. Only six genes in total showed potential co-localization (± 10 kb of TSS) of both epigenetic markers (**Fig. 2-25** A). However, genes identified by SICER, which gained repressive histone modifications during tolerance inductions (from **Fig. 2-22** B), often showed parallel enrichment in DNA methylation (no significant result, **Fig. 2-25** B).

Taken together, in contrast to the observed histone pattern, endotoxin tolerance mediated a global loss in repressive DNA methylation, which might be due to the first overnight LPS stimulus. Only a small proportion of genomic regions gained significant enrichment in DNA methylation in tolerant monocytes treated with LPS. Moreover, a direct interaction of DNA methylation with repressive histone modifications could not be confirmed by bioinformatical analyses.

2.2.3 Validation of Epigenetic Changes by Global mRNA Expression

As indicated by analyses of histone modifications and DNA methylation, endotoxin tolerance seemed to have a dramatic impact on the epigenetic landscape of human monocytes. However, whether the observed epigenetic changes were responsible for the characteristic gene expression in tolerant monocytes compared to naïve ones remains to be validated.
Therefore, human monocytes were subjected to the *in vitro* endotoxin tolerance model and extracted RNA was subjected to total mRNA-Sequencing (mRNA-Seq) to analyze the genome-wide expression pattern of naïve (N+L) and high-dose tolerized, human monocytes stimulated with LPS (T100+L) (see **Fig. 2-26** A).

Comparative analysis in global gene expression identified 3638 genes differentially expressed with a minimum fold change of 2 (*P* value ≤ 0.05); of these, 1758 genes were down regulated and 1880 genes were up regulated in high-dose tolerized monocytes stimulated with LPS (**Fig. 2-26** B). GO analyses of differentially expressed genes revealed that tolerant monocytes treated with LPS (T100+L) showed a prominence in phagocytosis- and metabolism-related processes, whereas mechanisms involved in gene expression, particularly RNA metabolism and translation, and immune responses were reduced (**Fig. 2-26** C). This gene expression pattern clearly demonstrated a profound gene reprogramming in endotoxin tolerance towards an immunosuppressive phenotype.
Finally, the identified gene sets were correlated with genes that underwent an epigenetic change in tolerant monocytes (within TSS ± 10 kb). Approximately 1000 of the differentially expressed genes (27 %) showed a transcriptional level and an epigenetic pattern consistent with the *histone code theory* (Strahl & Allis 2000). In particular, changes in activating histone modifications (H3K27ac, H4ac) – either enrichment or reduction in tolerant monocytes treated with LPS (T100+L) – correlated with genes expression (**Fig. 2-26** D). No significant correlation could be observed between changes in DNA methylation and transcriptional level (**Fig. 2-26** F), further confirming that DNA methylation plays only a minor role in endotoxin tolerance.

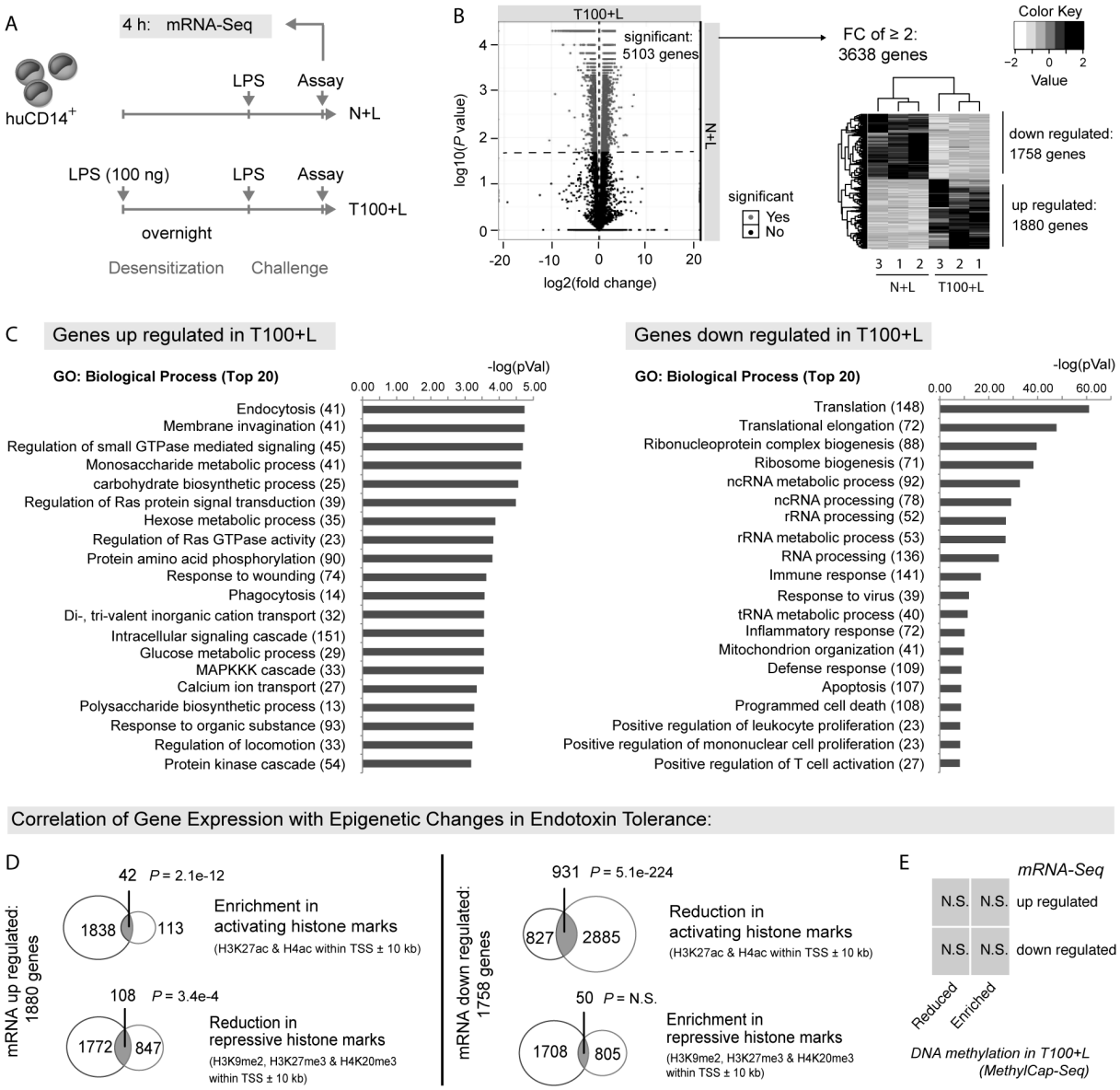

Fig. 2-26: Approximately 1000 differentially expressed genes show an expression pattern consistent with the *histone code theory*. (A) Naïve and high-dose tolerized monocytes were treated with LPS and subjected to mRNA-Seq analysis. (B) Overview of differentially expressed genes: Volcano plot (left) represents the relationship between significance and fold change (FC) illustrated using the Bioconductor package cummeRbund. Differentially expressed genes showing a minimum fold change of 2 in RPKM expression values are depicted as heat map (right). Heat map was built using R (Euclidean clustering, unsupervised). Three replicates per condition were used for expression analysis. (C) GO enrichment analysis of identified differentially expressed genes was performed using DAVID, with the count of genes found significantly over-represented in the given dataset is shown in brackets. (D and E) Differentially expressed genes were analyzed for potential gene overlap with genes identified showing either differences in histone modifications (D) or DNA methylation (E) within the TSS region using the Bioconductor package GeneOverlap. Significance was tested using Fisher's exact test (N.S. = not significant).

In summary, global transcriptomic analysis identified a clear reprogramming of gene expression in tolerant human monocytes. Correlation of transcription with specific epigenetic signatures demonstrated that gene expression was partially associated with histone

modifications representing active or repressive transcription. The analyzed changes in histone modifications (but not DNA methylation) indicate how a physiological condition of tolerant monocytes is mediated by promoting oxidative stress responses, while global repression of transcription and signaling-linked molecules is induced.

3. Discussion

Exposure of monocytes and macrophages to LPS results in expression of several genes encoding for pro-inflammatory and anti-inflammatory cytokines, chemokines and anti-microbial peptides and proteins. Moreover, LPS stimulation leads to tolerance induction and reprogramming of gene expression with transient silencing of a specific set of LPS-induced genes. This phenomenon known as endotoxin tolerance can be observed *in vivo* in humans and animals as well as *in vitro* in cell culture (Favorite & Morgan 1942, Fraker *et al.* 1988, Randow *et al.* 1995). Nowadays, it is common knowledge that LPS-inducible genes can be broadly classified into two distinct classes (Biswas & Lopez-Collazo 2009, Biswas & Shalova 2012, Cavaillon & Adib-Conquy 2006, Seeley & Ghosh 2014). Upon repeated exposure to LPS, one group of genes is transiently silenced to prevent excessive inflammation and immunopathology. These genes encode for pro-inflammatory cytokines, like TNF and IL-1β, and are termed class T genes or *tolerizable genes*. The tolerization effect on class T genes appears within different magnitudes (Erroi *et al.* 1993), whereas TNF is probably the best marker for endotoxin tolerance as assessed by its dramatically reduced production following LPS tolerization (Mathison *et al.* 1990). The second class of genes also termed *non-tolerizable genes* (class NT) contains antimicrobial mediators and effectors that remain inducible to maintain a basic antimicrobial host defense against invading pathogens without the destructive force of inflammation (Allantaz-Frager *et al.* 2013, Foster *et al.* 2007, Lehner *et al.* 2001, Rayhane *et al.* 2000, Wheeler *et al.* 2008).

Both classes of genes are induced by the same receptor named TLR4. Initial LPS stimulation induces a temporary downregulation of TLR4 cell surface expression and reduction of downstream signaling by *e.g*. decoupling of TLR4 from the signaling adapter MyD88 (Medvedev *et al.* 2002). But downregulation of major signaling pathways including NFκB and MAP kinase cascade activation would affect all LPS-induced genes. Thus, it is questioned how this differential gene regulation is mediated and how class NT – but not class T – genes remain highly inducible. There is increasing evidence that silencing one class of genes occurs by gene-specific rather than signal-specific mechanisms, through chromatin modifications at the level of individual promoters (Carson *et al.* 2011, Chan *et al.* 2005, El Gazzar *et al.* 2007, Foster *et al.* 2007, Foster & Medzhitov 2009, McCall & Yoza 2007, Neagos *et al.* 2015, Ramirez-Carrozzi *et al.* 2006). Moreover, sustained unresponsiveness of inflammatory reactions in endotoxin tolerance persists for several days (*in vitro*) and weeks (*in vivo*) even if the original source of inflammation is resolved (Kox *et al.* 2011) or when the transduction of major signaling pathways is recovered (Krüger 2006). Moreover, activation of monocytes and macrophages and subsequent restoration of endotoxin tolerance by IFNγ (Docke *et al.* 1997a) or IFNα2 treatment (Shi *et al.* 2015) seems to be mediated by recruitment of transcriptional activators and chromatin remodeling proteins without significant

alterations in TLR4 signaling defects (Chen & Ivashkiv 2010, Shi *et al.* 2015). These examples imply some kind of memory generation. As changes in epigenetic marks appear more stable than simple alterations in signaling molecules, it is very likely that the initial LPS stimulation remodels the epigenetic landscape to a transiently more tolerant phenotype.

The aim of this study was to elucidate the changes in the epigenetic landscape occurring during tolerance induction in a human experimental setup, thus providing new insights in the tolerance mechanisms leading to repression of individual genes.

3.1 Individual Class T Genes are Differentially Affected by Epigenetic Changes and Signaling Events in Endotoxin Tolerance

The first part of the study focused on the analysis of differences in transcription-linked histone modifications compared to repressive marks with a specific focus on immune-relevant genes that play an important role in endotoxin tolerance.

A common pattern to distinguish class NT genes from class T genes could not be identified in human monocytes. The study rather provided a detailed classification of class T genes in *intermediately tolerizable* and *highly tolerizable*. Comparative analysis of activating histone modifications and signaling strength in LPS-tolerant monocytes showed that the *IL6* and *IL1B* genes possessed activating H3K27ac and H4ac even in tolerant monocytes. Moreover, production of IL-6 and presumably IL-1β was signaling-dependent (*intermediately tolerizable*). In contrast, the *TNF* and *CXCL10* genes showed diminished induction of activating histone marks independent of signaling strength of tolerant cells (*highly tolerizable*). This type of discrimination seemed to be human-specific, as analysis of murine macrophages demonstrated diminished re-acetylation of H4 within the *Il6* gene, while the *Tnf* gene showed H4 re-acetylation in tolerant cells.

Further analysis of repressive histone modifications in human monocytes identified selective enrichment of repressive H3K9me2 and H4K20me3 in *IL1*-related genomic loci, whereas the *IL6* gene showed reduction in H3K27me3 in tolerant monocytes re-stimulated with LPS. Lastly, endotoxin tolerance had no impact in the DNA methylation status of the *IL6* and *TNF* genes.

3.1.1 The Role of Activating Events in Individual Genes

First, characterization of cytokine and chemokine secretion in human tolerant monocytes was performed to assure that the experimental setup used in this study followed the expression behavior described for endotoxin tolerance. Consistent with previous studies (Allantaz-Frager *et al.* 2013, Foster *et al.* 2007), a subset of LPS-inducible genes encoding for TNF, CXCL10/IP-10, CXCL8/IL-8, IL-6, IL1-RA and IL-1β was selectively reduced upon repetitive

exposure to LPS (class T). However, the tolerization behavior of these cytokines was quite diverse, demonstrating a high tolerization effect on TNF and CXCL10/IP-10 production, whereas IL-6 and IL-1β were only moderately tolerized by LPS treatment. Moreover, CXCL8/IL-8 showed a clear re-induction in tolerant monocytes reaching almost the same expression level as naïve monocytes treated with LPS. By contrast, expression of other chemokines like CCL2/MCP-1 and CCL7/MCP-3 was unaffected or even enhanced. Likewise, the mRNA expression of *FPR1* was clearly increased in tolerant monocytes compared to naïve ones (class NT). The expression of the genes mentioned is somewhat controversially discussed in the literature. Especially for CXCL8/IL-8, IL-1RA, IL-1β, CCL2/MCP-1 and CCL7/MCP-3, conflicting studies exist showing either enhanced/unaffected or reduced expression depending on the model and cell type used for analysis of endotoxin tolerance (reviewed in Biswas & Lopez-Collazo (2009), Cavaillon & Adib-Conquy (2006), Lopez-Collazo & Del Fresno (2013) and Nahid *et al.* (2011)).This implies that endotoxin tolerance is a very complex phenomenon and that cytokines do not all behave the same. Thus, interpretation of endotoxin tolerance and the resulting consequences must take into account the diverse nature of cells and the environmental and experimental setup.

To relate the differences in gene expression to potential changes in epigenetic modifications, the expression behavior of specific genes affected by endotoxin tolerance was analyzed by epigenetic changes. Primarily, the induction of histone modifications indicating transcriptionally active chromatin (H3K4me3, H3K27ac and H4ac) was characterized near the transcription start sites (TSS ± 1 kb) of *TNF*, *CXCL10*, *IL8*, *IL6* and *IL1B* (class T genes) compared to *FPR1* (class NT gene).

ChIP assays of tolerant monocytes challenged with a high dose of LPS (T100+L) compared to naïve cells (N+L) demonstrated that highly tolerant genes like *TNF* and *CXCL10* (class T genes) showed a diminished re-induction in activating histone modifications, in particular acetylation marks, which mirrored their reduced gene expression in endotoxin tolerance. By contrast, the TSS regions of *IL1B*, *IL6* and *IL8* (class T genes) were associated with a similar or even higher levels of activating histone modifications in tolerant cells stimulated with LPS. The histone pattern of these genes resembled that of the class NT gene *FPR1*. However, whereas the kinetics of induction of transcription-linked histone marks within the *FPR1* gene reflected its enhanced gene expression in tolerant monocytes, the positive histone patterns of *IL1B* and *IL6* were contrary to their reduced gene expression in endotoxin tolerance.

Moreover, species-specific differences in histone patterns of class T genes seem to exist. In particular, the promoter regions of *IL6* and *TNF* were differentially modified in human monocytes compared to murine macrophages. Whereas the human *IL6* gene still possessed the positive histone mark H3K4me3 and showed re-induction of H4ac in tolerant human

monocytes, the re-acetylation of H4 was reduced in murine macrophages. The diminished H4 acetylation in the murine *Il6* gene has also been shown in a publication by Foster *et al.* (2007). In contrast, H4ac was inducible in the murine *Tnf* gene while being inhibited in human monocytes. This further demonstrates that the mechanisms leading to gene repression in endotoxin tolerance might be different and likely depend on the experimental setup.

The variation in tolerance induction of the human cytokines TNF and CXCL10/IP-10 compared to IL-1β, IL-6 and CXCL8/IL-8 could be partially explained by differences in sensitivity towards LPS-signaling strength. For instance, signaling-dependent analyses of gene expression combined by histone modification assays revealed that the production of CXCL8/IL-8, IL-6 and presumably IL-1β were more sensitive to signaling strength. Monocytes tolerized by a low dose of LPS (1 ng/ml) showed a reduced but still clearly detectable signaling induction compared to cells treated with a high dose of LPS (100 ng/ml) as shown for *e.g.* the induction of MAP kinase p38 phosphorylation. The remaining signaling strength in low-dose tolerized monocytes was sufficient to induce CXCL8/IL-8, IL-6 and IL-1β expression, though the production level of particular IL-6 and IL-1β was not as high as in naïve monocytes stimulated with LPS. The parallel analysis of the transcription-linked histone modifications H3K27ac and H4ac revealed that the corresponding *IL8*, *IL6* and *IL1B* genes showed high induction in these activating histone marks during low-dose LPS treatment. Again, the histone patterns were very similar to the epigenetic signature of the class NT gene *FPR1*, which was even more highly expressed in low- and high-dose treated monocytes. It is not clear, why especially the *IL6* and *IL1B* genes still possessed high enrichment in activating histone marks in tolerant human monocytes while showing reduced gene expression capacity. It could be hypothesized that these genes were modified within their promoters to a more active, positive histone pattern indicating a kind of *'stand-by status'* for transcription during endotoxin tolerance, meaning that if the signaling level is strong enough, these genes will be transcribed. But nevertheless, the production of IL-6 and IL-1β in low-dose tolerized cells (1 ng/ml LPS) did not reach the same expression level as in naïve monocytes treated with LPS, indicating that additional repressive mechanisms besides signaling strength might exist to reduce their expression capacity. Moreover, signaling analysis was exclusively performed with a focus on p38 phosphorylation; it cannot be ruled out that other signaling mechanisms have an impact on the expression of these genes. For instance, a detailed study of TNF tolerance implied that low-dose TNF tolerance is mediated by glycogen synthase kinase 3, whereas high-dose tolerance is regulated by A20/glycogen synthase kinase 3- and protein phosphatase 1-dependent mechanisms (Gunther *et al.* 2014). Perhaps, this discriminative mechanism is also important in high and low-dose LPS tolerization.

By contrast, the promoter regions of *TNF* and *CXCL10* showed low acetylation status of H3K27 and H4 during low- and high-dose LPS tolerization, without regard to signaling strength. In particular, H4ac induction was completely diminished independently of the signaling capacity in low- and high-dose treated cells, indicating that the repression of these genes is likely mediated by the involvement of histone modifying enzymes *e.g.* histone deacetylases (HDACs) (Castellucci *et al.* 2015). Moreover, the discrimination described seems to be independent of so-called primary and secondary response genes in endotoxin tolerance. Primary or early response genes (PRG) *e.g. TNF* and *IL1B* are supposed to be kept in an open chromatin state in naïve monocytes and macrophages, whereas secondary or late response genes (SRG) like *IL6* need initial recruitment of the transcription machinery after stimulation (Ghisletti *et al.* 2009, Hargreaves *et al.* 2009, Ramirez-Carrozzi *et al.* 2006). As *IL6* (SRG) and *IL1B* (PRG) in this study behaved very similarly regarding their epigenetic changes, it is likely that the mechanisms involved in LPS tolerization are different than for transcription of PRGs and SRGs after initial LPS stimulation.

3.1.2 The Role of Repressive Events in Individual Genes

Besides changes in positive histone modification, it could be hypothesized that *tolerizable genes* were repressed by gaining repressive histone modifications rather than the loss of activating ones. For instance, Stender *et al.* reported that the repressive H4K20me3 served as a checkpoint for expression of TLR4 target genes and that NFκB-dependent erasure of H4K20me3 was necessary for gene expression (Stender *et al.* 2012). Moreover, H3K9me2 hypermethylation in tolerant monocytic THP1 cells within the promoter regions of *TNF* and *IL1B* was reported by other studies (Chan *et al.* 2005, El Gazzar *et al.* 2007). Thus, a selective enrichment in repressive histone modifications in class T genes might be very likely. However, analyses of H3K9me2, H3K27me3 and H4K20me3 by ChIP-Seq could only partially support an involvement of these repressive histone marks in endotoxin tolerance. The *IL1B* locus, for example, showed an increase in H3K9me2 in tolerant monocytes circa 7 kb upstream from its TSS. Moreover, ChIP-seq analyses revealed an increase in H4K20me3 near the TSS of *IL1A* and *IL1R1*, which are both involved in IL-1 signaling. However, no differences in repressive histone marks could be observed for the *TNF*, *CXCL10* and *IL8* genes in human monocytes. Strikingly, *IL6* displayed a reduction of the repressive mark H3K27me3 in tolerant cells compared to naïve monocytes treated with LPS, which negatively correlates with its gene repression.

Again, a common pattern in repressive histone modifications could not be observed in class T genes. Notably, not every known repressive histone mark was analyzed in the present study, and many have not yet been identified. Thus, it has to be further investigated how these modifications really affect gene expression in endotoxin tolerance.

Moreover, individual differences by using primary cells (here human monocytes) cannot be ruled out and might result in distinct results than using a cell line like THP-1.

To elucidate other epigenetic mechanisms (besides histone modifications) involved in tolerization of TNF and IL-6 production in primary human monocytes, the promoter regions of the encoding genes were investigated for *de novo* DNA methylation – an epigenetic marker for gene regression (Bird & Wolffe 1999). PCR-based bisulfite sequencing (BS-Seq) revealed no significant changes in DNA methylation in the promoter regions of human *TNF* and *IL6* in naïve and tolerant monocytes treated with LPS. The analysis of BS-Seq data in the present work only focused on canonical CpGs. Certainly, recent advances in the field of DNA methylation demonstrate that there is a higher diversity in DNA modifications than expected (reviewed in Breiling & Lyko (2015)). However, gene-covered analysis of *TNF* and *IL6* by MethylCap-Seq, which is a technique in which methylated DNA is indirectly analyzed, revealed no significant differences between naïve and tolerant monocytes, further confirming that DNA methylation might not play a prominent role in LPS tolerization. This is in contrast to previous reports. Detailed analyses of the *TNF* promoter in THP1 cells demonstrated that its repression by DNA methylation was mediated by a complex interplay of several molecules: Binding of the NFκB family member RelB and high-mobility group protein 1 (HMGB1) in tolerant THP1 cells within the *TNF* promoter led to recruitment of the histone H3K9 methyltransferase G9a, which induced the repressive mark H3K9me2. H3K9me2 in turn mediated DNA methylation by HP1-dependent recruitment of the DNA methylase DNMT3a/b at the *TNF* promoter (El Gazzar *et al.* 2009, El Gazzar *et al.* 2008). The discrepancy between the present study and the publications from El Gazzar *et al.* might arise because primary human monocytes may behave differentially than a monocytic cell line as discussed above. Moreover, the time frame of DNA methylation analysis might not be optimal in the present study. The establishment of DNA methylation is potentially different from those of histone modifications and may differ between cell type and species.

Generally, several defects in signaling events have been reported in endotoxin tolerance including suppressed phosphorylation of p38 and reduced degradation of the NFκB inhibitor molecule IκBα. LPS stimulation induces a negative feedback loop by parallel activation of several negative regulators of TLR4 signaling. These are induced by the same NFκB and MAP kinase pathways, and mediate termination of input signaling. LPS-induced inhibitors of signaling include: IL-1 receptor associated kinase M (IRAKM, which inhibits TRAF6 complex formation), A20 (which prevents ubiquitinylation of the signaling molecule TRAF6), A20-binding inhibitors of NFκB activation 3 (ABIN-3, which inhibits NFκB activation), and dual specificity phosphatase 1 (DUSP1, which dephosphorylates p38). Of note, not all of the mechanisms mentioned have been validated in humans (reviewed in Biswas & Shalova

(2012), Cavaillon & Adib-Conquy (2006), Grutz (2005), Medzhitov & Horng (2009) and Seeley & Ghosh (2014)). However, these mechanisms are basically not selective in that they prefer the expression of one subset of genes, while another one is inhibited. The signaling inhibitors mentioned act proximally to TLR4 and thus block gene expression in a global fashion (Medzhitov & Horng 2009).

Discrimination in gene expression can be mediated on the chromatin level by *e.g.* transcriptional repressors. LPS signaling increases expression of inactive p50/p50 homodimers of NFκB, which compete with active p65/p50 heterodimers for binding to the gene targets. Moreover, detailed analyses in tolerant, monocytic THP-1 cells revealed that repression within the promoter regions of *TNF* and *IL1B* relied on a change in the composition of the transcription factor NFκB from activating p65-p50 to repressive RelB-p50 complexes (Chan *et al.* 2005, El Gazzar *et al.* 2007). RelB-binding within the *Il1b* promoter has also been demonstrated in murine microglia subjected to LPS preconditioning (Schaafsma *et al.* 2015).

Active repression can be further mediated by induction of anti-inflammatory cytokine expression *e.g.* IL-10 and TGFβ, which downregulates the activation of immune cells including monocytes and macrophages and induces expression of transcriptional regulators. For instance, IL-10 influences *TNF* gene expression by blocking transcription elongation in human primary macrophages (Smallie *et al.* 2010). Moreover, upregulated IL-10 expression in murine macrophages activates B cell lymphoma 3 (BCL3) production that negatively regulates NFκB signaling by inhibiting p65/p50 binding to its promoter sites (Kuwata *et al.* 2003). This negative mechanism, however, is selective for the murine *Tnf* gene and has no influence on *Il6* expression, although both cytokine-encoding genes belong to class T genes. By contrast, another IL10-inducible molecule called IκBNS limits murine *Il6* expression (Hirotani *et al.* 2005, Kuwata *et al.* 2006). These examples indicate that LPS-induced transcriptional regulators act on individual class T genes and limit their expression in a gene-specific manner (Medzhitov & Horng 2009). Thus, a combinational effect of several transcriptional repressors can potentially lead to the discriminative gene expression in endotoxin tolerance.

Yan and colleagues (2012) further demonstrated that binding motifs for NFκB were significantly enhanced in promoters of class T genes, but not in class NT genes in murine macrophages. Additionally, repressive p50 binding was essential for generating LPS tolerance by induction of a stable repressor complex containing the nuclear receptor co-repressor 1 (NCoR). Thus, the selective use of an NFκB binding site in promoters of pro-inflammatory (class T genes) but not antimicrobial genes (class NT genes) could further explain selective down regulation of destructive immune responses (Yan *et al.* 2012). Yet, the finding described in Yan *et al.* (2012) does not explain why the TNF and CXCL10/IP-10

production were highly tolerizable compared to IL-6 and CXCL8/IL-8 in human monocytes in this study, if tolerization of class T genes is in general dictated by NFκB binding sites. It should be interesting to investigate whether specific transcription factor binding motifs are differentially enriched within class T genes in human monocytes.

Moreover, it could be demonstrated that several transcriptional regulators interact with chromatin modifying molecules. NCoR, for instance, was shown to interact with the histone deacetylase HDAC3 within the *Tnf* promoter in murine macrophages (Yan *et al.* 2012). The transcriptional regulator RelB seemed to bind the methyltransferase G9a, which methylates H3K9 in the *TNF* and *IL1B* genes of THP-1 cells (Chan *et al.* 2005, El Gazzar *et al.* 2008, El Gazzar *et al.* 2007, Schaafsma *et al.* 2015). In the present work, enrichment of H3K9me2 could only be confirmed for the *IL1B* gene in human monocytes as demonstrated by ChIP-Seq analysis (discussed above). Another transcriptional regulator is ATF3, which has been shown to negatively regulate gene expression of *e.g. Il6* and *Il12* in an HDAC1-dependent manner in murine macrophages (Gilchrist *et al.* 2006).

To investigate the potential role of histone modifying enzymes and repressor complexes leading to distinct chromatin patterns, ChIP assays identifying NCoR and HDAC3 recruitment to the promoter regions of human *TNF*, *IL6*, *IL1B* and *FPR1* were performed. However, no enrichment of these repressive mediators in individual genes could be observed (data not shown) implying that the specific mechanism by NCoR-HDAC3 might not be involved in human monocytes. However, it cannot be ruled out that other HDACs not analyzed in this study such as HDAC1 have an impact in deacetylation of particular genes *e.g. TNF* and *CXCL10*, as LPS stimulation leads to an increase in the production of several HDACs (Aung *et al.* 2006).

Taken together, the experimental results determined in this study and by others clearly show that endotoxin tolerance has a very complex interplay, which cannot be explained by one single mechanism. The combined effect of changes in signaling and epigenetic remodeling affects LPS-induced genes by different extents, which may lead to the discriminative expression pattern known for endotoxin tolerance.

3.1.3 Summary

The analyses of specific class T and NT genes by histone modifications in human monocytes showed that the histone patterns were inconsistently affected by LPS tolerization and that the modifications only partially reflected their gene expressions in endotoxin tolerance. After examining the class T genes encoding for the cytokines and chemokines TNF, CXCL10/ IP-10, IL-1β, IL-6 and CXCL8/IL-8 indicated that a common, selective histone pattern, which discriminates the class T genes from the class NT genes, unlikely exists. The present study

further showed that selective repression of specific genes is potentially a combined effect of several molecular mechanisms including epigenetic changes and signaling effects, which jointly contribute to the phenomenon known as endotoxin tolerance.

An earlier study from Foster *et al.* (2007) introduced the concept of non-heritable transcriptional memory based on epigenetic mechanisms in endotoxin tolerance. The authors analyzed murine macrophages in an *in vitro* endotoxin tolerance model and identified two distinct histone patterns discriminated by selective changes in H3K4me3 and H4ac, which contributed to the opposing gene expression manner of class T and NT genes. They demonstrated that H3K4me3 and H4ac persisted and were more highly induced in class NT genes, whereas these activating histone marks were lost in class T genes (Foster *et al.* 2007).

The present work suggests a more complex nature of endotoxin tolerance showing that tolerization in itself seems to be very discriminative. It is known that endotoxin tolerance leads to downregulation of signaling pathways, however the effect on gene expression is quite diverse. The data obtained suggest that initial LPS signaling induces chromatin remodeling, which combined with a complex interplay of signaling duration, has an impact on gene transcription in the tolerized state. Class NT genes probably undergo chromatin remodeling so that even reduced signaling is enough for their gene expression (Medzhitov & Horng 2009, Seeley & Ghosh 2014), whereas tolerization of class T genes occurs by signaling and epigenetic changes.

This study could identify different levels of regulation: First, the class T genes analyzed possessed different patterns in transcription-linked histone modifications. Whereas *IL6* and *IL1B* showed enrichment in activating histone marks, the re-induction in H4ac and H3K27ac was diminished in the promoter regions of *TNF* and *CXCL10* in tolerant monocytes. Second, IL-6 and presumably IL-1β production showed higher sensitivity towards LPS signaling compared to TNF and CXCL10/IP-10. Third, tolerization of the genes analyzed was not mediated by a specific enrichment in the repressive histone modifications investigated. This leads to a more detailed classification of class T genes into *highly tolerizable* and *intermediate tolerizable genes* (see **Fig. 3-1** A). For instance, TNF and CXCL10/IP-10 were highly affected by endotoxin tolerance showing only low production in tolerant monocytes. The encoding genes were mainly regulated by chromatin changes affecting gene expression (*highly tolerizable*, epigenetic-driven). By contrast, IL-6 and IL-1β showed reduced expression in tolerant cells, which was mainly dependent on diminished signaling strength (*intermediately tolerizable*, signaling-driven). Moreover, the *IL8* gene possessed a similar histone pattern like the *IL6*, *IL1B* and *FPR1* genes and was highly inducible even in tolerant monocytes. Thus, it should be questioned whether *IL8* belongs to class NT genes (*non-tolerizable*) or is a subgroup of *intermediately tolerizable genes* (see **Fig. 3-1** A and B).

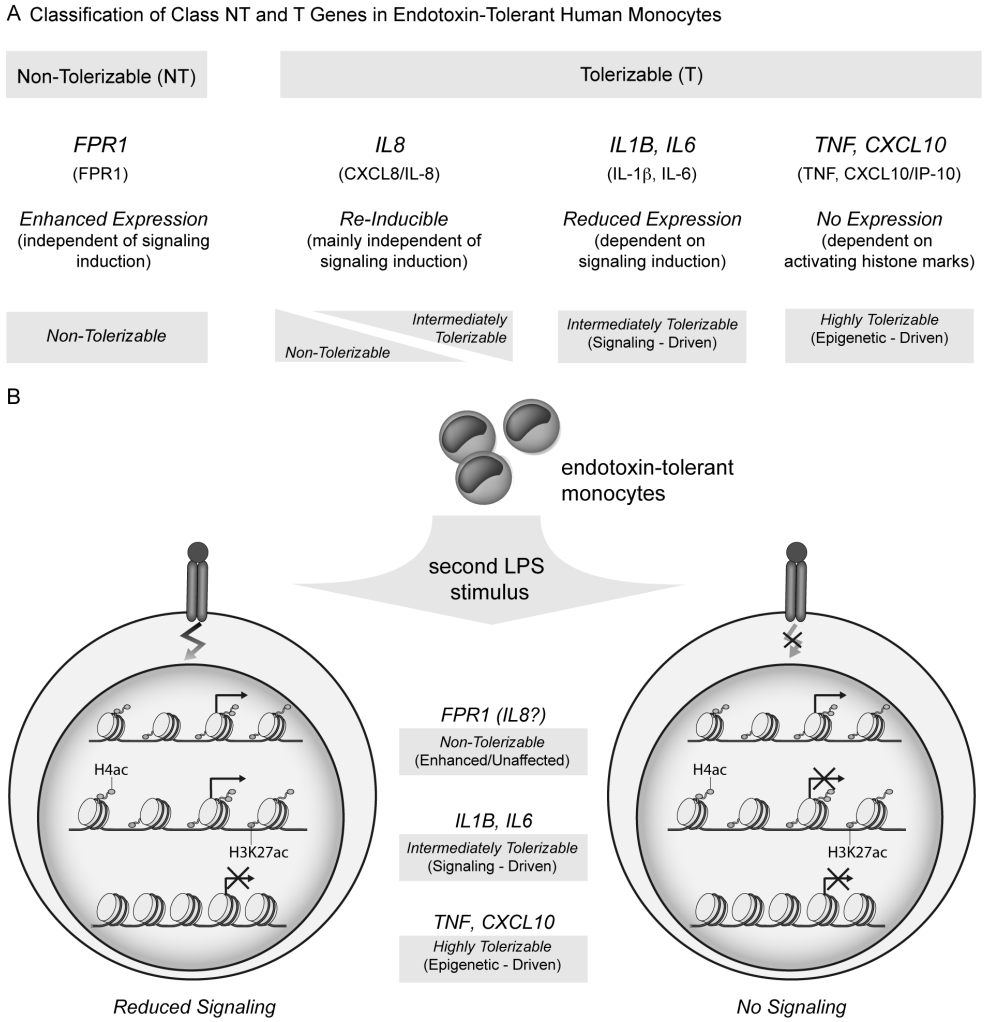

Fig. 3-1: Detailed classification of class T genes based on changes in signaling and histone modification
(A) Class T genes can be further subdivided into genes that show reduced expression in tolerant human monocytes (*intermediately tolerizable*) and genes that show an almost complete loss in gene expression (*highly tolerizable*). As CXCL8/IL-8 shows high induction capacity even in low-dose tolerized monocytes reaching almost the same expression level than naïve cells stimulated with LPS, it is a matter of debate whether the encoding *IL8* gene belongs to the *intermediately tolerizable* or *non-tolerizable* gene class. (B) In endotoxin-tolerant human monocytes, *FPR1* and *IL8* show an activating histone pattern and are expressed mainly independently of signaling strength (*non-tolerizable*). In contrast, production of IL-6 and presumably IL-1β is dictated by the signaling capacity of tolerant cells (*intermediately tolerizable*), whereas the *TNF* and *CXCL10* genes possess a *'negative'* histone pattern indicated by diminished re-enrichment in activating histone modifications, which potentially limits their gene expression (*highly tolerizable*).

3.2 Endotoxin Tolerance Alters Genome-Wide the Epigenetic Signature of Human Monocytes

Within the second part of the study, a genome-wide approach was used to investigate global epigenetic changes including histone modifications and DNA methylation induced by LPS tolerization in human monocytes.

Genome-wide analysis in histone modifications identified a shift from activating histone modifications in naïve human monocytes to repressive histone marks in endotoxin-tolerant

cells re-stimulated with LPS. The alterations in histone modifications affected mainly distinct gene cluster showing only limited co-regulations in histone marks. In naïve monocytes treated with LPS, most of the genes involved in immune responses were associated with activating histone modifications, which was reduced in tolerant cells. By contrast, genomic regions gaining enrichment particularly in repressive H3K9me2 and H4K20me3 were observed in tolerant monocytes. These regions were mainly found in intergenic loci and genes involved in signaling and transcription pathways. Analysis of transcription factor binding sites within these regions revealed a potential enrichment in the binding motifs for YY1 and SMAD3.

Moreover, endotoxin tolerance induced a global loss in DNA methylation. The identified changes in DNA methylation did not co-localized with alterations in repressive histone modifications. Finally, correlation of epigenetic changes with the gene expression pattern of tolerant monocytes identified approximately 27 % of differentially expressed genes that showed a histone pattern consistent with the histone code, while DNA methylation seemed to have no impact.

3.2.1 Global Analysis of Histone Modifications

Focusing on single genes in human monocytes provides only a glimpse into the epigenetic mechanisms involved in LPS tolerization. Therefore, genome-wide approaches using next generation techniques were applied to analyze the global changes occurring in endotoxin tolerance.

First, analyses of positive (H3K27ac, H4ac) and repressive histone marks (H3K9me2, H3K27me3 and H4K20me3) revealed a genome-wide change of differentially regulated genomic regions from a more activating histone signature in naïve human monocytes stimulated with LPS to a repressive one in LPS-tolerized cells. The identified gene clusters were characterized by an almost mutually exclusive possession of either activating (H4ac and H3K27ac) or repressive histone marks (H3K9me2, H3K27me3 and H4K20me3), implying that these epigenetic signatures do not act cooperatively in regulating gene expression of these distinct sets of genes. Comparative analyses revealed that naïve monocytes treated with LPS showed enrichment in positive histone marks, especially H4ac, in a huge gene cluster, which was lost in tolerant monocytes, probably due to the reduced signaling capacity of tolerant monocytes affecting *e.g.* NFκB and MAP kinase cascades. GO analysis of this gene cluster showed a dominance of immune response-related mechanisms. This implies that LPS tolerization minimizes the induction capacity of positive acetylation markers in genes important for immune defense processes.

In particular, intergenic sections gained an increase in repressive histone modifications implying a regulatory role of these regions in endotoxin tolerance. However, the remote

distance to potentially gene-coding regions makes it quite difficult to interpret their specific impact on LPS tolerization. Thus, genomic regions that showed differentially regulated histone modifications within the TSS ± 10 kb were further analyzed assessing a potential biological role in endotoxin tolerance. Regions that showed an increase in activating histone modifications in tolerant monocytes treated with LPS were particularly involved in metal binding and oxidative stress responses by *e.g.* metallothioneins as illustrated by GO enrichment analysis (Ruttkay-Nedecky *et al.* 2013). Indeed, mRNA expression analysis confirmed a positive correlation of *MT1L* and *MT1F* expression with enrichment in activating histone modifications in tolerant monocytes. In contrast, genomic regions that gained an increase in repressive histone marks, especially H3K9me2 and H4K20me3, during LPS tolerization were linked to transcription-involved molecules like zinc finger proteins. This implies that endotoxin tolerance might affect the gene transcription machinery in a global manner, which results in reduced gene expression. However, mRNA expression analysis of selected ZNFs in naïve and tolerant monocytes stimulated with LPS indicated that these transcription factors were expressed predominantly independently of their repressive histone pattern. Thus, the impact of enrichment in repressive histone marks needs to be validated in future studies. The induced changes may be important for the cell itself, but difficult to fully understand at the moment due to their complexity. Moreover, the present work focused on the analysis of genome-wide changes by comparing of naïve monocytes treated with LPS (N+L) with high-dose tolerized cells stimulated with LPS (T100+L). It cannot be ruled out, however, that the additional treatment of tolerant monocytes with LPS already changed the epigenetic signature of tolerant monocytes. Additionally, high-dose tolerization compared to low-dose treatment may differentially affect the epigenetic landscape. Thus, expanded analyses of the epigenetic profile of human monocytes using several tolerization conditions with or without LPS re-stimulation are required to answer this question.

Next, the differentially regulated genomic regions were analyzed for transcription factor binding sites to identify the transcription factor network associated within these genomic elements possibly leading to the observed histone patterns. The potential binding motifs in regions that were associated with an enrichment in H3K27ac and H4ac in tolerant monocytes can only be hypothesized due to the fact that only a limited number of genomic elements significantly gained activating histone modifications in tolerant monocytes treated with LPS. Regions that were co-localized by H3K27ac and H4ac most likely showed enrichment for the binding motif of AP1, implying a MAP kinase signaling-dependent mechanism of positive regulation of these genomic regions (see *Appendix* **5.6**).
Regions that showed enrichment in the repressive marks H3K9me2 and H4K20me3 in tolerant monocytes treated with LPS were significantly enhanced for the binding motif of YY1 and SMAD3, among others. Notably, the significance values obtained by HOMER were quite

low compared to the amount of peaks analyzed. Thus, only assumptions can be made regarding the possible transcription network in endotoxin tolerance.

The transcription factor YY1 can act as a transcriptional activator or repressor depending on interaction partners. In endotoxin tolerance, Liu *et al.* (2014) demonstrated that RelB, YY1 and the proto-oncogene protein Myc (c-Myc) were selectively recruited to chromatin and interacted with the H3K9me2 methyltransferase G9a, which further stabilized the repressosomal complex (Liu *et al.* 2014). Hence, YY1-mediated repression might play an important role in endotoxin tolerance. However, only approximately 1 % of genomic regions that showed enrichment in H3K9me2 and H4K20me3 in tolerant cells appeared to possess the specific binding motif for YY1. Noteably, most of the genomic regions analyzed possessed a binding motif for the transcription factor SCL, which is mainly involved in monocyte/macrophage differentiation and cell cycle (Dey *et al.* 2010), and for SMAD3, which plays an important role in TGFβ signaling (Li *et al.* 2006b, Massague 2012).

Similar to YY1, SMAD3 can act as transcriptional activator or suppressor. As activator, SMAD3 can interact with the histone acetyltransferase p300 to foster transcription (Feng *et al.* 1998, Janknecht *et al.* 1998). Interestingly, SMAD3-mediated activation of transcription can be inhibited by YY1, implying a regulatory network of both transcription factors (Kurisaki *et al.* 2003). Here, however, the association of SMAD3 binding motifs in genomic regions enriched for repressive histone modifications implies a TGFβ-mediated repression. This agrees with the observation that LPS tolerization can be partially mimicked by the administration of anti-inflammatory cytokines including IL-10 and TGFβ (Cavaillon *et al.* 1994, Randow *et al.* 1995). Inhibitory activities of TGFβ include inhibition of LPS-induced cytokine expression like IL-12, TNF and CCL3/MIP-1α, promotion of MyD88 degradation and reduction in CD14 expression, which attenuates TLR4 signaling (Reviewed in Li *et al.* (2006b)). Moreover, overexpression of NFκB p50/p50 homodimers, as shown in endotoxin tolerance, triggers gene transcription of IL-10 and TGFβ (Lawrence *et al.* 2001).

TGFβ signals through type I and type II receptors (TGFBR1/TGFBR2). Ligand binding brings both receptor types in close proximity leading to activation of type I receptors through type II receptor-mediated phosphorylation (see **Fig. 3-2**). Once activated, type I receptor phosphorylates SMAD2 and SMAD3, which dimerize and form a complex with SMAD4. The whole complex translocates into the nucleus, where it interacts with other transcription factors and chromatin-modifying enzymes to control targeted gene expression (Li *et al.* 2006b, Massague 2012). SMAD3-mediated inhibition of gene transcription is mediated through the binding of transcriptional corepressors. For instance, SMAD3 binds TGFβ-induced factor homeobox 1 (TGIF), which in turn recruits other repressors like C-terminal-binding protein (CtBP), and HDAC1 resulting in deacetylation of histone tails (Wotton *et al.* 2001, Wotton *et al.* 1999a, Wotton *et al.* 1999b). Moreover, SMAD-binding has also been

shown to be associated with repressive methylation marks. It was demonstrated that the H3K9 methyltransferase Suv39h1 binds to SMAD3, leading to suppression of IL-2 production in T cells (Wakabayashi *et al.* 2011). Additionally, SMAD3 can interact with the histone H3K9 methyltransferase G9a via the corepressor CtBP (Shi *et al.* 2003). Hence, H3K9 methylation may support silencing of the underlying gene loci. Previous advances highlighted a crucial interaction between H3K9 methylation and DNA methylation. For instance, H3K9 methylation (H3K9me2 and H3K9me3) can be recognized by adapter proteins like HP1, which can interact with DNA methyltransferases (*e.g.* DNMT3a) to promote genomic silencing. Moreover, HP1, but also H3K9 methylation itself, can be a binding platform for other histone methyltransferases like the Suv420h methyltransferases to induce repressive H4K20me3 (reviewed in Fuks (2005)).

To conclude, the transcription factor network analysis revealed that repressive modification of mainly intergenic genomic regions by repressive H3K9me2 and H4K20me3 might be potentially mediated by TGFβ/SMAD3-signaling. This provides the molecular basis for the observation that SMAD3 and SMAD4 are detrimental for the development of endotoxin tolerance (Pan *et al.* 2010, Werner *et al.* 2000). Interestingly, a negative feedback loop of SMAD3 seems to exist as the SMAD3 gene region itself was associated with enrichment in repressive histone marks in tolerant monocytes treated with LPS (see GO analysis in *Appendix* **5.7**). Thus, this study provides a mechanistic picture in which endotoxin tolerance mediates epigenetic remodeling of intergenic regions and genes involved in signaling and transcription machineries by TGFβ/SMAD3-dependent signaling. These events are likely induced during the first LPS treatment (**Fig. 3-2**). Notably, a direct link between repressive histone modifications and DNA methylation remains to be validated (discussed in **3.2.2**).

3.2.2 Global Analysis of DNA Methylation

Genome-wide changes in *de novo* DNA methylation were analyzed to elucidate its potential role in transcriptional repression in endotoxin tolerance. Whereas histone modifications are easily reversible, DNA methylation leads to stable long-term repression (Senner 2011). Surprisingly, tolerant human monocytes treated with LPS showed a general reduction in DNA methylation implying a global facilitation of gene expression. The observed decline in DNA methylation might be induced by the first LPS stimulus and its biological function needs to be analyzed in future studies.

Only a small set of genomic loci (approximately 570) near the TSS regions showed significant enrichment in DNA methylation. GO enrichment analysis indicated an over-representation of genes involved in ribonucleotide-binding, indicating a negative impact of endotoxin tolerance on the transcription machinery by DNA methylation.

As mentioned above, recent advances indicate that DNA methylation and repressive histone modifications highly cooperate to induce a silenced status in genomic regions and that both repressive marks can be dependent on each other (reviewed in Brenner & Fuks (2007), Cedar & Bergman (2009) and Rose & Klose (2014)). However, in the present work, no direct correlation between methylated DNA and repressive H3K9me2 and H4K20me3 near TSS regions could be identified. This suggests that both repressive mechanisms act independently of each other in tolerant monocytes or possibly that other histone marks not analyzed in the present study like trimethylation of H3K9 (H3K9me3) might appear in genomic regions showing parallel enrichment in DNA methylation. Furthermore, not identifying potential interactions between repressive histone marks and DNA methylation by bioinformatical analyses might be due to either excluding genomic regions by the cut-off criteria of a 2-fold change for this study or by not examining more distantly localized regions. As already mentioned above in **3.1.2**, the timepoint for the establishment of DNA methylation might be different from when histone modifications take place (no optimal timing for analysis). As only preliminary data was shown, the impact of DNA methylation and its interaction with repressive histone marks in endotoxin tolerance needs to be validated in future studies.

3.2.3 Epigenetic Changes Partially Correlate with Gene Expression

The present study illustrates that endotoxin tolerance mediates a global change in the epigenetic make-up of human monocytes. This concurs with recent studies demonstrating that epigenetic mechanisms have an impact on innate immune cell function. Saeed *et al.* (2014), for instance, analyzed the epigenome and transcriptome of naïve monocytes and compared them with naïve, tolerant and trained macrophages. The term *'trained immunity'* is understood as enhanced innate immune responses upon re-stimulation (Netea *et al.* 2011). Saeed and colleagues identified exclusive epigenetic signatures, which classify the different cell subsets.

To further elucidate the impact of the epigenetic changes observed in endotoxin tolerance (described above in **3.2.1** and **3.2.2**), the mRNA transcriptome in naïve and tolerant monocytes treated with LPS was analyzed in the present study. Consistent with the literature (Allantaz-Frager *et al.* 2013, Foster *et al.* 2007, Pena *et al.* 2011), endotoxin-tolerant monocytes showed increased transcription of genes involved in phagocytosis and wound healing (class NT genes) to maintain anti-microbial defense mechanisms, whereas gene expression for inflammatory immune responses was inhibited (class T genes). Moreover, the gene expression machinery was reduced globally. The observed expression profile was also consistent with a recent publication from Shalova *et al.* (2015), who globally analyzed the transcriptome of monocytes from sepsis patients (Shalova *et al.* 2015). The authors further

revealed a hypoxia-inducible factor 1 α (HIF1α)-dependent mechanism in functional reprogramming of monocytes to a more immunosuppressive status. HIF1α-mediated enhanced phagocytosis and tissue repair, while simultaneously inducing IRAKM, which negatively regulated TLR signaling. They also stated that the phenotypes of the monocytes analyzed were more complex than a simplified M1 (classical-activated) or M2 polarization (alternative-activated) (Shalova *et al.* 2015). A detrimental role of HIF1α was also demonstrated by two other publications from Saeed *et al.* (2014) and Cheng *et al.* (2014) in trained immunity. The authors showed that trained monocytes changed their energy balance from oxidative towards glycolytic metabolism by an mTOR/HIF1α-mediated pathway (Cheng *et al.* 2014, Saeed *et al.* 2014).
These publications indicate that HIF1α is a potential master regulator in programming monocytes and macrophages towards inflammatory settings. Thus, its role in TGFβ-mediated induction of repressive histone marks is of high interest in future studies.

The observed gene expression pattern in tolerant monocytes partially correlated with the identified epigenetic changes induced by endotoxin tolerance. Approximately 1000 of 3638 differentially expressed genes (27 %) showed expression patterns consistent with the histone code. Especially alterations in activating H4ac and H3K27ac highly correlated with gene transcription. By contrast, no significant correlation could be identified between gene expression and DNA methylation.
Strikingly, several thousand genomic regions (> 10 000) were identified by ChIP-Seq, which showed significant enrichment in repressive H3K9me2 and H4K20me3 in endotoxin tolerance. However, genes that possessed a reduced expression behavior appeared far less with 1758 genes identified. The high abundance of these repressive histone marks without a concurrent reduction in expression, especially in intergenic regions, implies a regulatory function in endotoxin tolerance. Thus, LPS tolerization may require multiple LPS-related enhancer sites for each gene. It further suggests that the given epigenome provides the framework and allows higher plasticity in what can potentially be expressed, whereas the endotoxin tolerance-induced transcriptional regulators mediate *de facto* the tolerant phenotype of monocytes. This is in agreement with data from the research group of Prof. Joachim L. Schultze (Life & Medical Sciences Institute (LIMES), Bonn, Germany), who demonstrated that irrespective of gene expression, most genes possessed similar epigenetic marks in IFNγ-, IL-4- or TNF+PGE2+P3C (TPP)-treated human macrophages; and that basically the master transcription factors in each condition were responsible for the different macrophage phenotypes (Xue *et al.* (2014) and personal communication). However, the main question remains as to whether the outcome of these transcriptional regulators is affected by epigenetic signatures. Alternatively, regarding the fact that LPS stimulation

means cellular stress, these regulatory elements may help to regulate constitutively expressed genes, which are critical for the biological setting (Smale 2010b).

To conclude, only a subset of differentially expressed genes could be linked to a specific epigenetic signature in the present work. However, chromatin remodeling by histone modifications and DNA methylation is not the only *'gatekeeper'* for transcriptional activity and additional factors are essential for the final regulation of gene transcription. Recent studies indicate that the specific network of transcriptional regulators have a crucial impact in the macrophage phenotype (Saeed *et al.* 2014, Xue *et al.* 2014). A study by Lavin *et al.* (2014) could also show that the local microenvironment has a higher influence in shaping the chromatin landscape of macrophages than expected (Lavin *et al.* 2014). The recent advances in macrophage immunity imply that one key protagonist does not solely mediate endotoxin tolerance.

Moreover, processes that go beyond the mechanisms analyzed in this study such as nuclear translocation of transcription factors and post-transcriptional regulations could additionally regulate gene expression. The MAP kinase p38, for instance, influences stability of mRNA transcripts bearing AU-rich elements (ARE) (Dean *et al.* 2004) and plays a crucial role in LPS/TLR4-induced systemic inflammation (Schottelius *et al.* 2010). Following p38 signaling, MAP kinase-activated protein kinase 2 (MK2) activates ARE-binding proteins, which in turn binds to AREs of mRNAs and mediates either stabilization or destabilization of target transcripts (Barreau *et al.* 2005). The stability of several cytokine mRNAs, including those of *TNF*, *IL6* and *IL8*, have been reported to be regulated by ARE-binding proteins (reviewed in Palanisamy *et al.* (2012)). For instance, a well-known destabilizer of TNF-mRNA-transcripts is tristetraproline (TTP, also known as ZFP36) (Carballo *et al.* 1998), whereas work from our group showed that Tis11d (ZFP36L2), another member of the TTP family, has a more stabilizing effect on TNF-mRNA-transcripts compared to TTP (Bossmann 2009). Furthermore, post-transcriptional regulation by microRNAs (miRNAs) resulting in selective downregulation of protein expression have been implicated in endotoxin tolerance (Nahid *et al.* 2011, Seeley & Ghosh 2014). MiRNAs are short non-coding RNAs, which regulate gene expression by complementary gene interference resulting in degradation of targeted mRNA or inhibition of translation. For instance, miR-221, miR-579 and miR-125b are involved in *TNF* transcript degradation, which may explain the strong hyporesponsiveness of TNF (El Gazzar & McCall 2010). Additionally, miRNA-146a, miRNA-155 and miRNA-12 are thought to downregulate LPS/TLR signaling (Taganov *et al.* 2006). Sheedy *et al.* (2010) demonstrated that miR-21 suppressed NFκB activation and transcription of *IL6* mRNA, but simultaneously promoted production of IL-10 (Sheedy *et al.* 2010).

Finally, a direct link between epigenetic modifications and miRNAs does exist. Whilst DNA methylation and histone modifications influence miRNA expression, miRNAs itself can affect epigenetic modifications by targeting chromatin-modifying enzymes (Sato *et al.* 2011, Wang *et al.* 2015). But again, no single miRNA could be identified, which could completely account for the characteristic phenotype of endotoxin tolerance (Seeley & Ghosh 2014). This further implies that the phenomenon of LPS tolerance relies on a complex machinery of several interaction partners, which together results in the phenotypic characteristics known for endotoxin tolerance.

3.2.4 Summary

The present study provides a detailed description of the epigenetic changes occurring during endotoxin tolerance. A bottom-up approach was used by focusing on chromatin alterations rather than analyzing transcriptome changes. Site-specific post-translational modifications of histone proteins and DNA methylation mediate recruitment of transcription factors and other chromatin-modifying proteins, and provide a more stable picture of what occurs during tolerization than simple gene expression analyses. These changes may have an impact for a longer time period, as transcriptome analyses only provide a snapshot of the current gene expression.

Endotoxin tolerance induced a genome-wide change in the epigenetic make-up of human monocytes. As these changes occurred in higher abundance than the actual number of differentially expressed genes, the present results imply that global alterations in chromatin structure are required for tolerance induction resulting in the characteristic expression behavior of tolerant monocytes.

Treatment of human monocytes with LPS induced a global change from activating, positive histone modifications in naïve monocytes to repressive histone marks in tolerant cells. Detailed analyses of endotoxin-tolerant human monocytes revealed that a large gene cluster including immune response genes showed limited induction capacity in acetylation of H4 and H3K27 (probably due to reduced signaling induction in tolerant cells), whereas only a small set of genomic regions was associated with an enrichment in activating histone modifications. These chromatin changes clearly correlated with gene transcription. Moreover, LPS tolerization induced a global enrichment in repressive histone modifications, particularly H3K9me2 and H4K20me3, in mainly intergenic regions. The high abundance of these repressive marks was mainly independent of gene expression, which implies a regulatory function of these regions in induction of endotoxin tolerance. Strikingly, genomic regions located near the TSS, which showed induction of repressive H3K9me2 and H4K20me3 in endotoxin-tolerant monocytes, were preferentially linked to molecules involved within the

transcription and signaling network as indicated by GO analysis. Thus, induction of repressive histone modifications by LPS tolerization may influence gene expression in an indirect manner by targeting the signaling/transcription framework.

Transcription factor binding site analyses within genomic regions that showed enrichment in the repressive histone marks H3K9me2 and H4K20me3 were potentially enriched for the binding motif of SMAD3, implying a TGFβ-dependent mechanism in endotoxin tolerance (**Fig. 3-2**).

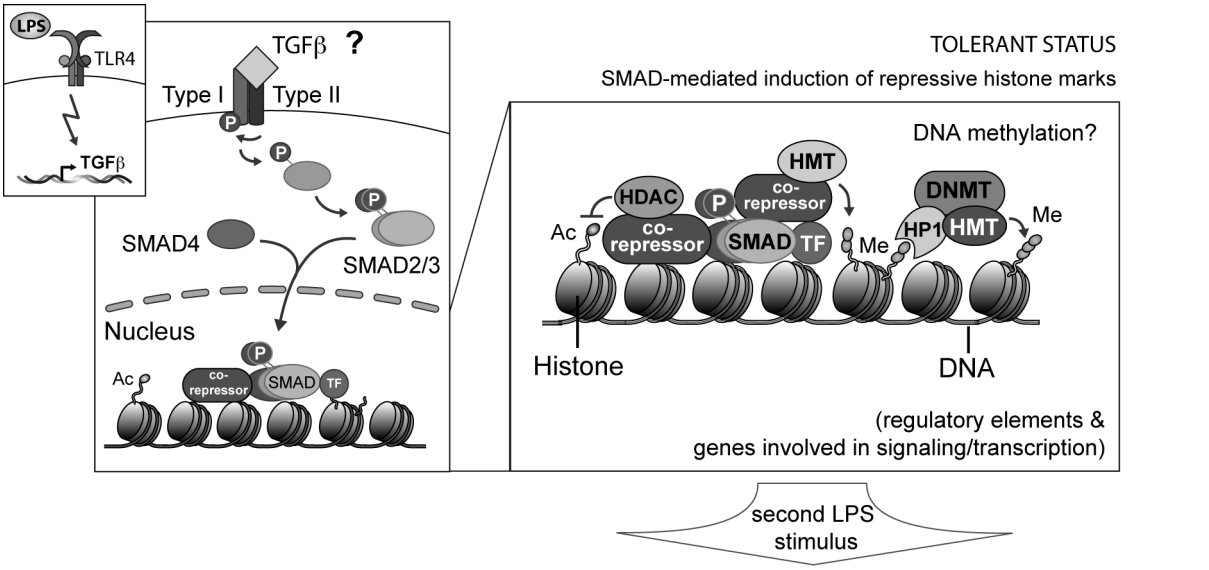

Fig. 3-2: Model for regulation of endotoxin tolerance by TGFβ signaling. First, LPS treatment leads to induction of TGFβ expression as a negative feedback loop to downregulate inflammation. Subsequently, TGFβ itself acts on monocytes to establish a repressive histone pattern. Signaling of TGFβ involves two types of transmembrane serine/threonine receptors. TGFβ ligands bind first to type II receptors, which recruit and engage type I receptors to form a complex. Type II receptors then activate the type I components, which in turn phosphorylate intracellular SMAD transcription factors (SMAD2 and SMAD3). These molecules are also called receptor-regulated SMAD proteins (R-SMADs). Phosphorylated SMAD2 and SMAD3 dimerize and associate with the common SMAD4, also termed Co-SMAD, leading to translocation into the nucleus (Massague 2012). Lineage-specific transcription factors (TF) direct SMAD transcription factors to specific genomic regions. In endotoxin tolerance, activated SMADs potentially interact with co-repressors (TGIF, CtBP) to induce a repressive epigenetic pattern at target regions. TGIF, for instance, can interact with HDACs resulting in deacetylation of histone tails. Moreover, CtBP recruits histone methyltransferases (HMTs) like G9a, which induce methylation of H3K9. An amplification of repression can be generated by DNA methylation. For instance, the adapter protein HP1 can recognize the repressive histone mark H3K9me2 (reviewed in Shinkai (2011)) and recruit DNA methyltransferases (DNMTs), but also other HMTs like the H4K20me3 methyltransferase Suv4-20h (reviewed in Fuks (2005)). Eventually, induction of a repressive epigenetic signature by TGFβ in intergenic regions and genes involved in signaling and transcription may indirectly influence the signaling capacity in tolerant monocytes leading to a reduced induction of activating acetylation marks at histone proteins located in immune response genes. Notably, a direct link between repressive histone marks and DNA methylation could not be confirmed in this work and is shown only to complete the regulatory picture.

TGFβ signaling may influence the epigenetic signature towards a more repressive status, which impacts intergenic regions and mainly signaling- and transcription-linked molecules. By targeting these molecules within the complexity of signaling network, downstream targets are affected as well, which leads to a kind of domino effect in tolerization resulting in direct and indirect repression, see **Fig. 3-2**.

LPS tolerization further influenced DNA methylation in human monocytes in a global fashion. In contrast to histone modifications, however, endotoxin tolerance induction led to a global decrease in DNA methylation indicating a reduction in gene silencing. Moreover, changes in DNA methylation did not directly co-localize with alterations in histone modifications. Thus, its impact in induction of endotoxin tolerance has to be the focus of future studies.
Correlation of the identified epigenetic changes with global mRNA transcriptome analysis indicated that not all differentially expressed genes were regulated or affected by the epigenetic signature found. This also correlates with results obtained by the detailed analysis of individual immune response genes in endotoxin tolerance (*TNF* & *CXCL10* versus *IL6* & *IL1B*, see *Discussion* section **3.1**) implying that the specific epigenetic changes and signaling events might distinctly affect genes or gene classes.

3.3 Impact of Epigenetic Changes in Endotoxin Tolerance and Sepsis

Endotoxin tolerance provides a protective mechanism against excessive inflammation, however, its incidence also plays a critical role in sepsis. Here, initial tolerance induction serves as host protection against uncontrolled inflammation due to tissue damage and massive release of pro-inflammatory mediators (*'cytokine storm'*). But prolonged unresponsiveness of immune cells leads to a higher risk of developing secondary infections, which results in the increased mortality of sepsis patients (Biswas & Lopez-Collazo 2009). Although endotoxin tolerance does not completely cover the complexity of sepsis, several events of sepsis can be mimicked by endotoxin tolerance. Thus, understanding the molecular mechanisms in tolerance induction is critical for the development of novel treatment strategies in order to activate immunosuppressed immune cells when necessary for sepsis patients.

The results presented here clearly demonstrated that endotoxin tolerance influenced the epigenetic signature of human monocytes far beyond the actual gene expression pattern of tolerant human monocytes. These findings agree with recent discoveries showing that distinct epigenetic programming of innate immunity is shaped by environmental factors (Chen *et al.* 2014, Cheng *et al.* 2014, Lavin *et al.* 2014, Saeed *et al.* 2014).
Moreover, a publication by Weiterer *et al.* (2015) showed that global epigenetic changes also occur in sepsis patients. The authors demonstrated that sepsis induced a specific change in

H3K4me3 and H3K27me3 in distinct promoter regions of immunologically relevant genes (Weiterer *et al.* 2015). Another recent publication further implied that a combinational treatment with epigenetic modifiers which affect both histone modifications and DNA methylation modulated murine macrophages in endotoxin-induced acute lung injury (Thangavel *et al.* 2015).

Finally, LPS tolerization can last for several days. This is more profound for sepsis, where immunosuppression can persist for weeks or even years as indicated by studies showing a reduction in long-term survival of patients who survived sepsis (Iwashyna *et al.* 2010, Perl *et al.* 1995, Quartin *et al.* 1997). This implies that even newly generated immune cells from the bone marrow may not restore an efficient immune system and that epigenetic changes mediated by LPS tolerization occur at the level of hematopoietic stem cells (Carson *et al.* 2011). Moreover, bacterial infections generate a heritable change or a kind of fingerprint that persists even when the pathogen is eradicated (reviewed in Bierne *et al.* (2012)).

Hence, endotoxin tolerance and sepsis are highly complex and multifaceted phenomena, which involve changes in signaling events and remodeling of chromatin structure by histone modifications and DNA methylation as analyzed in this study, but also post-transcriptional control by microRNAs as discussed above. Still, the mechanisms as a whole are not completely understood and we are currently starting to elucidate the global changes in the epigenetic and transcriptional programs, which directly or indirectly influence the gene re-programming associated with endotoxin tolerance and sepsis. Thus, controlling these genome-wide changes may provide new opportunities in the treatment of sepsis patients.

3.4 Outlook

The study presented showed that endotoxin tolerance mediated a global change in the epigenetic makeup of primary, human monocytes. So far, only genomic regions near the TSS of genes were analyzed in detail, but the results clearly illustrate that endotoxin tolerance mainly influenced intergenic regions such as enhancers. A general marker for enhancers is H3K4me1 (Heintzman *et al.* 2007). Future analysis of enhancers in endotoxin tolerance will be achieved by *e.g.* performing ChIP-Seq assays directed towards H3K4me1 or utilizing the sequencing data provided by the Encyclopedia of DNA Elements (ENCODE) Project (Consortium 2012). Co-localization analysis with H3K27ac excluding promoter regions will give an insight into potentially activated enhancers. Moreover, Ghisletti *et al.* (2010) identified dynamic enhancers in murine macrophages by LPS-inducible binding of the acetyltransferase p300 to chromatin exploiting enhancers associated with inducible genes. The underlying DNA sequences provide binding for the tissue-restricted transcription factor

PU.1 and stimulus-activated transcription factors like NFκB and AP1 (Ghisletti *et al.* 2010). Thus, it will be of huge interest in future studies to determine how this regulatory network will work in endotoxin-tolerant cells.

The present results did not show a major role for DNA methylation in endotoxin tolerance, however these data are preliminary. Consequently, future studies in DNA methylation, probably in combination with other repressive histone marks *e.g.* H3K9me3, are essential to clarify the impact of methylated DNA regions in endotoxin tolerance.

In addition, transcription factor motif analyses in genomic regions that gained repressive H3K9me2 and H4K20me3 in tolerant monocytes treated with LPS revealed a possible role for SMAD3. ChIP-Seq assays using antibodies directed towards activated (phosphorylated) SMAD3 will be necessary to confirm its role in the regulation of endotoxin tolerance and to identify the genomic target regions.

Finally, regarding the fact that endotoxin tolerance lasts for several days, analysis of the observed epigenetic changes in LPS-tolerant monocytes for more than one day will be of interest for future research to elucidate the stability and functions of these alterations. Additionally, comparing *in vitro* data to the analysis of epigenetic markers in sepsis patients both during and after recovery will provide a detailed insight in the molecular, epigenetic processes occurring during sepsis.

4. Materials & Methods

4.1 Software & Programs

Software/Program	Notes
BEDTools	Software suite for the comparison, manipulation and annotation of genomic features (Quinlan & Hall 2010).
BigWig tools	Converts BedGraph file to BigWig file. Part of UCSC's command line utilities (Kent *et al.* 2010).
Bioconductor project	Contains software packages for implementation in R. Available online (as of October 2015): http://www.bioconductor.org/. (Gentleman *et al.* 2004, Huber *et al.* 2015).
BiQ Analyzer HiMod	Software for analysis of bisulfite sequencing data (Becker *et al.* 2014).
BWA Aligner	Alignment of NGS data to a reference genome (Li & Durbin 2009).
CellQuest	Acquisition of flow cytometry data, BD Biosciences (Franklin Lakes, NJ, USA).
ChIPseeker	Tool for analysis and visualization of ChIP-Seq data (Yu *et al.* 2015).
cummeRbund	Bioconductor package for analysis of Cufflinks data (RNA-Seq analysis). (Goff *et al.* 2013)
DAVID	Database for Annotation, Visualization and Integrated Discovery, GO enrichment analysis (Huang *et al.* 2009a, b).
FACSDiva	Acquisition of flow cytometry data, BD Biosciences (Franklin Lakes, NJ, USA).
FastQC	Quality control of fastq files. Available online (as of October 2015): http://www.bioinformatics.babraham.ac.uk/projects/fastqc/ (Andrew 2010).
FlowJo	Analysis of flow cytometry data, FlowJo, LLC (Ashland, Oregon, USA).
Galaxy project	Platform for NGS data analysis. Available online (as of October 2015): http://galaxyproject.org/ . (Blankenberg *et al.* 2010, Giardine *et al.* 2005, Goecks *et al.* 2010).
GeneOverlap	Bioconductor package for analysis of gene lists (Shen & Sinai 2013).
GraphPad Prism	Data analysis tool, GraphPad Software (La Jolla, USA).
GREAT	Genomic Regions Enrichment of Annotations Tool for ChIP-Seq data. GO enrichment analysis, available online (as of October 2015): http://bejerano.stanford.edu/great/public/html/ (McLean *et al.* 2010).
gplots	R tool for plotting data (Warnes *et al.* 2015).
HOMER	Motif discovery and analysis of ChIP-Seq data. Available online (as of October 2015): http://homer.salk.edu/homer/index.html (Heinz *et al.* 2010).
Integrative Genome Viewer (IGV)	Genome browser for visualization of binding profiles. Available online (as of October 2015): https://www.broadinstitute.org/igv/. (Robinson *et al.* 2011, Thorvaldsdottir *et al.* 2013).
MEDIPS	Bioconductor package for analysis of differential DNA methylation (Lienhard *et al.* 2014).
R language	Statistical computing and graphics. Available online (as of October 2015): http://www.R-project.org/. (RCoreTeam 2014).
SAMtools	Converts SAM files to BAM files (Li *et al.* 2009).
SICER	Detection of significant DNA-histone protein interactions (Zang *et al.* 2009).
TopHat / Cufflinks	Software tools for analysis of RNA-Seq data. (Trapnell *et al.* 2009, Trapnell *et al.* 2010)
UCSC Genome Browser	Genome browser for visualization of binding profiles. Available online (as of Octber 2015): https://genome.ucsc.edu/. (Kent *et al.* 2002).

4.2 Materials

All reagents and substances described in the *Methods* section **4.3** were purchased from Abcam (Cambridge, United Kingdom), Agilent Technologies (Santa Clara, California, USA), Applied Biosystems (by Thermo Fisher Scientific; Waltham, Massachusetts, USA), BD Biosciences (Franklin Lakes, New Jersey, USA), Biochrom AG (Berlin, Germany), BioLegend (San Diego, California, USA), Calbiochem (by Merck Millipore; Billerica, Massachusetts, USA), Carl Roth (Karlsruhe, Germany), Diagenode (Seraing (Ougrée), Belgium), eBioscience (by Affymetrix; Santa Clara, California, USA), GE Healthcare (Chalfont St Giles, United Kingdom), Gibco (by Thermo Fisher Scientific; Waltham, Massachusetts, USA), Invitrogen (by Thermo Fisher Scientific; Waltham, Massachusetts, USA), Macherey-Nagel (Dueren, Germany), Merck Millipore (Billerica, Massachusetts, USA), Miltenyi Biotech (Bergisch Gladbach, Germany), New England BioLabs (Ipswich, Massachusetts, USA), PAA (by GE Healthcare; Chalfont St Giles, United Kingdom), PAN-Biotech (Aidenbach, Germany), Qiagen (Hilden, Germany), R&D Systems (Minneapolis, Minnesota, USA), Roche (Basel, Swiss), Sarstedt (Nuembrecht, Germany), SERVA Electrophoresis (Heidelberg, Germany), Sigma-Aldrich (St. Louis, Missouri, USA) and Thermo Fisher Scientific (Waltham, Massachusetts, USA).

Necessary catalog numbers (*Cat. No.*) and lot numbers (*Lot No.*) are indicated within the *Methods* section **4.3**.

4.3 Methods

4.3.1 Cell Culture

4.3.1.a Human Peripheral Blood Mononuclear Cell (PBMC) Isolation

Human peripheral blood mononuclear cells (PBMCs) were isolated from buffy coat preparations via density gradient (Boyum 1968, Ulmer *et al.* 1984). In brief, heparinized blood was diluted 1:2 with phosphate buffered saline (PBS, Gibco). Thirty-five ml of diluted blood was carefully layered over 15 ml Ficoll (Biocoll, Biochrom AG, density: 1.077 g/ml) and centrifuged for 20 min at room temperature (RT) and 1000 x g (without deceleration). The interface containing PBMCs was transferred into fresh tubes and was washed twice with PBS (Gibco). Subsequently, cells were used for human $CD14^+$ MACS separation (see **4.3.1.b**).

4.3.1.b Human Monocyte Isolation by Magnetic Cell Separation

$CD14^+$ human monocytes were isolated from PBMCs using magnetic-activated cell sorting (MACS) according to the manufacturer's protocol (Miltenyi Biotec) with the following modifications: Human CD14 MicroBeads (Milteny Biotec, *Cat. No. 130-050-201*) were added in a ratio of 1:25 (beads:buffer volume) to 1 x 10^7 PBMCs in 80 µl of cold MACS buffer containing PBS (Gibco), 0.5 % low-endotoxin fetal calf serum (FCS, Biochrom AG) and 2 mM EDTA (Merck Millipore, sterile-filtered) and incubated for 30 min at 4 °C with occasional gentle shaking. Subsequently, cells were washed and isolated using a MACS separator. The purity was tested by CD14 labeling and flow cytometric analysis. Generally, a

purity of ≥ 90 % of CD14-positive living cells was achieved (see **4.3.2.a** for staining). Approximately 1 x 10^8 $CD14^+$ monocytes were isolated from 1 x 10^9 PBMCs generated from buffy coat preparations.

4.3.1.c Human Monocyte Cultures and the Endotoxin Tolerance Model

Human $CD14^+$ monocytes were cultured at a density of 2 x 10^6/ml in IMDM medium (PAA or Biochrom AG) supplemented with 10 % human AB serum (PAN-Biotech, *Cat. No. P30-2901, Lot No. P073305*), 4 mM L-alanyl-L-glutamine, 100 U/ml penicillin and 100 µg/ml streptomycin (all Biochrom AG) at 37 °C and 5 % CO_2 in low cell binding multiwell plates (Nunc™, Sigma-Aldrich, *Cat. No. Z721050-7EA or Z721077-7EA*). For a detailed description of the optimization of culture conditions for cultivation of human monocytes see **4.3.1.d** (below).

For induction of endotoxin tolerance, $CD14^+$ monocytes were treated with either 1 ng/ml or 100 ng/ml LPS (from *Escherichia coli*, serotype O111:B4, TLRgrade, Enzo Life Sciences, *Cat. No. ALX-581-012*) overnight for 16 to 24 h (tolerant, T). If not otherwise stated, tolerized cells with 100 ng/ml LPS were termed either T or T100, whereas tolerized cells with 1 ng/ml were indicated as T1. In parallel, unstimulated cells served as control (naïve, N). Subsequently, cells were washed with PBS (Gibco), cultured in fresh, complete IMDM medium and challenged with 100 ng/ml LPS for the times indicated (termed N+L, T+L, T1+L or T100+L).

4.3.1.d Optimization of Culture Conditions for Cultivation of Human Monocytes

Isolated monocytes were cultured in three different types of cell culture plates (tissue culture-, non- and MPC-treated), two different media (RPMI 1640 and IMDM) and sera (human AB and FCS).

Tissue culture-treated plates have a hydrophilic surface promoting cell attachment, whereas non-treated plates provide a more hydrophobic environment ideal for low cell binding[3]. Plates covered by the polymer MPC (2-methacryroyloxy-ethylphosphorylcholine) (Koike *et al.* 2005), which mimics cell membrane surfaces, offer a very low cell binding platform, therefore, limiting unwanted differentiation and providing a better physiological conditions for monocytes[4].

A very popular medium for cultivation of a wide range of immune cells is RPMI 1640 medium developed in the Rosewell Park Memorial Institute, which is a modification of MEM medium (Eagle's Minimum Essential Medium). Another common medium also based originally on the MEM medium is Iscove's modified Dulbecco's medium (IMDM) that supports cultivation of B and T lymphocytes, macrophages and monocytes (Reviewed in Langdon (2004) and Schmitz (2011a)).

For cell growth and metabolism, the supplementation of culture media with serum is very common. The most widely used animal serum is fetal calf serum (FCS). Besides addition of FSC, cultivation of cells in species-specific serum, in this case human serum, provides a more physiologically comparable environment. For minimizing immunoreactivity, human serum from type AB blood is generally used, since it does not contain anti-A and anti-B antibodies against antigens on erythrocytes (reviewed in Schmitz (2011b)).

[3] Indicated by distributor: https://www.fishersci.com/shop/products/falcon-tissue-culture-plates/p-154828 (as of October 2015)

[4] Indicated by distributor: http://www.sigmaaldrich.com/catalog/product/sigma/z721050?lang=de&region=DE (as of Occtober 2015)

Monocytes isolated from PBMCs following CD14-positive magnetic separation were cultured in either tissue culture-, non- or MPC-treated plates in RPMI or IMDM medium supplemented with human AB or FCS serum. The viability was determined by flow cytometric analysis (see *Material* section **4.3.2.a** and **4.3.2.c** for staining). Cells were stained with the dye 7AAD to indicate dead cells, and the monocytic marker CD14. Viable cells were considered 7AAD-negative and CD14-positive.

Cells cultured in MPC-treated plates in combination with IMDM medium supplemented with human AB serum showed the highest viability (**Fig. 4-1** A), whereas cultivation of cells in tissue culture-treated plates in RPMI medium and FCS decreased the expression of CD14 by 5 times (**Fig. 4-1** B). Comparison of all three factors (plates, media and sera) indicated that serum selection had the most striking effect on monocyte viability, followed by the type of medium and the cell culture plate. The cumulative effect of the optimal serum (human serum), the optimal medium (IMDM) and the optimal plate (MPC-treated) offered the highest viability of human monocytes (**Fig. 4-1** C and D).

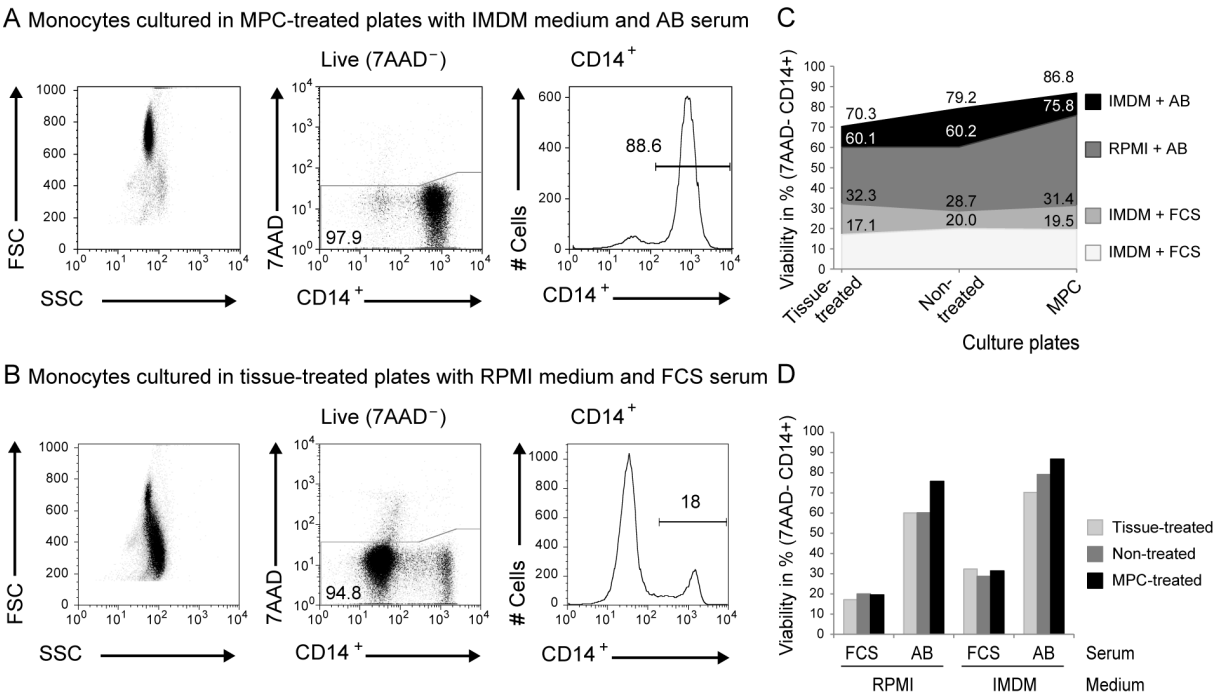

Fig. 4-1: Cultivation of human CD14⁺ monocytes in different culture plates, media and sera. PBMCs were isolated from buffy coat preparations followed by CD14-positive isolation by magnetic-cell sorting. Human $CD14^+$ monocytes were cultured for one day either in tissue culture-, non- or MPC-treated plates in RPMI or IMDM medium supplemented with human AB or FCS. The viability of cells was analyzed by 7AAD and CD14 staining following flow cytometric analysis. (A and B) Gating strategy for analysis of cell viability: Living monocytes were considered 7AAD-negative and CD14-positive. (C and D) Cell viability of cultured human monocytes (% of $7AAD^-$ $CD14^+$) is depicted dependent on cell culture plates (C) or different kinds of media and sera (D). Data represents one experiment out of two. Human AB serum was kindly provided by the research group of *Prof. Carmen Scheibenbogen* (Charité – Institut für Medizinische Immunologie, Berlin, Germany).

The human AB serum for the initial viability test (see above) was kindly provided by the research group of *Prof. Carmen Scheibenbogen* (Charité – Institut für Medizinische Immunologie, Berlin, Germany). To obtain a human AB serum suitable for further use in monocyte cultivation, several human sera from different companies and batches were tested for stimulation capacity measured by the production of the pro-inflammatory cytokine TNF.

From the sera tested (**Fig. 4-2** A and B), only one human AB serum from PAN-Biotech (PB-2, **Fig. 4-2** B) showed similar characteristics compared to the control serum provided by the research group of *Prof. Carmen Scheibenbogen*. Both sera showed low levels of pre-stimulation of untreated monocytes indicated by low TNF release into the cell culture supernatant, yet high induction of TNF production after LPS stimulation. Notably, the release of TNF after LPS stimulation in PB-2 or control serum was lower than for all of the other tested sera, but the overall ratio of LPS-treated monocytes compared to untreated ones was similar or even higher than the other sera.

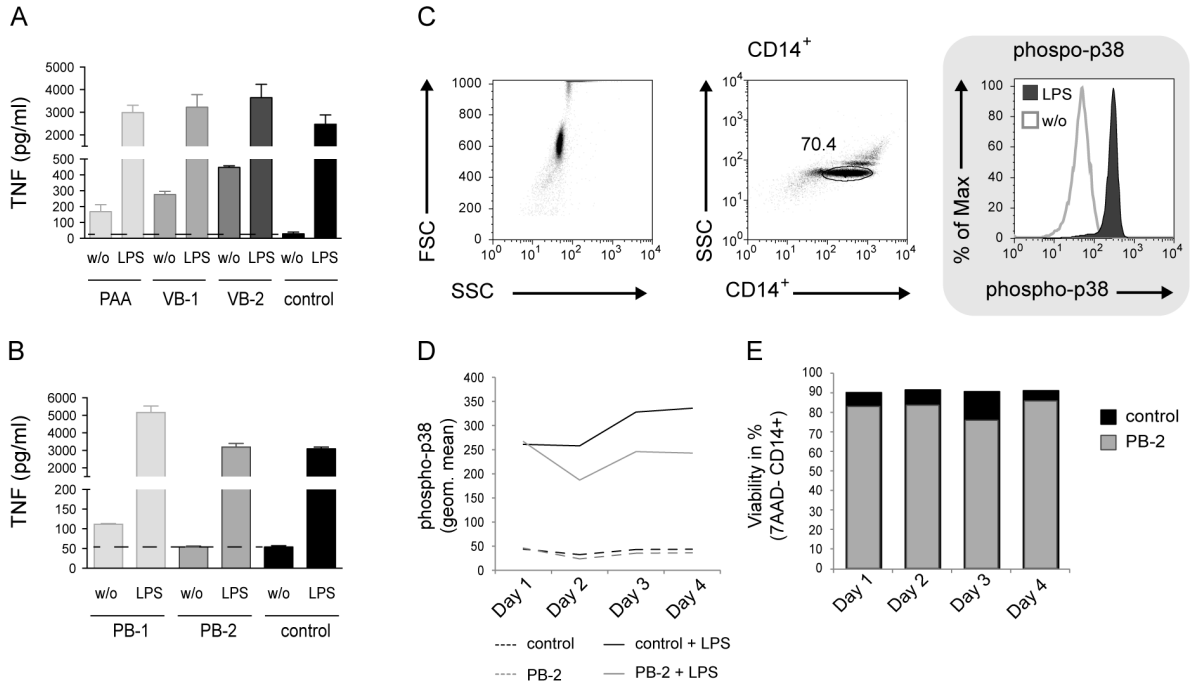

Fig. 4-2: Cultivation of human CD14$^+$ monocytes in several human AB sera. Following PBMC and CD14-positive isolation, human monocytes were cultured in MPC-treated plates in IMDM medium supplemented with different human AB sera. All sera were heat-inactivated and sterile-filtered. (A and B) Cells were cultured in the following sera: from PAA / *Cat. No.* C05-021 / *Lot No.* C02111-3986 (PAA), Valley Biomedicals / *Cat. No.* HS1017HI / *Lot No.* 2A0084 (VB-1), Valley Biomedicals / *Cat. No.* HS1017HI / *Lot No.* 2C0431 (VB-2), PAN-Biotech / *Cat. No.* P30-2901M / *Lot No.* P442000 (PB-1) and PAN-Biotech / *Cat. No.* P30-2901M / *Lot No.* P073305 (PB-2). Human AB serum kindly provided by the research group from *Prof. Carmen Scheibenbogen* was used as control. Cells were stimulated for 4 h with 100 ng/ml LPS or left untreated (w/o). Supernatants were subjected to TNF measurement by ELISA. Data are representative out of 2 independent experiments; shown are mean ± standard deviation. (C) Signaling in monocytes: Gating strategy for evaluation of p38 phosphorylation by flow cytometric analysis. (D and E) Monocytes cultured for up to 4 days in serum from PAN-Biotech (PB-2) or control (Scheibenbogen) were checked every day by flow cytometric analysis for stimulation capacity indicated by p38 phosphorylation after 15 min treatment with 100 ng/ml LPS (D) and for viability (E). Data represent one experiment out of two.

Finally, human CD14$^+$ monocytes were cultured for up to four days in MPC-treated plates and IMDM medium supplemented with control or PB-2 serum and checked every day for stimulation capacity and viability by flow cytometric analysis. Cultivation of primary human monocytes for experimental procedures normally lasted two to three days.

Signaling capacity (see **4.3.2.d** below for staining) was analyzed by induction of intracellular p38 phosphorylation after LPS stimulation for 15 min compared to untreated cells (**Fig. 4-2** C and D). Moreover, untreated cells were analyzed for viability by staining monocytes for 7AAD and CD14 (**Fig. 4-2** E). In general, monocytes cultured in PB-2 showed lower p38 MAP kinase signaling induction

and lower viability compared to control serum during the four days of cultivation. However, these effects were consistent over the time analyzed. Thus, PB-2 from PAN-Biotech (*Cat. No.:* P30-2901M, *Lot No.:* P073305) was considered as a suitable surrogate for the human AB serum provided by the research group of *Prof. Carmen Scheibenbogen* for the cultivation of human monocytes.

4.3.1.e Isolation and Cultivation of Murine Bone Marrow-Derived Macrophages

Bone marrow cells were isolated from mice with a C57BL/6 background and cultured for five to seven days in tissue culture treated plates (BD Biosciences) in RPMI-1640 medium (Biochrom AG) supplemented with 50 ng/ml murine M-CSF (Miltenyi Biotech), 10 % low-endotoxin FCS, 2 mM L-alanyl-L-glutamine, 100 U/ml penicillin and 100 µg/ml streptomycin (all Biochrom AG) at 37 °C and 5 % CO_2. Differentiated murine macrophages were checked for purity by flow cytometry using CD11b and F4/80 surface staining, **4.3.2.c**, replated at a density of 1 – 2 x 10^6/ml, and stimulated the following day with 100 ng/ml LPS (from *Escherichia coli*, serotype O111:B4, TLRgrade, Enzo Life Sciences, *Cat. No. ALX-581-012*) for 24 h (tolerant, T). Untreated cells served as a control (naïve, N). Subsequently, cells were washed, given fresh media and challenged with 100 ng/ml LPS for the time points indicated (N+L, T+L).

4.3.2 Flow Cytometry

Fluorochrome-labeled antibodies used for flow cytometric analyses are listed in **Table 4-1**.

Table 4-1: List of antibodies and staining dyes used for flow cytometric analyses.

Molecule (Clone)	Conjugate	Company	Cat. No.
Anti-human CD14 (MϕP9)	PE	BD Biosciences	345785
Anti-human CD14 (M5E2)	BV510	BioLegend	301842
Anti-human FPR1 (5F1)	PE	BD Biosciences	556016
Anti-human IL-1β (JK1B-1)	A647	BioLegend	508208
Anti-human IL-6 (MQ2-13A5)	FITC	BioLegend	501104
Anti-human/mouse p38 MAPK (36/p38 (pT180/pY182))	A647	BD Biosciences	612595
Anti-human TNF (MAb11)	A700	BioLegend	502928
Anti-mouse CD11b (M1/70)	APC-Cy7	BD Biosciences	557657
Anti-mouse F4/80 (BM8)	A700	BioLegend	123130
Zombie NIR™ Fixable Viability Kit	/ (APC-Cy7)	BioLegend	423105
Fixable Viability Dye eFluor® 506	/ (AmCyan)	eBioscience	65-0866
7AAD	/ (PerCP)	BD Biosciences	559925

Flow cytometric analysis of purity/viability and p38 MAPK signaling of human monocytes was performed on a BD FACSCalibur device (BD Biosciences) with CellQuest software (version 5.2). A minimum of 5 000 monocytes was acquired. Intracellular cytokines and the FPR1 surface expression of human monocytes were analyzed on a BD LSRFortessa device (BD Biosciences) using FACSDiva software (version 6.2). A minimum of 50 000 human $CD14^+$ cells was acquired.

Analysis of murine macrophages was performed on an BD LSRFortessa device with a minimum of 5 000 murine macrophages acquired. Settings for FACS devices are listed in *Appendix* **5.3**.

Flow cytometric data were analyzed by FlowJo software (FlowJo LLC, Ashland, OR, USA, version 9).

4.3.2.a Determination of Purity and Cell Viability with 7AAD

The viability of human monocytes was determined with 7AAD (BD Biosciences, *Cat. No. 559925*), which stains only dead cells. After extracellular staining of CD14-positive monocytes (PE-conjugate, see **4.3.2.c**) to check the purity obtained, cell viability staining with 7AAD was performed according to the manufacturer's instructions.

4.3.2.b Live/Dead Discrimination with a Fixable Dye

For live/dead discrimination prior to permeabilization, either the Zombie NIR™ Fixable Viability Kit (BioLegend, *Cat. No. 423105*) or the Fixable Viability Dye eFluor® 506 (eBioscience, *Cat. No. 65-0866*) were used according to the manufacturer's instructions.

4.3.2.c Extracellular Staining of Cell Surface Molecules

One to two million cells per milliliter were washed twice with staining buffer containing PBS (Gibco) supplemented with 2 % serum and 0.1 % sodium azide (SERVA Electrophoresis GmbH) and stained for 15 min at 4 °C with antibodies directed towards surface molecules. Antibodies used for surface staining were as follows: human anti-CD14 (BV510-conjugate, clone M5E2, or PE-conjugate, clone MϕP9), human anti-FPR1 (PE-conjugate, clone 5F1), murine anti-CD11b (APCCy7-conjugate, clone M1/70) and murine anti-F4/80 (A700-conjugate, clone BM8).

4.3.2.d Intracellular Signaling Analysis of p38 MAP Kinase (MAPK)

Phosphorylation of p38 MAPK was measured using the Phosflow system from BD Biosciences according to their protocol. In brief, 2×10^5 cells in 100 µl cell culture medium were stimulated for 15 min with 100 ng/ml LPS (Enzo Life Sciences, *Cat. No. ALX-581-012*) and immediately fixed by the addition of 2 volumes of Fix Buffer 1 (BD Biosciences, *Cat. No. 557870*). After incubation for 10 min at 37 °C, cells were permeabilized in Perm/Wash Buffer I (BD Biosciences, *Cat. No. 557885*) for 30 min at RT and subsequently stained for 20 min at 4 °C with anti-p38 MAPK (A647-conjugate, clone 36/p38 (pT180/pY182)) and anti-CD14 (PE-conjugate, clone MϕP9) for human monocytes or anti-CD11b (APCCy7-conjugate, clone M1/70) and anti-F4/80 (A700-conjugate, clone BM8) for murine macrophages. Stained cells were washed and resuspended in staining buffer (see point **4.3.2.c** above) prior to flow cytometric analysis.

4.3.2.e Intracellular Cytokine Staining

For intracellular analysis of cytokine production, naïve or tolerant human monocytes were washed with PBS (Gibco), resuspended in fresh medium and stimulated for 6 h with 100 ng/ml LPS (Enzo Life Sciences, *Cat. No. ALX-581-012*) in the presence of Brefeldin A (10 µg/ml, Sigma-Aldrich).

After incubation, 1 x 10^6 cells were stained for the surface molecule CD14, fixed and permeabilizied using the Cytofix/Cytoperm kit (BD Biosciences, *Cat. No. 554714*) as recommended by the manufacturer before staining for intracellular cytokines. Antibodies for flow cytometric analysis were as follows: human anti-CD14 (BV510-conjugate, clone M5E2), human anti-IL-1β (A647-conjugate, clone JK1B-1), human anti-IL-6 (FITC-conjugate, clone MQ2-13A5) and human anti-TNF (A700-conjugate, clone MAb11).

4.3.3 ELISA and Multiplex

Naïve and tolerant monocytes stimulated with either 1 or 100 ng/ml LPS were challenged with 100 ng/ml LPS (Enzo Life Sciences, *Cat. No. ALX-581-012*) for the times indicated. After incubation, cell culture medium (supernatant) was collected by centrifugation (300 x g for 5 min at 4 °C) and stored at -80 °C until use. Cytokines within the supernatant were determined by ELISAs or Multiplex Assays according to the manufacturer's protocols (see **Table 4-2**).

Table 4-2: List of ELISAs and Multiplex Panel used for cytokine detection in the cell culture supernatant.

Molecule	Company	Cat. No.
CXCL8/IL-8	R&D Systems	DY208
CXCL10/IP-10	R&D Systems	DY266
IL-1β	eBioscience	88-7010
IL-6	R&D Systems	DY206
TNF	eBioscience	88-7346
MILLIPLEX® MAP Human Cytokine/Chemokine	Merck Millipore	HCYTOMAG-60K

4.3.4 RNA Isolation, cDNA Synthesis and Quantitative Real Time PCR (qRT-PCR)

Naïve and tolerant human $CD14^+$ monocytes were stimulated with LPS (Enzo Life Sciences, *Cat. No. ALX-581-012*) for the times indicated. Following stimulation, the expression profiles of several inflammatory molecules were evaluated by quantitative real time PCR (qRT-PCR) analysis.
Total RNA from 1 x 10^6 monocytes was isolated using the NucleoSpin® RNA Kit (Macherey-Nagel, *Cat. No. 740955*) according to the manufacturer´s protocols. After determination of RNA purity and concentration by *NanoDrop 2000* spectrophotometer measurement (Thermo Fisher Scientific), RNA was reverse-transcribed into cDNA using the QuantiTect Rev. Transcription Kit (Qiagen, *Cat. No. 205311*). The generated cDNA was amplified with 1 x TaqMan® Universal PCR Master Mix (Invitrogen, *Cat. No. 4304437*) by qRT-PCR on the 7500 Real Time PCR System (Applied Biosystems).

The specific primers and TaqMan Gene Expression Assays (Invitrogen) used for amplification are listed in **Table 4-3**.

Table 4-3: TaqMan Gene Expression Assays and primer pairs used for qRT-PCR.

Gene		
huCXCL10	Assay ID (Invitrogen)	Hs01124251_g1
huFPR1	Assay ID (Invitrogen)	Hs04235426_s1
huHPRT	Forward Primer (5'→3')	AGTCTGGCTTATATCCAACACTTCG (300 nM)
	Reverse Primer (5'→3')	GACTTTGCTTTCCTTGGTCAGG (300 nM)
	Probe (5'→3')	Fam-TTTCACCAGCAAGCTTGCGACCTTGA-Tamra (100 µM)
huIL1B	Forward Primer (5'→3')	GGCAATGAGGATGACTTGTTCTTT (300 nM)
	Reverse Primer (5'→3')	GTAGTGGTGGTCGGAGATTCGTAG (300 nM)
	Probe (5'→3')	Fam-ATGGCCCTAAACAGATGAAGTGCTCCTTCC-Tamra (100 µM)
huIL6	Assay ID (Invitrogen)	Hs00985639_m1
	or	
huIL6	Forward Primer (5'→3')	CCACTCACCTCTTCAGAACGAATT (300 nM)
	Reverse Primer (5'→3')	AGTGCCTCTTTGCTGCTTTCAC (50 nM)
	Probe (5'→3')	Fam-ATGTCTCCTTTCTCAGGGCTGAGATGCC-Tamra (100 µM)
huIL8	Assay ID (Invitrogen)	Hs00174103_m1
huMT1F	Assay ID (Invitrogen)	Hs00744661_sH
huMT1L	Assay ID (Invitrogen)	Hs01591331_g1
huTNF	Forward Primer (5'→3')	TCTCGAACCCCGAGTGACAA (50 nM)
	Reverse Primer (5'→3')	TCAGCACTGGAGCTGCC (900 nM)
	Probe (5'→3')	Fam-TGTAGCCCATGTTGTAGCAAACCCTCAAGC-Tamra (100 µM)
huZSCAN18	Assay ID (Invitrogen)	Hs00225073_m1
huZNF316	Assay ID (Invitrogen)	Hs00418202_m1

The PCR conditions were as follows: An initial 50 °C (2 min) followed by 95 °C (10 min), 40 cycles of 95 °C (15 sec) followed by 60 °C (1 min, combined annealing and extension) and a final hold at 4 °C.

The relative mRNA expression level of each target gene was normalized to the expression level of human *HPRT* ($2^{-\Delta CT}$, with CT = cycle threshold). All PCR reactions were carried out in duplicates and data analysis was performed using the 7500 System SDS Software (Version 1.4.0, Applied Biosystems).

4.3.5 Chromatin Immunoprecipitation (ChIP)

Interactions between proteins or modified forms of proteins (*e.g.* histone modifications) and a genomic DNA can be identified by chromatin immunoprecipitation (ChIP).

At first, the ChIP assay requires crosslinking of the chromatin structure with formaldehyde to stabilize the interaction between protein factors and DNA. The cross-linked chromatin is further broken down into smaller fragments to achieve high resolution. After immunoprecipitation with specific antibodies directed towards the target of interest (*e.g.* histone modifications), the associated DNA is isolated and

analyzed by PCR (Northrup & Zhao 2011). For genome-wide resolution, the ChIP DNA is sequenced by next generation sequencing techniques (see **4.3.6**).

4.3.5.a Sample Preparation (ChIP)

ChIP was performed according to a protocol from Dr. Daniel Ibrahim and Dr. Jochen Hecht (MPI for Molecular Genetics, Berlin, Germany / Center for Genomic Regulation, Barcelona, Spain), which was adapted from a publication by Lee *et al.* (2006) with following modifications:

Cell Fixation

Ten million human monocytes were stimulated for the indicated times (see **4.3.1.c** for experimental design) and immediately fixed in cell culture medium with 1 % formaldehyde (37 % solution, Sigma-Aldrich) for 7.5 min at 4 °C with gentle shaking. Formaldehyde fixation was stopped by the addition of glycine (125 mM final concentration, SERVA Electrophoresis). Cells were washed twice with ice cold PBS (Gibco) and the pellet was frozen at -80 °C until proceeding with cell lysis.

Cell Lysis and Sonication

Cell lysis and chromatin isolation was performed by incubating the cell pellet in 2.5 ml Lysis Buffer 1 (LB1) at 4 °C for 10 min with gentle rotation and subsequent centrifugation at 1350 x g for 5 min at 4 °C, followed by removal of supernatant and incubation of the pellet in 2.5 ml Lysis Buffer 2 (LB2) for 10 min at RT. After centrifugation (1350 x g, 5 min, 4 °C), the nuclei pellet was dissolved in 200 µl Lysis Buffer 3 (LB3) and transferred to 1.5 ml microtubes (Sarstedt). Freed chromatin was sonicated using the Bioruptor from Diagenode (for 10 min with 30 sec pulse on / 30 sec pulse off, set to high power) to obtain fragments ranging from 200 to 1000 bp. After sonication, cell debris was removed by addition of 1 % Triton X-100 (Sigma-Aldrich) and subsequent centrifugation of samples for 10 min at 16 000 x g and 4 °C. Supernatant (200 µl) containing sheared chromatin was transferred to fresh 1.5 ml microtubes.

Quality Control of Sonicated Chromatin and Determination of DNA Concentration

From a small aliquot (normally 1/20th of the total volume), DNA was purified for determination of DNA fragment size and concentration. Reversal of cross-linking was achieved by incubation of the fixed chromatin for 15 min at 95 °C with shaking in the presence of NaCl (for more details see *Washing and Recovery of DNA* below). After RNA and protein digestion, ethanol precipitated DNA was resolved in 20 µl H_2O. DNA concentration was determined by *NanoDrop 2000* spectrophotometer measurement (Thermo Fisher Scientific) and used for recalculation of DNA concentration in the original chromatin sample. Optimal DNA fragment size was checked on a 1.2 % agarose gel by gel electrophoresis (see **4.3.5.b**). The sonicated DNA should have a fragment range of 200 to 1000 bp with the major peak at around 400 to 500 bp.

Preparation of Magnetic Beads and Immunoprecipitation

Prior to immunoprecipitation (IP), magnetic protein G beads (Dynabeads® Protein G from Invitrogen, *Cat. No. 100.04D*) were pre-incubated with ChIP antibodies (3 to 5 µg per IP) for a minimum of 3 h at 4 °C with rotation in the presence of blocking solution (0.5 % BSA in PBS). In general, 20 µl of beads were used per IP.

Equal amounts of sonicated chromatin (5 to 20 µg) were incubated with antibody-bead complexes overnight with constant rotation. ChIP antibodies to H3K4me3 (*Cat. No. 07-473*), H3K27ac (*Cat. No. 17-683 or 07-360*), H3K27me3 (*Cat. No. 07-449*) and H4ac (*Cat. No. 06-866*) were purchased from Merck Millipore. ChIP-antibodies to H3K9me2 (*Cat. No. ab1220*) and H4K20me3 (*Cat. No. ab9053*) were purchased from Abcam. Sonicated chromatin incubated with a non-specific IgG antibody (Merck Millipore, *Cat. No. 12-370*) served as a negative control. Ten percent of sonicated total chromatin (not immunoprecipitated) was reserved as positive control input DNA and was stored at -20 °C until further processing (see below).

Washing and Recovery of DNA

Chromatin-antibody-bead-complexes were captured using a magnet and the supernatants were discarded. After washing with RIPA Wash Buffer 5 times and a final washing step with TE Buffer, protein-DNA complexes were eluted from beads in 110 µl Elution Buffer for 30 min at 65 °C with shaking. Beads were spun down for 1 min at 16 000 x g and the supernatants (100 µl) containing immunoprecipitated DNA-protein complexes were carefully transferred to fresh microtubes.

From now on, the input DNA sample representing total DNA was treated the same way as the ChIP DNA. For reversal of cross-linking, immunoprecipitated and input DNA were treated with NaCl (500 mM final concentration, Sigma-Aldrich) at 65 °C overnight if DNA was subjected to ChIP-Seq (see **4.3.6.a**), or 95 °C for 15 min if DNA was subjected to qRT-PCR analysis (see **4.3.5.c**). RNA and protein were removed by RNase A digestion for 30 min at 37 °C (0.4 mg/ml final concentration, Sigma-Aldrich, *Cat. No. R4642*), followed by Proteinase K treatment for 1 h at 55 °C (0.4 mg/ml final concentration, Sigma-Aldrich, *Cat. No. P4850*). For analysis of single DNA-protein interactions by qRT-PCR (see **4.3.5.c**), the resulting DNA was recovered by ethanol precipitation with addition of glycogen (Roche, *Cat. No. 10901393001*) and 3 volumes of cold 100 % ethanol with subsequent centrifugation for 30 min at 4 °C, followed by a washing step with 70 % ethanol. Immunoprecipitated DNA and input DNA were resolved in 80 to 100 µl H_2O.

For genome-wide resolution of DNA-protein interactions (ChIP-Seq), precipitated DNA was further processed and sequenced at the Core Facility for Next Generation Sequencing (NGS) at the Berlin-Brandenburg Center for Regenerative Therapies (BCRT), Charité – University Medicine Berlin, Germany (see **4.3.6.a**).

Buffers used for ChIP:

Lysis Buffer 1 (LB1)	Company
50 mM HEPES-KOH (pH 7.5)	Sigma-Aldrich
140 mM NaCl	Sigma-Aldrich
1 mM EDTA	Merck Millipore
10 % Glycerin (glycerol)	SERVA
0.5 % NP-40	Calbiochem
0.25 % Triton X-100	Sigma-Aldrich

Lysis Buffer 2 (LB2)	Company
10 mM Tris-HCl (pH 8.0)	Carl Roth
200 mM NaCl	Sigma-Aldrich
1 mM EDTA	Merck Millipore
0.5 mM EGTA	Merck Millipore

Lysis Buffer 3 (LB3)	Company
10 mM Tris-HCl (pH 8.0)	Carl Roth
100 mM NaCl	Sigma-Aldrich
1 mM EDTA	Merck Millipore
0.5 mM EGTA	Merck Millipore
0.1 % Na-Deoxycholate	Sigma-Aldrich
0.5 % N-Laroylsarcosine	Sigma-Aldrich

RIPA Wash Buffer (WB)	Company
50 mM HEPES-KOH (pKa 7.55)	Sigma-Aldrich
500 mM LiCl	Sigma-Aldrich
1 mM EDTA	Merk Millipore
1.0 % NP-40	Calbiochem
0.7 % Na-Deoxycholate	Sigma-Aldrich

TE Buffer (TE)	Company
10 mM Tris-HCl (pH 8.0)	Carl Roth
1 mM EDTA	Merck Millipore

Elution Buffer (EB)	Company
50 mM Tris-HCl (pH 8.0)	Carl Roth
10 mM EDTA	Merck Millipore
1.0 % SDS	SERVA

All buffers were sterile-filtered, aliquoted and stored at -20 °C until use. Protease inhibitors (1 x cOmplete Protease Inhibitor Tablets, Roche, *Cat. No. 11697498001*) and 20 mM sodium butyrate for analysis of acetylated histones (Sigma-Aldrich, *Cat. No. B5887*) were freshly added to LB1, LB2, LB3, WB and TE just before use.

4.3.5.b Detection of DNA Fragments by Agarose Gel Electrophoresis

For detection of correct DNA fragment size after sonication (see **4.3.5.a**, *Quality Control of Sonicated Chromatin and Determination of DNA Concentration*), purified DNA was mixed with 6 x Loading Dye and analyzed on a 1.2 % agarose gel (SERVA Electrophoresis) with 0.3 µg/ml ethidium bromide (Carl Roth) by gel electrophoresis in 1 x TAE buffer with a constant voltage of 100 for 30 min.

1x TAE Buffer	Company
40 mM Tris	Carl Roth
0.5 mM EDTA	Merck Millipore
Adjusted to pH 7.5	
(with acetic acid)	Merck Millipore

6x Loading Dye	Company
50 % Glycerol	SERVA
1 % SDS	SERVA
100 mM EDTA	Merck Millipore
0.1 % Bromphenol blue	

4.3.5.c Quantitative Real Time PCR (qRT-PCR) of ChIP DNA

Immunoprecipitated DNA and input DNA were amplified by qRT-PCR with the gene-specific primer pairs listed in **Table 4-4**. Prior to PCR, input DNA (10 %) was further diluted 1:10 for a final concentration of 1 %. The PCR reaction (25 µl) contained 2.5 µl DNA, 12.5 µl of 2x SYBR® Green PCR Mastermix (Invitrogen, *Cat. No. 4309155*) or SYBR® Select Master Mix (Invitrogen, *Cat. No. 4472908*) and gene specific forward and reverse primers with the specific concentrations indicated in **Table 4-4**. Samples were analyzed in triplicate. The PCR conditions were as follows: Initial incubation at 50 °C (2 min) and 95 °C (10 min), followed by 40 cycles at 95 °C (15 sec) and 60 °C (1 min), with a final melting curve for specificity analysis using the 7500 Real Time PCR System (Applied Biosystems). ChIP data were calculated as % of input DNA and normalized to IgG control

(fold enrichment). All data are presented as fold change relative to enriched DNA from naïve (N) untreated cells (relative fold enrichment).

Calculation of enriched ChIP DNA:

(1) The samples were first adjusted to the total input fraction:

What is the CT value of the 1 % input at 100 %?	Log2 of 100 = 6.64
The raw CT of 1 % input was *e.g.* 25	
Adjustment of 1 % to 100 %:	25 – 6.64 = 18.36 (= 100 %)
CT of antibody sample was *e.g.* 23	2 ^ (18,36 – 23) = 0.04 (= 4 %)
CT of IgG control was *e.g.* 28	2 ^ (18,36 – 28) = 0.001 (= 0.1 %)

(2) Fold enrichment of specific antibody to IgG control:

Correlation of specific antibody (in %) to IgG control (in %)	4 % / 0.1 % = 40 (fold enrichment)

(3) Relative fold enrichment by normalization to naïve (N) control

Table 4-4: Primers used for qRT-PCR analysis of ChIP DNA.

Gene	Concentration	Forward primer (5'→3')	Reverse primer (5'→3')
huCXCL10	300/300 nM	ACCCAAATGAGCAATGTTTTCCC	GGACTGGCCTGCTTTGACAG
huFPR1	900/900 nM	AGAGGCAAGGGCATCAGCTT	CTCATTTCCCCATGACCCATC
huIL1B	900/900 nM	GGCAAACAGGGTGCCAAGTA	AGGAAGCCCTTGCAACAACAC
huIL6 (Park *et al.* 2011)	900/900 nM	ACCCTCACCCTCCAACAAAG	GCAGAATGAGCCTCAGACATC
huIL8	300/300 nM	AGAGACAGCAGAGCACACAAGC	GCTGCCAAGAGAGCCACGG
huTNF	300/300 nM	CGGGGATGCAGAAAGAGATG	GCACCTTCCATGTGCCAGAC
muFpr1	300/300 nM	TGCATCCTGCAGATTGGAGA	ACCCAGGCTTTGTGTGTGCT
muGapdh	300/300 nM	CCGCATCTTCTTGTGCAGTG	ACTTCGCACCAGCATCCCTA
muIl1b	300/300 nM	GAGGCCAGAGAGTCCCCAAC	GGGCTTGGGAGTGAAGAGGT
muIl6	300/300 nM	CCCCACCCTCCAACAAAGAT	GTGGGCTCCAGAGCAGAATG
muTnf	300/300 nM	GCCACCACGCTCTTCTGTCT	TTGCCCTCCTAACCCGTTTT

Binding sites of human primer pairs within the genome are depicted in *Appendix* **5.2**. Data analysis was performed using the 7500 System SDS Software (Applied Biosystems, version 1.4.0).

4.3.5.d Optimization of ChIP

The fixation and shearing conditions for human monocytes were optimized to gain reliably uniform chromatin fragments ranging from 200 to 1000 bp for ChIP assays (**Fig. 4-3**). A balance between fixation temperature and time as well as shearing conditions was needed to avoid over fixation on the one hand, but reliable fixed interactions of DNA and proteins on the other hand. Briefly, $CD14^+$ monocytes were fixed followed by chromatin isolation. Subsequently, cross-linked chromatin was sheared by sonication and DNA was accessed by reversal of cross-linking and purification (for more details see **4.3.5.a**). To find the optimal ChIP conditions, variations in fixation temperature (**Fig. 4-3** B), fixation time (**Fig. 4-3** C) and shearing time (**Fig. 4-3** D) were performed. Proper fragment size of DNA was checked by agarose gel electrophoresis (see also **4.3.5.b**).
Optimal DNA fragment size ranging from 200 to 1000 bp was achieved by cell fixation on ice (ca. 4 °C) for 7.5 min and shearing for 10 cycles (**Fig. 4-3** D).

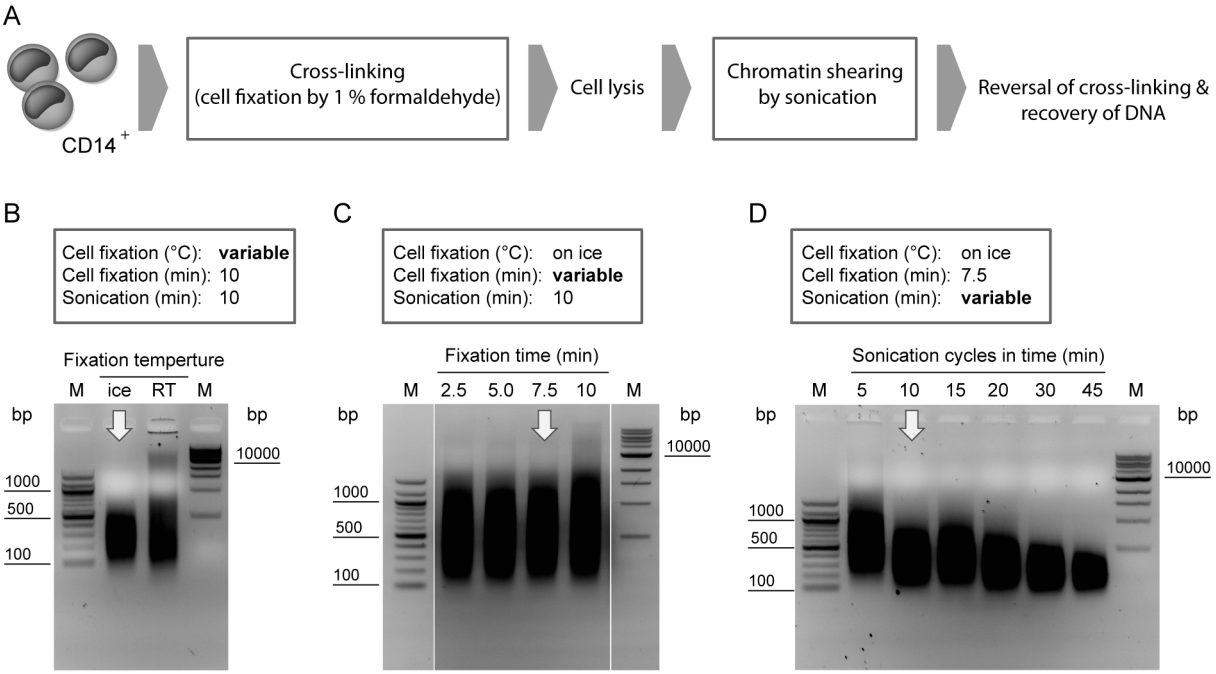

Fig. 4-3: Optimization of fixation and shearing conditions of ChIP assays for human monocytes. (A) Schematic overview of determining optimal ChIP fixation and shearing conditions: Human CD14$^+$ monocytes were cross-linked with formaldehyde following cell lysis and isolation of fixed chromatin. After shearing of chromatin by sonication, DNA was accessed by reversing the cross-linking following DNA purification. Optimal shearing of DNA was analyzed on an agarose gel (1.2 %). (B, C and D) Agarose gel with purified DNA: Either fixation temperature (B), fixation time (C) or shearing time (D) was varied. Best results are indicated by arrows. M = ladder, RT = room temperature (circa 21 °C).

4.3.6 ChIP-Sequencing (ChIP-Seq)

For epigenetic characterization of the chromatin status and recovery of all binding sites within a genome, ChIP DNA is sequenced and the short sequences called *'reads'* are aligned to a reference genome. As a control for ChIP-Seq data analysis, a library with input DNA (pre-immunoprecipitated total DNA) is generated, which allows an accurate estimation of biases produced by sonication of chromatin and sequencing. If no input DNA is available, specific enrichment of ChIP DNA is compared to different conditions. The generated binding profile of target proteins can be visualized in a genome browser.

Finally, the sequence data are converted to position data by alignment with a reference genome and analyzed by peak-calling algorithms to identify ChIP-enriched regions that correspond to histone modifications or transcription factor binding sites (Northrup & Zhao 2011).

4.3.6.a Next Generation Sequencing (NGS) of ChIP DNA

For genome-wide analysis of histone modifications, the ChIP DNA was subjected to sequencing: Ethanol-precipitated DNA from ChIP assays (see **4.3.5.a**) was further processed by the BCRT Core Facility for Next Generation Sequencing (Jochen Hecht/Ulrike Krüger, Charité-Berlin, Germany).

In brief, library preparation (ligation of barcoded adapters to DNA fragments) was performed using the NEBNext ChIP-seq Library Prep Master Mix for Illumina (New England Biolabs) according to the manufacturer's instructions. A limited PCR amplification was performed for enrichment of ChIP-Seq library, followed by size selection of desired DNA fragments ranging from 300 to 450 bp using the

BioAnalyzer (Agilent Technologies). Subsequently, DNA samples were sequenced on an Illumina Genome Analyzer IIx generating 36 bp single-end reads using TruSeq Cluster Kit and TruSeq SBS Kit or on an Illumina HiSeq 1500 generating 50 bp single-end reads using HiSeq Cluster Kit and HiSeq SBS Kit (all Illumina).

As the Illumina technology was used for DNA sequencing, this technique is briefly introduced in this section (see **Fig. 4-4**). The technology basically involves attachment of smaller fragments of DNA to a surface followed by massively parallel sequencing.

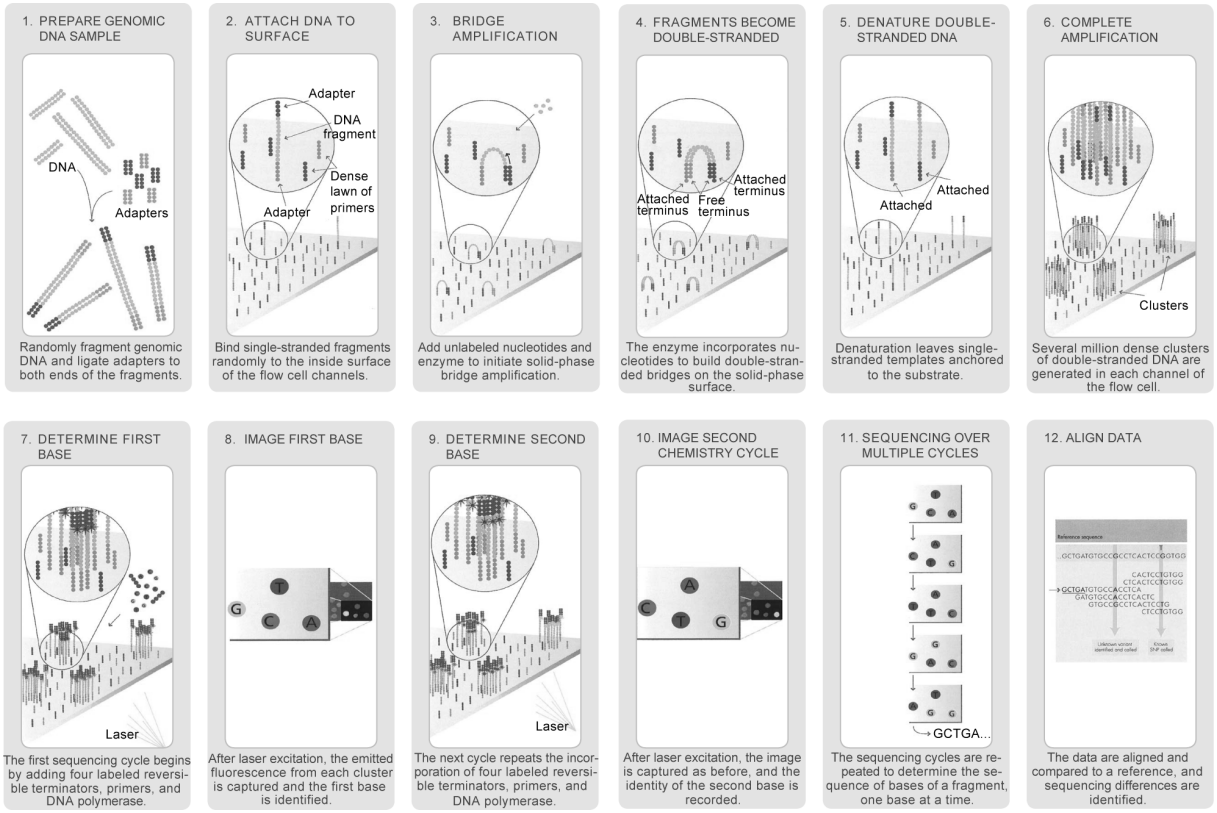

Fig. 4-4: Pipeline of DNA sequencing by Illumina technology. All information and illustrations are adopted from the illumina website (online available (as of October 2015): http://www.illumina.com/).

First, DNA fragments are ligated to barcoded adapters with a known sequence. This allows attachment of single-stranded DNA to a solid surface called a *'flow cell'* and subsequent solid-phase bridge amplification of the DNA templates. Here, the DNA molecule bends over and hybridizes to a free complementary adapter which functions as a primer allowing synthesis of the complementary DNA strand. The amplification results in a flow cell with millions of clusters with the exact number depending on the sequencing device used, each containing about 1000 identical copies of the initial template in close proximity. Sequencing is mediated in a massively parallel fashion by a *'DNA Sequencing by Synthesis'* approach: First, the DNA strand is denatured leaving the forward DNA strand bound to the flow cell and then a sequencing primer complementarily hybridizes to the adapter sequence. Subsequently, a single fluorescence-labeled terminator nucleotide is incorporated into the nucleic acid chain allowing imaging of a successive nucleotide addition after each sequencing cycle.

Finally, enzymatic cleavage of the terminator dye allows the incorporation of the next nucleotide starting a new sequencing cycle.

4.3.6.b Pre-Processing: Quality Filtering and Read Mapping of ChIP-Seq Data

ChIP experiments followed by NGS produce millions of short read sequences, which are aligned to a known reference genome to identify locations of specific DNA-protein interactions.
The computational analysis starts with so-called fastq files that store the sequence information of all reads. The pre-processing pipeline involves quality assessment, mapping to a reference genome, duplicate filtering of reads and transformation of the aligned data to coverage vectors.

(Pipeline was adapted from Dr. Daniel Ibrahim)
The sequencing data was converted to fastq files and controlled for general quality characteristics using FastQC. All reads that had an average Phred-score < 28 were discarded. Subsequently, the remaining reads were aligned to the human hg19 genome assembly (Feb. 2009) using the mapping algorithm BWA with default parameters allowing two mismatches per reads. The parameters were as follows: aln -n=0, aln -o=1, aln -e=1, aln -d=16, aln -i=5, aln -l=-1, aln -k=2, aln -M=3, aln -O=11, aln -E=4, aln -R=FALSE, aln -N=FALSE, samse/sampe -n=3, sampe=-N10, sampe -a=500, sampe -o=100000, samse/sampe -r=NO. The SAM file created containing aligned read data was used for follow-up processing. Reads that repetitively bound within the genome were discarded and only uniquely mapped reads were kept for subsequent filtering of duplicates (removal of PCR artifacts by the SAMtool rmdup). The final alignment file (BAM file) contained only non-redundant reads. The BAM file is the binary and indexed format of the SAM file that stores the final sequence data.
The quality of the ChIP enriched data was evaluated by calculating the relative strand correlation (RSC) and normalized strand correlation (NSC) from the cross-correlation following the ChIP-Seq guidelines suggested by the ENCODE consortium (The Encyclopedia of DNA Elements) (Bailey *et al.* 2013, Landt *et al.* 2012).
The pre-processing was conducted on a server at the Charité (Berlin, Germany) using a locally installed version of the Galaxy platform (Blankenberg *et al.* 2010, Giardine *et al.* 2005, Goecks *et al.* 2010). The infrastructure of the server was set up and maintained by Peter Hansen from the Computational Biology Group of Prof. Dr. Peter Robinson.

The ChIP-Seq assays performed are listed in **Table 4-5**. According to the ChIP-Seq guidelines (Bailey *et al.* 2013, Landt *et al.* 2012), the sequencing depth should be a minimum of 10 million reads, whereas the percentage of uniquely mapped reads should lie above 50 %. The percentage of non-redundant reads known as non-redundancy fraction (NFR) within the uniquely mapped ones should be ≥ 80 %. The NSC (≥ 1.05) and the RSC (≥ 0.8) are important indexes for assessing signal-to-noise ratios in a ChIP-Seq experiment.
The quality of the conducted ChIP-Seq experiments was good. Most of the quality criteria, especially the most important ones (NSC and RSC), were met by all samples. Solely the NFR was achieved by 10 of 16 ChIP-Seq analyses.

Table 4-5: Overview of performed ChIP-Seq assays. Naïve (N) or tolerant cells (treated with 100 ng/ml LPS overnight) were stimulated for 1.5 h with 100 ng/ml LPS (N+L, T100+L) prior to ChIP-Seq analyses.

Histone modifications	Conditions	Replicates	Total reads	Total reads (FastQC-filtered)	Uniquely mapped reads	Uniquely mapped reads (in %)	Non-redundant reads (duplicates filtered)	Non-redundant reads within uniquely mapped (in %)	NSC	RSC
H3K9me2	N+L	1	24990613	24937781	18210519	73.02	13198844	72.48	1.103	5.785
H3K9me2	N+L	2	30326140	30184109	20672630	68.49	16674211	80.66	1.092	6.554
H3K9me2	T100+L	1	23940783	23892929	17226306	72.10	11119768	64.55	1.100	4.865
H3K9me2	T100+L	2	31607282	31447721	22287481	70.87	16640784	74.66	1.090	3.584
H3K27me3	N+L	1	17952199	17899832	12429386	69.44	8852687	71.22	1.171	2.628
H3K27me3	N+L	2	39883441	39650973	31657613	79.84	25603692	80.88	1.088	1.919
H3K27me3	T100+L	1	13360964	13322746	9109428	68.38	6221161	68.29	1.155	2.197
H3K27me3	T100+L	2	31821055	31616484	22730043	71.89	18853318	82.94	1.099	1.613
H4K20me3	N+L	1	26648298	26589310	15996756	60.16	13358495	83.51	1.057	1.949
H4K20me3	N+L	2	35180756	35007444	23065502	65.89	19690983	85.37	1.052	3.052
H4K20me3	T100+L	1	36067558	35988056	20324041	56.47	15562998	76.57	1.057	1.576
H4K20me3	T100+L	2	40740966	40524889	25170417	62.11	20489596	81.40	1.054	1.633
H3K27ac	N	1	44910266	44693987	34090192	76.27	30042303	88.13	1.055	3.866
H3K27ac	N+L	1	34033741	33846109	25349055	74.90	21698557	85.60	1.069	3.281
H3K27ac	T100+L	1	36474027	36299868	26669802	73.47	22528742	84.47	1.051	3.714
H4ac	N	1	41176243	40953900	32242936	78.73	27712381	85.95	1.084	2.158
H4ac	N+L	1	38083744	37868972	29285769	77.33	24722675	84.42	1.116	1.707
H4ac	T100+L	1	41578935	41369787	31806813	76.88	28126000	88.43	1.051	2.053

H3K9me2 = dimethylation of lysine 9 (K9) at histone 3 (H3), H3K27me3 = trimethylation of K27 at H3, H4K20me3 = trimethylation of K20 at histone 4 (H4), H3K27ac = acetylation of K27 at H3, H4ac = pan-acetylation of several lysines at H4, RSC = relative strand correlation and NSC = normalized strand correlation.

4.3.6.c Visualization of Binding Profiles

The final alignment result of the pre-processed analysis is a BAM file including all non-redundant reads with an index file (BAI file), which can be displayed in the Integrative Genome Viewer (IGV, Broad Institute, version 2.3). For better handling and visualization in the IGV, the alignments within the BAM file were converted into bedgraph-files (using BEDTools).

For visualization within the UCSC Genome Browser from the University of California (Santa Cruz, California, USA), read lengths were extended to fragment size and ChIPSeq data was normalized to one million aligned sequencing reads. Converted BigWig files were uploaded on a local server from the MPI for Molecular Genetics (Berlin, Germany) and displayed in the UCSC Genome Browser (Kent *et al.* 2002).

4.3.6.d Peak Calling

Significant enrichment of regions by ChIP representing DNA-protein interactions known as *'peaks'* are determined by specifically developed algorithms that identify truly enriched ChIP DNA over a given background. Here, ChIP samples are either compared with the input DNA or significant differences are detected by comparing two conditions. The latter approach was used in this study. As the sequencing is performed from the 5' end (single-end), the alignment of the short sequencing reads results in two enrichment profiles, representing one on each strand. Most peak callers, therefore, correct the real binding location of the protein of interest by length extractions of reads and shifting the binding sites according the 3' end by one half of the fragment size (**Fig. 4-5**). The fragment length can be estimated based on the size selection during library preparation or computationally by maximizing the cross-correlation between the sense and anti-sense strand (Kharchenko *et al.* 2008).

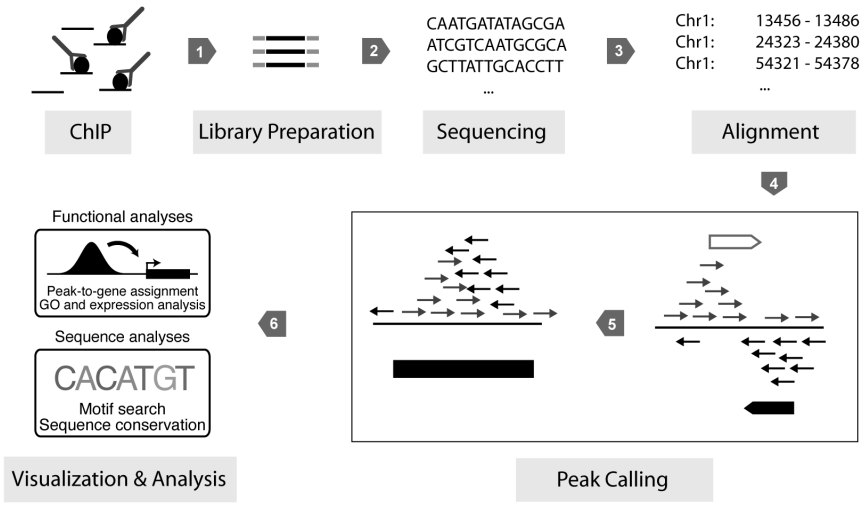

Fig. 4-5: Pipeline of the central steps in analysis of ChIP-Seq data (adapted from Liu *et al.* (2010) and Bardet *et al.* (2012)). For more details see text.

The peak shape is an important factor in choosing the right peak caller. ChIP-Seq experiments using an antibody directed towards a transcription factor (TF) result in sharp peaks because of the binding characteristics of TFs to attach to specific DNA sequences (TFBS, transcription factor binding site). By contrast, peaks of histone modifications result in broader peaks ranging from 300 bp to several kbs depending on the type of histone mark.

The output file of peak calling is normally a BED file that contains the chromosome name, start point and end point of enriched regions. Moreover, it provides a score (normally specific to each peak caller), a *P* value and a false discovery rate (FDR) for evaluation of significantly enriched genomic regions indicating specific DNA-protein interactions.

4.3.6.e Spatial Clustering Approach for the Identification of ChIP-Enriched Regions (SICER)

(Performed by Carolin Walter)

SICER (Zang *et al.* 2009) is a spatial clustering approach to detect large domains of enriched histone modifications. The genome is divided into non-overlapping bins of size w (window). For histone modifications, a window size of 200 bp representing a nucleosome is normally used. Each bin is categorized as *'eligible'* or *'ineligible'* based on a Poisson null hypothesis with a fixed λ parameter. SICER detects eligible windows (enriched read sequences) that are separated by gaps. A gap of size m contains m ineligible windows. A scoring system of detected clusters is delivered together with *P* values and FDRs. The specific SICER score represents the negative logarithm of the probability of finding the number of reads observed to be in the current window. The higher the score, the less likely the observed interaction occurs by chance (Fischl 2010, Xu *et al.* 2014, Zang *et al.* 2009).

For a comprehensive view of SICER peak calling see **Fig. 4-6**.

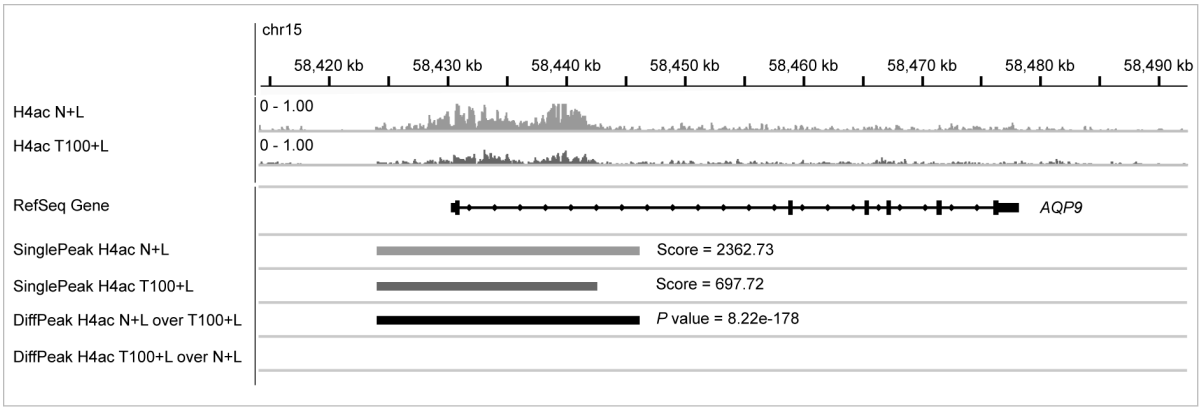

Fig. 4-6: Peak Calling by SICER. The SICER algorithm identifies enriched regions (peaks) within each condition (N+L, T100+L) provided with a score representing the likelihood of the identified interaction (termed as *SinglePeak*). Moreover, SICER compares two ChIP-Seq data sets by treating one condition as a control. The *DiffPeak* is counted here for the condition N+L. The significance is provided by a *P* value. An IGV snapshot is displayed as representative ChIP-Seq data of the histone modification H4ac. Chr = chromosome, N+L = naïve cells treated with LPS, T100+L = tolerant cells (tolerized with 100 ng/ml LPS) stimulated with LPS, RefSeq = reference sequence, AQP9 = Aquaporin-9.

Before peak calling, the two replicates for the repressive histone marks H3K9me2, H3K27me3 and H4K20me3 were merged together (see also **Table 4-5**). The final ten data sets (BAM files) used for peak calling consisted of the combination of N+L compared to T100+L for each of the five different histone marks; H3K9me2, H3K27me3, H4K20me3, H3K27ac and H4ac.

Peak calling for each data set was performed using SICER with default parameters applying a window (w) size of 200 bp and a gap (g) size of 600 bp (effective human genome length was assumed by 74.3 %). As no input control data were available, a random E-value threshold of 100 and a random background were used to determine the statistical significance of each identified peak (script used: SICER-rb.sh). The resulting peak list containing significant genomic regions with a corresponding SICER score was titled as *'SinglePeaks'*.

Moreover, SICER provides a differential analysis modus: For identification of differential enrichment between two ChIP data sets, *e.g.* the comparison of the condition N+L over T100+L and vice versa for a single histone mark, the data sets were analyzed by SICER-df-rb.sh with an FDR of 0.01 (g = 600, w = 200). The specific script first identified enriched regions in the two conditions (as above), then merged the regions together and identified significantly enriched peaks compared to the defined control condition. The output peak lists containing regions with increased or decreased enrichment over the control condition were provided with an FDR, *P* value and fold change (FC). These peak sets were termed *'DiffPeaks'*. The data files containing significantly enriched regions were provided in BED format.

4.3.6.f Determining the Final Peak Lists

(Performed by Carolin Walter)

Single peak lists called by SICER for each histone mark and every condition were filtered for a minimum score of 100 (*SinglePeaks*). Differential peak lists comparing naïve monocytes treated with LPS (N+L) and tolerant cells stimulated with LPS (T100+L) were filtered for a minimum fold change (FC) of 2 and a *P* value of ≤ 1e-6 (*DiffPeaks*).

The *DiffPeak* data sets were further filtered for *histone-limited DiffPeak data sets*. To identify genomic regions with enhanced H4ac-enrichment in tolerant monocytes treated with LPS (T100+L) compared to naïve cells (N+L), differentially enriched H4ac in T100+L (*DiffPeaks* from SICER, 2-fold change) were selected and all regions positive for *DiffPeaks* in repressive histone marks were discarded. The same was performed for H3K27ac.

Moreover, for identifying induction of repressive histone marks in tolerant cells compared to naïve ones, specific genomic regions significantly enriched for H3K9me3, H3K27me3 or H4K20me3 (minimum 2-fold change) in T100+L with a negative correlation in positive histone marks (H3K27ac or H4ac) were chosen for down-stream analyses.

The final peak lists for (1) enrichment of the activating histone marks H4ac or H3K27ac and (2) enrichment for the repressive histone modifications H3K9me2, H3K27me3 or H4K20me3 in tolerant cells (T100+L) were subjected to down-stream functional analysis. An overview of the final peak lists used in this study is given in **Table 4-6**.

Table 4-6: Overview of the final ChIP-Seq peak lists used in this thesis.

SinglePeaks		
Histone/Name	**Condition**	**Notes**
H3K27ac	N+L	SICER Score ≥ 100
H3K27ac	T100+L	SICER Score ≥ 100
H4ac	N+L	SICER Score ≥ 100
H4ac	T100+L	SICER Score ≥ 100
H3K9me2	N+L	SICER Score ≥ 100
H3K9me2	T100+L	SICER Score ≥ 100
H3K27me3	N+L	SICER Score ≥ 100
H3K27me3	T100+L	SICER Score ≥ 100
H4K20me3	N+L	SICER Score ≥ 100
H4K20me3	T100+L	SICER Score ≥ 100

Table 4-6: Overview of the final ChIP-Seq peak lists used in this thesis (*continued*).

DiffPeaks		
Histone/Name	**Counted For**	**Notes**
H3K27ac_N	N+L	FC ≥ 2, *P* value of minimum 1e-6
H3K27ac_T	T100+L	FC ≥ 2, *P* value of minimum 1e-6
H4ac_N	N+L	FC ≥ 2, *P* value of minimum 1e-6
H4ac_T	T100+L	FC ≥ 2, *P* value of minimum 1e-6
H3K9me2_N	N+L	FC ≥ 2, *P* value of minimum 1e-6
H3K9me2_T	T100+L	FC ≥ 2, *P* value of minimum 1e-6
H3K27me3_N	N+L	FC ≥ 2, *P* value of minimum 1e-6
H3K27me3_T	T100+L	FC ≥ 2, *P* value of minimum 1e-6
H4K20me3_N	N+L	FC ≥ 2, *P* value of minimum 1e-6
H4K20me3_T	T100+L	FC ≥ 2, *P* value of minimum 1e-6
DiffPeaks (Histone-limited)		
Histone/Name	**Counted For**	
H3K27ac_T_no_RepX	T100+L	No overlap with *DiffPeaks* in repressive histone marks
H4ac_T_no_RepX	T100+L	No overlap with *DiffPeaks* in repressive histone marks
H3K9me2_T_no_AcX	T100+L	No overlap with *DiffPeaks* in activating histone marks
H3K27me3_T_no_AcX	T100+L	No overlap with *DiffPeaks* in activating histone marks
H4K20me3_T_no_AcX	T100+L	No overlap with *DiffPeaks* in activating histone marks

4.3.7 Bioinformatical Downstream Analyses of ChIP-Seq Data

For the identification of potential functional relevance of the DNA-protein interaction, several downstream analyses are available including genomic annotation of peaks, discovery of TFBSs within the significantly enriched regions and comparison with DNA methylation or RNA expression data.
The vast majority of downstream analyses were conducted using the open-source R language (version 3.1.2) as well as the open-source Bioconductor project (version 3.1), and HOMER (see **4.1** for software overview).

4.3.7.a Gene Annotation and Gene Body Distribution

(Performed by Carolin Walter)
Identified peaks (genomic regions) were assigned to the nearest transcription start site (TSS) of a gene using Hypergeometric Optimization of Motif EnRichment (HOMER, Heinz *et al.* (2010)) and categorized into following gene body elements: TSS (by default defined from -1 kb to +100 bp), transcription termination site (TTS, by default defined from -100 bp to +1 kb), coding DNA sequence (CDS Exons), 5' untranslated (UTR) Exons, 3' UTR Exons, Introns and Intergenic regions (Heinz *et al.* 2010).

4.3.7.b Binding Profiles around the Transcription Start Site (TSS)

Peak binding profiles of ChIP-Seq data to TSS regions were generated by the Bioconductor package ChIPseeker (version 1.2.6). Moreover, it supported annotation of ChIP peaks and functional visualization (Yu *et al.* 2015).

4.3.7.c Cluster Analysis of Chromatin Signatures (Heat map)

(In cooperation with Dr. Stephan Schlickeiser)

Differentially enriched regions were visualized with an unsupervised clustering heat map (Euclidean) using R. First, peak sets identified by SICER were annotated to the nearest gene using HOMER. *DiffPeaks* for each histone and every condition (minimum fold change of 2, *P* value of ≤ 1e-6) were unified to a single gene list by discarding duplicates. As *DiffPeaks* were counted for either one of the two conditions, the given gene list was compared to the *SinglePeak* data set (with a minimum SICER score of 100) to obtain values for both conditions. If multiple regions were associated with a single gene, the region with the highest SICER score was used. Genes and corresponding SICER scores were scaled over the samples and clustered using heatmap.2 (gplot R package, version 2.17.0, Warnes *et al.* (2015)).

4.3.7.d Analysis of Gene Overlap between Gene Lists

Significant overlap between gene lists was investigated by the Bioconductor package GeneOverlap (version 1.2.0) (Shen & Sinai 2013).

4.3.7.e Gene Ontology (GO) Enrichment Analysis of ChIP-Seq Data

Peak lists as BED files were subjected to Genomic Regions Enrichment of Annotations Tool (GREAT, version 3) analyses. GREAT not only attributes significant enrichment of genes to specific functional processes, it also identifies putative cis-regulatory regions, which is useful for intergenic analyses (McLean *et al.* 2010).

Moreover, gene ontology analyses of identified gene lists were performed using Database for Annotation, Visualization and Integrated Discovery (DAVID, version 6.7) (Huang *et al.* 2009a, b).

4.3.7.f Identification of Transcription Factor Binding Sites (TFBSs)

(Performed by Carolin Walter)

The enriched genomic regions identified by SICER were analyzed for *de novo* motif discovery of known TFBSs using HOMER (Heinz *et al.* 2010).

4.3.8 Specific DNA Methylation Analysis of the Human *IL6* and *TNF* Promoter Using Short Bisulfite Sequencing (BS-Seq)

Methylation of DNA molecules is a general marker for repressive gene expression. Methylated cytosine can be detected by modification with sodium bisulfite treatment. Here, unmethylated cytosines are de-aminated to uracil, whereas methylated cytosines are protected and remain unchanged. After sequence-specific PCR, uracil is exchanged with the structural analog tyrosine. PCR products can be subjected to sequencing, where formerly methylated cytosine is read as *'C'* while unmethylated cytosine is read as *'T'* in the DNA sequence. The generated sequence data can be compared to the original reference DNA (Li & Tollefsbol 2011, Northrup & Zhao 2011).

4.3.8.a DNA Preparation and Bisulfite Conversion

For DNA methylation analysis of the *IL6* and *TNF* promoter regions, DNA was subjected to bisulfite treatment followed by PCR and sequencing analysis.
Genomic DNA was isolated using the QIAamp DNA Mini Kit (Qiagen, *Cat. No. 51304*) following the manufacturer's instructions. Before elution, columns were dried for additional 10 min and DNA was eluted in 200 µl Buffer AE. Bisulfite conversion of isolated DNA was performed with the Epitect Bisulfite Kit® (Qiagen, *Cat. No. 59194*) according to the "Sodium Bisulfite Conversion of Unmethylated Cytosines in DNA" protocol. Bisulfite-converted DNA was eluted twice in 25 µl Buffer EB for a final volume of 50 µl. DNA was aliquoted and stored at -20 °C until further use.

4.3.8.b PCR of Target Promoter

Bisulfite-converted DNA was subjected to sequence-specific PCR. For the human *TNF* promoter, the primers were specifically designed to screen a promoter fragment from -360 to +50 bp containing 12 CpG doublets surrounding the NFκB binding site at -98 bp (Campion *et al.* 2009). The human *IL6* promoter region spanning over 1200 bp was subdivided into 3 sections ranging from 350 to 400 bp (Nile *et al.* 2008). The primer sequences are listed in **Table 4-7**.

Table 4-7: Primer pairs used for promoter-specific PCR of bisulfite-converted DNA.

Gene/Amplicon	Forward primer (5'→3')	Reverse primer (5'→3')
TNF (Campión *et al.* 2009)	TTAAAAGAAATGGAGGTAATAG	CTTCTCTCCCTCTTAACTAATC
IL6_section1 (Nile *et al.* 2008)	TATTATTTTGAGGGAAGAGGGTTTT	TACTCTCCCCACTACCACTAAATCT
IL6_section2 (Nile *et al.* 2008)	TTTTTTTAAGTGGGTTGAAGTAGGT	CAAAAAATAAAACTAAAATCATACA
IL6_section3 (Nile *et al.* 2008)	TAAAGTGTTGAGTTATTAATAAAAG	TCATAACTAAACTCCTAAAAAAAA

The specific primer pairs used for promoter amplification already included adapter sequences for direct sequencing with Illumina (Adaptor1: 5'-CTACACGACGCTCTTCCGATCT-*primer-specific sequence*-3', Adaptor2: 5'-CAGACGTGTGCTCTTCCGATCT-*primer-specific sequence*-3'). The PCR reactions were performed in 25 µl containing 1 x AmpliTaq Gold Mastermix (Invitrogen, *Cat. No. 4398881*), 500 nM of forward and reverse primers and 2.5 µl of bisulfite-converted DNA (circa 100 ng). The PCR reaction was carried out as touchdown PCR with the following conditions: Initial denaturation at 95 °C (10 min), followed by 10 cycles at 95 °C (30 sec), the sequence-specific annealing temperature plus 10 °C for 1 min with decreasing annealing temperature by 1 °C each cycle and elongation at 72 °C (1 min), followed by 30 cycles at 95 °C (30 sec), sequence-specific annealing temperature (30 sec) and 72 °C (1 min), and a final elongation step at 72 °C (7 min). The specific annealing temperatures were as follows: 53 °C (TNF), 58 °C (IL6_section1), 50 °C (IL6_section2) and 47 °C (IL6_section3).

Sequences of the promoter regions of *TNF* and *IL6* used for DNA methylation analyses are found in the *Appendix* **5.4**.

4.3.8.c Purification of PCR Products

PCR products were purified using the QIAquick PCR Purification Kit (Qiagen, *Cat. No. 28104*) according to the manufacturer's instructions with the following changes: After DNA binding, columns were washed twice with PE Buffer and dried for 10 min to remove residual ethanol. Subsequently, DNA was eluted in two serial elution steps, each with 30 µl Elution Buffer.

4.3.8.d Detection of PCR Products by Gel Electrophoresis

Purified PCR products were checked on an agarose gel (2 %, SERVA Electrophoresis in 1 x TAE buffer) for proper product sizes (see also **4.3.5.b**).

4.3.8.e Restriction Enzyme Digestion for Specificity Analysis of PCR Products

Specificity of PCR products was further evaluated by restriction enzyme digestion and subsequent gel electrophoresis. PCR products were digested with SspI (AATATT) or DraI (TTTAAA) in the enzyme-corresponding buffer (New England BioLabs). The standard digestion reaction (final volume 10 µl) contained 5 µl of purified PCR product, 1 x NEBuffer (No. 2 for SspI, No. 4 for DraI) and 1 µl of restriction enzyme. PCR products were digested for 1 h at 37 °C followed by 20 min at 65 °C for heat inactivation of the enzyme. Digestion products were checked for correct sizes on a 2 % agarose gel (**Fig. 4-7**). Restriction sites of enzymes are shown in *Appendix* **5.4**.

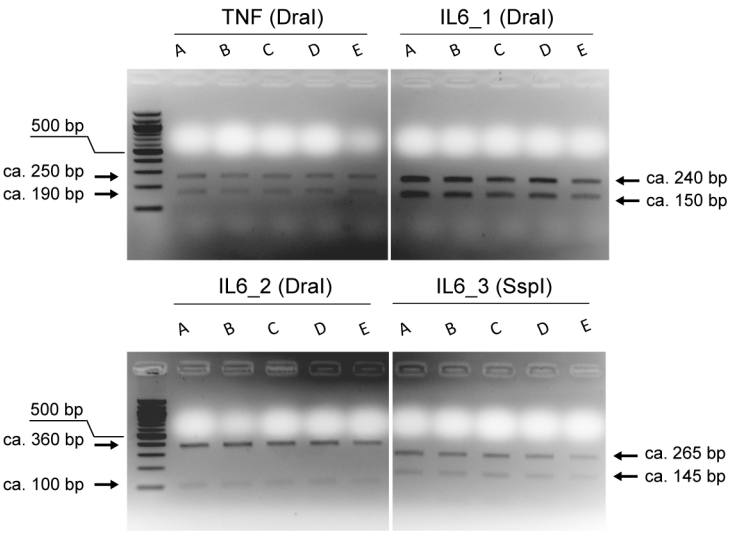

Fig. 4-7: Analysis of restriction enzyme digestion of PCR products by gel electrophoresis. *TNF* and *IL6* promoter-specific PCR products of bisulfite-converted DNA were digested with the restriction enzymes DraI or SspI. Digestion fragments were checked for correct sizes on a 2 % agarose gel. The total amplicon sizes of the PCR products were as follows: TNF = ca. 400 bp (+ 40 bp adapter), IL6_1 = ca. 350 bp (+ 40 bp adapter), IL6_2 = 420 bp (+ 40 bp adapter) and IL6_3 = 370 bp (+ 40 bp adapter). A, B, C, D and E represent different experiments.

4.3.8.f Sequencing of PCR Products

PCR products were subjected to sequencing. DNA sequencing was carried out on a Illumina MiSeq generating 250 bp single-end reads at the BCRT Core Facility for Next Generation Sequencing (Jochen Hecht/Ulrike Krüger, Charité-Berlin, Germany). BS-Seq libraries were constructed as directional.

4.3.8.g Pre-processing and Computational Analysis

(In cooperation with Peter Hansen)

The workflow proposed by Krueger *et al.* was used for data processing (Krueger *et al.* 2012). After trimming of possible adapter sequences, reads were checked for quality by FastQC and reads with a Phred-score below 28 were discarded. Fastq files were generated for each amplicon and each sample.

Quality filtered reads were analyzed using BiQ Analyzer HiMod (Becker *et al.* 2014) and compared with reference sequences representing unmethylated, fully C to T converted DNA (reported as % of cytosine methylation).

4.3.9 DNA Methylation Analysis by MethylCap-Sequencing (MethylCap-Seq)

Genome-wide analysis of DNA methylation profiles by NGS-based bisulfite *'shotgun'* sequencing is highly cost-effective. Therefore, alternative strategies focus on the enrichment of sheared, methylated DNA by affinity purification using proteins containing methyl-DNA binding domains (MBDs) and subsequent analysis of enriched DNA fragments by massive parallel sequencing. One method is called MethylCap-Seq that is based on *in vitro* capture of methylated DNA using the MBD domain of MeCP2 (methyl CpG binding protein 2) combined by next generation sequencing of eluted DNA (**Fig. 4-8**) (Brinkman *et al.* 2010, Serre *et al.* 2010).

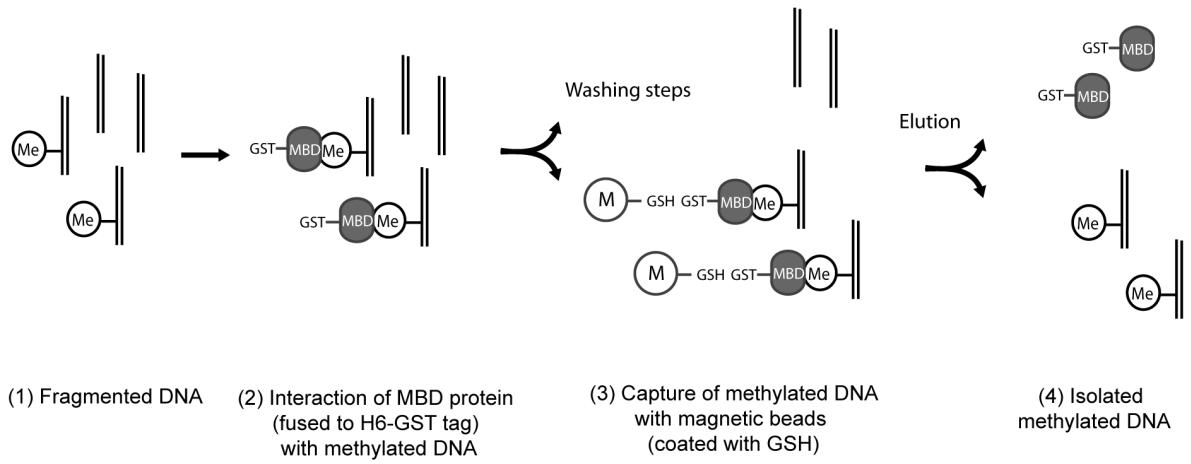

Fig. 4-8: Principle of MethylCap. Isolated DNA is fragmented by sonication and subjected to MethylCap. Methylated DNA (Me) is enriched by binding to the high affinity H6-GST-MBD fusion protein and subsequent magnetic (M) separation. The protein H6-GST-MBD consists of the methyl binding domain (MBD) of human MeCP2 that is fused to glutathione-S-transferase (GST) containing an N-terminal His6-tag (H6). GST possesses a high affinity to glutathione (GSH). Isolated DNA can be further processed by sequencing analysis. Figure was adapted from the Diagenode website (as of October 2015): http://www.diagenode.com/en/catalog/kits-2/dna-methylation-11/product/methylcap-kit-11.

4.3.9.a Sample Preparation (MethylCap)

MethylCap-Seq was performed at the BCRT Core Facitlity for Next Generation Sequencing (Jochen Hecht/Ulrike Krüger, Charité-Berlin, Germany). Briefly, isolated genomic DNA (from point **4.3.8.a**) was sheared by sonication and subjected to MethylCap following the instructions of the MethylCap® kit

from Diagenode. Elution of captured DNA was performed by a single total elution in High Elution Buffer. Sequencing of eluted DNA fragments was performed on an Illumina HiSeq 1500 generating 50 bp long reads.

4.3.9.b Pre-Processing and Visualization of MethylCap-Seq Data

Pre-processing of sequenced data was performed similarly as for ChIP-Seq data, as outlined in **4.3.6.b**. Briefly, sequenced reads were mapped to the human hg19 reference genome (Feb. 2009) and filtered for uniquely mapped and non-redundant reads. Aligned reads in BAM files were converted to BigWig files and visualized in the UCSC Genome Browser.

4.3.9.c Identification of Genome-Wide DNA-Methylated Regions

(Performed in cooperation with Dr. Karsten Jürchott)

Analysis of enriched DNA fragments representing methylated DNA was performed with the Bioconductor package MEDIPS (version 1.16.0) (Lienhard *et al.* 2014). The workflow provides a quality control (QC) followed by differential methylation analysis.

The QC included saturation analysis, CpG coverage analysis and CpG enrichment calculation. An overview of the quality control is shown in **Table 4-8**. The most important QC parameter is the CpG enrichment, which represents the frequency of CpGs observed in the sequenced sample compared to the expected frequency in the reference genome (Rodriguez *et al.* 2012). Samples were generally excluded with CpG enrichment values less than 1.4 and saturation values less than 0.5. The samples which passed the quality control were further analyzed for differential DNA methylation.

Table 4-8: QC values of MethylCap-Seg data provided by the Bioconductor package MEDIPS.

Samples	Saturation analysis	CpG coverage rate	CpG enrichment	
			enrichment.score.relH	enrichment.score.GoGe
N	0.89	22.60 %	3.73	1.87
N+L	0.83	23.97 %	3.02	1.68
T1	0.71	12.96 %	2.65	1.58
T1+L	0.78	9.95 %	3.76	1.90
T100	0.81	14.75 %	3.60	1.84
T100+L	0.78	12.19 %	3.47	1.81

QC parameter: Saturation (library complexity) > 0.05, CpG coverage rate (5x; fraction of CpGs sequenced at least five times) > 5 %, CpG enrichment scores (compared to reference genome) > 1.4.

Analysis of differentially methylated genomic regions was performed with default parameters (uniq=TRUE, extend=300, shift=0 and ws=100) over the complete human genome ("BSgenome.Hsapiens,UCSC.hg19", chromosome 1 to 22, chromosome X and chromosome Y).
The analysis was performed by identifying differential methylation between N+L with T100+L conditions. As no replicates were available, the differential coverage was calculated by edgeR (p.adj = "none") and differentially methylated regions were identified by a minimum fold change of 2

(*P* value = 0.01). Regions of interest were annotated with the nearest genes (annotation = GENE, tssSz =c(-10000,10000)).

4.3.9.d Gene Ontology (GO) Enrichment Analysis of MethylCap-Seq Data

GO enrichment analyses of identified gene lists were performed using Database for Annotation, Visualization and Integrated Discovery (DAVID, version 6.7) (Huang *et al.* 2009a, b).

4.3.10 Expression Profiling by mRNA Sequencing (mRNA-Seq)

4.3.10.a Sample Preparation (mRNA)

Total isolated RNA from section **4.3.4** was subjected to mRNA-Seq for genome-wide analysis of mRNA expression in human monocytes. In total, three replicates per condition (N+L, T100+L) were used. Illumina deep sequencing was performed at the genomics core facility of the Center of Excellence for Fluorescent Bioanalytics (KFB, University of Regensburg, Germany).

4.3.10.b Data Processing and Determining of Differentially Expressed Genes

(Performed in cooperation with Peter Hansen)

Data preprocessing and analysis were performed on a locally installed version of the Galaxy platform (Blankenberg *et al.* 2010, Giardine *et al.* 2005, Goecks *et al.* 2010) at the Charité (Berlin, Germany). Data analysis was performed in principle according to the tuxedo workflow proposed by Trapnell *et al.* (Trapnell *et al.* 2012).

In brief, mRNA-Seq data was quality controlled using FastQC. Sequenced reads were mapped to the reference genome (human hg19) using TopHat (version 2.0.9) (Trapnell *et al.* 2009) with known gene model annotations (human reference .GTF annotation) to disable novel splice discovery. The aligned reads were directly tested for differential expression using Cuffdiff (version 2.1.1) (Trapnell *et al.* 2010) with the human reference annotation used as transcript assembly. Geometric normalization was applied to normalize between samples and replicates (as proposed by Anders & Huber (2010)). Default parameters were used for TopHat and Cuffdiff analysis. Data visualization was performed by the Bioconductor package cummeRbund (version 2.8.2) (Goff *et al.* 2013).

RNA-Seq analysis results were controlled for normalization and quality (**Fig. 4-9**). To quantify the transcript expression and compare between samples, Cuffdiff determines the *reads per kilobase of transcripts per million mapped reads* (RPKM) for all genes.

The expression profile for naïve monocytes treated with LPS (N+L) was compared to the transcriptome of high-dose tolerized cells stimulated with LPS (T100+L). Differentially expressed genes (DEG), which showed at least a 2-fold change and a *P* value smaller than 0.05, were used for downstream analyses.

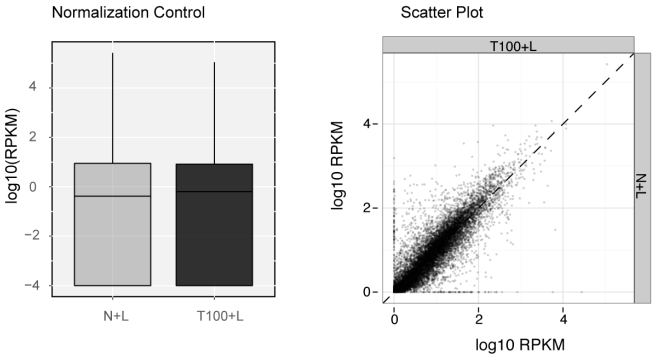

Fig. 4-9: Quality control of mRNA-Seq data. Box plot (left) represents proper normalization of data. Scatter plot (right) evaluates good quality based on low deviation from the dashed line. Replicates were combined to one condition. Data was visualized by the Bioconductor package cummeRbund.

4.3.10.c Heat map of Differentially Expressed Genes

A heat map of RPKM expression values of selected genes (DEG) was generated using R. Data matrix was scaled over the samples before hierarchical clustering (Euclidean) using heatmap.2 (gplot R package, version 2.17.0, Warnes *et al.* (2015)).

4.3.10.d GO Enrichment Analysis of mRNA-Seq Data

GO enrichment analysis of identified genes was performed using DAVID (version 6.7) (Huang *et al.* 2009a, b).

4.3.10.e Analysis of Gene Overlap between Gene Lists

Significant overlap between gene lists was investigated by the Bioconductor package GeneOverlap (version 1.2.0, Shen & Sinai (2013)).

4.4 Statistical Analysis

Data were analyzed by GraphPad Prism (La Jolla, California, USA, version 5 and 6) and are presented as mean ± standard error of the mean (SEM) of more than three independent experiments. Statistical analysis was performed for a sample size > 5 and relied on the general comparison of naïve cells with tolerant monocytes. Wilcoxon matched-pairs signed-rank test was used to determine significant differences between two related groups (non-parametric, for comparison of samples from one source with different conditions). *P* values of < 0.05 were considered statistically significant and were displayed in figures as follows: *p ≤ 0.05 and **p ≤ 0.01.

For analysis of gene overlap between identified gene lists, the Bioconductor package GeneOverlap (version 1.2.0) was used (Shen & Sinai 2013). Significance was tested using the Fisher's exact test.

5. Appendix

5.1 Cytokines and Chemokines – An Overview

Information about the following cytokines and chemokines is reviewed in Ramnath *et al.* (2006), Schulte *et al.* (2013) and Turner *et al.* (2014).

The 17 kDa protein **TNF** is one of the primary master regulators of inflammation (Parameswaran & Patial 2010) and is responsible for the pathophysiological conditions associated with sepsis (Carswell *et al.* 1975).
The primary function of TNF is the upregulation of multiple pro-inflammatory proteins like cytokines, chemokines and adhesion molecules. In local inflammatory responses, TNF is important for activation of macrophages and their production from progenitor cells (Fahlman *et al.* 1994, Witsell & Schook 1992). Furthermore, it induces phagocytosis, increases vascular permeability, and enhances adhesion molecules on endothelial cells to facilitate infiltration of leucocytes to the site of infection and allow clearance of infectious agents (Nakae *et al.* 1996, Shimaoka & Park 2008). TNF is mainly produced by activated immune cells like monocytes and macrophages, lymphocytes and polymorphonuclear cells; and by non-immune cells like fibroblasts in response to infectious and/or inflammatory stimuli (Schulte *et al.* 2013, Striz *et al.* 2014, Turner *et al.* 2014).
However, once invading pathogens infiltrate the blood stream, TNF is systemically produced leading to a dramatic loss of liquid, and vascular occlusion resulting in organ failure and sometimes death as seen in sepsis (see **1.5** in *Introduction* section) (Roman *et al.* 1993).

IL-1β was originally identified as an endogenous pyrogen, which can induce fever on its own. It is mainly produced by monocytes and macrophages, neutrophils and hepatocytes (Striz *et al.* 2014, Turner *et al.* 2014). IL-1β activates neutrophils, induces production of cytokines and chemokines production like IL-6, CXCL8/IL-8 and TNF (Cavaillon *et al.* 1994, O'Neill 2008), and upregulates adhesion molecules on leukocytes and endothelial cells (Striz *et al.* 2014, Turner *et al.* 2014).
The production and secretion of IL-1β and other cytokine family members need two signals. First, TLR4 signaling leads to activation of NFκB signaling followed by expression of biologically inactive pro-IL-1β. Second, inflammasome-dependent activation of caspase-1 mediates posttranslational processing of the propeptide into the active IL-1β form and subsequent secretion via exocytosis (Kostura *et al.* 1989, Schroder & Tschopp 2010).
The **IL-1 receptor antagonist (IL-1RA)** is a competitive inhibitor of IL-1β signaling (McIntyre *et al.* 1991). It inhibits the function of IL-1β through binding to the IL-1 receptor but fails to induce intracellular signaling. It is secreted by neutrophils, monocytes, macrophages and hepatocytes as an acute phase protein (Arend & Guthridge 2000).

TNF and IL-1β share a remarkable array of biological effects (Elias *et al.* 1989, Okusawa *et al.* 1988). Both cytokines are main activators of the coagulation system (Schouten *et al.* 2008) and operate synergistically to induce a shock-like status characterized by vascular permeability, severe pulmonary edema and hemorrhage (Schulte *et al.* 2013). TNF and IL-1β are released within the first 30 to 90 min after exposure to LPS (Creasey *et al.* 1991, Kuhns *et al.* 1995) and act on other immune cells such as macrophages, endothelial cells and neutrophils. Binding to their receptors orchestrates a second level of inflammatory cascades. Activation of MAP kinases and the transcription factor NFκB result in the induction of downstream immunoregulatory mediators including cytokines like IL-6 and CXCL8/IL-8, and lipid mediators (Cohen 2002, Schulte *et al.* 2013).

IL-6 is a 21 kDa glycoprotein and is a pleiotropic cytokine with a wide range of functions including activation and differentiation of macrophages, dendritic cells, B and T cells. However, application of IL-6 alone cannot induce a shock-like status. It can be produced by a variety of cells including T and B cells, monocytes and macrophages, dendritic cells, fibroblasts and endothelial cells (Schulte *et al.* 2013, Striz *et al.* 2014, Turner *et al.* 2014). The key functions of IL-6 are the induction of fever and mediation of the acute phase response (Castell *et al.* 1988, Gauldie *et al.* 1989, Leon *et al.* 1998). In an acute infection, IL-6 stimulates hepatic synthesis of acute phase proteins such as C-reactive protein and complement components, and mediates activation of the coagulation system (fibrinogen, ferritin) (Kishimoto 2010).

A potent activator for monocytes and macrophages is **IFNγ**, which is preferentially produced by activated NK cells, NKT cells and some T cell subtypes including cytotoxic CD8+ T cells and T helper 1 cells. Its production is tightly regulated by macrophage-derived cytokines like TNF and IL-12 (Schulte *et al.* 2013). IFNγ induces phagocytic effector functions, activates anti-microbial activity and increases antigen processing, thereby promoting antigen presentation to lymphocytes through MHCs and activation of adaptive immunity (Giacomini *et al.* 1988, Young & Hardy 1995). Moreover, IFNγ enhances killing of intracellular pathogens, *e.g.* viruses (Muller *et al.* 1994), *Leishmania major* (Wang *et al.* 1994), *Listeria monocytogenes* (Huang *et al.* 1993) and Mycobacteria (Cooper *et al.* 1993). Administration of IFNγ can rescue monocyte function and reverse *'immunoparalysis'* in sepsis (Bozinovski *et al.* 2002, Docke *et al.* 1997a, Flohe *et al.* 2008, Leentjens *et al.* 2012, Schefold *et al.* 2008, Volk *et al.* 1996).

The main function of chemokines is chemotaxis, although their role is more complex and involves homeostatic and housekeeping functions (Turner *et al.* 2014). Chemokines are a group of small proteins (8-12 kDa), characterized by the presence of three to four conserved cysteine residues, subdivided into four families based on the arrangement of the N-terminal

residues (Nomiyama *et al.* 2013). The majority of chemokines belong to the CXC and CC subfamily (Striz *et al.* 2014, Turner *et al.* 2014).
Chemokines have an important role within the cytokines as they regulate the recruitment of immune cells to sites of infection or injury.

IL-8 belongs to the CXC subfamily and is also known as **CXCL8**. The chemokine is a critical inflammatory mediator and was originally identified as neutrophilic chemoattractant (Baggiolini *et al.* 1992, Hammond *et al.* 1995). However, CXCL8/IL-8 also recruits monocytes, lymphocytes, basophils and eosinophils to sites of infection (Turner *et al.* 2014), and induces the expression of adhesion molecules (Takami *et al.* 2002).
Whereas CXCL8/IL-8 basically regulates the recruitment and phagocytosis activity of neutrophils to inflamed tissues, other chemokines like monocyte chemoattractant protein-1 (**MCP-1** also known as **CCL2**), macrophage inflammatory protein-1α (**MIP-1α** also known as **CCL3**) and IFN-inducible protein of 10 kDa (**IP-10** also known as **CXCL10**) are important regulators for the attraction of mainly monocytes and macrophages but also T cells, NK cells and dendritic cells. Thus, early chemokine expression appears in two phases: First, recruitment of neutrophils by *e.g.* IL8/CXCL8 followed by attraction of monocytes, NK cells and T cells by CCL2/MCP1, CCL3/MIP1α and CXCL10/IP-10 (Striz *et al.* 2014).

After clearance of infectious agents, several mechanisms are involved in downregulation of effector mechanisms and tissue healing. These processes are also orchestrated by cytokines like IL-10 and TGFβ.
The 35 kDa homodimeric cytokine **IL-10** is produced by NK cells, T cells and monocytes. IL-10 has mainly immunosuppressive functions and is involved in termination of inflammatory processes (Schulte *et al.* 2013, Striz *et al.* 2014). For instance, it inhibits the production of pro-inflammatory cytokines and chemokines (de Waal Malefyt *et al.* 1991, Fiorentino *et al.* 1991), thereby preventing tissue damage (van der Poll *et al.* 1997). Moreover, IL-10 reduces the antigen-presenting capacity of dendritic cells by downregulation of MHCs and costimulatory molecules, leading to inhibition of T lymphocyte activation (O'Keefe *et al.* 1999).
Another anti-inflammatory cytokine is **TGFβ**, which is widely produced by platelets, macrophages, lymphocytes, endothelial and epithelial cells, eosinophils and others. It plays an important role in tissue repair and fibrosis (Sporn & Roberts 1989), suppression of TNF and IL-1β release (Bogdan & Nathan 1993), and inhibition of T cell function and proliferation (Gilbert *et al.* 1997, Li *et al.* 2006a). Additionally, TGFβ is an important mediator of sepsis-induced immunosuppression (Blobe *et al.* 2000) and mediates tolerance induction of monocytes and macrophages to LPS together with IL-10 (Randow *et al.* 1995).

5.2 Binding Sites of Primer Pairs for ChIP-qPCR Analysis of Human Monocytes and Murine Macrophages

Human

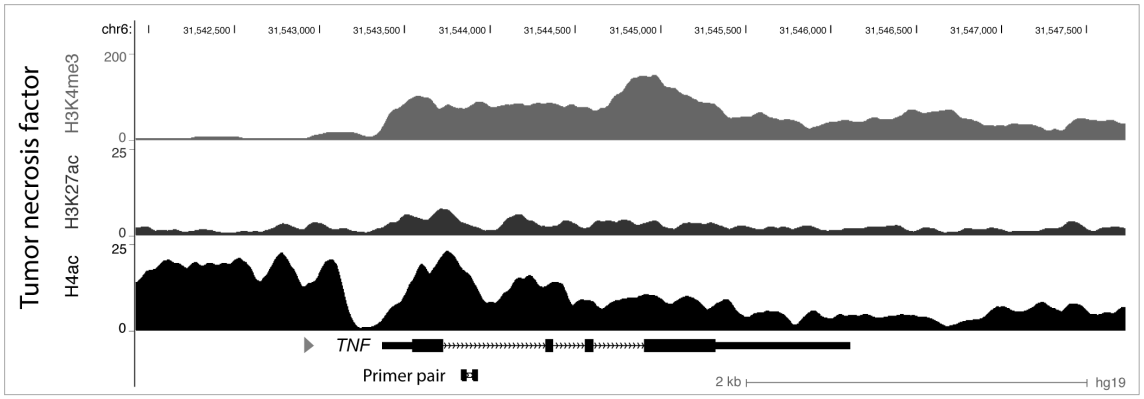

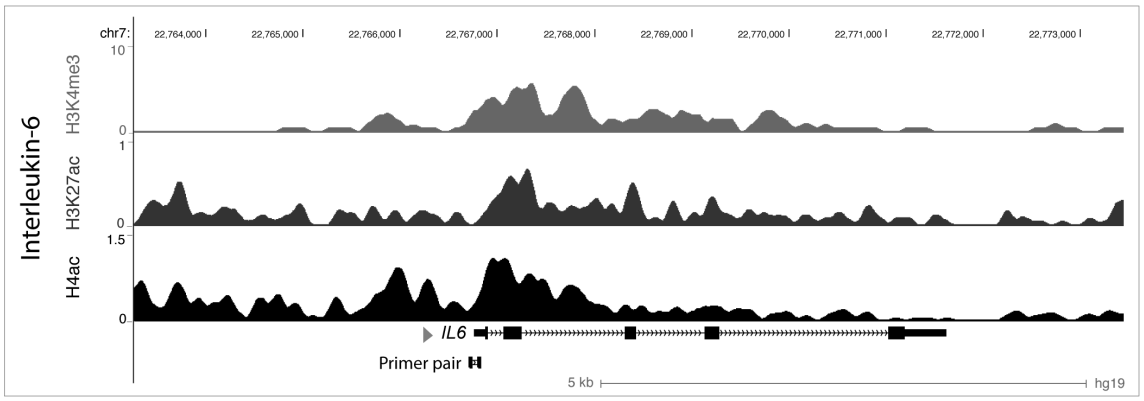

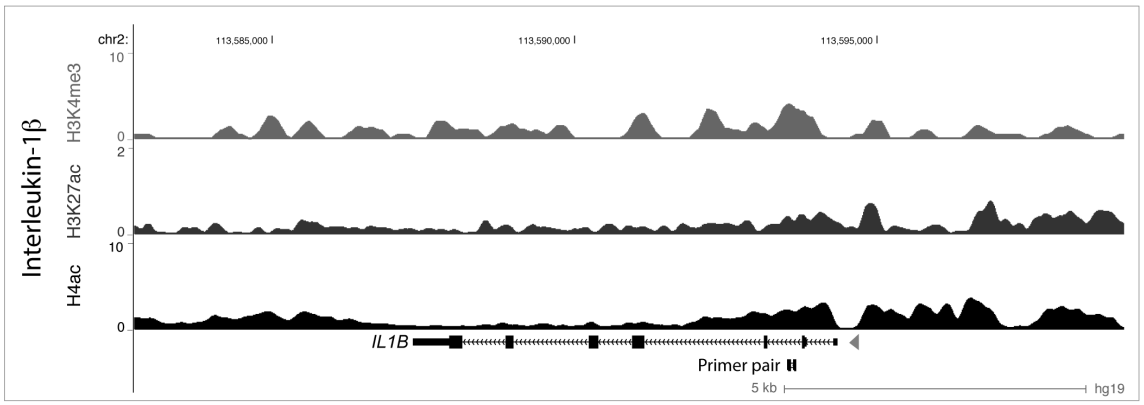

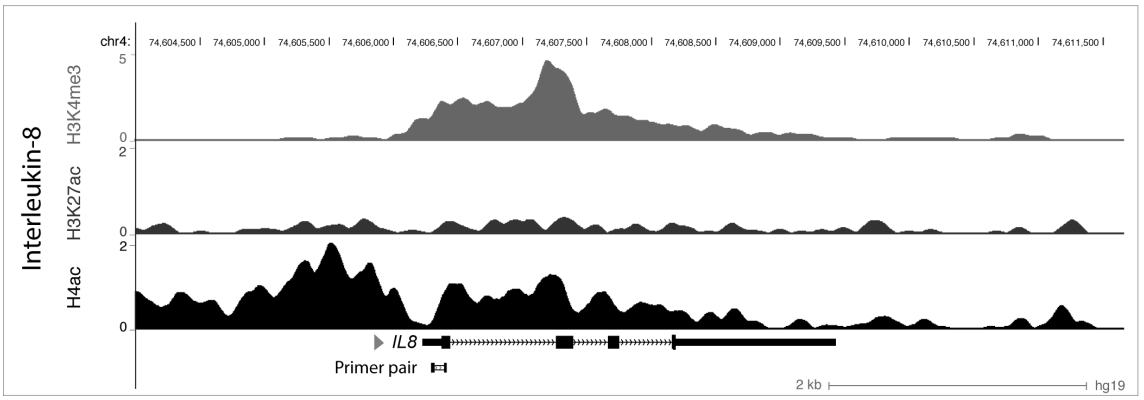

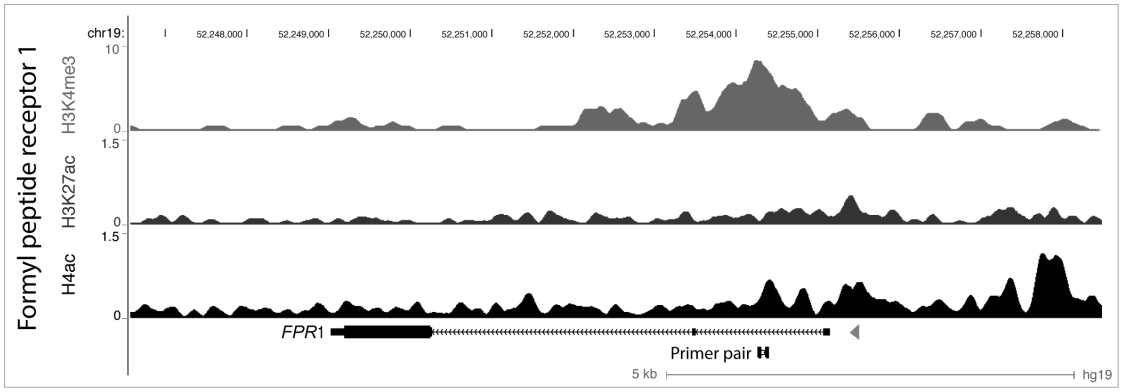
Formyl peptide receptor 1
chr19:
52,248,000
52,249,000
52,250,000
52,251,000
52,252,000
52,253,000
52,254,000
52,255,000
52,256,000
52,257,000
52,258,000
H3K4me3
H3K27ac
H4ac
10
0
1.5
0
1.5
0
FPR1
Primer pair
5 kb
hg19

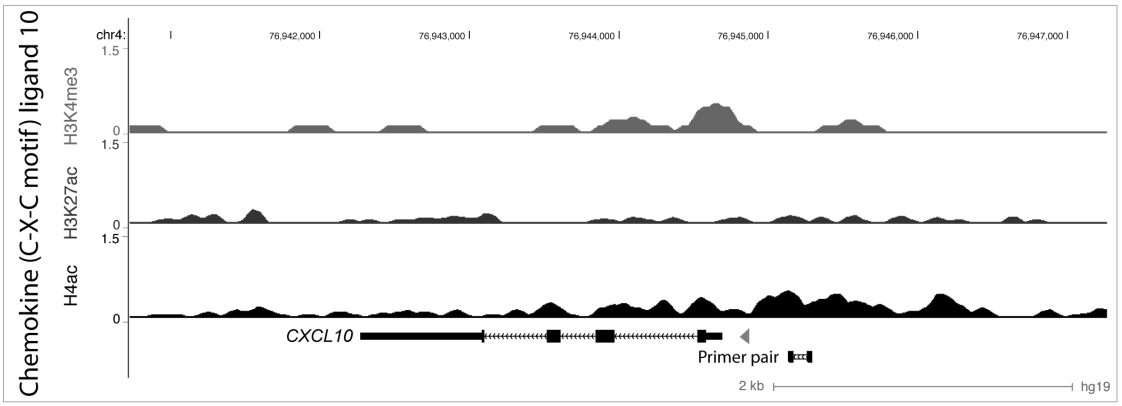
Chemokine (C-X-C motif) ligand 10
chr4:
76,942,000
76,943,000
76,944,000
76,945,000
76,946,000
76,947,000
H3K4me3
H3K27ac
H4ac
1.5
0
1.5
0
1.5
0
CXCL10
Primer pair
2 kb
hg19

Murine

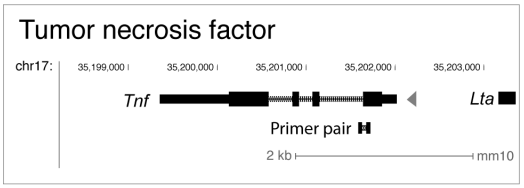
Tumor necrosis factor
chr17:
35,199,000
35,200,000
35,201,000
35,202,000
35,203,000
Tnf
Lta
Primer pair
2 kb
mm10

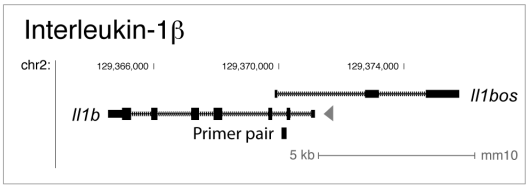
Interleukin-1β
chr2:
129,366,000
129,370,000
129,374,000
Il1bos
Il1b
Primer pair
5 kb
mm10

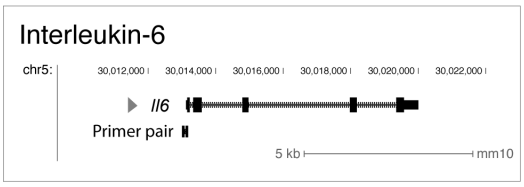
Interleukin-6
chr5:
30,012,000
30,014,000
30,016,000
30,018,000
30,020,000
30,022,000
Il6
Primer pair
5 kb
mm10

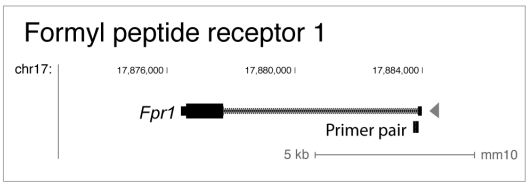
Formyl peptide receptor 1
chr17:
17,876,000
17,880,000
17,884,000
Fpr1
Primer pair
5 kb
mm10

5.3 Cytometer Settings

BD FACSCalibur

Laser	Detector	1. Pass	2. Pass	PMT	Fluorochrome
Blue 488 nm (15 mW)	A	560 SP	530/30 BP	FL1	FITC, Alexa 488, GFP, CSFE
	B		480/10 BP	SSC	
	C	640 LP	585/42 BP	FL2	PE
	D	640 LP	670 LP	FL3	PerCP, PE-Cy5, PE-Cy7, 7AAD
Red 640 nm (10 mW)	C	640 LP	660/20 BP	FL4	APC, Alexa 647

BD LSRFortessa

Laser	Detector	1. Pass	2. Pass	PMT	Fluorochrome
Blue 488 nm (100 mW)	A	685 LP	696/40 BP	Blue 695/40	PerCP, PerCP-Cy5.5, 7AAD
	B	505 LP	525/50 BP	Blue 525/50	FITC, Alexa 488, GFP, CFSE
	C	Empty	488/10 BP	SSC	
YellowGreen (YG) 561 nm (100 mW)	A	750 LP	780/60 BP	YG 780/60	PE-Cy7, PE-H7, PE-A750, PC7
	B	685 LP	710/50 BP	YG 710/50	PE-Cy5.5
	C	635 LP	670/30 BP	YG 670/30	PE-Cy5, PC5
	D	600 LP	610/20 BP	YG 610/20	PE-TexasRed (ECD), PI, PE-A610
	E	Empty	585/15 BP	YG 585/15	PE
	F	Empty	Empty		
	G	Empty	Empty		
	H	Empty	Empty		
Red 639 nm (40 mW)	A	750 LP	780/60 BP	Red 780/60	APC-Cy7, APC-A750
	B	685 LP	710/50 BP	Red 710/50	Alexa 700, APC-A700
	C	Empty	670/14 BP	Red 670/14	APC, Alexa 647
Violet (Vio) 404 nm (50 mW)	A	705	780/60	Vio 780/60	Horizon V800, Qdot 800
	B	685	710/50 BP	Vio 710/50	Qdot 705, Qdot 700
	C	635	660/20 BP	Vio 660/20	Qdot 655
	D	600	610/20	Vio 610/20	Qdot 605
	E	505	525/50 BP	Vio 525/50	Amcyan, Horizon V450, Qdot 525
	F	Empty	450/50 BP	Vio 450/50	Pacific Blue, Alexa 405, Horizon V450
	G	Empty	Empty		
	H	Empty	Empty		
Ultra-Violet (UV) 355 nm (60 mW)	A	505	530/30	UV 530/30	Indo-1 (free $Ca2^+$)
	B	Empty	405/20	UV 405/20	Indo-1 (bound $Ca2^+$), DAPI, Hoechst
	C	Empty	Empty		

FSC = forward scatter

LP = long pass

mW = milliwatts

PMT = photomultiplier tube with specific band pass filter

SP = short pass

SSC = sideward scatter

5.4 DNA Methylation Analysis by BS-Seq

Sequence of untreated and bisulfite-treated DNA (displayed by MethPrimer, Li & Dahiya (2002))

Explanations:		
	Upper row:	Original sequence
	Lower row:	Bisulfite modified sequence
	++	CpG site
	::	Non-CpG *'C'* converted to *'T'*
	>>>>>>	Primer position
	DraI / SspI	Restriction site for specific enzyme

Human *TNF* promoter region (Campion 2009)

```
  1 CCAAAAGAAATGGAGGCAATAGGTTTTGAGGGGCATGGGGACGGGGTTCAGCCTCCAGGG
    ::|||||||||||||||:||||||||||||||||:|||||||++|||||:||::|::||||
  1 TTAAAAGAAATGGAGGTAATAGGTTTTGAGGGGTATGGGGACGGGGTTTAGTTTTTAGGG
    >>>>>>>>>>>>>>>>>>>>>>

 61 TCCTACACACAAATCAGTCAGTGGCCCAGAAGACCCCCCTCGGAATCGGAGCAGGGAGGA
    |::|||:|:|:||||:|||:|||||:::|||||||:::::::|++||||++||||:||||||||
 61 TTTTATATATAAATTAGTTAGTGGTTTAGAAGATTTTTTTCGGAATCGGAGTAGGGAGGA

121 TGGGGAGTGTGAGGGGTATCCTTGATGCTTGTGTGTCCCCAACTTTCCAAATCCCCGCCC
    |||||||||||||||||||::|||||||:|||||||:::::||:|||::|||||:::++:::
121 TGGGGAGTGTGAGGGGTATTTTTGATGTTTGTGTGTTTTTAATTTTTTAAATTTTCGTTT
                                                      DraI

181 CCGCGATGGAGAAGAAACCGAGACAGAAGGTGCAGGGCCCACTACCGCTTCCTCCAGATG
    :++++|||||||||||||:++|||:||||||||:||||:::|:||:++:||::|::||||||
181 TCGCGATGGAGAAGAAATCGAGATAGAAGGTGTAGGGTTTATTATCGTTTTTTTTAGATG

241 AGCTCATGGGTTTCTCCACCAAGGAAGTTTTCCGCTGGTTGAATGATTCTTTCCCCGCCC
    ||:|:||||||||:|::|::||||||||||||:++:|||||||||||||:|||:::++:::
241 AGTTTATGGGTTTTTTTATTAAGGAAGTTTTTCGTTGGTTGAATGATTTTTTTTTCGTTT
                                                    TSS

301 TCCTCTCGCCCCAGGGACATATAAAGGCAGTTGTTGGCACACCCAGCCAGCAGACGCTCC
    |::|:|++::::|||||:|||||||||:|||||||||:|:|:::||::||:|||++:|::
301 TTTTTTCGTTTTAGGGATATATAAAGGTAGTTGTTGGTATATTTAGTTAGTAGACGTTTT

361 CTCAGCAAGGACAGCAGAGGACCAGCTAAGAGGGAGAGAAG
    :|:||:|||||:||:|||||::||:|||||||||||||||
361 TTTAGTAAGGATAGTAGAGGATTAGTTAAGAGGGAGAGAAG
                       <<<<<<<<<<<<<<<<<<<<<<
```

Human *IL6* promoter region (Nile 2008)

```
   1 CACCATCCTGAGGGAAGAGGGCTTCTGAACCAGCTTGACCCAATAAGAAATTCTTGGGTG
     :|::||::|||||||||||||||:||:|||||::||:||||:::||||||||||||:|||||||
   1 TATTATTTTGAGGGAAGAGGGTTTTTGAATTAGTTTGATTTAATAAGAAATTTTTGGGTG
IL6_1 >>>>>>>>>>>>>>>>>>>>>>>>>
  61 CCGACGCGGAAGCAGATTCAGAGCCTAGAGCCGTGCCTGCGTCCGTAGTTTCCTTCTAGC
     :++|++++||||:|||||:||||::||||||:++||::||++|:++||||||::||:|||:
  61 TCGACGCGGAAGTAGATTTAGAGTTTAGAGTCGTGTTTGCGTTCGTAGTTTTTTTTTAGT

 121 TTCTTTTGATTTCAAATCAAGACTTACAGGGAGAGGGAGCGATAAACACAAACTCTGCAA
     ||:|||||||||:||||:||||:|||:||||||||||||++|||||:|:||||:|:|||:||
 121 TTTTTTTGATTTTAAATTAAGATTTATAGGGAGAGGGAGCGATAAATATAAATTTTGTAA
                 DraI
 181 GATGCCACAAGGTCCTCCTTTGACATCCCCAACAAAGAGGTGAGTAGTATTCTCCCCCTT
     ||||::|:|||||::|::||||||:||::::||:||||||||||||||||||:|:::::||
 181 GATGTTATAAGGTTTTTTTTTGATATTTTTAATAAAGAGGTGAGTAGTATTTTTTTTTTT

 241 TCTGCCCTGAACCAAGTGGGCTTCAGTAATTTCAGGGCTCCAGGAGACCTGGGGCCCATG
     |:||:::|||||::|||||||:||:|||||||||:||||:|::|||||||::||||||:::|||
 241 TTTGTTTTGAATTAAGTGGGTTTTAGTAATTTTAGGGTTTTAGGAGATTTGGGGTTTATG

 301 CAGGTGCCCCAGTGAAACAGTGGTGAAGAGACTCAGTGGCAATGGGGAGAGCACTGGCAG
     :|||||::::|||||||:|||||||||||||:|:|||||:||||||||||||:|:||||:||
 301 TAGGTGTTTTAGTGAAATAGTGGTGAAGAGATTTAGTGGTAATGGGGAGAGTATTGGTAG
                                 IL6_1 <<<<<<<<<<<<<<<<<<<<<<<<<
 361 CACAAGGCAAACCTCTGGCACAGAGAGCAAAGTCCTCACTGGGAGGATTCCCAAGGGGTC
     :|:||||:|||::|:||||:|:|||||||:||||||::|:|:||||||||||:::|||||||:
 361 TATAAGGTAAATTTTTGGTATAGAGAGTAAAGTTTTTATTGGGAGGATTTTTAAGGGGTT

 421 ACTTGGGAGAGGGCAGGGCAGCAGCCAACCTCCTCTAAGTGGGCTGAAGCAGGTGAAGAA
     |:||||||||||||:||||:|||:||:::|||::|:::|:||||||||:||||||:||||||||||
 421 ATTTGGGAGAGGGTAGGGTAGTAGTTAATTTTTTTTTAAGTGGGTTGAAGTAGGTGAAGAA
                                   IL6_2 >>>>>>>>>>>>>>>>>>>>>>>>>
 481 AGTGGCAGAAGCCACGCGGTGGCAAAAAGGAGTCACACACTCCACCTGGAGACGCCTTGA
     |||||:||||||::|++++||||:||||||||||:|:|:|:|::|::||||||++:::||||
 481 AGTGGTAGAAGTTACGCGGTGGTAAAAAGGAGTTATATATTTTATTTGGAGACGTTTTGA

 541 AGTAACTGCACGAAATTTGAGGATGGCCAGGCAGTTCTACAACAGCCGCTCACAGGGAGA
     |||||:||:|++|||||||||||||::|||:||||:||:||:||:++:|:|:|||||||
 541 AGTAATTGTACGAAATTTGAGGATGGTTAGGTAGTTTTATAATAGTCGTTTATAGGGAGA

 601 GCCAGAACACAGAAGAACTCAGATGACTGGTAGTATTACCTTCTTCATAATCCCAGGCTT
     |::|||||:|:||||||||:|:|||||||:||||||||||||::||:||:|||||:::||||:||
 601 GTTAGAATATAGAAGAATTTAGATGATTGGTAGTATTATTTTTTTTATAATTTTAGGTTT
```

```
 661 GGGGGGCTGCGATGGAGTCAGAGGAAACTCAGTTCAGAACATCTTTGGTTTTTACAAATA
     ||||||:||++|||||||:||||||||:|:||||:||||:||:||||||||||||:|||||
 661 GGGGGGTTGCGATGGAGTTAGAGGAAATTTAGTTTAGAATATTTTTGGTTTTTATAAATA
                                             SssPI
 721 CAAATTAACTGGAACGCTAAATTCTAGCCTGTTAATCTGGTCACTGAAAAAAAATTTTTT
     :|||||||:|||||++:||||||:|||::|||||||:||||:|:|||||||||||||||
 721 TAAATTAATTGGAACGTTAAATTTTAGTTTGTTAATTTGGTTATTGAAAAAAAATTTTTT

 781 TTTTTTCAAAAAACATAGCTTTAGCTTATTTTTTTTCTCTTTGTAAAACTTCGTGCATGA
     ||||||:||||||:||||:|||||:||||||||||:|:|||||||||:||++||:||||
 781 TTTTTTTAAAAAATATAGTTTTAGTTTATTTTTTTTTTTTTTGTAAAATTTCGTGTATGA
         DraI                                                IL6_2 <<<<<<<
 841 CTTCAGCTTTACTCTTTGTCAAGACATGCCAAAGTGCTGAGTCACTAATAAAAGAAAAAA
     :||:||:|||||:|:||||||:||||:|||::||||||:||||||:|:|||||||||||||
 841 TTTTAGTTTTATTTTTTGTTAAGATATGTTAAAGTGTTGAGTTATTAATAAAAGAAAAAA
     <<<<<<<<<<<<<<<<<<<       IL6_3 >>>>>>>>>>>>>>>>>>>>>>>>>>

 901 AGAAAGTAAAGGAAGAGTGGTTCTGCTTCTTAGCGCTAGCCTCAATGACGACCTAAGCTG
     |||||||||||||||||||||||:||:||:||||++:|||::|:|||||++|::|||||:||
 901 AGAAAGTAAAGGAAGAGTGGTTTTGTTTTTTAGCGTTAGTTTTAATGACGATTTAAGTTG

 961 CACTTTTCCCCCTAGTTGTGTCTTGCCATGCTAAAGGACGTCACATTGCACAATCTTAAT
     :|:||||:::::|||||||||:|||::|||:|||||||++|:|:|||||:|:|||:|||||
 961 TATTTTTTTTTTTAGTTGTGTTTTGTTATGTTAAAGGACGTTATATTGTATAATTTTAAT

1021 AAGGTTTCCAATCAGCCCCACCCGCTCTGGCCCCACCCTCACCCTCCAACAAAGATTTAT
     |||||||::|||:||:::::|::++:|:|||::::|:::|:|:::|::|||:||||||||||
1021 AAGGTTTTTAATTAGTTTTATTCGTTTTGGTTTTATTTTTATTTTTTAATAAAGATTTAT

1081 CAAATGTGGGATTTTCCCATGAGTCTCAATATTAGAGTCTCAACCCCCAATAAATATAGG
     :|||||||||||||||:::||||||:|:||||||||||||:|:||:::::||||||||||||
1081 TAAATGTGGGATTTTTTTATGAGTTTTAATATTAGAGTTTTAATTTTTAATAAATATAGG
                       TSS ↓        SssPI
1141 ACTGGAGATGTCTGAGGCTCATTCTGCCCTCGAGCCCACCGGGAACGAAAGAGAAGCTCT
     |:||||||||||:||||||:|:||||:||:::|++||:::|:++||||++|||||||||:|:|
1141 ATTGGAGATGTTTGAGGTTTATTTTGTTTTCGAGTTTATCGGGAACGAAAGAGAAGTTTT

1201 ATCTCCCCTCCAGGAGCCCAGCTATGA
     ||:|::::|::||||||:::||:|||||
1201 ATTTTTTTTTAGGAGTTTAGTTATGA
  IL6_3 <<<<<<<<<<<<<<<<<<<<<<<<<
```

5.5 MethylCap-Seq Binding Profiles within the *FPR1*, *IL8*, *IL1B* & *CXCL10* Genes

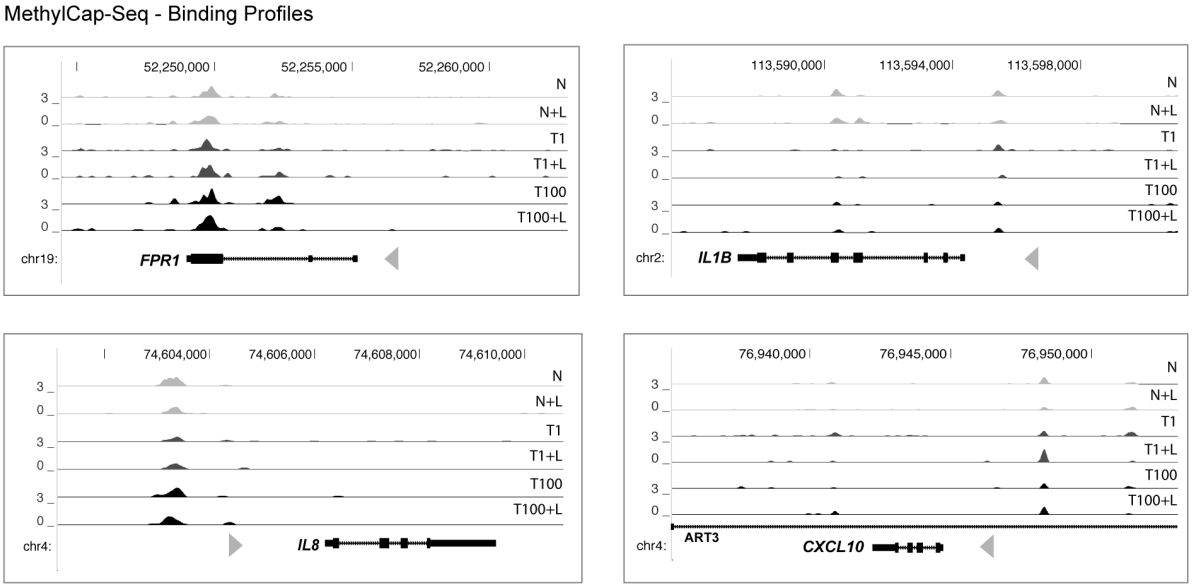

Naïve (N), low (T1, 1 ng/ml) and high-dose tolerized monocytes (T100, 100 ng/ml) were treated with 100 ng/ml LPS for 1.5 h and subjected to MethylCap-Seq. Binding profile of MBD-protein indicating methylated DNA within the genomic loci is displayed in the UCSC Genome Browser.

5.6 Transcription Factor Binding Sites (TFBSs) Identified by HOMER

H3K9me2_T_no_AcX (*DiffPeak* for T100+L, no co-enrichment in activating histone modifications)
Total Target Sequences = 11 558

Rank	Motif (known)	Name	*P* value	% of Targets Sequences with Motif
1		YY1(Zf)/Promoter/Homer	1e-8	0.77%
2		MyoD(HLH)/Myotube-MyoD-ChIP-Seq/Homer	1e-7	5.43%
3		Sp1(Zf)/Promoter/Homer	1e-5	0.81%
4		AP2gamma(AP2)/MCF7-TFAP2c-ChIP-Seq/Homer	1e-4	5.64%
5		MyoG(HLH)/C2C12-MyoG-ChIP-Seq(GSE36024)/Homer	1e-4	7.59%
6		HNF4a(NR/DR1)/HepG2-HNF4a-ChIP-Seq/Homer	1e-4	4.38%
7		Ap4(HLH)/AML-Tfap4-ChIP-Seq(GSE45738)/Homer	1e-4	9.16%
8		Tcf12(HLH)/GM12878-Tcf12-ChIP-Seq/Homer	1e-4	6.92%
9		SCL/HPC7-Scl-ChIP-Seq/Homer	1e-4	39.50%
10		MafA(bZIP)/Islet-MafA-ChIP-Seq(GSE30298)/Homer	1e-3	6.17%
11		FXR(NR/IR1)/Liver-FXR-ChIP-Seq/Homer	1e-3	3.30%
12		Myf5(bHLH)/GM-Myf5-ChIP-Seq(GSE24852)/Homer	1e-2	4.96%
13		HEB?/mES-Nanog-ChIP-Seq/Homer	1e-2	4.18%
14		ZBTB33/GM12878-ZBTB33-ChIP-Seq/Homer	1e-2	0.13%
15		RUNX2(Runt)/PCa-RUNX2-ChIP-Seq(GSE33889)/Homer	1e-2	8.52%
16		MafF(bZIP)/HepG2-MafF-ChIP-Seq(GSE31477)/Homer	1e-2	4.26%
17		Smad3(MAD)/NPC-Smad3-ChIP-Seq(GSE36673)/Homer	1e-2	26.84%
18		NFY(CCAAT)/Promoter/Homer	1e-2	8.23%
19		NFkB-p65(RHD)/GM12787-p65-ChIP-Seq/Homer	1e-2	4.67%

Rank	Motif (known)	Name	*P* value	% of Targets Sequences with Motif
20		Atoh1(bHLH)/Cerebellum-Atoh1-ChIP-Seq/Homer	1e-2	8.53%
21		EKLF(Zf)/Erythrocyte-Klf1-ChIP-Seq(GSE20478)/Homer	1e-2	1.81%
22		GFX(?)/Promoter/Homer	1e-2	0.09%
23		STAT6/Macrophage-Stat6-ChIP-Seq/Homer	1e-2	6.09%
24		STAT6(Stat)/CD4-Stat6-ChIP-Seq/Homer	1e-2	6.26%
25		AP-2alpha(AP2)/Hela-AP2alpha-ChIP-Seq/Homer	1e-2	4.77%
26		Sox3(HMG)/NPC-Sox3-ChIP-Seq(GSE33059)/Homer	1e-2	21.40%

H3K27me3_T_no_meX (*DiffPeak* for T100+L, no co-enrichment in activating histone modifications)
Total Target Sequences = 161

Rank	Motif (known)	Name	*P* value	% of Targets Sequences with Motif
1		Tcf12(HLH)/GM12878-Tcf12-ChIP-Seq/Homer	1e-2	13.04%
2		FOXA1:AR/LNCAP-AR-ChIP-Seq(GSE27824)/Homer	1e-2	3.73%
3		NF1(CTF)/LNCAP-NF1-ChIP-Seq/Homer	1e-2	6.83%

H4K20me3_T_no_meX (*DiffPeak* for T100+L, no co-enrichment in activating histone modifications)
Total Target Sequences = 2 758

Rank	Motif (known)	Name	*P* value	% of Targets Sequences with Motif
1		Tbox:Smad/ESCd5-Smad2_3-ChIP-Seq(GSE29422)/Homer	1e-9	3.30%
2		YY1(Zf)/Promoter/Homer	1e-8	1.34%
3		GFY-Staf/Promoters/Homer	1e-8	0.98%
4		Foxa2(Forkhead)/Liver-Foxa2-ChIP-Seq/Homer	1e-6	10.04%

Rank	Motif (known)	Name	*P* value	% of Targets Sequences with Motif
5		Sox3(HMG)/NPC-Sox3-ChIP-Seq(GSE33059)/Homer	1e-5	20.91%
6		NFY(CCAAT)/Promoter/Homer	1e-4	8.88%
7		Fox:Ebox(Forkhead:HLH)/Panc1-Foxa2-ChIP-Seq(GSE47459)/Homer	1e-4	10.98%
8		HEB?/mES-Nanog-ChIP-Seq/Homer	1e-3	6.92%
9		VDR(NR/DR3)/GM10855-VDR+vitD-ChIP-Seq/Homer	1e-3	2.54%
10		SCL/HPC7-Scl-ChIP-Seq/Homer	1e-3	46.10%
11		FOXA1(Forkhead)/MCF7-FOXA1-ChIP-Seq/Homer	1e-3	12.90%
12		Sox2(HMG)/mES-Sox2-ChIP-Seq/Homer	1e-3	9.89%
13		Smad3(MAD)/NPC-Smad3-ChIP-Seq(GSE36673)/Homer	1e-3	30.81%
14		RUNX2(Runt)/PCa-RUNX2-ChIP-Seq(GSE33889)/Homer	1e-3	9.53%
15		Sp1(Zf)/Promoter/Homer	1e-3	1.92%
16		RUNX-AML(Runt)/CD4+-PolII-ChIP-Seq/Homer	1e-3	8.23%
17		NFkB-p65(RHD)/GM12787-p65-ChIP-Seq/Homer	1e-2	5.94%
18		FOXP1(Forkhead)/H9-FOXP1-ChIP-Seq(GSE31006)/Homer	1e-2	5.11%
19		AR-halfsite(NR)/LNCaP-AR-ChIP-Seq(GSE27824)/Homer	1e-2	38.46%
20		RUNX1(Runt)/Jurkat-RUNX1-ChIP-Seq/Homer	1e-2	11.34%
21		FOXA1(Forkhead)/LNCAP-FOXA1-ChIP-Seq(GSE27824)/Homer	1e-2	14.90%
22		NFkB-p65-Rel(RHD)/LPS-exp(GSE23622)/Homer	1e-2	0.80%

H3K27ac_T_no_RepX (*DiffPeak* for T100+L, no co-enrichment in repressive histone modifications)
Total Target Sequences = 377

Rank	Motif (known)	Name	*P* value	% of Targets Sequences with Motif
1		Atoh1(bHLH)/Cerebellum-Atoh1-ChIP-Seq/Homer	1e-3	15.92%
2		CEBP:AP1(bZIP)/ThioMac-CEBPb-ChIP-Seq(GSE21512)/Homer	1e-2	10.88%

H4ac_T_no_RepX (*DiffPeak* for T100+L, no co-enrichment in repressive histone modifications)
Total Target Sequences = 236

Rank	Motif (known)	Name	*P* value	% of Targets Sequences with Motif
1		Tcf3(HMG)/mES-Tcf3-ChIP-Seq/Homer	1e-2	5.08%

Overlap in several histone modifications

Combined activating histone modifications in LPS-tolerant monocytes

H3K27acT_H4acT_no_RepX
Total Target Sequences = 32

Rank	Motif (known)	Name	*P* value	% of Targets Sequences with Motif
1		NFAT:AP1/Jurkat-NFATC1-ChIP-Seq/Homer	1e-2	12.50%

Combined repressive histone modifications in LPS-tolerant monocytes

H3K9me2T_H4K20me3T_no_AcX
Total Target Sequences = 350

Rank	Motif (known)	Name	*P* value	% of Targets Sequences with Motif
1		Tbox:Smad/ESCd5-Smad2_3-ChIP-Seq(GSE29422)/Homer	1e-2	4.29%

5.7 Gene Ontology (GO) Enrichment Analysis by DAVID

Histone Modifications (Annotated Genomic Regions, TSS ± 10 kb): H3K9me2T_no_AcX (Enrichment in H3K9me2 in endotoxin tolerant monocytes; no co-localization with activating histone modifications)

BIOLOGICAL PROCESS (BP)				
Term	**Count**	**%**	***P* value**	**Genes**
GO:0007166~cell surface receptor linked signal transduction	58	17.37	1.32E-06	OPRM1, TAS2R1, BTRC, OR5L1, GNA12, OR5L2, LPAR3, RHOQ, OR4C3, LPHN2, OR4C13, OR4C15, OR4S2, OR4C12, OR8K3, OR4C11, OR7C1, TRPV4, SHC3, OR5AN1, SYK, GABRG1, GABRG2, OR10S1, LY96, OR10AG1, OR5M8, OR4K15, OR8J1, GRM7, OR4K13, OR8J3, OR6Q1, OR5D14, OR2T1, OR5J2, OR5D16, TFG, FPR3, HCRTR1, IL12RB1, OR9I1, NPFFR2, PTN, OR5F1, UBE2D1, OR2M7, OR5P3, OR5M11, VAV1, OR5T3, OR5I2, OR3A3, OR5AK2, OR8H1, EMR3, OR8D4, OR4C46
GO:0050877~neurological system process	55	16.47	5.65E-12	OPRM1, TAS2R1, OR5L1, OR5L2, HPS1, LPAR3, OR4C3, OR4C13, OR4C15, OR4S2, OR8K3, OR4C12, OR4C11, OR7C1, IL1B, SHC3, OR5AN1, CDH23, GABRG1, GABRG2, OR10S1, PCDHB6, PCDHB3, PCDHB4, OR10AG1, OR5M8, OR4K15, OR8J1, GRM7, OR4K13, OR8J3, OR6Q1, OR5D14, OR2T1, OR5J2, OR5D16, CACNB2, HCRTR1, OR9I1, IMPG1, PTN, OR5F1, OR2M7, OR5P3, OR5M11, CRYZ, OR5T3, OR5I2, OR5AK2, OR3A3, GRIA1, TMOD2, OR8H1, OR8D4, OR4C46
GO:0045449~regulation of transcription	54	16.17	4.87E-02	ZNF208, ZNF582, ZNF17, ZNF534, ZNF80, ZNF155, ZNF676, RHOQ, ZNF16, ZNF578, IL1B, RARA, ZNF732, KDM5A, DEDD2, ZNF43, ZNF45, ZNF547, SP100, ZNF285, ZNF479, ZNF354C, ZNF812, ZNF790, ZNF502, ZFP28, ZNF549, PRDM8, ZFP82, PRDM9, ZNF134, ZNF716, MED18, ZSCAN18, ZNF98, ZNF483, ING4, VENTXP7, SOX5, ZNF35, ZNF660, SUMO1, ZNF226, ZNF599, ZNF569, ZFP3, ZNF221, ZSCAN1, ZNF585B, PKNOX1, ZNF419, SRFBP1, TRPS1, ZIK1
GO:0050890~cognition	48	14.37	1.12E-12	OPRM1, TAS2R1, OR5D14, OR2T1, OR5L1, OR5D16, OR5J2, OR5L2, HPS1, CACNB2, OR4C3, OR4C13, OR4C15, OR4S2, OR9I1, OR8K3, OR4C12, IMPG1, OR4C11, OR7C1, PTN, IL1B, OR5F1, SHC3, CDH23, OR5AN1, OR2M7, OR5P3, OR10S1, OR5M11, CRYZ, OR10AG1, OR5T3, OR5M8, OR5I2, OR5AK2, OR3A3, GRIA1, OR4K15, OR8J1, GRM7, OR4K13, OR8J3, TMOD2, OR8H1, OR6Q1, OR8D4, OR4C46
GO:0007186~G-protein coupled receptor protein signaling pathway	47	14.07	4.84E-09	OPRM1, TAS2R1, OR5D14, OR2T1, OR5L1, GNA12, OR5D16, OR5J2, OR5L2, LPAR3, FPR3, OR4C3, LPHN2, OR4C13, HCRTR1, OR4C15, OR4S2, OR9I1, OR8K3, OR4C12, OR4C11, NPFFR2, OR7C1, OR5F1, OR5AN1, GABRG1, OR2M7, GABRG2, OR5P3, OR10S1, OR5M11, OR10AG1, OR5T3, OR5M8, OR5I2, OR5AK2, OR3A3, OR4K15, OR8J1, GRM7, OR4K13, OR8J3, OR8H1, EMR3, OR6Q1, OR8D4, OR4C46
GO:0006350~transcription	45	13.47	4.92E-02	ZNF582, ZNF17, ZNF534, ZNF80, SOX5, ZNF155, ZNF676, ZNF35, ZNF16, ZNF660, ZNF226, ZNF578, RARA, ZNF732, ZNF599, KDM5A, DEDD2, ZNF43, ZNF45, ZNF547, ZNF285, ZNF479, ZNF812, ZNF354C, ZNF569, ZNF790, ZNF502, ZFP3, ZNF221, ZSCAN1, ZFP28, ZNF549, ZNF585B, PRDM8, ZFP82, PRDM9, SRFBP1, ZNF134, ZNF419, TRPS1, MED18, ZIK1, ZSCAN18, ZNF483, ZNF98
GO:0007600~sensory perception	43	12.87	2.06E-11	OPRM1, TAS2R1, OR5D14, OR2T1, OR5L1, OR5D16, OR5J2, OR5L2, HPS1, CACNB2, OR4C3, OR4C13, OR4C15, OR4S2, OR9I1, OR8K3, OR4C12, IMPG1, OR4C11, OR7C1, OR5F1, CDH23, OR5AN1, OR2M7, OR5P3, OR10S1, OR5M11, CRYZ, OR10AG1, OR5T3, OR5M8, OR5I2, OR5AK2, OR3A3, OR4K15, OR8J1, GRM7, OR4K13, OR8J3, OR8H1, OR6Q1, OR8D4, OR4C46
GO:0006355~regulation of transcription, DNA-dependent	43	12.87	8.55E-03	ZNF208, ZNF582, ING4, ZNF17, ZNF534, VENTXP7, ZNF80, SOX5, ZNF155, ZNF676, RHOQ, ZNF35, ZNF226, RARA, ZNF732, ZNF599, ZNF43, ZNF45, ZNF547, SP100, ZNF285, ZNF479, ZNF812, ZNF354C, ZNF569, ZNF790, ZNF221, ZSCAN1, ZFP28, ZNF549, ZNF585B, ZFP82, PRDM9, PKNOX1, ZNF134, ZNF419, TRPS1, ZNF716, MED18, ZIK1, ZSCAN18, ZNF483, ZNF98
GO:0051252~regulation of RNA metabolic process	43	12.87	1.23E-02	ZNF208, ZNF582, ING4, ZNF17, ZNF534, VENTXP7, ZNF80, SOX5, ZNF155, ZNF676, RHOQ, ZNF35, ZNF226, RARA, ZNF732, ZNF599, ZNF43, ZNF45, ZNF547, SP100, ZNF285, ZNF479, ZNF812, ZNF354C, ZNF569, ZNF790, ZNF221, ZSCAN1, ZFP28, ZNF549, ZNF585B, ZFP82, PRDM9, PKNOX1, ZNF134, ZNF419, TRPS1, ZNF716, MED18, ZIK1, ZSCAN18, ZNF483, ZNF98
GO:0007606~sensory perception of chemical stimulus	37	11.08	1.36E-14	TAS2R1, OR5D14, OR2T1, OR5L1, OR5D16, OR5J2, OR5L2, OR4C3, OR4C13, OR4C15, OR4S2, OR9I1, OR8K3, OR4C12, OR4C11, OR7C1, OR5F1, OR5AN1, OR2M7, OR5P3, OR10S1, OR5M11, OR10AG1, OR5M8, OR5T3, OR5I2, OR5AK2, OR3A3, OR4K15, OR8J1, GRM7, OR4K13, OR8J3, OR8H1, OR6Q1, OR8D4, OR4C46
GO:0007608~sensory perception of smell	36	10.78	3.43E-15	OR5D14, OR2T1, OR5L1, OR5D16, OR5J2, OR5L2, OR4C3, OR4C13, OR4C15, OR4S2, OR9I1, OR8K3, OR4C12, OR4C11, OR7C1, OR5F1, OR5AN1, OR2M7, OR5P3, OR10S1, OR5M11, OR10AG1, OR5M8, OR5T3, OR5I2, OR5AK2, OR3A3, OR4K15, OR8J1, GRM7, OR4K13, OR8J3, OR8H1, OR6Q1, OR8D4, OR4C46
GO:0016337~cell-cell adhesion	13	3.89	2.04E-03	CD84, ATP2C1, PCDHB6, CDH18, PCDHB3, PCDHA5, PCDHB4, PCDHA10, CNTN4, PCDHGA3, SELPLG, CDH23, SYK
GO:0007268~synaptic transmission	12	3.89	1.03E-02	GABRG1, GABRG2, HCRTR1, GRIA1, PCDHB6, GRM7, PCDHB3, PCDHB4, TMOD2, LPAR3, CACNB2, SHC3
GO:0019226~transmission of nerve impulse	12	3.89	2.98E-02	GABRG1, GABRG2, HCRTR1, GRIA1, PCDHB6, GRM7, PCDHB3, PCDHB4, TMOD2, LPAR3, CACNB2, SHC3
GO:0007156~homophilic cell adhesion	9	2.69	1.42E-03	CD84, PCDHB6, CDH18, PCDHB3, PCDHA5, PCDHB4, PCDHA10, PCDHGA3, CDH23
GO:0045321~leukocyte activation	9	2.69	4.62E-02	CD48, PKNOX1, RPL22, MS4A1, STXBP2, KIR2DS4, VAV1, HSH2D, SYK

Histone Modifications (Annotated Genomic Regions, TSS ± 10 kb): H3K9me2T_no_AcX (Enrichment in H3K9me2 in endotoxin tolerant monocytes; no co-localization with activating histone modifications) ***cont.***

	Term	Count	%	*P* value	Genes
BP	GO:0046649~lymphocyte activation	8	2.40	4.63E-02	CD48, PKNOX1, RPL22, MS4A1, KIR2DS4, VAV1, HSH2D, SYK
	GO:0007611~learning or memory	6	1.80	3.60E-02	GRIA1, GRM7, TMOD2, PTN, IL1B, SHC3
	GO:0016339~calcium-dependent cell-cell adhesion	5	1.50	4.89E-04	ATP2C1, PCDHB6, PCDHB3, PCDHB4, CDH23
MOLECULAR FUNCTION (MF)	GO:0043167~ion binding	91	27.25	9.80E-04	ZNF208, ZNF582, SLC9A8, ZNF17, ZNF534, ZAK, ZNF80, PCDHA5, ZNF676, ZNF155, ADH1A, ZNF16, PCDHGA3, RABGEF1, ZNF578, TRPV4, RARA, ZNF732, KDM5A, RNF148, CDH23, ZNF43, GABRG1, GABRG2, ZNF45, SP100, ZNF547, ZNF285, PCDHB6, ZNF479, ADAMTS20, ZNF812, PCDHB3, ZNF354C, PCDHB4, ZNF790, ZNF502, ZFP28, ZNF549, NUCB1, PRDM8, PITPNM1, ZFP82, PPM1G, MYRIP, RNF133, PRDM9, NAPEPLD, ZNF134, ATP2C1, GRM7, ZNF716, ZSCAN18, ZNF98, ZNF483, ENOX1, ING4, KCNA2, CACNB2, ADH6, MKRN9P, ZNF35, ZNF365, ZNF660, MTMR3, ZNF226, PCDHA10, ZNF599, TEC, ACSL5, PTGR1, TRPC6, CYP2C9, ZNF569, FSCB, IDO2, ZFP3, ZNF221, CRYZ, ZSCAN1, U2AF1L4, VAV1, ZNF585B, TEX13A, ZNF419, EFHB, CDH18, TRPS1, EMR3, ZIK1, TSSK6
	GO:0046872~metal ion binding	89	26.65	1.11E-03	ZNF208, ZNF582, SLC9A8, ZNF17, ZNF534, ZAK, ZNF80, PCDHA5, ZNF676, ZNF155, ADH1A, ZNF16, PCDHGA3, RABGEF1, ZNF578, TRPV4, RARA, ZNF732, KDM5A, RNF148, CDH23, ZNF43, ZNF45, SP100, ZNF547, ZNF285, PCDHB6, ZNF479, ADAMTS20, ZNF812, ZNF354C, PCDHB3, PCDHB4, ZNF790, ZNF502, ZFP28, ZNF549, NUCB1, PRDM8, PITPNM1, ZFP82, PPM1G, MYRIP, RNF133, PRDM9, NAPEPLD, ZNF134, ATP2C1, GRM7, ZNF716, ZSCAN18, ZNF98, ZNF483, ENOX1, ING4, KCNA2, CACNB2, ADH6, MKRN9P, ZNF35, ZNF365, ZNF660, MTMR3, ZNF226, PCDHA10, ZNF599, TEC, ACSL5, PTGR1, TRPC6, CYP2C9, ZNF569, FSCB, IDO2, ZFP3, ZNF221, CRYZ, ZSCAN1, U2AF1L4, VAV1, ZNF585B, TEX13A, ZNF419, EFHB, CDH18, TRPS1, EMR3, ZIK1, TSSK6
	GO:0043169~cation binding	89	26.65	1.53E-03	ZNF208, ZNF582, SLC9A8, ZNF17, ZNF534, ZAK, ZNF80, PCDHA5, ZNF676, ZNF155, ADH1A, ZNF16, PCDHGA3, RABGEF1, ZNF578, TRPV4, RARA, ZNF732, KDM5A, RNF148, CDH23, ZNF43, ZNF45, SP100, ZNF547, ZNF285, PCDHB6, ZNF479, ADAMTS20, ZNF812, ZNF354C, PCDHB3, PCDHB4, ZNF790, ZNF502, ZFP28, ZNF549, NUCB1, PRDM8, PITPNM1, ZFP82, PPM1G, MYRIP, RNF133, PRDM9, NAPEPLD, ZNF134, ATP2C1, GRM7, ZNF716, ZSCAN18, ZNF98, ZNF483, ENOX1, ING4, KCNA2, CACNB2, ADH6, MKRN9P, ZNF35, ZNF365, ZNF660, MTMR3, ZNF226, PCDHA10, ZNF599, TEC, ACSL5, PTGR1, TRPC6, CYP2C9, ZNF569, FSCB, IDO2, ZFP3, ZNF221, CRYZ, ZSCAN1, U2AF1L4, VAV1, ZNF585B, TEX13A, ZNF419, EFHB, CDH18, TRPS1, EMR3, ZIK1, TSSK6
	GO:0046914~transition metal ion binding	67	20.06	3.80E-04	ZNF208, ZNF582, ZNF17, ZNF534, ZNF80, ZNF155, ZNF676, ADH1A, ZNF16, ZNF578, RABGEF1, RARA, ZNF732, RNF148, KDM5A, ZNF43, ZNF45, SP100, ZNF547, ZNF285, ADAMTS20, ZNF479, ZNF812, ZNF354C, ZNF790, ZNF502, ZFP28, ZNF549, PRDM8, ZFP82, PPM1G, MYRIP, RNF133, PRDM9, NAPEPLD, ZNF134, ATP2C1, ZNF716, ZSCAN18, ZNF98, ZNF483, ENOX1, ING4, MKRN9P, ADH6, ZNF35, ZNF365, ZNF660, MTMR3, ZNF226, ZNF599, TEC, PTGR1, CYP2C9, ZNF569, IDO2, ZFP3, ZNF221, ZSCAN1, CRYZ, U2AF1L4, VAV1, ZNF585B, TEX13A, ZNF419, TRPS1, ZIK1
	GO:0008270~zinc ion binding	62	18.56	3.20E-05	ZNF208, ZNF582, ZNF17, ZNF534, ZNF80, ZNF155, ZNF676, ADH1A, ZNF16, ZNF578, RABGEF1, RARA, ZNF732, RNF148, KDM5A, ZNF43, ZNF45, ZNF547, SP100, ZNF285, ADAMTS20, ZNF479, ZNF812, ZNF354C, ZNF790, ZNF502, ZFP28, ZNF549, PRDM8, ZFP82, MYRIP, RNF133, PRDM9, NAPEPLD, ZNF134, ZNF716, ZSCAN18, ZNF98, ZNF483, ING4, MKRN9P, ADH6, ZNF35, ZNF365, ZNF660, MTMR3, ZNF226, ZNF599, TEC, PTGR1, ZNF569, ZFP3, ZNF221, ZSCAN1, CRYZ, U2AF1L4, VAV1, ZNF585B, TEX13A, ZNF419, TRPS1, ZIK1
	GO:0003677~DNA binding	50	14.97	2.58E-02	ZNF208, ZNF582, ZNF17, ZNF534, ZNF80, ZNF155, ZNF676, ZNF16, ZNF578, RABGEF1, RARA, ZNF732, KDM5A, DEDD2, ZNF43, C5ORF51, ZNF45, ZNF547, SP100, ZNF285, ZNF479, ZNF354C, ZNF812, ZNF790, ZNF502, ZFP28, ZNF549, PRDM8, NUCB1, ZFP82, ZNF134, ZNF716, ZSCAN18, ZNF98, ZNF483, VENTXP7, SOX5, ZNF35, ZNF660, ZNF226, ZNF599, ZNF569, ZFP3, ZNF221, ZSCAN1, VAV1, PKNOX1, ZNF419, TRPS1, ZIK1
	GO:0004984~olfactory receptor activity	35	10.48	1.07E-14	OR5D14, OR2T1, OR5L1, OR5D16, OR5J2, OR5L2, OR4C3, OR4C13, OR4C15, OR9I1, OR4S2, OR8K3, OR4C12, OR4C11, OR7C1, OR5F1, OR5AN1, OR2M7, OR5P3, OR10S1, OR5M11, OR10AG1, OR5M8, OR5T3, OR51I2, OR5AK2, OR3A3, OR4K15, OR8J1, OR4K13, OR8J3, OR8H1, OR6Q1, OR8D4, OR4C46
	GO:0004022~alcohol dehydrogenase (NAD) activity	3	0.90	5.14E-03	PTGR1, ADH6, ADH1A
	GO:0017022~myosin binding	3	0.90	4.82E-02	TRIOBP, MYRIP, CALD1
	GO:0004370~glycerol kinase activity	2	0.60	4.75E-02	GK2, GK5
PATHWAY	hsa04740:Olfactory transduction	36	10.78	7.42E-18	OR5D14, OR2T1, OR5L1, OR5D16, OR5J2, OR5L2, PRKG2, OR4C3, OR4C13, OR4C15, OR4S2, OR9I1, OR8K3, OR4C12, OR4C11, OR7C1, OR5F1, OR5AN1, OR2M7, OR5P3, OR10S1, OR5M11, OR10AG1, OR5M8, OR5T3, OR51I2, OR5AK2, OR3A3, OR4K15, OR8J1, OR4K13, OR8J3, OR8H1, OR6Q1, OR8D4, OR4C46
	P00012:Cadherin signaling pathway	8	2.40	3.37E-03	PCDHB6, CDH18, PCDHB3, PCDHA5, PCDHB4, PCDHA10, PCDHGA3, CDH23
	REACT_14797:Signaling by GPCR	33	9.88	3.17E-09	OPRM1, OR5D14, OR2T1, OR5L1, OR5D16, OR5J2, OR5L2, LPAR3, OR4C3, HCRTR1, OR4C13, OR4C15, OR4S2, OR4C12, OR4C11, NPFFR2, OR5F1, OR5AN1, OR2M7, OR5P3, OR10S1, OR5M11, OR10AG1, OR5M8, OR5T3, OR51I2, OR3A3, OR5AK2, OR4K15, GRM7, OR4K13, OR6Q1, OR4C46

Histone Modifications (Annotated Genomic Regions, TSS ± 10 kb): H3K27me3_T_no_AcX (Enrichment in H3K27me3 in endotoxin tolerant monocytes; no co-localization with activating histone modifications)

	Term	Count	%	*P* value	Genes
BIOLOGICAL PROCESS	GO:0032233~positive regulation of actin filament bundle	2	6.90	2.05E-02	SMAD3, SYNPO
	GO:0051492~regulation of stress fiber formation	2	6.90	2.77E-02	SMAD3, SYNPO
	GO:0050877~neurological system process	6	20.69	2.83E-02	PRX, CD9, OR10A3, KCNQ3, OR13H1, OR4N5
	GO:0032231~regulation of actin filament bundle formation	2	6.90	3.06E-02	SMAD3, SYNPO
	GO:0019228~regulation of action potential in neuron	2	6.90	7.69E-02	PRX, CD9
	GO:0034330~cell junction organization	2	6.90	8.10E-02	CD9, SMAD3
	GO:0019226~transmission of nerve impulse	3	10.34	9.34E-02	PRX, CD9, KCNQ3
	GO:0001508~regulation of action potential	2	6.90	9.59E-02	PRX, CD9

Histone Modifications (Annotated Genomic Regions, TSS ± 10 kb): H4K20me3_T_no_AcX (Enrichment in H4K20me3 in endotoxin tolerant monocytes; no co-localization with activating histone modifications)

	Term	Count	%	*P* value	Genes
BIOLOGICAL PROCESS	GO:0042981~regulation of apoptosis	18	7.59	2.71E-02	COL18A1, PHB, GRIN1, CBX4, ACTN1, PRDX2, DLX1, MYD88, SARM1, NME3, HMOX1, CSTB, FAIM, TRAF7, CASP1, IL1A, FGD3, FGF4
	GO:0043067~regulation of programmed cell death	18	7.59	2.94E-02	COL18A1, PHB, GRIN1, CBX4, ACTN1, PRDX2, DLX1, MYD88, SARM1, NME3, HMOX1, CSTB, FAIM, TRAF7, CASP1, IL1A, FGD3, FGF4
	GO:0010941~regulation of cell death	18	7.59	3.04E-02	COL18A1, PHB, GRIN1, CBX4, ACTN1, PRDX2, DLX1, MYD88, SARM1, NME3, HMOX1, CSTB, FAIM, TRAF7, CASP1, IL1A, FGD3, FGF4
	GO:0006952~defense response	15	6.33	2.52E-02	IL1R1, NMI, DEFB125, TLR1, CHST2, PRDX2, FPR2, COTL1, MYD88, SARM1, HMOX1, SERPINA1, XCR1, ORM2, IL1A
	GO:0006954~inflammatory response	11	4.64	8.69E-03	NMI, MYD88, HMOX1, TLR1, CHST2, PRDX2, SERPINA1, FPR2, XCR1, ORM2, IL1A
	GO:0046903~secretion	10	4.22	1.46E-02	CADPS, ARFGAP3, HMOX1, OXT, FAM3B, RPH3AL, EXOC3, NMU, EXOC1, SYK
	GO:0060341~regulation of cellular localization	9	3.80	1.40E-02	HMOX1, OXT, RPH3AL, CALM3, TRAF7, CASP1, NMU, IL1A, SYK
	GO:0051046~regulation of secretion	8	3.38	1.47E-02	HMOX1, OXT, RPH3AL, TRAF7, CASP1, NMU, IL1A, SYK
	GO:0001817~regulation of cytokine production	7	2.95	2.81E-02	MYD88, HMOX1, GATA4, TLR1, CASP1, IL1A, SYK
	GO:0032940~secretion by cell	7	2.95	4.88E-02	CADPS, ARFGAP3, FAM3B, RPH3AL, EXOC3, EXOC1, SYK
	GO:0045165~cell fate commitment	6	2.53	3.23E-02	ISL2, HOXA2, DLX1, CDON, DSCAML1, PRDM1
	GO:0034976~response to endoplasmic reticulum stress	4	1.69	9.05E-03	COL4A3BP, EIF2AK2, PPP1R15A, OS9
	GO:0017157~regulation of exocytosis	4	1.69	9.05E-03	HMOX1, RPH3AL, TRAF7, SYK
	GO:0042108~positive regulation of cytokine biosynthetic process	4	1.69	2.30E-02	HMOX1, TLR1, IL1A, SYK
	GO:0007617~mating behavior	3	1.27	1.32E-02	OXT, GRIN1, MTNR1A
	GO:0019098~reproductive behavior	3	1.27	2.15E-02	OXT, GRIN1, MTNR1A
	GO:0007618~mating	3	1.27	4.58E-02	OXT, GRIN1, MTNR1A
	GO:0060179~male mating behavior	2	0.84	3.77E-02	OXT, GRIN1
MF	GO:0019899~enzyme binding	13	5.49	3.62E-02	DMXL2, HMOX1, AKAP8L, CBX4, RPH3AL, CSTB, SERPINA1, SKIL, CDH2, AKAP11, PTPRN, COTL1, FGD3
PATHWAY	hsa04740:Olfactory transduction	11	4.64	4.28E-02	OR2B6, OR4C13, OR2A5, OR4S2, OR5M10, OR1L6, CALM3, OR4Q3, OR10H4, OR10P1, OR4C46
	REACT_14797:Signaling by GPCR	15	6.33	4.12E-02	OPRM1, OR2B6, OR5M10, OXT, OR1L6, PTH1R, FPR2, OR10H4, OR4C13, OR4S2, OR4Q3, XCR1, OR4C46, OR10P1, MTNR1A

Histone Modifications (Annotated Genomic Regions, TSS ± 10 kb): H4ac_T_no_RepX (Enrichment in H4ac in endotoxin tolerant monocytes; no co-localization with repressive histone modifications)

	Term	Count	%	*P* value	Genes
MF	GO:0046870~cadmium ion binding	4	1.62	5.03E-07	MT1L, MT1M, MT1A, MT1G
	GO:0005507~copper ion binding	4	1.62	2.06E-04	MT1L, MT1M, MT1A, MT1G

Histone Modifications (Annotated Genomic Regions, TSS ± 10 kb): H3K27ac_T_no_RepX (Enrichment in H3K27ac in endotoxin tolerant monocytes; no co-localization with repressive histone modifications)

	Term	Count	%	*P* value	Genes
BIOLOGICAL PROCESS	GO:0006955~immune response	10	11.49	6.70E-03	CXCL1, CSF3, GPI, IL2RA, CXCL5, MASP2, LILRB4, MS4A1, FCGRT, PAG1
	GO:0032101~regulation of response to external stimulus	4	4.60	4.42E-02	MYOD1, NPC1, IL2RA, PTGS2
	GO:0006979~response to oxidative stress	4	4.60	4.77E-02	DHRS2, PTGS2, MMP14, TRPM2
	GO:0000041~transition metal ion transport	3	3.46	4.83E-02	STEAP3, SLC39A11, TRPM2
MOLECULAR FUNCTION	GO:0005509~calcium ion binding	10	11.49	2.20E-02	FKBP8, RAB11FIP3, BEST1, MASP2, TGM3, TRPV6, MMP14, CDH4, SYT17, TRPM2
	GO:0008083~growth factor activity	5	5.75	6.11E-03	CXCL1, CSF3, GPI, WISP3, NDP
	GO:0005507~copper ion binding	3	3.45	3.92E-02	STEAP3, MT1L, MT1E, MT1F
	GO:0046870~cadmium ion binding	2	2.30	4.45E-02	MT1L, MT1E, MT1F
PATHWAY	hsa04060:Cytokine-cytokine receptor interaction	5	5.75	4.21E-02	CXCL1, TNFRSF6B, CSF3, IL2RA, CXCL5

DNA Methylation (Annotated Genomic Regions (TSS ± 10 kb)): Enrichment in DNA methylation in endotoxin tolerant monocytes

	Term	Count	%	*P* value	Genes
BIOLOGICAL FUNCTION	GO:0006793~phosphorus metabolic process	19	8.19	0.006	CTBP1, LTK, FLT1, MAP2K2, WNK2, SRPK1, CAMKK1, TBCK, CD74, IKBKE, DUSP13, CLK2, EPHA8, DUSP14, DLD, MERTK, SIK1, DUSP7, MATK
	GO:0006796~phosphate metabolic process	19	8.19	0.006	CTBP1, LTK, FLT1, MAP2K2, WNK2, SRPK1, CAMKK1, TBCK, CD74, IKBKE, DUSP13, CLK2, EPHA8, DUSP14, DLD, MERTK, SIK1, DUSP7, MATK
	GO:0016310~phosphorylation	16	6.90	0.010	CTBP1, LTK, FLT1, MAP2K2, WNK2, CAMKK1, TBCK, CD74, SRPK1, IKBKE, CLK2, EPHA8, DLD, MERTK, SIK1, MATK
	GO:0006468~protein amino acid phosphorylation	15	6.47	0.005	CTBP1, LTK, FLT1, MAP2K2, WNK2, CAMKK1, TBCK, CD74, SRPK1, IKBKE, CLK2, EPHA8, MERTK, SIK1, MATK
	GO:0006357~regulation of transcription from RNA polymerase II promoter	14	6.03	0.024	KLF6, CTBP1, TCF7, TFAP4, GRIN1, HDAC10, ZNF367, HES7, NR2E3, IRF8, ZGLP1, ABRA, TFAP2C, SIK1
	GO:0031327~negative regulation of cellular biosynthetic process	11	4.74	0.046	KHDRBS1, ENPP7, CTBP1, PDGFA, IRF8, ZGLP1, ZNF24, HDAC10, HES7, NR2E3, SIK1
	GO:0007167~enzyme linked receptor protein signaling pathway	8	3.45	0.049	DOK2, FLT1, GP6, LTK, PDGFA, EPHA8, FGF22, CD7
	GO:0007169~transmembrane receptor protein tyrosine kinase signaling pathway	7	3.02	0.022	DOK2, FLT1, LTK, PDGFA, EPHA8, FGF22, CD7
	GO:0000122~negative regulation of transcription from RNA polymerase II promoter	7	3.02	0.045	CTBP1, IRF8, ZGLP1, HDAC10, HES7, NR2E3, SIK1
	GO:0007018~microtubule-based movement	6	2.59	0.005	KIF14, KIF1A, KIF24, TUBA3C, TUBB1, KIF3C
	GO:0007030~Golgi organization	3	1.29	0.017	CTBP1, COG1, VCPIP1
	GO:0035121~tail morphogenesis	2	0.86	0.047	CHST11, HES7
MOLECULAR FUNCTION	GO:0000166~nucleotide binding	34	14.66	0.007	KIF24, RP2, NT5C1A, RTKN, SNORA67, CAMKK1, TPK1, CLK2, ACTR1A, TUBA3C, PMS2, UCK1, SIK1, DHX30, TUBB1, RTEL1, MATK, KIF14, ACTB, CTBP1, FLT1, LTK, MAP2K2, WNK2, KIF3C, HNRNPR, SRPK1, TBCK, IKBKE, KIF1A, ATP2A2, EPHA8, DLD, MERTK
	GO:0017076~purine nucleotide binding	31	13.36	0.004	KIF24, RP2, RTKN, SNORA67, CAMKK1, TPK1, CLK2, ACTR1A, TUBA3C, PMS2, UCK1, DHX30, SIK1, TUBB1, RTEL1, MATK, KIF14, ACTB, LTK, FLT1, MAP2K2, WNK2, KIF3C, TBCK, SRPK1, IKBKE, KIF1A, ATP2A2, EPHA8, DLD, MERTK
	GO:0032555~purine ribonucleotide binding	30	12.93	0.004	KIF24, RP2, RTKN, SNORA67, CAMKK1, TPK1, CLK2, ACTR1A, TUBA3C, PMS2, UCK1, DHX30, SIK1, TUBB1, RTEL1, MATK, KIF14, ACTB, LTK, FLT1, MAP2K2, WNK2, KIF3C, TBCK, SRPK1, IKBKE, KIF1A, ATP2A2, EPHA8, MERTK
	GO:0030554~adenyl nucleotide binding	28	12.93	0.002	KIF24, RP2, SNORA67, CAMKK1, TPK1, CLK2, ACTR1A, PMS2, UCK1, DHX30, SIK1, RTEL1, MATK, KIF14, ACTB, LTK, FLT1, MAP2K2, WNK2, KIF3C, TBCK, SRPK1, IKBKE, KIF1A, ATP2A2, EPHA8, DLD, MERTK
	GO:0001883~purine nucleoside binding	28	12.07	0.002	KIF24, RP2, SNORA67, CAMKK1, TPK1, CLK2, ACTR1A, PMS2, UCK1, DHX30, SIK1, RTEL1, MATK, KIF14, ACTB, LTK, FLT1, MAP2K2, WNK2, KIF3C, TBCK, SRPK1, IKBKE, KIF1A, ATP2A2, EPHA8, DLD, MERTK
	GO:0001882~nucleoside binding	28	12.07	0.003	KIF24, RP2, SNORA67, CAMKK1, TPK1, CLK2, ACTR1A, PMS2, UCK1, DHX30, SIK1, RTEL1, MATK, KIF14, ACTB, LTK, FLT1, MAP2K2, WNK2, KIF3C, TBCK, SRPK1, IKBKE, KIF1A, ATP2A2, EPHA8, DLD, MERTK
	GO:0005524~ATP binding	27	12.07	0.002	KIF24, RP2, SNORA67, CAMKK1, TPK1, CLK2, ACTR1A, PMS2, UCK1, DHX30, SIK1, RTEL1, MATK, KIF14, ACTB, LTK, FLT1, MAP2K2, WNK2, KIF3C, TBCK, SRPK1, IKBKE, KIF1A, ATP2A2, EPHA8, MERTK
	GO:0032559~adenyl ribonucleotide binding	27	11.64	0.002	KIF24, RP2, SNORA67, CAMKK1, TPK1, CLK2, ACTR1A, PMS2, UCK1, DHX30, SIK1, RTEL1, MATK, KIF14, ACTB, LTK, FLT1, MAP2K2, WNK2, KIF3C, TBCK, SRPK1, IKBKE, KIF1A, ATP2A2, EPHA8, MERTK
	GO:0004672~protein kinase activity	13	11.64	0.014	LTK, FLT1, MAP2K2, WNK2, CAMKK1, TBCK, SRPK1, IKBKE, EPHA8, CLK2, SIK1, MERTK, MATK
	GO:0019904~protein domain specific binding	8	5.60	0.041	KHDRBS1, CTBP1, PHRF1, GRIA2, DLGAP2, INPP5A, PMEPA1, SNTA1
	GO:0004713~protein tyrosine kinase activity	7	3.45	0.005	FLT1, LTK, CLK2, MAP2K2, EPHA8, MERTK, MATK
	GO:0004713~protein tyrosine kinase activity	7	3.02	0.005	FLT1, LTK, CLK2, MAP2K2, EPHA8, MERTK, MATK
	GO:0032403~protein complex binding	6	2.59	0.041	DOK2, FCER2, ICAM2, PMS2, FCGR2A, TIMP2
	GO:0004714~transmembrane receptor protein tyrosine kinase activity	4	1.72	0.027	FLT1, LTK, EPHA8, MERTK
	GO:0003777~microtubule motor activity	4	1.72	0.038	KIF14, KIF1A, KIF24, KIF3C
	GO:0004970~ionotropic glutamate receptor activity	3	1.29	0.013	GRIA2, GRIN1, GRIK5
	GO:0005234~extracellular-glutamate-gated ion channel activity	3	1.29	0.014	GRIA2, GRIN1, GRIK5
	GO:0008066~glutamate receptor activity	3	1.29	0.036	GRIA2, GRIN1, GRIK5

mRNA Expression: Genes Up-Regulated in Endotoxin Tolerance

	Term	Count	%	*P* value	Genes
BIOLOGICAL FUNCTION	GO:0006897~endocytosis	41	2.29	1.83E-05	ABCA7, CAV1, SLC9A3, MYO7A, SNCA, HFE, EPS15L1, ITSN1, SLC11A1, DAB2, DOCK1, DNER, ZFYVE9, FCER1G, SCARB1, EHD2, MICALL2, PLD2, CEBPE, STXBP1, MFGE8, CDK5, LDLRAP1, CORO1C, SH3BP4, CORO1A, ADRB2, LRP1, UNC13D, ULK1, IGF2R, CD209, SH3KBP1, OPHN1, RIN1, LRP8, MERTK, BIN1, CD14, LRP5, RIN3
	GO:0010324~membrane invagination	41	2.29	1.83E-05	ABCA7, CAV1, SLC9A3, MYO7A, SNCA, HFE, EPS15L1, ITSN1, SLC11A1, DAB2, DOCK1, DNER, ZFYVE9, FCER1G, SCARB1, EHD2, MICALL2, PLD2, CEBPE, STXBP1, MFGE8, CDK5, LDLRAP1, CORO1C, SH3BP4, CORO1A, ADRB2, LRP1, UNC13D, ULK1, IGF2R, CD209, SH3KBP1, OPHN1, RIN1, LRP8, MERTK, BIN1, CD14, LRP5, RIN3
	GO:0051056~regulation of small GTPase mediated signal transduction	45	2.51	2.04E-05	TBC1D8, AKAP13, LPAR2, ITSN1, RGL2, TBC1D16, PLEKHG3, PLEKHG2, RASGRP4, PTK2B, TBC1D14, PLEKHG6, RASAL3, TBC1D7, RAP1GAP2, FGD6, FGD3, AGAP3, IQSEC1, FGD4, TBC1D2, GIT1, ARHGEF1, TBC1D10C, VAV3, TBC1D10B, ARHGEF6, SIPA1L2, SCAI, ARHGEF17, SIPA1L3, TBC1D22A, DNMBP, TBC1D25, NOTCH2, TBC1D24, WDR67, ADAP2, SGSM2, ACAP3, ACAP1, ACAP2, DGKZ, SYNGAP1, ARAP3
	GO:0005996~monosaccharide metabolic process	41	2.29	2.27E-05	PRKAG3, ALDOA, GNPDA1, FUT8, PFKFB4, PHKB, ALDOC, SLC37A4, HEXB, PGAM2, HIBADH, PPP1R3E, TPI1, NISCH, HK3, ENO2, FUT2, CHST15, GAPDH, PDK1, PDK2, WDTC1, IRS2, PDK4, BAD, PFKM, ADIPOQ, PMM1, CPT1A, PGM2L1, CSGALNACT1, GPI, RENBP, AMDHD2, G6PD, CHST7, SDS, CHST6, MAPK14, PGM1, GHRL
	GO:0016051~carbohydrate	25	1.40	2.78E-05	PRKAG3, NDST1, FUT8, PGAM2, HS2ST1, B3GNT8, TPI1, GOT1, XYLT2, XYLT1, CHST14, ENO2, CHST15, CMAS, CERCAM, GLCE, PMM1, CSGALNACT1, GPI, G6PD, CHST7, SDS, CHST6, HAS1, PGM1
	GO:0046578~regulation of Ras protein signal transduction	39	2.18	3.27E-05	TBC1D8, AKAP13, LPAR2, ITSN1, TBC1D16, PLEKHG3, PLEKHG2, RASGRP4, PTK2B, TBC1D14, PLEKHG6, TBC1D7, FGD6, FGD3, AGAP3, IQSEC1, FGD4, TBC1D2, GIT1, ARHGEF1, TBC1D10C, VAV3, TBC1D10B, ARHGEF6, SCAI, ARHGEF17, TBC1D22A, DNMBP, TBC1D25, NOTCH2, TBC1D24, WDR67, ADAP2, ACAP3, SGSM2, ACAP1, ACAP2, DGKZ, ARAP3
	GO:0019318~hexose metabolic process	35	1.95	1.29E-04	PRKAG3, ALDOA, FUT8, PFKFB4, PHKB, ALDOC, SLC37A4, PGAM2, HIBADH, PPP1R3E, TPI1, NISCH, HK3, ENO2, FUT2, CHST15, GAPDH, PDK1, PDK2, WDTC1, IRS2, PDK4, BAD, PFKM, ADIPOQ, PMM1, CPT1A, PGM2L1, GPI, RENBP, G6PD, SDS, MAPK14, PGM1, GHRL
	GO:0032318~regulation of Ras GTPase activity	23	1.28	1.49E-04	GIT1, TBC1D10C, TBC1D8, TBC1D10B, TBC1D22A, TBC1D25, TBC1D16, TBC1D24, WDR67, ADAP2, SGSM2, ACAP3, PTK2B, TBC1D14, ACAP1, ACAP2, TBC1D7, ARAP3, FGD6, AGAP3, FGD3, TBC1D2, FGD4
	GO:0006468~protein amino acid phosphorylation	90	5.02	1.59E-04	CDK19, RNASEL, ACVRL1, NUAK2, STK38, STK36, PASK, PINK1, LPAR3, AURKA, LPAR2, CAMKK1, DMPK, MAP3K6, MAP3K4, CXCR4, AAK1, GAB1, PRKACA, PAK1, CSK, INSR, MAP2K5, PIK3CG, PRKCA, C5AR1, ADAM10, MADD, MINK1, PKN1, WNK2, MARK4, CDK5, MAST3, MAPK1, PROK2, PRKD2, ACVR2B, HIPK2, MAPK3, TESK1, RIPK3, GHRL, CAMK1, NEK4, MAP3K14, ERC1, LRRK2, ACVR1, NRBP2, FGFR2, CCL2, NEK1, CAMK2G, MAP4K2, MKNK2, ABI3, MAPKAPK3, ADRBK1, PXK, ULK4, STK32C, IGF1R, EPHB6, ERCC6, TTBK2, PTK2B, FGD4, FYB, PDK1, PDK2, MAK, ALPK2, MEX3B, PDK4, MET,
	GO:0009611~response to wounding	74	4.13	2.39E-04	ACVRL1, NRP1, NDST1, S100A8, TRPV1, S100A9, MMP25, TLR9, CFP, FOS, S1PR3, NLRC4, APOA2, SLC1A2, DYSF, LTB4R, CXCR4, VNN1, XCR1, TFPI2, F11R, F12, PDPN, RXRA, STXBP1, WAS, CDK5, SIGIRR, CD163, PROK2, UNC13D, GNAQ, EREG, KIAA1715, VCAN, CTSB, PROS1, ACVR1, TPST1, ITGAL, CCL2, NFKBID, C3, CLU, NINJ2, MST1, ABHD2, PXK, GPR68, TPM1, CCL7, IL17C, SLC11A1, LAMB2, PROCR, SCARB1, RTN4RL2, ENTPD1, NFATC3, PAPSS2, KL, CCL18, CD180, S100A12, HDAC5, NOTCH3, NOTCH2, HDAC4, P2RX1, C1RL, LTA4H, ID3, PLAU, CD14
	GO:0006909~phagocytosis	14	0.78	2.70E-04	ABCA7, CEBPE, MYO7A, MFGE8, CORO1C, SLC11A1, CORO1A, UNC13D, LRP1, DOCK1, FCER1G, SCARB1, MERTK, CD14
	GO:0015674~di-, tri-valent inorganic cation transport	32	1.79	2.78E-04	CAV1, TRPV1, CAMK2G, CACNB1, SFXN3, HFE, CACNB3, FKBP1B, TPCN1, SFXN5, ANXA6, SLC11A1, ATP2B4, CYP27B1, SLC24A4, PKD1, MCOLN1, XCR1, TRPM4, CACNG8, SLC3A2, STIM1, ITPR3, ITPR1, TRPM2, ITPR2, CACNA2D4, CORO1A, FYN, ATP2A3, CACNA1G, SLC25A37
	GO:0007242~intracellular signaling cascade	151	8.43	2.80E-04	ADCY4, STK38, LPAR3, RRAD, RGL4, LPAR2, AURKA, FOXO4, ITSN1, TLR9, RGL2, S1PR3, MAP3K6, ARL11, MAP3K4, LTB4R, GAB1, SPRED2, RAB23, RRAS, PRKACA, DDAH2, INSR, MAP2K5, PIK3CG, PLD2, RARG, C5AR1, PLXNB1, MADD, RREB1, RXRA, ARID1A, WNK2, DEPDC5, MAPK1, ACAP1, MAPK3, REM2, RIPK3, ERC1, LRRK2, CAV1, CCL2, MAPKAPK3, DUSP10, MAP4K2, AKAP13, CORO2A, DOCK1, CDC42EP1, DUSP16, HIST1H4F, FGD4, DVL2, VAV3, MET, ALMS1, BRIP1, ATM, DNMBP, LAT, CBLB, TULP4, ULK1, CD209, PCNA, CDC42BPA, GRK5, ABL1, SLC9A1, PRKAG3, NDST1, PINK1, NOD2, ARHGAP5, MCTP2, NISCH, STAC2, CXCR4, DLG5, PAK1, XCR1, CSK, DEDD2, TUBB3, AGAP3, PRKCA, ARHGEF1, ARHGEF6, PKN1, ADIPOR1, MINK1, MBD4, ARL6, CDK5, ARL3, SH2D3C, PRKD2, PROK2, DOK2, CARD14, ADRB2, NCOA2, DOK3, GNAQ, HIPK2, DEF8, GHRL, TREM1, ARL4C, ING4, RAB3D, PLEK2, MKNK2, GNG11, CALCOCO1, RAB42, DGKA, IGF1R, ERCC6, PTK2B, SQSTM1, RASGRP4, PLCD3, TGM2, PKD1, PLCD4, KDM3A, SH2B1, MT1H, FYB, PDK1, OPRL1, SPSB3, RGS19, FZD2, RACGAP1, RCAN3, RPS6KA5, SH3BP5, DUSP4, FYN, MAPK14, NLRP12, DGKZ, MAPK8IP3, EPOR, IRF3, APBB3, DUSP6
	GO:0006006~glucose metabolic process	29	1.62	2.82E-04	PRKAG3, ALDOA, PHKB, ALDOC, SLC37A4, PGAM2, HIBADH, PPP1R3E, TPI1, NISCH, HK3, ENO2, GAPDH, PDK1, PDK2, IRS2, WDTC1, PDK4, BAD, PFKM, ADIPOQ, CPT1A, PGM2L1, GPI, G6PD, SDS, MAPK14, PGM1, GHRL
	GO:0000165~MAPKKK cascade	33	1.84	2.83E-04	CAV1, NDST1, MAP4K2, DUSP10, LPAR3, LPAR2, MAP3K6, ERCC6, MAP3K4, CXCR4, PTK2B, GAB1, DUSP16, SPRED2, PAK1, INSR, FGD4, MAP2K5, PRKCA, C5AR1, MADD, ARHGEF6, MET, PKN1, MINK1, MAPK1, DUSP4, PROK2, SH2D3C, GHRL, MAPK8IP3, LRRK2, DUSP6
	GO:0006816~calcium ion transport	27	1.51	4.54E-04	CAV1, TRPV1, CAMK2G, CACNB1, CACNB3, FKBP1B, TPCN1, ANXA6, ATP2B4, CYP27B1, SLC24A4, PKD1, MCOLN1, XCR1, TRPM4, CACNG8, SLC3A2, STIM1, ITPR3, ITPR1, TRPM2, ITPR2, CACNA2D4, CORO1A, ATP2A3, FYN, CACNA1G
	GO:0000271~polysaccharide biosynthetic process	13	0.73	5.38E-04	PRKAG3, NDST1, CMAS, CERCAM, GLCE, HS2ST1, CSGALNACT1, B3GNT8, XYLT2, CHST7, CHST6, HAS1, XYLT1
	GO:0010033~response to organic substance	93	5.19	5.68E-04	ADCY4, SLC9A3, PTGS1, PPARG, SNCA, ARNT2, FOXO1, AURKA, FOXO4, XRCC1, ASAH1, FOS, EIF4EBP1, APOA2, SLC1A2, NOD2, GOT1, GAB1, ATF6B, VKORC1, TMEM102, PRKACA, DNAJC4, DDAH2, XCR1, INSR, EGR1, PRKCA, F12, IRS2, STS, ADAM10, RXRA, ADIPOR1, MFGE8, MMP14, CDK5, MAPK1, RETN, GLUL, ACVR2B, EP300, SQLE, PIAS3, GHRL, CTSC, CA2, CAV1, GCLC, CYP1B1, CCL2, ALDOC, GNG11, TIMP4, TRIM16, ADRBK1, LIN28A, FKBP1B, SERPINH1, SLC11A1, IGF1R, CYP27B1, PLIN2, PTK2B, ENO2, IDH1, SCARB1, KDM3A, WDTC1, GNRH1, FADS1, NR4A2, CRIPAK, ADIPOQ, ABCG1, ABCB4, HDAC5, DUSP4, HDAC4, CORO1A, P2RX1, FYN, MAPK14, ARSA, SMPD1, IRF3, DNAJB2, CHRNB1, ID3, ABCC5, MGST1, CD14, SLC9A1
	GO:0040012~regulation of locomotion	33	1.84	6.13E-04	ACVRL1, IL16, MMP9, SNCA, ABI3, ABHD2, TPM1, VCL, IGF1R, NISCH, ARHGAP5, CXCR4, PTK2B, GAB1, RRAS, SCARB1, LAMB1, INSR, PRKCA, IRS2, ADAM10, PTPRM, PDPN, SCAI, MYO1F, CDK5, VASH1, HDAC5, MAPK1, BBS2, CORO1A, GHRL, ARAP3
	GO:0007243~protein kinase cascade	54	3.01	6.64E-04	PRKAG3, NDST1, STK38, PINK1, LPAR3, LPAR2, TLR9, MAP3K6, MAP3K4, CXCR4, GAB1, SPRED2, PRKACA, PAK1, INSR, MAP2K5, PRKCA, C5AR1, MADD, ARHGEF6, MINK1, PKN1, WNK2, CDK5, MAPK1, SH2D3C, PROK2, CARD14, RIPK3, GHRL, LRRK2, ERC1, CAV1, CCL2, DUSP10, MKNK2, MAP4K2, IGF1R, ERCC6, PTK2B, DUSP16, PKD1, FGD4, FYB, MET, RPS6KA5, DUSP4, FYN, MAPK14, NLRP12, MAPK8IP3, IRF3, DUSP6, SLC9A1

mRNA Expression: Genes Down-Regulated in Endotoxin Tolerance

	Term	Count	%	*P* value	Genes
BIOLOGICAL FUNCTION	GO:0006412~translation	148	8.70	9.90E-62	RPL17, RPL19, RPL14, RPL13, RBM3, RPL15, EIF5B, EIF5A, RPLP2, RPL22L1, MRPS30, RPLP0, EIF1AX, RPLP1, EIF1AY, MRPL36, FAU, EIF1, RPL11, RPL12, MRPL32, EIF2B3, RPS27A, EIF2B5, RPL36AL, RPL35A, YARS, AARS, EARS2, RSL1D1, RPS18, RPS19, RPS16, MRPS18B, RPS14, RARS, EIF2S1, EIF2S2, RPS12, RPS13, RPS10, MRPL47, YARS2, RPS11, EIF2AK2, MRPS17, EEF1B2, PTRH1, MRPS15, MRPS14, MRPS12, WARS2, PTRH2, KARS, RPS25, QRSL1, EIF3A, RPS27, EIF3B, RPS29, RPL7, RPL6, GFM1, RPL9, EIF3E, RPL8, RPL3, EIF3I, RPL5, EIF3J, RPL10A, RPL7A, RPL4, RPS21, EIF3M, RPS23, RPS24, EEF1A1, RPSA, MRPS24, RPL23A, AARSD1, RPS6, RPS5, RPS8, RPS7, RPL18A, RPL37A, ABCF1, ZNFX1, DPH1, EIF2A, RPS2, RPS3, WARS, RPS3A, TRMT6, EEF2K, TNIP1, MRPL1, MRPL4, MRPL3, MRPS5, MRPL9, EIF1B, RPS4X, GTF2B, TARS, RPL41, MRPS9, FARSB, UBB, RPL27A, RPL35, RPL36, RPS15A, RPL37, RPL38, VARS, RPL39, CYLD, RPL30, MRPL13, MRPL12, MRPL15, RPL32, RPL31, MRPL14, ICT1, RPL34, MRPL17, LARS, MARS2, MRPL18, RSL24D1, AIMP1, RRBP1, RPL26, RPL27, RPL24, RPL29, MRPL24, MRPL21, GSPT1, RPL23, RPL22, MRPL27, RPL7L1
	GO:0006414~translational elongation	72	4.23	1.98E-48	RPL17, RPL19, RPL14, RPL13, RPL15, RPLP2, RPS2, RPS3, RPS3A, RPLP0, RPLP1, EEF2K, FAU, RPL11, RPL12, RPS27A, RPL35A, RPS4X, RPS18, RPS19, RPL41, RPS16, RPS14, RPS12, RPS13, RPS10, RPS11, UBB, EEF1B2, RPL27A, RPL35, RPS15A, RPL36, RPL37, RPL38, RPL39, VARS, RPS25, RPL30, RPS27, RPL7, RPL32, RPS29, RPL31, RPL6, GFM1, RPL9, RPL34, RPL8, RPL3, RPL5, RPL10A, RPL7A, RPL4, RPS21, RPS23, RPS24, EEF1A1, RPSA, RPL26, RPL27, RPL24, RPL23A, RPS6, RPS5, RPS8, RPL29, RPS7, RPL23, RPL18A, RPL22, RPL37A
	GO:0022613~ribonucleoprotein complex biogenesis	88	5.17	2.96E-40	NCBP2, NAF1, RPL14, UTP18, SURF6, GAR1, UTP15, SNRPD1, SNRPD2, EIF2A, EBNA1BP2, DCAF13, SBDS, WDR36, DKC1, PRMT5, RPLP0, TFB2M, RPL11, TGS1, GNL2, IMP4, CLNS1A, RPL35A, KRR1, GTPBP4, EXOSC9, EMG1, EXOSC7, NIP7, EXOSC4, BYSL, EXOSC2, EXOSC3, RRP8, RRP9, MBNL1, MRTO4, RCL1, PA2G4, RPS19, NOP2, RPS16, RPS14, ZNHIT6, SNRPF, SNRPE, NHP2, SNRPG, SDAD1, UTP6, NUFIP1, BOP1, BMS1, UTP11L, EIF3A, RPL7, NPM1, BRIX1, NPM3, RPL5, RSL24D1, RPL7A, GEMIN6, GEMIN4, NSA2, RPS24, GEMIN5, PDCD11, TSR1, RPL26, DDX1, MPHOSPH10, RPL24, RPS6, FBL, SF3A3, RPS7, NOP14, DIS3, DDX56, NOLC1, NOP58, RRS1, WDR3, NOP56, UTP14A, PES1
	GO:0042254~ribosome biogenesis	71	4.17	5.74E-39	NAF1, RPL14, SURF6, UTP18, GAR1, UTP15, EIF2A, DCAF13, EBNA1BP2, SBDS, WDR36, DKC1, RPLP0, TFB2M, RPL11, GNL2, IMP4, RPL35A, KRR1, GTPBP4, EXOSC9, EMG1, EXOSC7, NIP7, BYSL, EXOSC4, EXOSC2, EXOSC3, RRP8, RRP9, MRTO4, RCL1, PA2G4, RPS19, NOP2, RPS16, RPS14, NHP2, SDAD1, UTP6, BOP1, BMS1, UTP11L, RPL7, NPM1, BRIX1, NPM3, RPL5, RPL7A, RSL24D1, GEMIN4, NSA2, RPS24, PDCD11, TSR1, MPHOSPH10, RPL26, RPL24, RPS6, FBL, RPS7, DIS3, NOP14, DDX56, NOLC1, NOP58, RRS1, WDR3, NOP56, UTP14A, PES1
	GO:0034660~ncRNA metabolic process	92	5.41	1.79E-33	NAF1, RPL14, ZNFX1, UTP18, GAR1, UTP15, RG9MTD1, MKI67IP, TRMT1, WARS, DCAF13, SBDS, WDR36, DKC1, CTU1, TRMT6, TRMT5, TFB2M, RPL11, IMP4, TSEN15, RPL35A, KRR1, YARS, EXOSC9, EMG1, EXOSC7, EXOSC4, AARS, EXOSC2, EXOSC3, RRP8, RRP9, TRMT61A, EARS2, TARS, PA2G4, RPS19, NOP2, RPS16, RPS14, RARS, FARSB, YARS2, TRUB2, NHP2, PUS3, PUS1, PUS10, UTP6, TYW3, WARS2, QTRT1, BOP1, VARS, PUS7, KARS, UTP11L, RPL7, METTL1, LARS, THG1L, MARS2, NPM3, RPL5, NSUN2, GEMIN4, NSA2, RPS24, DUS3L, PDCD11, AIMP1, RPL26, MPHOSPH10, SSB, AARSD1, RPS6, FBL, RPS7, NOP14, TRNT1, DIS3, CCDC76, DDX56, NOLC1, WDR4, POP1, NOP58, WDR3, NOP56, UTP14A, PES1
	GO:0034470~ncRNA processing	78	4.59	7.45E-30	NAF1, RPL14, UTP18, GAR1, UTP15, RG9MTD1, TRMT1, DCAF13, SBDS, WDR36, DKC1, CTU1, TRMT6, TRMT5, TFB2M, RPL11, IMP4, TSEN15, RPL35A, KRR1, EXOSC9, EMG1, EXOSC7, EXOSC4, AARS, EXOSC2, EXOSC3, RRP8, RRP9, TRMT61A, PA2G4, RPS19, NOP2, RPS16, RPS14, NHP2, TRUB2, PUS3, PUS1, UTP6, PUS10, TYW3, QTRT1, BOP1, PUS7, UTP11L, RPL7, METTL1, THG1L, NPM3, RPL5, NSUN2, GEMIN4, NSA2, RPS24, DUS3L, PDCD11, MPHOSPH10, RPL26, SMAD3, SSB, SMAD1, RPS6, FBL, RPS7, TRNT1, DIS3, CCDC76, NOP14, DDX56, NOLC1, WDR4, POP1, NOP58, WDR3, NOP56, UTP14A, PES1
	GO:0006364~rRNA processing	52	3.06	9.97E-28	NAF1, RPL14, GAR1, UTP18, UTP15, DCAF13, SBDS, WDR36, DKC1, TFB2M, RPL11, IMP4, KRR1, RPL35A, EXOSC9, EXOSC7, EMG1, EXOSC4, EXOSC2, EXOSC3, RRP8, RRP9, PA2G4, NOP2, RPS19, RPS16, RPS14, NHP2, UTP6, BOP1, UTP11L, RPL7, NPM3, RPL5, GEMIN4, NSA2, RPS24, PDCD11, MPHOSPH10, RPL26, RPS6, FBL, RPS7, DIS3, NOP14, DDX56, NOLC1, WDR3, NOP58, NOP56, PES1, UTP14A
	GO:0016072~rRNA metabolic process	53	3.12	1.36E-27	NAF1, RPL14, GAR1, UTP18, UTP15, MKI67IP, DCAF13, SBDS, WDR36, DKC1, TFB2M, RPL11, IMP4, KRR1, RPL35A, EXOSC9, EXOSC7, EMG1, EXOSC4, EXOSC2, EXOSC3, RRP8, RRP9, PA2G4, NOP2, RPS19, RPS16, RPS14, NHP2, UTP6, BOP1, UTP11L, RPL7, NPM3, RPL5, GEMIN4, NSA2, RPS24, PDCD11, MPHOSPH10, RPL26, RPS6, FBL, RPS7, DIS3, NOP14, DDX56, NOLC1, WDR3, NOP58, NOP56, PES1, UTP14A
	GO:0006396~RNA processing	136	8.00	7.86E-25	NCBP2, NAF1, RNMT, RPL14, RBM3, SNRPD1, SNRPD2, SYNCRIP, WTAP, RBM8A, LSM5, TFB2M, RPL11, TGS1, IMP4, CLNS1A, SNRPA1, KRR1, RPL35A, EMG1, AARS, RRP8, RRP9, CSTF2T, HNRNPR, MRM1, RSL1D1, PA2G4, RPS19, NOP2, RPS16, RPS14, SNRPF, SNRPE, SNRPG, PUS3, PUS1, STRAP, PPIL1, PNPT1, SNRPB2, BOP1, PUS7, PPAN, HNRNPM, MOV10, RPL7, METTL1, NPM3, RPL5, HNRNPC, RPL10A, RPS24, PRPF40A, CSTF3, DDX1, MPHOSPH10, SMAD3, SSB, SMAD1, RPS6, HNRNPA1, RPS7, NOP14, TRNT1, PPIE, DDX56, PPIG, NOLC1, POP1, WDR4, WDR3, UTP14A, ADAR, GAR1, UTP18, RG9MTD1, UTP15, TRMT1, YBX1, DCAF13, SBDS, WDR36, DKC1, CTU1, PRMT5, TRMT6, TRMT5, MAGOHB, TSEN15, MRPL1, EXOSC9, EXOSC7, EXOSC4, EXOSC2, EXOSC3, MBNL1, TRMT61A, TTF2, NHP2, TRUB2, THOC1, PPP4R2, POLR2K, TRA2B, TRA2A, PUS10, UTP6, TYW3, NUFIP1, QTRT1, SF3B5, POLR2D, IVNS1ABP, PRPF19, UTP11L, DHX15, THG1L, GEMIN6, NSUN2, RBM28, GEMIN4, DUS3L, NSA2, GEMIN5, PDCD11, RPL26, FBL, SF3A3, DIS3, CCDC76, NOP58, PHF5A, NOP56, PES1, RBM17

mRNA Expression: Genes Down-Regulated in Endotoxin Tolerance ***continued***

	Term	Count	%	*P* value	Genes
BIOLOGICAL FUNCTION	GO:0006955~immune response	141	8.29	1.84E-17	AQP9, IL18, IL19, TNFSF15, APOBEC3G, TLR5, IL15, CXCL11, TLR7, C1QC, IL10, TLR8, CXCL10, NUDCD1, LILRA5, IL1B, CLEC4D, CFD, EBI3, IL1A, CIITA, GTPBP1, GBP5, BST2, IL27, SERPING1, HLA-DQA2, PDCD1LG2, HLA-DQA1, HLA-F, C1QA, IGSF6, C1QB, HLA-DPA1, GBP4, VSIG4, GBP3, GBP2, GBP1, HLA-DRA, ORAI1, IL1R2, IL1R1, CCL3, IFIH1, HLA-DRB1, ENPP2, IFITM3, OAS3, CCL8, OAS1, CD70, OAS2, CCL5, CCL4, CD74, IFI35, ADA, IL23A, HLA-DRB5, HLA-DPB1, HLA-DOA, DEFB1, DHX58, DNAJA3, CFB, IL1RN, CD276, SMAD3, SLAMF7, VAV1, AIM2, FOXP1, PSMB9, DDX58, OASL, TNFSF10, APOL1, ETS1, CD274, POMP, HSPD1, IFI6, NBN, IFI44L, NFKB2, HLA-DMB, HLA-DMA, CD97, HAMP, IL4R, IL1RAP, FCGR3A, ICAM1, SP100, IL18RAP, EXOSC9, PTGER4, CTSS, CD83, CD86, TNFSF13B, PSEN2, IL12B, TREM2, ICOSLG, LCP2, PSMB10, HLA-DQB1, TNF, RSAD2, IL7R, TNFRSF4, CLEC10A, GCH1, CCL24, CCL22, CCL23, CCL20, XBP1, BCL2, TAP2, FCN1, POU2F2, TAP1, CD4, PTX3, IL18R1, IL6, IL2RA, OLR1, IL7, CCL19, SAMHD1, TNFSF9, TRIM22, TNFSF8, CYBB, FCGR2B, ILF2, FCGR2C, IRF8
	GO:0009615~response to virus	39	2.29	1.27E-12	IFIH1, TNF, ZC3HAV1, RPS15A, RSAD2, CCL8, APOBEC3G, IVNS1ABP, CCL5, CCL4, TLR7, IFI35, TLR8, ISG20, TRIM5, CCL22, IL23A, ISG15, BCL2, MX1, DNAJC3, IFNGR2, MX2, FOSL1, ABCE1, IL6, BST2, CCL19, SAMHD1, IFI44, IFI16, STAT1, TRIM22, STAT2, IRF9, DDX58, PLSCR1, IRF7, EIF2AK2
	GO:0006399~tRNA metabolic process	40	2.35	4.38E-12	PUS3, PUS1, ZNFX1, PUS10, RG9MTD1, TYW3, TRMT1, WARS2, QTRT1, VARS, PUS7, KARS, WARS, CTU1, TRMT6, METTL1, TRMT5, LARS, THG1L, MARS2, NSUN2, TSEN15, DUS3L, YARS, AIMP1, AARS, SSB, AARSD1, TRMT61A, FBL, EARS2, CCDC76, TRNT1, TARS, RARS, FARSB, POP1, WDR4, YARS2, TRUB2
	GO:0006954~inflammatory response	72	4.23	8.95E-11	ABCF1, A2M, NFKB1, TLR5, IL15, CXCL11, C1QC, TLR7, TLR8, IL10, CXCL10, CD97, NOD1, IL1RAP, IL1B, CFD, IL1A, CIITA, NFKBIZ, IL18RAP, IL27, LYZ, SERPING1, CD40, C1QA, C1QB, SIGLEC1, TNFAIP6, F3, RIPK2, VSIG4, KDM6B, CCL3, TNF, NMI, ADORA2A, CCL8, CCL5, TNFRSF4, CCL4, CCL24, CCL22, HRH1, IL23A, CCL23, MEFV, CCL20, PTX3, SPP1, FN1, IL6, IL2RA, LIPA, AIMP1, OLR1, CFB, SAAL1, MAP2K3, IL1RN, CCL19, IDO1, SMAD1, STAT3, SELS, APOL2, CYBB, P2RX7, TFRC, NUPR1, IRF7, HDAC9, IGFBP4
	GO:0007005~mitochondrion organization	41	2.41	2.27E-10	NDUFAF4, GRPEL2, GRPEL1, GGCT, COX10, TIMM17A, TIMM10, RNASEH1, TIMM50, TIMM13, BCL2L1, PMAIP1, TFAM, TOMM7, MRPL12, TOMM5, GFM1, BCL2, CASP7, TIMM9, SYNJ2, TFB2M, MYC, DNAJA3, HSP90AA1, MSTO1, SSBP1, SMAD3, TOMM40, TMEM70, PIM2, TIMM23, TIMM8B, C10ORF2, TIMM8A, TRNT1, P2RX7, TOMM70A, PTCD2, TOMM22, IFI6
	GO:0006952~defense response	109	6.41	1.58E-09	A2M, APOBEC3G, TLR5, IL15, CXCL11, C1QC, TLR7, TLR8, IL10, CXCL10, CD48, CSF3R, IL1B, CFD, MX1, MX2, IL1A, CIITA, IL27, CST3, SERPING1, CD40, SP140, C1QA, TNFAIP6, C1QB, F3, MNDA, RIPK2, VSIG4, HLA-DRA, IL1R1, CCL3, IFIH1, ADORA2A, CCL8, CCL5, CCL4, CD74, IL23A, DEFB1, DNAJA3, DHX58, FN1, SPP1, CFB, MAP2K3, IL1RN, SMAD1, SLAMF7, DDX58, APOL2, P2RX7, APOL1, HDAC9, ABCF1, NFKB1, CD97, NOD1, HAMP, IL1RAP, TNIP1, FOSL1, NFKBIZ, IL18RAP, SP100, LYZ, CD83, SIGLEC1, INHBA, ICOSLG, KDM6B, PRF1, NMI, TNF, RSAD2, VARS, TNFRSF4, GCH1, CCL24, CCL22, HRH1, CCL23, MEFV, CCL20, BCL2, TAP2, TAP1, PTX3, IL18R1, IL6, IL2RA, LIPA, AIMP1, OLR1, SAAL1, RNASE6, CCL19, SAMHD1, IDO1, STAT3, SELS, LSP1, KCNN4, CYBB, TFRC, NUPR1, IRF7, IGFBP4
	GO:0006915~apoptosis	107	6.29	1.91E-09	FASTKD2, IL19, TNFSF15, PMAIP1, MRPS30, CRADD, MAP3K5, RAD21, TIAM1, IL1B, IL1A, RPS27A, CUL1, YARS, BCL2L14, FAM82A2, BCL2A1, TBRG4, ESPL1, PIM2, BCL2L11, F3, TNFAIP8, RIPK2, TNFAIP3, EIF2AK2, NEK6, TRAF1, FGD2, GGCT, LITAF, ADORA2A, NFKBIA, PPT1, BCL2L1, PTRH2, GREM1, MST4, PEA15, ECE1, HSPE1, FAIM, DNAJA3, SRGN, CFLAR, SMAD3, VAV1, TRADD, TNFSF10, CSRNP1, HSPD1, PDCD5, IFI6, IER3, PPARD, NFKB1, RPS3, CASP5, TRIAP1, CASP4, NOD1, CASP7, AEN, CASP1, MYC, DHCR24, CYCS, GZMB, DAPK1, TNFRSF10A, BNIP1, TNFRSF10D, HIPK3, PSEN2, GADD45G, PSME3, UBB, GADD45B, THOC1, PRF1, TNFRSF21, TNF, PML, TRIB3, BCL2, TNFRSF18, ZC3H12A, XAF1, PHLDA3, PHLDA2, RNF144B, IL6, IL2RA, AIMP1, FAM188A, TNFSF9, BIRC3, STAT1, BIRC2, NRAS, RASSF5, GSPT1, IFT57, JAK2, PERP, DRAM1, TP53INP1
	GO:0012501~programmed cell death	108	6.35	2.22E-09	FASTKD2, IL19, TNFSF15, PMAIP1, MRPS30, CRADD, TOP1, MAP3K5, RAD21, TIAM1, IL1B, IL1A, RPS27A, CUL1, YARS, BCL2L14, FAM82A2, BCL2A1, TBRG4, ESPL1, PIM2, BCL2L11, F3, TNFAIP8, RIPK2, TNFAIP3, EIF2AK2, NEK6, TRAF1, FGD2, GGCT, LITAF, ADORA2A, NFKBIA, PPT1, BCL2L1, PTRH2, GREM1, MST4, PEA15, ECE1, HSPE1, FAIM, DNAJA3, SRGN, CFLAR, SMAD3, VAV1, TRADD, TNFSF10, CSRNP1, HSPD1, PDCD5, IFI6, IER3, PPARD, NFKB1, RPS3, CASP5, TRIAP1, NOD1, CASP4, CASP7, AEN, CASP1, MYC, DHCR24, CYCS, GZMB, DAPK1, TNFRSF10A, BNIP1, TNFRSF10D, HIPK3, PSEN2, GADD45G, PSME3, UBB, GADD45B, THOC1, PRF1, TNFRSF21, TNF, PML, TRIB3, BCL2, TNFRSF18, ZC3H12A, XAF1, PHLDA3, PHLDA2, RNF144B, IL6, IL2RA, AIMP1, FAM188A, TNFSF9, BIRC3, STAT1, BIRC2, NRAS, RASSF5, GSPT1, IFT57, JAK2, PERP, DRAM1, TP53INP1
	GO:0070665~positive regulation of leukocyte proliferation	23	1.35	5.36E-09	IL6, IL2RA, IL7, IL6ST, STAT5A, CSF1, IL18, CD276, CD40, IL15, TNFRSF4, PDCD1LG2, ADA, CD38, NCK2, TNFSF13B, CD80, RIPK2, IL1B, IL12B, DNAJA3, ICOSLG, EBI3
	GO:0032946~positive regulation of mononuclear cell proliferation	23	1.35	5.36E-09	IL6, IL2RA, IL7, IL6ST, STAT5A, CSF1, IL18, CD276, CD40, IL15, TNFRSF4, PDCD1LG2, ADA, CD38, NCK2, TNFSF13B, CD80, RIPK2, IL1B, IL12B, DNAJA3, ICOSLG, EBI3
	GO:0050870~positive regulation of T cell activation	27	1.59	7.11E-09	IL6ST, STAT5A, IL18, IL15, IL7R, HLA-DMA, ADA, CD74, IL4R, IL1B, CD4, DNAJA3, EBI3, IL6, IL2RA, IL7, CD276, PDCD1LG2, CD83, NCK2, CD86, TNFSF13B, CD80, RIPK2, HSPD1, IL12B, ICOSLG

6. References

Adib-Conquy M & Cavaillon JM (2009): Compensatory anti-inflammatory response syndrome. *Thromb Haemost* **101**: 36-47.

Akira S & Hoshino K (2003): Myeloid differentiation factor 88-dependent and -independent pathways in toll-like receptor signaling. *J Infect Dis* **187 Suppl 2**: S356-363.

Akira S, Uematsu S & Takeuchi O (2006): Pathogen recognition and innate immunity. *Cell* **124**: 783-801.

Allantaz-Frager F, Turrel-Davin F, Venet F, Monnin C, De Saint Jean A, Barbalat V, Cerrato E, Pachot A, Lepape A & Monneret G (2013): Identification of biomarkers of response to IFNg during endotoxin tolerance: application to septic shock. *PLoS One* **8**: e68218.

Anders S & Huber W (2010): Differential expression analysis for sequence count data. *Genome Biol* **11**: R106.

Andrew S (2010): FastQC: a quality control tool for high throughput sequence data.

Angus DC, Pereira CA & Silva E (2006): Epidemiology of severe sepsis around the world. *Endocr Metab Immune Disord Drug Targets* **6**: 207-212.

Angus DC & van der Poll T (2013): Severe sepsis and septic shock. *N Engl J Med* **369**: 840-851.

Arend WP & Guthridge CJ (2000): Biological role of interleukin 1 receptor antagonist isoforms. *Ann Rheum Dis* **59 Suppl 1**: i60-64.

Artis D & Spits H (2015): The biology of innate lymphoid cells. *Nature* **517**: 293-301.

Aung HT, Schroder K, Himes SR, Brion K, van Zuylen W, Trieu A, Suzuki H, Hayashizaki Y, Hume DA, Sweet MJ *et al.* (2006): LPS regulates proinflammatory gene expression in macrophages by altering histone deacetylase expression. *FASEB J* **20**: 1315-1327.

Baggiolini M, Imboden P & Detmers P (1992): Neutrophil activation and the effects of interleukin-8/neutrophil-activating peptide 1 (IL-8/NAP-1). *Cytokines* **4**: 1-17.

Bailey T, Krajewski P, Ladunga I, Lefebvre C, Li Q, Liu T, Madrigal P, Taslim C & Zhang J (2013): Practical guidelines for the comprehensive analysis of ChIP-seq data. *PLoS Comput Biol* **9**: e1003326.

Banerji J, Rusconi S & Schaffner W (1981): Expression of a beta-globin gene is enhanced by remote SV40 DNA sequences. *Cell* **27**: 299-308.

Bardet AF, He Q, Zeitlinger J & Stark A (2012): A computational pipeline for comparative ChIP-seq analyses. *Nat Protoc* **7**: 45-61.

Barreau C, Paillard L & Osborne HB (2005): AU-rich elements and associated factors: are there unifying principles? *Nucleic Acids Res* **33**: 7138-7150.

Barski A, Cuddapah S, Cui K, Roh TY, Schones DE, Wang Z, Wei G, Chepelev I & Zhao K (2007): High-resolution profiling of histone methylations in the human genome. *Cell* **129**: 823-837.

Becker D, Lutsik P, Ebert P, Bock C, Lengauer T & Walter J (2014): BiQ Analyzer HiMod: an interactive software tool for high-throughput locus-specific analysis of 5-methylcytosine and its oxidized derivatives. *Nucleic Acids Res* **42**: W501-507.

Beeson PB (1946): Devolpment of tolerance to typhoid bacterial pyrogen and its abolition by reticulo-endothelial blockade. *Proc Soc Exp Biol Med* **61**: 248-250.

Berger SL (2007): The complex language of chromatin regulation during transcription. *Nature* **447**: 407-412.

Bernstein BE, Kamal M, Lindblad-Toh K, Bekiranov S, Bailey DK, Huebert DJ, McMahon S, Karlsson EK, Kulbokas EJ, 3rd, Gingeras TR *et al.* (2005): Genomic maps and comparative analysis of histone modifications in human and mouse. *Cell* **120**: 169-181.

Bernstein BE, Meissner A & Lander ES (2007): The mammalian epigenome. *Cell* **128**: 669-681.

Beutler B (2004): Innate immunity: an overview. *Mol Immunol* **40**: 845-859.

Bierne H, Hamon M & Cossart P (2012): Epigenetics and bacterial infections. *Cold Spring Harb Perspect Med* **2**: a010272.

Bird AP & Wolffe AP (1999): Methylation-induced repression--belts, braces, and chromatin. *Cell* **99**: 451-454.

Biswas SK & Lopez-Collazo E (2009): Endotoxin tolerance: new mechanisms, molecules and clinical significance. *Trends Immunol* **30**: 475-487.

Biswas SK & Shalova IN (2012). Endotoxin Tolerance as a Key Mechanism for Immunosuppression. In Immunosuppression - Role in Health and Diseases, Kapur DS, ed. (InTech), pp. 21-40.

Black JC, Van Rechem C & Whetstine JR (2012): Histone lysine methylation dynamics: establishment, regulation, and biological impact. *Mol Cell* **48**: 491-507.

Blankenberg D, Von Kuster G, Coraor N, Ananda G, Lazarus R, Mangan M, Nekrutenko A & Taylor J (2010): Galaxy: a web-based genome analysis tool for experimentalists. *Curr Protoc Mol Biol* **Chapter 19**: Unit 19 10 11-21.

Blobe GC, Schiemann WP & Lodish HF (2000): Role of transforming growth factor beta in human disease. *N Engl J Med* **342**: 1350-1358.

Bogdan C & Nathan C (1993): Modulation of macrophage function by transforming growth factor beta, interleukin-4, and interleukin-10. *Ann N Y Acad Sci* **685**: 713-739.

Bone RC (1996): Sir Isaac Newton, sepsis, SIRS, and CARS. *Crit Care Med* **24**: 1125-1128.

Bone RC, Balk RA, Cerra FB, Dellinger RP, Fein AM, Knaus WA, Schein RM & Sibbald WJ (1992): Definitions for sepsis and organ failure and guidelines for the use of innovative therapies in sepsis. The ACCP/SCCM Consensus Conference Committee. American College of Chest Physicians/Society of Critical Care Medicine. *Chest* **101**: 1644-1655.

Bossmann K (2009). Dissertation: Regulation der TNF-α-mRNA-Stabilität durch das anti-inflammatorische Zytokin IL-10 (Humboldt-Universität zu Berlin).

Boyer LA, Plath K, Zeitlinger J, Brambrink T, Medeiros LA, Lee TI, Levine SS, Wernig M, Tajonar A, Ray MK *et al.* (2006): Polycomb complexes repress developmental regulators in murine embryonic stem cells. *Nature* **441**: 349-353.

Boyum A (1968): Isolation of mononuclear cells and granulocytes from human blood. Isolation of monuclear cells by one centrifugation, and of granulocytes by combining centrifugation and sedimentation at 1 g. *Scand J Clin Lab Invest Suppl* **97**: 77-89.

Bozinovski S, Jones JE, Vlahos R, Hamilton JA & Anderson GP (2002): Granulocyte/macrophage-colony-stimulating factor (GM-CSF) regulates lung innate immunity to lipopolysaccharide through Akt/Erk activation of NFkappa B and AP-1 in vivo. *J Biol Chem* **277**: 42808-42814.

Bracken AP, Dietrich N, Pasini D, Hansen KH & Helin K (2006): Genome-wide mapping of Polycomb target genes unravels their roles in cell fate transitions. *Genes Dev* **20**: 1123-1136.

Breiling A & Lyko F (2015): Epigenetic regulatory functions of DNA modifications: 5-methylcytosine and beyond. *Epigenetics Chromatin* **8**: 24.

Brenner C & Fuks F (2007): A methylation rendezvous: reader meets writers. *Dev Cell* **12**: 843-844.

Brinkman AB, Simmer F, Ma K, Kaan A, Zhu J & Stunnenberg HG (2010): Whole-genome DNA methylation profiling using MethylCap-seq. *Methods* **52**: 232-236.

Campion J, Milagro FI, Goyenechea E & Martinez JA (2009): TNF-alpha promoter methylation as a predictive biomarker for weight-loss response. *Obesity (Silver Spring)* **17**: 1293-1297.

Carballo E, Lai WS & Blackshear PJ (1998): Feedback inhibition of macrophage tumor necrosis factor-alpha production by tristetraprolin. *Science* **281**: 1001-1005.

Caretti G, Salsi V, Vecchi C, Imbriano C & Mantovani R (2003): Dynamic recruitment of NF-Y and histone acetyltransferases on cell-cycle promoters. *J Biol Chem* **278**: 30435-30440.

Carson WF, Cavassani KA, Dou Y & Kunkel SL (2011): Epigenetic regulation of immune cell functions during post-septic immunosuppression. *Epigenetics* **6**: 273-283.

Carswell EA, Old LJ, Kassel RL, Green S, Fiore N & Williamson B (1975): An endotoxin-induced serum factor that causes necrosis of tumors. *Proc Natl Acad Sci U S A* **72**: 3666-3670.

Castell JV, Gomez-Lechon MJ, David M, Hirano T, Kishimoto T & Heinrich PC (1988): Recombinant human interleukin-6 (IL-6/BSF-2/HSF) regulates the synthesis of acute phase proteins in human hepatocytes. *FEBS Lett* **232**: 347-350.

Castellucci M, Rossato M, Calzetti F, Tamassia N, Zeminian S, Cassatella MA & Bazzoni F (2015): IL-10 disrupts the Brd4-docking sites to inhibit LPS-induced CXCL8 and TNF-alpha expression in monocytes: Implications for chronic obstructive pulmonary disease. *J Allergy Clin Immunol* **136**: 781-791 e789.

Cavaillon JM & Adib-Conquy M (2006): Bench-to-bedside review: endotoxin tolerance as a model of leukocyte reprogramming in sepsis. *Crit Care* **10**: 233.

Cavaillon JM, Pitton C & Fitting C (1994): Endotoxin tolerance is not a LPS-specific phenomenon: partial mimicry with IL-1, IL-10 and TGFβ. *J Endotoxin Res* **1**: 21-29.

Cedar H & Bergman Y (2009): Linking DNA methylation and histone modification: patterns and paradigms. *Nat Rev Genet* **10**: 295-304.

Celsus AD (circa 30 AD): De Medicina.

Chan C, Li L, McCall CE & Yoza BK (2005): Endotoxin tolerance disrupts chromatin remodeling and NF-kappaB transactivation at the IL-1beta promoter. *J Immunol* **175**: 461-468.

Chaplin DD (2010): Overview of the immune response. *J Allergy Clin Immunol* **125**: S3-23.

Chen J & Ivashkiv LB (2010): IFN-gamma abrogates endotoxin tolerance by facilitating Toll-like receptor-induced chromatin remodeling. *Proc Natl Acad Sci U S A* **107**: 19438-19443.

Chen L, Kostadima M, Martens JH, Canu G, Garcia SP, Turro E, Downes K, Macaulay IC, Bielczyk-Maczynska E, Coe S *et al.* (2014): Transcriptional diversity during lineage commitment of human blood progenitors. *Science* **345**: 1251033.

Cheng SC, Quintin J, Cramer RA, Shepardson KM, Saeed S, Kumar V, Giamarellos-Bourboulis EJ, Martens JH, Rao NA, Aghajanirefah A *et al.* (2014): mTOR- and HIF-1alpha-mediated aerobic glycolysis as metabolic basis for trained immunity. *Science* **345**: 1250684.

Clapier CR & Cairns BR (2009): The biology of chromatin remodeling complexes. *Annu Rev Biochem* **78**: 273-304.

Cohen J (2002): The immunopathogenesis of sepsis. *Nature* **420**: 885-891.

Consortium EP (2012): An integrated encyclopedia of DNA elements in the human genome. *Nature* **489**: 57-74.

Cook DN, Pisetsky DS & Schwartz DA (2004): Toll-like receptors in the pathogenesis of human disease. *Nat Immunol* **5**: 975-979.

Cooper AM, Dalton DK, Stewart TA, Griffin JP, Russell DG & Orme IM (1993): Disseminated tuberculosis in interferon gamma gene-disrupted mice. *J Exp Med* **178**: 2243-2247.

Cooper MD & Alder MN (2006): The evolution of adaptive immune systems. *Cell* **124**: 815-822.

Creasey AA, Stevens P, Kenney J, Allison AC, Warren K, Catlett R, Hinshaw L & Taylor FB, Jr. (1991): Endotoxin and cytokine profile in plasma of baboons challenged with lethal and sublethal Escherichia coli. *Circ Shock* **33**: 84-91.

Creyghton MP, Cheng AW, Welstead GG, Kooistra T, Carey BW, Steine EJ, Hanna J, Lodato MA, Frampton GM, Sharp PA *et al.* (2010): Histone H3K27ac separates active from poised enhancers and predicts developmental state. *Proc Natl Acad Sci U S A* **107**: 21931-21936.

de Waal Malefyt R, Abrams J, Bennett B, Figdor CG & de Vries JE (1991): Interleukin 10(IL-10) inhibits cytokine synthesis by human monocytes: an autoregulatory role of IL-10 produced by monocytes. *J Exp Med* **174**: 1209-1220.

Dean JL, Sully G, Clark AR & Saklatvala J (2004): The involvement of AU-rich element-binding proteins in p38 mitogen-activated protein kinase pathway-mediated mRNA stabilisation. *Cell Signal* **16**: 1113-1121.

del Fresno C, Garcia-Rio F, Gomez-Pina V, Soares-Schanoski A, Fernandez-Ruiz I, Jurado T, Kajiji T, Shu C, Marin E, Gutierrez del Arroyo A *et al.* (2009): Potent phagocytic activity with impaired antigen presentation

identifying lipopolysaccharide-tolerant human monocytes: demonstration in isolated monocytes from cystic fibrosis patients. *J Immunol* **182**: 6494-6507.

Delves PJ & Roitt IM (2000): The immune system. First of two parts. *N Engl J Med* **343**: 37-49.

Depken M & Schiessel H (2009): Nucleosome shape dictates chromatin fiber structure. *Biophys J* **96**: 777-784.

Dey S, Curtis DJ, Jane SM & Brandt SJ (2010): The TAL1/SCL transcription factor regulates cell cycle progression and proliferation in differentiating murine bone marrow monocyte precursors. *Mol Cell Biol* **30**: 2181-2192.

Docke WD, Randow F, Syrbe U, Krausch D, Asadullah K, Reinke P, Volk HD & Kox W (1997a): Monocyte deactivation in septic patients: restoration by IFN-gamma treatment. *Nat Med* **3**: 678-681.

Docke WD, Reinke P, Syrbe U, Platzer C, Asadullah K, Krausch D, Zuckermann H & HD V (1997b): Immunoparalysis in sepsis – From phenomenon to treatment strategies. *Tex Med* **9**: 55-65.

Dormann HL, Tseng BS, Allis CD, Funabiki H & Fischle W (2006): Dynamic regulation of effector protein binding to histone modifications: the biology of HP1 switching. *Cell Cycle* **5**: 2842-2851.

Eichacker PQ, Parent C, Kalil A, Esposito C, Cui X, Banks SM, Gerstenberger EP, Fitz Y, Danner RL & Natanson C (2002): Risk and the efficacy of antiinflammatory agents: retrospective and confirmatory studies of sepsis. *Am J Respir Crit Care Med* **166**: 1197-1205.

El Gazzar M & McCall CE (2010): MicroRNAs distinguish translational from transcriptional silencing during endotoxin tolerance. *J Biol Chem* **285**: 20940-20951.

El Gazzar M, Yoza BK, Chen X, Garcia BA, Young NL & McCall CE (2009): Chromatin-specific remodeling by HMGB1 and linker histone H1 silences proinflammatory genes during endotoxin tolerance. *Mol Cell Biol* **29**: 1959-1971.

El Gazzar M, Yoza BK, Chen X, Hu J, Hawkins GA & McCall CE (2008): G9a and HP1 couple histone and DNA methylation to TNFalpha transcription silencing during endotoxin tolerance. *J Biol Chem* **283**: 32198-32208.

El Gazzar M, Yoza BK, Hu JY, Cousart SL & McCall CE (2007): Epigenetic silencing of tumor necrosis factor alpha during endotoxin tolerance. *J Biol Chem* **282**: 26857-26864.

Elias JA, Reynolds MM, Kotloff RM & Kern JA (1989): Fibroblast interleukin 1 beta: synergistic stimulation by recombinant interleukin 1 and tumor necrosis factor and posttranscriptional regulation. *Proc Natl Acad Sci U S A* **86**: 6171-6175.

Erroi A, Fantuzzi G, Mengozzi M, Sironi M, Orencole SF, Clark BD, Dinarello CA, Isetta A, Gnocchi P, Giovarelli M *et al.* (1993): Differential regulation of cytokine production in lipopolysaccharide tolerance in mice. *Infect Immun* **61**: 4356-4359.

Ertel W, Kremer JP, Kenney J, Steckholzer U, Jarrar D, Trentz O & Schildberg FW (1995): Downregulation of proinflammatory cytokine release in whole blood from septic patients. *Blood* **85**: 1341-1347.

Fahlman C, Jacobsen FW, Veiby OP, McNiece IK, Blomhoff HK & Jacobsen SE (1994): Tumor necrosis factor-alpha (TNF-alpha) potently enhances in vitro macrophage production from primitive murine hematopoietic progenitor cells in combination with stem cell factor and interleukin-7: novel stimulatory role of p55 TNF receptors. *Blood* **84**: 1528-1533.

Falkenberg KJ & Johnstone RW (2014): Histone deacetylases and their inhibitors in cancer, neurological diseases and immune disorders. *Nat Rev Drug Discov* **13**: 673-691.

Fan H & Cook JA (2004): Molecular mechanisms of endotoxin tolerance. *J Endotoxin Res* **10**: 71-84.

Favorite GO & Morgan HR (1942): Effects Produced by the Intravenous Injection in Man of a Toxic Antigenic Material Derived from Eberthella Typhosa: Clinical, Hematological, Chemical and Serological Studies. *J Clin Invest* **21**: 589-599.

Feng XH, Zhang Y, Wu RY & Derynck R (1998): The tumor suppressor Smad4/DPC4 and transcriptional adaptor CBP/p300 are coactivators for smad3 in TGF-beta-induced transcriptional activation. *Genes Dev* **12**: 2153-2163.

Fiorentino DF, Zlotnik A, Mosmann TR, Howard M & O'Garra A (1991): IL-10 inhibits cytokine production by activated macrophages. *J Immunol* **147**: 3815-3822.

Fischl KD (2010): Comparison of Histone Protein Locatin Algorithm. *MERIT Bien 2010 Final Report*.

Flajnik MF & Kasahara M (2010): Origin and evolution of the adaptive immune system: genetic events and selective pressures. *Nat Rev Genet* **11**: 47-59.

Flohe SB, Agrawal H, Flohe S, Rani M, Bangen JM & Schade FU (2008): Diversity of interferon gamma and granulocyte-macrophage colony-stimulating factor in restoring immune dysfunction of dendritic cells and macrophages during polymicrobial sepsis. *Mol Med* **14**: 247-256.

Forster R, Davalos-Misslitz AC & Rot A (2008): CCR7 and its ligands: balancing immunity and tolerance. *Nat Rev Immunol* **8**: 362-371.

Foster SL, Hargreaves DC & Medzhitov R (2007): Gene-specific control of inflammation by TLR-induced chromatin modifications. *Nature* **447**: 972-978.

Foster SL & Medzhitov R (2009): Gene-specific control of the TLR-induced inflammatory response. *Clin Immunol* **130**: 7-15.

Fraker DL, Stovroff MC, Merino MJ & Norton JA (1988): Tolerance to tumor necrosis factor in rats and the relationship to endotoxin tolerance and toxicity. *J Exp Med* **168**: 95-105.

Freudenberg MA & Galanos C (1988): Induction of tolerance to lipopolysaccharide (LPS)-D-galactosamine lethality by pretreatment with LPS is mediated by macrophages. *Infect Immun* **56**: 1352-1357.

Fuks F (2005): DNA methylation and histone modifications: teaming up to silence genes. *Curr Opin Genet Dev* **15**: 490-495.

Gauldie J, Richards C, Northemann W, Fey G & Baumann H (1989): IFN beta 2/BSF2/IL-6 is the monocyte-derived HSF that regulates receptor-specific acute phase gene regulation in hepatocytes. *Ann N Y Acad Sci* **557**: 46-58; discussion 58-49.

Gentleman RC, Carey VJ, Bates DM, Bolstad B, Dettling M, Dudoit S, Ellis B, Gautier L, Ge Y, Gentry J *et al.* (2004): Bioconductor: open software development for computational biology and bioinformatics. *Genome Biol* **5**: R80.

Ghisletti S, Barozzi I, Mietton F, Polletti S, De Santa F, Venturini E, Gregory L, Lonie L, Chew A, Wei CL *et al.* (2010): Identification and characterization of enhancers controlling the inflammatory gene expression program in macrophages. *Immunity* **32**: 317-328.

Ghisletti S, Huang W, Jepsen K, Benner C, Hardiman G, Rosenfeld MG & Glass CK (2009): Cooperative NCoR/SMRT interactions establish a corepressor-based strategy for integration of inflammatory and anti-inflammatory signaling pathways. *Genes Dev* **23**: 681-693.

Giacomini P, Tecce R, Gambari R, Sacchi A, Fisher PB & Natali PG (1988): Recombinant human IFN-gamma, but not IFN-alpha or IFN-beta, enhances MHC- and non-MHC-encoded glycoproteins by a protein synthesis-dependent mechanism. *J Immunol* **140**: 3073-3081.

Giardine B, Riemer C, Hardison RC, Burhans R, Elnitski L, Shah P, Zhang Y, Blankenberg D, Albert I, Taylor J *et al.* (2005): Galaxy: a platform for interactive large-scale genome analysis. *Genome Res* **15**: 1451-1455.

Gilbert KM, Thoman M, Bauche K, Pham T & Weigle WO (1997): Transforming growth factor-beta 1 induces antigen-specific unresponsiveness in naive T cells. *Immunol Invest* **26**: 459-472.

Gilchrist M, Thorsson V, Li B, Rust AG, Korb M, Roach JC, Kennedy K, Hai T, Bolouri H & Aderem A (2006): Systems biology approaches identify ATF3 as a negative regulator of Toll-like receptor 4. *Nature* **441**: 173-178.

Gilmour DS & Lis JT (1985): In vivo interactions of RNA polymerase II with genes of Drosophila melanogaster. *Mol Cell Biol* **5**: 2009-2018.

Glass CK & Saijo K (2010): Nuclear receptor transrepression pathways that regulate inflammation in macrophages and T cells. *Nat Rev Immunol* **10**: 365-376.

Goecks J, Nekrutenko A, Taylor J & Galaxy T (2010): Galaxy: a comprehensive approach for supporting accessible, reproducible, and transparent computational research in the life sciences. *Genome Biol* **11**: R86.

Goff L, Trapnell C & Kelley D (2013): cummeRbund: Analysis, exploration, manipulation, and visualization of Cufflinks high-throughput sequencing data. R package version 2.8.0.

Goll MG & Bestor TH (2005): Eukaryotic cytosine methyltransferases. *Annu Rev Biochem* **74**: 481-514.

Goyert SM, Ferrero EM, Seremetis SV, Winchester RJ, Silver J & Mattison AC (1986): Biochemistry and expression of myelomonocytic antigens. *J Immunol* **137**: 3909-3914.

Grutz G (2005): New insights into the molecular mechanism of interleukin-10-mediated immunosuppression. *J Leukoc Biol* **77**: 3-15.

Gunther J, Vogt N, Hampel K, Bikker R, Page S, Muller B, Kandemir J, Kracht M, Dittrich-Breiholz O, Huber R *et al.* (2014): Identification of two forms of TNF tolerance in human monocytes: differential inhibition of NF-kappaB/AP-1- and PP1-associated signaling. *J Immunol* **192**: 3143-3155.

Hammond ME, Lapointe GR, Feucht PH, Hilt S, Gallegos CA, Gordon CA, Giedlin MA, Mullenbach G & Tekamp-Olson P (1995): IL-8 induces neutrophil chemotaxis predominantly via type I IL-8 receptors. *J Immunol* **155**: 1428-1433.

Hargreaves DC, Horng T & Medzhitov R (2009): Control of inducible gene expression by signal-dependent transcriptional elongation. *Cell* **138**: 129-145.

Hawkins RD, Hon GC, Yang C, Antosiewicz-Bourget JE, Lee LK, Ngo QM, Klugman S, Ching KA, Edsall LE, Ye Z *et al.* (2011): Dynamic chromatin states in human ES cells reveal potential regulatory sequences and genes involved in pluripotency. *Cell Res* **21**: 1393-1409.

Heintzman ND, Stuart RK, Hon G, Fu Y, Ching CW, Hawkins RD, Barrera LO, Van Calcar S, Qu C, Ching KA *et al.* (2007): Distinct and predictive chromatin signatures of transcriptional promoters and enhancers in the human genome. *Nat Genet* **39**: 311-318.

Heinz S, Benner C, Spann N, Bertolino E, Lin YC, Laslo P, Cheng JX, Murre C, Singh H & Glass CK (2010): Simple combinations of lineage-determining transcription factors prime cis-regulatory elements required for macrophage and B cell identities. *Mol Cell* **38**: 576-589.

Hirotani T, Lee PY, Kuwata H, Yamamoto M, Matsumoto M, Kawase I, Akira S & Takeda K (2005): The nuclear IkappaB protein IkappaBNS selectively inhibits lipopolysaccharide-induced IL-6 production in macrophages of the colonic lamina propria. *J Immunol* **174**: 3650-3657.

Hoflich C & Volk HD (2002): [Immunomodulation in sepsis]. *Chirurg* **73**: 1100-1104.

Hotchkiss RS & Karl IE (2003): The pathophysiology and treatment of sepsis. *N Engl J Med* **348**: 138-150.

Hotchkiss RS, Monneret G & Payen D (2013): Immunosuppression in sepsis: a novel understanding of the disorder and a new therapeutic approach. *Lancet Infect Dis* **13**: 260-268.

Hotchkiss RS, Swanson PE, Freeman BD, Tinsley KW, Cobb JP, Matuschak GM, Buchman TG & Karl IE (1999): Apoptotic cell death in patients with sepsis, shock, and multiple organ dysfunction. *Crit Care Med* **27**: 1230-1251.

Hotchkiss RS, Tinsley KW, Swanson PE, Grayson MH, Osborne DF, Wagner TH, Cobb JP, Coopersmith C & Karl IE (2002): Depletion of dendritic cells, but not macrophages, in patients with sepsis. *J Immunol* **168**: 2493-2500.

Hotchkiss RS, Tinsley KW, Swanson PE, Schmieg RE, Jr., Hui JJ, Chang KC, Osborne DF, Freeman BD, Cobb JP, Buchman TG *et al.* (2001): Sepsis-induced apoptosis causes progressive profound depletion of B and CD4+ T lymphocytes in humans. *J Immunol* **166**: 6952-6963.

Huang DW, Sherman BT & Lempicki RA (2009a): Bioinformatics enrichment tools: paths toward the comprehensive functional analysis of large gene lists. *Nucleic Acids Res* **37**: 1-13.

Huang DW, Sherman BT & Lempicki RA (2009b): Systematic and integrative analysis of large gene lists using DAVID bioinformatics resources. *Nat Protoc* **4**: 44-57.

Huang S, Hendriks W, Althage A, Hemmi S, Bluethmann H, Kamijo R, Vilcek J, Zinkernagel RM & Aguet M (1993): Immune response in mice that lack the interferon-gamma receptor. *Science* **259**: 1742-1745.

Huber W, Carey VJ, Gentleman R, Anders S, Carlson M, Carvalho BS, Bravo HC, Davis S, Gatto L, Girke T *et al.* (2015): Orchestrating high-throughput genomic analysis with Bioconductor. *Nat Methods* **12**: 115-121.

Hutchins NA, Unsinger J, Hotchkiss RS & Ayala A (2014): The new normal: immunomodulatory agents against sepsis immune suppression. *Trends Mol Med* **20**: 224-233.

Iizuka M & Smith MM (2003): Functional consequences of histone modifications. *Curr Opin Genet Dev* **13**: 154-160.

Iskander KN, Osuchowski MF, Stearns-Kurosawa DJ, Kurosawa S, Stepien D, Valentine C & Remick DG (2013): Sepsis: multiple abnormalities, heterogeneous responses, and evolving understanding. *Physiol Rev* **93**: 1247-1288.

Ivashkiv LB (2011): Inflammatory signaling in macrophages: transitions from acute to tolerant and alternative activation states. *Eur J Immunol* **41**: 2477-2481.

Iwasaki A & Medzhitov R (2010): Regulation of adaptive immunity by the innate immune system. *Science* **327**: 291-295.

Iwashyna TJ, Ely EW, Smith DM & Langa KM (2010): Long-term cognitive impairment and functional disability among survivors of severe sepsis. *JAMA* **304**: 1787-1794.

Jackson V (1978): Studies on histone organization in the nucleosome using formaldehyde as a reversible cross-linking agent. *Cell* **15**: 945-954.

Jair KW, Bachman KE, Suzuki H, Ting AH, Rhee I, Yen RW, Baylin SB & Schuebel KE (2006): De novo CpG island methylation in human cancer cells. *Cancer Res* **66**: 682-692.

Janeway CA, Jr. (1989): Approaching the asymptote? Evolution and revolution in immunology. *Cold Spring Harb Symp Quant Biol* **54 Pt 1**: 1-13.

Janeway CA, Jr. (2001): How the immune system works to protect the host from infection: a personal view. *Proc Natl Acad Sci U S A* **98**: 7461-7468.

Janeway CA, Jr. & Medzhitov R (2002): Innate immune recognition. *Annu Rev Immunol* **20**: 197-216.

Janknecht R, Wells NJ & Hunter T (1998): TGF-beta-stimulated cooperation of smad proteins with the coactivators CBP/p300. *Genes Dev* **12**: 2114-2119.

Jeannin P, Jaillon S & Delneste Y (2008): Pattern recognition receptors in the immune response against dying cells. *Curr Opin Immunol* **20**: 530-537.

Jenuwein T & Allis CD (2001): Translating the histone code. *Science* **293**: 1074-1080.

Kaczmarek A, Vandenabeele P & Krysko DV (2013): Necroptosis: the release of damage-associated molecular patterns and its physiological relevance. *Immunity* **38**: 209-223.

Kawai T & Akira S (2010): The role of pattern-recognition receptors in innate immunity: update on Toll-like receptors. *Nat Immunol* **11**: 373-384.

Kawai T & Akira S (2011): Toll-like receptors and their crosstalk with other innate receptors in infection and immunity. *Immunity* **34**: 637-650.

Kelly NM, Young L & Cross AS (1991): Differential induction of tumor necrosis factor by bacteria expressing rough and smooth lipopolysaccharide phenotypes. *Infect Immun* **59**: 4491-4496.

Kent WJ, Sugnet CW, Furey TS, Roskin KM, Pringle TH, Zahler AM & Haussler D (2002): The human genome browser at UCSC. *Genome Res* **12**: 996-1006.

Kent WJ, Zweig AS, Barber G, Hinrichs AS & Karolchik D (2010): BigWig and BigBed: enabling browsing of large distributed datasets. *Bioinformatics* **26**: 2204-2207.

Kharchenko PV, Tolstorukov MY & Park PJ (2008): Design and analysis of ChIP-seq experiments for DNA-binding proteins. *Nat Biotechnol* **26**: 1351-1359.

Kishimoto T (2010): IL-6: from its discovery to clinical applications. *Int Immunol* **22**: 347-352.

Klose RJ & Bird AP (2006): Genomic DNA methylation: the mark and its mediators. *Trends Biochem Sci* **31**: 89-97.

Koike M, Kurosawa H & Amano Y (2005): A Round-bottom 96-well Polystyrene Plate Coated with 2-methacryloyloxyethyl Phosphorylcholine as an Effective Tool for Embryoid Body Formation. *Cytotechnology* **47**: 3-10.

Kooistra SM & Helin K (2012): Molecular mechanisms and potential functions of histone demethylases. *Nat Rev Mol Cell Biol* **13**: 297-311.

Kostura MJ, Tocci MJ, Limjuco G, Chin J, Cameron P, Hillman AG, Chartrain NA & Schmidt JA (1989): Identification of a monocyte specific pre-interleukin 1 beta convertase activity. *Proc Natl Acad Sci U S A* **86**: 5227-5231.

Kouzarides T (2007): Chromatin modifications and their function. *Cell* **128**: 693-705.

Kox M, de Kleijn S, Pompe JC, Ramakers BP, Netea MG, van der Hoeven JG, Hoedemaekers CW & Pickkers P (2011): Differential ex vivo and in vivo endotoxin tolerance kinetics following human endotoxemia. *Crit Care Med* **39**: 1866-1870.

Krueger F, Kreck B, Franke A & Andrews SR (2012): DNA methylome analysis using short bisulfite sequencing data. *Nat Methods* **9**: 145-151.

Krüger M (2006). Diplomarbeit: Interleukin-10-abhängige und -unabhängige Lipopolysaccharid-Desensibiliserung (Humboldt-Universität zu Berlin).

Krüger M (2009). Dissertation: Unterschiede zwischen LPS- und Lipid A-Desensibilisierung und die Rolle von Interleukin 10 (Humboldt-Universität zu Berlin).

Kuhns DB, Alvord WG & Gallin JI (1995): Increased circulating cytokines, cytokine antagonists, and E-selectin after intravenous administration of endotoxin in humans. *J Infect Dis* **171**: 145-152.

Kumari MV, Hiramatsu M & Ebadi M (1998): Free radical scavenging actions of metallothionein isoforms I and II. *Free Radic Res* **29**: 93-101.

Kumpf O & Schumann RR (2010): Genetic variation in innate immunity pathways and their potential contribution to the SIRS/CARS debate: evidence from human studies and animal models. *J Innate Immun* **2**: 381-394.

Kuo MH & Allis CD (1999): In vivo cross-linking and immunoprecipitation for studying dynamic Protein:DNA associations in a chromatin environment. *Methods* **19**: 425-433.

Kurisaki K, Kurisaki A, Valcourt U, Terentiev AA, Pardali K, Ten Dijke P, Heldin CH, Ericsson J & Moustakas A (2003): Nuclear factor YY1 inhibits transforming growth factor beta- and bone morphogenetic protein-induced cell differentiation. *Mol Cell Biol* **23**: 4494-4510.

Kuwata H, Matsumoto M, Atarashi K, Morishita H, Hirotani T, Koga R & Takeda K (2006): IkappaBNS inhibits induction of a subset of Toll-like receptor-dependent genes and limits inflammation. *Immunity* **24**: 41-51.

Kuwata H, Watanabe Y, Miyoshi H, Yamamoto M, Kaisho T, Takeda K & Akira S (2003): IL-10-inducible Bcl-3 negatively regulates LPS-induced TNF-alpha production in macrophages. *Blood* **102**: 4123-4129.

Landt SG, Marinov GK, Kundaje A, Kheradpour P, Pauli F, Batzoglou S, Bernstein BE, Bickel P, Brown JB, Cayting P *et al.* (2012): ChIP-seq guidelines and practices of the ENCODE and modENCODE consortia. *Genome Res* **22**: 1813-1831.

Langdon SP (2004). Introduction to Cancer Cell Cultivation. In Cancer Cell Culture: Methods and Protocols (Methods in Molecular Medicine) (Heidelberg: Springer Science & Business Media), pp. 3-30.

Lavin Y, Winter D, Blecher-Gonen R, David E, Keren-Shaul H, Merad M, Jung S & Amit I (2014): Tissue-resident macrophage enhancer landscapes are shaped by the local microenvironment. *Cell* **159**: 1312-1326.

Lawrence T, Gilroy DW, Colville-Nash PR & Willoughby DA (2001): Possible new role for NF-kappaB in the resolution of inflammation. *Nat Med* **7**: 1291-1297.

Lee TI, Johnstone SE & Young RA (2006): Chromatin immunoprecipitation and microarray-based analysis of protein location. *Nat Protoc* **1**: 729-748.

Leentjens J, Kox M, Koch RM, Preijers F, Joosten LA, van der Hoeven JG, Netea MG & Pickkers P (2012): Reversal of immunoparalysis in humans in vivo: a double-blind, placebo-controlled, randomized pilot study. *Am J Respir Crit Care Med* **186**: 838-845.

Lehner MD, Ittner J, Bundschuh DS, van Rooijen N, Wendel A & Hartung T (2001): Improved innate immunity of endotoxin-tolerant mice increases resistance to Salmonella enterica serovar typhimurium infection despite attenuated cytokine response. *Infect Immun* **69**: 463-471.

Lemaitre B, Nicolas E, Michaut L, Reichhart JM & Hoffmann JA (1996): The dorsoventral regulatory gene cassette spatzle/Toll/cactus controls the potent antifungal response in Drosophila adults. *Cell* **86**: 973-983.

Leon LR, White AA & Kluger MJ (1998): Role of IL-6 and TNF in thermoregulation and survival during sepsis in mice. *Am J Physiol* **275**: R269-277.

Li H & Durbin R (2009): Fast and accurate short read alignment with Burrows-Wheeler transform. *Bioinformatics* **25**: 1754-1760.

Li H, Handsaker B, Wysoker A, Fennell T, Ruan J, Homer N, Marth G, Abecasis G, Durbin R & Genome Project Data Processing S (2009): The Sequence Alignment/Map format and SAMtools. *Bioinformatics* **25**: 2078-2079.

Li LC & Dahiya R (2002): MethPrimer: designing primers for methylation PCRs. *Bioinformatics* **18**: 1427-1431.

Li MO, Sanjabi S & Flavell RA (2006a): Transforming growth factor-beta controls development, homeostasis, and tolerance of T cells by regulatory T cell-dependent and -independent mechanisms. *Immunity* **25**: 455-471.

Li MO, Wan YY, Sanjabi S, Robertson AK & Flavell RA (2006b): Transforming growth factor-beta regulation of immune responses. *Annu Rev Immunol* **24**: 99-146.

Li Y & Tollefsbol TO (2011): DNA methylation detection: bisulfite genomic sequencing analysis. *Methods Mol Biol* **791**: 11-21.

Lienhard M, Grimm C, Morkel M, Herwig R & Chavez L (2014): MEDIPS: genome-wide differential coverage analysis of sequencing data derived from DNA enrichment experiments. *Bioinformatics* **30**: 284-286.

Liew FY, Xu D, Brint EK & O'Neill LA (2005): Negative regulation of toll-like receptor-mediated immune responses. *Nat Rev Immunol* **5**: 446-458.

Liu C, Yu Y, Liu F, Wei X, Wrobel JA, Gunawardena HP, Zhou L, Jin J & Chen X (2014): A chromatin activity-based chemoproteomic approach reveals a transcriptional repressome for gene-specific silencing. *Nat Commun* **5**: 5733.

Liu ET, Pott S & Huss M (2010): Q&A: ChIP-seq technologies and the study of gene regulation. *BMC Biol* **8**: 56.

Lopez-Collazo E & Del Fresno C (2013): Pathophysiology of endotoxin tolerance: mechanisms and clinical consequences. *Crit Care* **17**: 242.

Luger K, Mader AW, Richmond RK, Sargent DF & Richmond TJ (1997): Crystal structure of the nucleosome core particle at 2.8 A resolution. *Nature* **389**: 251-260.

Majno G (1975). Galen - and into the Night. In The Healing Hand: Man and Wound in the Ancient World (Cambridge, Massachusetts: Harvard UP), pp. 395-424.

Majno G (1991): The ancient riddle of sigma eta psi iota sigma (sepsis). *J Infect Dis* **163**: 937-945.

Manjuck J, Saha DC, Astiz M, Eales LJ & Rackow EC (2000): Decreased response to recall antigens is associated with depressed costimulatory receptor expression in septic critically ill patients. *J Lab Clin Med* **135**: 153-160.

Marshall JC (2014): Why have clinical trials in sepsis failed? *Trends Mol Med* **20**: 195-203.

Martin GS (2012): Sepsis, severe sepsis and septic shock: changes in incidence, pathogens and outcomes. *Expert Rev Anti Infect Ther* **10**: 701-706.

Martin GS, Mannino DM & Moss M (2006): The effect of age on the development and outcome of adult sepsis. *Crit Care Med* **34**: 15-21.

Massague J (2012): TGFbeta signalling in context. *Nat Rev Mol Cell Biol* **13**: 616-630.

Mathison JC, Virca GD, Wolfson E, Tobias PS, Glaser K & Ulevitch RJ (1990): Adaptation to bacterial lipopolysaccharide controls lipopolysaccharide-induced tumor necrosis factor production in rabbit macrophages. *J Clin Invest* **85**: 1108-1118.

McCall CE, Grosso-Wilmoth LM, LaRue K, Guzman RN & Cousart SL (1993): Tolerance to endotoxin-induced expression of the interleukin-1 beta gene in blood neutrophils of humans with the sepsis syndrome. *J Clin Invest* **91**: 853-861.

McCall CE & Yoza BK (2007): Gene silencing in severe systemic inflammation. *Am J Respir Crit Care Med* **175**: 763-767.

McIntyre KW, Stepan GJ, Kolinsky KD, Benjamin WR, Plocinski JM, Kaffka KL, Campen CA, Chizzonite RA & Kilian PL (1991): Inhibition of interleukin 1 (IL-1) binding and bioactivity in vitro and modulation of acute inflammation in vivo by IL-1 receptor antagonist and anti-IL-1 receptor monoclonal antibody. *J Exp Med* **173**: 931-939.

McLean CY, Bristor D, Hiller M, Clarke SL, Schaar BT, Lowe CB, Wenger AM & Bejerano G (2010): GREAT improves functional interpretation of cis-regulatory regions. *Nat Biotechnol* **28**: 495-501.

Medvedev AE, Lentschat A, Wahl LM, Golenbock DT & Vogel SN (2002): Dysregulation of LPS-induced Toll-like receptor 4-MyD88 complex formation and IL-1 receptor-associated kinase 1 activation in endotoxin-tolerant cells. *J Immunol* **169**: 5209-5216.

Medzhitov R (2001): Toll-like receptors and innate immunity. *Nat Rev Immunol* **1**: 135-145.

Medzhitov R (2008): Origin and physiological roles of inflammation. *Nature* **454**: 428-435.

Medzhitov R & Horng T (2009): Transcriptional control of the inflammatory response. *Nat Rev Immunol* **9**: 692-703.

Medzhitov R & Janeway C, Jr. (2000): Innate immunity. *N Engl J Med* **343**: 338-344.

Medzhitov R & Janeway CA, Jr. (2002): Decoding the patterns of self and nonself by the innate immune system. *Science* **296**: 298-300.

Medzhitov R, Preston-Hurlburt P & Janeway CA, Jr. (1997): A human homologue of the Drosophila Toll protein signals activation of adaptive immunity. *Nature* **388**: 394-397.

Medzhitov R, Schneider DS & Soares MP (2012): Disease tolerance as a defense strategy. *Science* **335**: 936-941.

Michalek SM, Moore RN, McGhee JR, Rosenstreich DL & Mergenhagen SE (1980): The primary role of lymphoreticular cells in the mediation of host responses to bacterial endotoxim. *J Infect Dis* **141**: 55-63.

Monneret G, Venet F, Pachot A & Lepape A (2008): Monitoring immune dysfunctions in the septic patient: a new skin for the old ceremony. *Mol Med* **14**: 64-78.

Mosser DM & Edwards JP (2008): Exploring the full spectrum of macrophage activation. *Nat Rev Immunol* **8**: 958-969.

Muller U, Steinhoff U, Reis LF, Hemmi S, Pavlovic J, Zinkernagel RM & Aguet M (1994): Functional role of type I and type II interferons in antiviral defense. *Science* **264**: 1918-1921.

Munoz C, Carlet J, Fitting C, Misset B, Bleriot JP & Cavaillon JM (1991): Dysregulation of in vitro cytokine production by monocytes during sepsis. *J Clin Invest* **88**: 1747-1754.

Murad S (2014): Toll-like receptor 4 in inflammation and angiogenesis: a double-edged sword. *Front Immunol* **5**: 313.

Muralidharan S & Mandrekar P (2013): Cellular stress response and innate immune signaling: integrating pathways in host defense and inflammation. *J Leukoc Biol* **94**: 1167-1184.

Murphy K, Travers P, Walport M & Janeway CA (2012a). Basic Concepts in Immunology. In Janeway's Immunobiology (New York, NY u.a.: Garland), pp. 1-36.

Murphy K, Travers P, Walport M & Janeway CA (2012b). The Generation of Lymphocyte Antigen Receptors. In Janeway's Immunobiology (New York, NY u.a.: Garland), pp. 157-200.

Nahid MA, Satoh M & Chan EK (2011): MicroRNA in TLR signaling and endotoxin tolerance. *Cell Mol Immunol* **8**: 388-403.

Nakae H, Endo S, Inada K, Takakuwa T & Kasai T (1996): Changes in adhesion molecule levels in sepsis. *Res Commun Mol Pathol Pharmacol* **91**: 329-338.

Nathan C (2002): Points of control in inflammation. *Nature* **420**: 846-852.

Nathan D, Ingvarsdottir K, Sterner DE, Bylebyl GR, Dokmanovic M, Dorsey JA, Whelan KA, Krsmanovic M, Lane WS, Meluh PB *et al.* (2006): Histone sumoylation is a negative regulator in Saccharomyces cerevisiae and shows dynamic interplay with positive-acting histone modifications. *Genes Dev* **20**: 966-976.

Neagos J, Standiford TJ, Newstead MW, Zeng X, Huang SK & Ballinger MN (2015): Epigenetic Regulation of Tolerance to TLR Ligands in Alveolar Epithelial Cells. *Am J Respir Cell Mol Biol*.

Netea MG, Quintin J & van der Meer JW (2011): Trained immunity: a memory for innate host defense. *Cell Host Microbe* **9**: 355-361.

Nikaido H (1962): Studies on the biosynthesis of cell wall polysaccharide in mutant strains of Salmonella. II. *Proc Natl Acad Sci U S A* **48**: 1542-1548.

Nile CJ, Read RC, Akil M, Duff GW & Wilson AG (2008): Methylation status of a single CpG site in the IL6 promoter is related to IL6 messenger RNA levels and rheumatoid arthritis. *Arthritis Rheum* **58**: 2686-2693.

Nomiyama H, Osada N & Yoshie O (2013): Systematic classification of vertebrate chemokines based on conserved synteny and evolutionary history. *Genes Cells* **18**: 1-16.

Northrup DL & Zhao K (2011): Application of ChIP-Seq and related techniques to the study of immune function. *Immunity* **34**: 830-842.

O'Keefe GM, Nguyen VT & Benveniste EN (1999): Class II transactivator and class II MHC gene expression in microglia: modulation by the cytokines TGF-beta, IL-4, IL-13 and IL-10. *Eur J Immunol* **29**: 1275-1285.

O'Neill LA (2008): The interleukin-1 receptor/Toll-like receptor superfamily: 10 years of progress. *Immunol Rev* **226**: 10-18.

Okusawa S, Gelfand JA, Ikejima T, Connolly RJ & Dinarello CA (1988): Interleukin 1 induces a shock-like state in rabbits. Synergism with tumor necrosis factor and the effect of cyclooxygenase inhibition. *J Clin Invest* **81**: 1162-1172.

Oldenburg M, Kruger A, Ferstl R, Kaufmann A, Nees G, Sigmund A, Bathke B, Lauterbach H, Suter M, Dreher S *et al.* (2012): TLR13 recognizes bacterial 23S rRNA devoid of erythromycin resistance-forming modification. *Science* **337**: 1111-1115.

Osborn MJ (1963): Studies on the Gram-Negative Cell Wall. I. Evidence for the Role of 2-Keto- 3-Deoxyoctonate in the Lipopolysaccharide of Salmonella Typhimurium. *Proc Natl Acad Sci U S A* **50**: 499-506.

Otto GP, Sossdorf M, Claus RA, Rodel J, Menge K, Reinhart K, Bauer M & Riedemann NC (2011): The late phase of sepsis is characterized by an increased microbiological burden and death rate. *Crit Care* **15**: R183.

Palanisamy V, Jakymiw A, Van Tubergen EA, D'Silva NJ & Kirkwood KL (2012): Control of cytokine mRNA expression by RNA-binding proteins and microRNAs. *J Dent Res* **91**: 651-658.

Pan H, Ding E, Hu M, Lagoo AS, Datto MB & Lagoo-Deenadayalan SA (2010): SMAD4 is required for development of maximal endotoxin tolerance. *J Immunol* **184**: 5502-5509.

Parameswaran N & Patial S (2010): Tumor necrosis factor-alpha signaling in macrophages. *Crit Rev Eukaryot Gene Expr* **20**: 87-103.

Park SH, Park-Min KH, Chen J, Hu X & Ivashkiv LB (2011): Tumor necrosis factor induces GSK3 kinase-mediated cross-tolerance to endotoxin in macrophages. *Nat Immunol* **12**: 607-615.

Parkin J & Cohen B (2001): An overview of the immune system. *Lancet* **357**: 1777-1789.

Pena OM, Pistolic J, Raj D, Fjell CD & Hancock RE (2011): Endotoxin tolerance represents a distinctive state of alternative polarization (M2) in human mononuclear cells. *J Immunol* **186**: 7243-7254.

Perl TM, Dvorak L, Hwang T & Wenzel RP (1995): Long-term survival and function after suspected gram-negative sepsis. *JAMA* **274**: 338-345.

Peterson CL & Laniel MA (2004): Histones and histone modifications. *Curr Biol* **14**: R546-551.

Pfeiffer R (1892): Untersuchungen über das Choleragift. *Zeitschrift für Hygiene und Infektionskrankheiten* **11**: 393-412.

Poltorak A, He X, Smirnova I, Liu MY, Van Huffel C, Du X, Birdwell D, Alejos E, Silva M, Galanos C *et al.* (1998a): Defective LPS signaling in C3H/HeJ and C57BL/10ScCr mice: mutations in Tlr4 gene. *Science* **282**: 2085-2088.

Poltorak A, Smirnova I, He X, Liu MY, Van Huffel C, McNally O, Birdwell D, Alejos E, Silva M, Du X *et al.* (1998b): Genetic and physical mapping of the Lps locus: identification of the toll-4 receptor as a candidate gene in the critical region. *Blood Cells Mol Dis* **24**: 340-355.

Quartin AA, Schein RM, Kett DH & Peduzzi PN (1997): Magnitude and duration of the effect of sepsis on survival. Department of Veterans Affairs Systemic Sepsis Cooperative Studies Group. *JAMA* **277**: 1058-1063.

Quinlan AR & Hall IM (2010): BEDTools: a flexible suite of utilities for comparing genomic features. *Bioinformatics* **26**: 841-842.

Rada-Iglesias A, Bajpai R, Swigut T, Brugmann SA, Flynn RA & Wysocka J (2011): A unique chromatin signature uncovers early developmental enhancers in humans. *Nature* **470**: 279-283.

Raetz CR & Whitfield C (2002): Lipopolysaccharide endotoxins. *Annu Rev Biochem* **71**: 635-700.

Ramirez-Carrozzi VR, Nazarian AA, Li CC, Gore SL, Sridharan R, Imbalzano AN & Smale ST (2006): Selective and antagonistic functions of SWI/SNF and Mi-2beta nucleosome remodeling complexes during an inflammatory response. *Genes Dev* **20**: 282-296.

Ramnath RD, Weing S, He M, Sun J, Zhang H, Singh BM & Bhatia M (2006): Inflammatory mediators in sepsis: Cytokines, chemokines, adhesion molecules and gases. *J Organ Dysfunct* **2**: 80-92.

Randow F, Syrbe U, Meisel C, Krausch D, Zuckermann H, Platzer C & Volk HD (1995): Mechanism of endotoxin desensitization: involvement of interleukin 10 and transforming growth factor beta. *J Exp Med* **181**: 1887-1892.

Rather LJ (1971): Disturbance of function (functio laesa): the legendary fifth cardinal sign of inflammation, added by Galen to the four cardinal signs of Celsus. *Bull N Y Acad Med* **47**: 303-322.

Rayhane N, Fitting C, Lortholary O, Dromer F & Cavaillon JM (2000): Administration of endotoxin associated with lipopolysaccharide tolerance protects mice against fungal infection. *Infect Immun* **68**: 3748-3753.

RCoreTeam (2014): R: A language and environment for statistical computing. R Foundation for Statistical Computing, Vienna, Austria. URL http://www.R-project.org/.

Rittirsch D, Flierl MA & Ward PA (2008): Harmful molecular mechanisms in sepsis. *Nat Rev Immunol* **8**: 776-787.

Robinson JT, Thorvaldsdottir H, Winckler W, Guttman M, Lander ES, Getz G & Mesirov JP (2011): Integrative genomics viewer. *Nat Biotechnol* **29**: 24-26.

Rock KL, Latz E, Ontiveros F & Kono H (2010): The sterile inflammatory response. *Annu Rev Immunol* **28**: 321-342.

Rodriguez BA, Frankhouser D, Murphy M, Trimarchi M, Tam HH, Curfman J, Huang R, Chan MW, Lai HC, Parikh D *et al.* (2012): Methods for high-throughput MethylCap-Seq data analysis. *BMC Genomics* **13 Suppl 6**: S14.

Roman J, Fernandez F, Velasco F, Rojas R, Roldan MR & Torres A (1993): Serum TNF levels in neonatal sepsis and septic shock. *Acta Paediatr* **82**: 352-354.

Rose NR & Klose RJ (2014): Understanding the relationship between DNA methylation and histone lysine methylation. *Biochim Biophys Acta* **1839**: 1362-1372.

Rosin DL & Okusa MD (2011): Dangers within: DAMP responses to damage and cell death in kidney disease. *J Am Soc Nephrol* **22**: 416-425.

Ruttkay-Nedecky B, Nejdl L, Gumulec J, Zitka O, Masarik M, Eckschlager T, Stiborova M, Adam V & Kizek R (2013): The role of metallothionein in oxidative stress. *Int J Mol Sci* **14**: 6044-6066.

Saeed S, Quintin J, Kerstens HH, Rao NA, Aghajanirefah A, Matarese F, Cheng SC, Ratter J, Berentsen K, van der Ent MA *et al.* (2014): Epigenetic programming of monocyte-to-macrophage differentiation and trained innate immunity. *Science* **345**: 1251086.

Santos-Rosa H, Schneider R, Bannister AJ, Sherriff J, Bernstein BE, Emre NC, Schreiber SL, Mellor J & Kouzarides T (2002): Active genes are tri-methylated at K4 of histone H3. *Nature* **419**: 407-411.

Sato F, Tsuchiya S, Meltzer SJ & Shimizu K (2011): MicroRNAs and epigenetics. *FEBS J* **278**: 1598-1609.

Schaafsma W, Zhang X, van Zomeren KC, Jacobs S, Georgieva PB, Wolf SA, Kettenmann H, Janova H, Saiepour N, Hanisch UK *et al.* (2015): Long-lasting pro-inflammatory suppression of microglia by LPS-preconditioning is mediated by RelB-dependent epigenetic silencing. *Brain Behav Immun*.

Schefold JC, Hasper D, Volk HD & Reinke P (2008): Sepsis: time has come to focus on the later stages. *Med Hypotheses* **71**: 203-208.

Schmitz S (2011a). Medien. In Der Experimentator: Zellkultur (Heidelberg: Spectrum), pp. 103-114.

Schmitz S (2011b). Zellkultursupplemente und andere Zusätze. In Der Experimentator: Zellkultur (Heidelberg: Spectrum), pp. 115-128.

Schneider R, Bannister AJ, Myers FA, Thorne AW, Crane-Robinson C & Kouzarides T (2004): Histone H3 lysine 4 methylation patterns in higher eukaryotic genes. *Nat Cell Biol* **6**: 73-77.

Schottelius AJ, Zugel U, Docke WD, Zollner TM, Rose L, Mengel A, Buchmann B, Becker A, Grutz G, Naundorf S *et al.* (2010): The role of mitogen-activated protein kinase-activated protein kinase 2 in the p38/TNF-alpha pathway of systemic and cutaneous inflammation. *J Invest Dermatol* **130**: 481-491.

Schouten M, Wiersinga WJ, Levi M & van der Poll T (2008): Inflammation, endothelium, and coagulation in sepsis. *J Leukoc Biol* **83**: 536-545.

Schroder K & Tschopp J (2010): The inflammasomes. *Cell* **140**: 821-832.

Schulte W, Bernhagen J & Bucala R (2013): Cytokines in sepsis: potent immunoregulators and potential therapeutic targets--an updated view. *Mediators Inflamm* **2013**: 165974.

Schumann RR, Leong SR, Flaggs GW, Gray PW, Wright SD, Mathison JC, Tobias PS & Ulevitch RJ (1990): Structure and function of lipopolysaccharide binding protein. *Science* **249**: 1429-1431.

Seeley JJ & Ghosh S (2014): Tolerization of Inflammatory Gene Expression. *Cold Spring Harb Symp Quant Biol*.

Senner CE (2011): The role of DNA methylation in mammalian development. *Reprod Biomed Online* **22**: 529-535.

Serhan CN (2007): Resolution phase of inflammation: novel endogenous anti-inflammatory and proresolving lipid mediators and pathways. *Annu Rev Immunol* **25**: 101-137.

Serhan CN & Savill J (2005): Resolution of inflammation: the beginning programs the end. *Nat Immunol* **6**: 1191-1197.

Serre D, Lee BH & Ting AH (2010): MBD-isolated Genome Sequencing provides a high-throughput and comprehensive survey of DNA methylation in the human genome. *Nucleic Acids Res* **38**: 391-399.

Shakespear MR, Halili MA, Irvine KM, Fairlie DP & Sweet MJ (2011): Histone deacetylases as regulators of inflammation and immunity. *Trends Immunol* **32**: 335-343.

Shalova IN, Lim JY, Chittezhath M, Zinkernagel AS, Beasley F, Hernandez-Jimenez E, Toledano V, Cubillos-Zapata C, Rapisarda A, Chen J *et al.* (2015): Human monocytes undergo functional re-programming during sepsis mediated by hypoxia-inducible factor-1alpha. *Immunity* **42**: 484-498.

Sheedy FJ, Palsson-McDermott E, Hennessy EJ, Martin C, O'Leary JJ, Ruan Q, Johnson DS, Chen Y & O'Neill LA (2010): Negative regulation of TLR4 via targeting of the proinflammatory tumor suppressor PDCD4 by the microRNA miR-21. *Nat Immunol* **11**: 141-147.

Shen L & Sinai M (2013): GeneOverlap: Test and visualize gene overlaps. R package version 1.2.0. http://shenlab-sinai.github.io/shenlab-sinai/.

Shi L, Song L, Maurer K, Sharp J, Zhang Z & Sullivan KE (2015): Endotoxin tolerance in monocytes can be mitigated by alpha2-interferon. *J Leukoc Biol*.

Shi Y, Sawada J, Sui G, Affar el B, Whetstine JR, Lan F, Ogawa H, Luke MP, Nakatani Y & Shi Y (2003): Coordinated histone modifications mediated by a CtBP co-repressor complex. *Nature* **422**: 735-738.

Shiio Y & Eisenman RN (2003): Histone sumoylation is associated with transcriptional repression. *Proc Natl Acad Sci U S A* **100**: 13225-13230.

Shimaoka M & Park EJ (2008): Advances in understanding sepsis. *Eur J Anaesthesiol Suppl* **42**: 146-153.

Shlyueva D, Stampfel G & Stark A (2014): Transcriptional enhancers: from properties to genome-wide predictions. *Nat Rev Genet* **15**: 272-286.

Smale ST (2010a): Selective transcription in response to an inflammatory stimulus. *Cell* **140**: 833-844.

Smale ST (2010b): Seq-ing LPS-induced enhancers. *Immunity* **32**: 296-298.

Smallie T, Ricchetti G, Horwood NJ, Feldmann M, Clark AR & Williams LM (2010): IL-10 inhibits transcription elongation of the human TNF gene in primary macrophages. *J Exp Med* **207**: 2081-2088.

Smallwood A, Esteve PO, Pradhan S & Carey M (2007): Functional cooperation between HP1 and DNMT1 mediates gene silencing. *Genes Dev* **21**: 1169-1178.

Solomon MJ, Larsen PL & Varshavsky A (1988): Mapping protein-DNA interactions in vivo with formaldehyde: evidence that histone H4 is retained on a highly transcribed gene. *Cell* **53**: 937-947.

Solomon MJ & Varshavsky A (1985): Formaldehyde-mediated DNA-protein crosslinking: a probe for in vivo chromatin structures. *Proc Natl Acad Sci U S A* **82**: 6470-6474.

Sporn MB & Roberts AB (1989): Transforming growth factor-beta. Multiple actions and potential clinical applications. *JAMA* **262**: 938-941.

Sriskandan S & Altmann DM (2008): The immunology of sepsis. *J Pathol* **214**: 211-223.

Stender JD & Glass CK (2013): Epigenomic control of the innate immune response. *Curr Opin Pharmacol* **13**: 582-587.

Stender JD, Pascual G, Liu W, Kaikkonen MU, Do K, Spann NJ, Boutros M, Perrimon N, Rosenfeld MG & Glass CK (2012): Control of proinflammatory gene programs by regulated trimethylation and demethylation of histone H4K20. *Mol Cell* **48**: 28-38.

Strahl BD & Allis CD (2000): The language of covalent histone modifications. *Nature* **403**: 41-45.

Striz I, Brabcova E, Kolesar L & Sekerkova A (2014): Cytokine networking of innate immunity cells: a potential target of therapy. *Clin Sci (Lond)* **126**: 593-612.

Taganov KD, Boldin MP, Chang KJ & Baltimore D (2006): NF-kappaB-dependent induction of microRNA miR-146, an inhibitor targeted to signaling proteins of innate immune responses. *Proc Natl Acad Sci U S A* **103**: 12481-12486.

Takami M, Terry V & Petruzzelli L (2002): Signaling pathways involved in IL-8-dependent activation of adhesion through Mac-1. *J Immunol* **168**: 4559-4566.

Takeuch O & Akira S (2011): Epigenetic control of macrophage polarization. *Eur J Immunol* **41**: 2490-2493.

Takeuchi O & Akira S (2010): Pattern recognition receptors and inflammation. *Cell* **140**: 805-820.

Tang BM, Huang SJ & McLean AS (2010): Genome-wide transcription profiling of human sepsis: a systematic review. *Crit Care* **14**: R237.

Thangavel J, Samanta S, Rajasingh S, Barani B, Xuan YT, Dawn B & Rajasingh J (2015): Epigenetic modifiers reduce inflammation and modulate macrophage phenotype during endotoxemia-induced acute lung injury. *J Cell Sci*.

Thomas L (1972): Germs. *N Engl J Med* **287**: 553-555.

Thorvaldsdottir H, Robinson JT & Mesirov JP (2013): Integrative Genomics Viewer (IGV): high-performance genomics data visualization and exploration. *Brief Bioinform* **14**: 178-192.

Tobias PS, Soldau K & Ulevitch RJ (1986): Isolation of a lipopolysaccharide-binding acute phase reactant from rabbit serum. *J Exp Med* **164**: 777-793.

Trapnell C, Pachter L & Salzberg SL (2009): TopHat: discovering splice junctions with RNA-Seq. *Bioinformatics* **25**: 1105-1111.

Trapnell C, Roberts A, Goff L, Pertea G, Kim D, Kelley DR, Pimentel H, Salzberg SL, Rinn JL & Pachter L (2012): Differential gene and transcript expression analysis of RNA-seq experiments with TopHat and Cufflinks. *Nat Protoc* **7**: 562-578.

Trapnell C, Williams BA, Pertea G, Mortazavi A, Kwan G, van Baren MJ, Salzberg SL, Wold BJ & Pachter L (2010): Transcript assembly and quantification by RNA-Seq reveals unannotated transcripts and isoform switching during cell differentiation. *Nat Biotechnol* **28**: 511-515.

Turner MD, Nedjai B, Hurst T & Pennington DJ (2014): Cytokines and chemokines: At the crossroads of cell signalling and inflammatory disease. *Biochim Biophys Acta* **1843**: 2563-2582.

Ulevitch RJ & Tobias PS (1995): Receptor-dependent mechanisms of cell stimulation by bacterial endotoxin. *Annu Rev Immunol* **13**: 437-457.

Ulmer AJ, Scholz W, Ernst M, Brandt E & Flad HD (1984): Isolation and subfractionation of human peripheral blood mononuclear cells (PBMC) by density gradient centrifugation on Percoll. *Immunobiology* **166**: 238-250.

van der Poll T, Jansen PM, Montegut WJ, Braxton CC, Calvano SE, Stackpole SA, Smith SR, Swanson SW, Hack CE, Lowry SF *et al.* (1997): Effects of IL-10 on systemic inflammatory responses during sublethal primate endotoxemia. *J Immunol* **158**: 1971-1975.

Vincent JL, Opal SM, Marshall JC & Tracey KJ (2013): Sepsis definitions: time for change. *Lancet* **381**: 774-775.

Virca GD, Kim SY, Glaser KB & Ulevitch RJ (1989): Lipopolysaccharide induces hyporesponsiveness to its own action in RAW 264.7 cells. *J Biol Chem* **264**: 21951-21956.

Voigt P, Tee WW & Reinberg D (2013): A double take on bivalent promoters. *Genes Dev* **27**: 1318-1338.

Volk HD, Reinke P, Falck P, Staffa G, Briedigkeit H & R vB (1989). Diagnostic-value of an immune monitoring program for the clinical management of immunosuppressed patients with septic complications. In Clinical Transplantation (Oxford u.: Wiley-Blackwell), pp. 246-252.

Volk HD, Reinke P, Krausch D, Zuckermann H, Asadullah K, Muller JM, Docke WD & Kox WJ (1996): Monocyte deactivation--rationale for a new therapeutic strategy in sepsis. *Intensive Care Med* **22 Suppl 4**: S474-481.

Volk HD, Thieme M, Heym S, Docke WD, Ruppe U, Tausch W, Manger D, Zuckermann S, Golosubow A, Nieter B *et al.* (1991): Alterations in function and phenotype of monocytes from patients with septic disease--predictive value and new therapeutic strategies. *Behring Inst Mitt*: 208-215.

Wakabayashi Y, Tamiya T, Takada I, Fukaya T, Sugiyama Y, Inoue N, Kimura A, Morita R, Kashiwagi I, Takimoto T *et al.* (2011): Histone 3 lysine 9 (H3K9) methyltransferase recruitment to the interleukin-2 (IL-2) promoter is a mechanism of suppression of IL-2 transcription by the transforming growth factor-beta-Smad pathway. *J Biol Chem* **286**: 35456-35465.

Wang X, Zheng G & Dong D (2015): Coordinated action of histone modification and microRNA regulations in human genome. *Gene*.

Wang Z, Zang C, Rosenfeld JA, Schones DE, Barski A, Cuddapah S, Cui K, Roh TY, Peng W, Zhang MQ *et al.* (2008): Combinatorial patterns of histone acetylations and methylations in the human genome. *Nat Genet* **40**: 897-903.

Wang ZE, Reiner SL, Zheng S, Dalton DK & Locksley RM (1994): CD4+ effector cells default to the Th2 pathway in interferon gamma-deficient mice infected with Leishmania major. *J Exp Med* **179**: 1367-1371.

Warnes GR, Bolker B, Bonebakker L, Gentleman R, Liaw WHA, Lumley T, Maechler M, Magnusson A, Moeller S, Schwartz M *et al.* (2015): gplots: various R programming tools for plotting data. R package version 2.17.0. http://CRAN.R-project.org/package=gplots.

Weber A, Wasiliew P & Kracht M (2010): Interleukin-1 (IL-1) pathway. *Sci Signal* **3**: cm1.

Weinmann AS & Farnham PJ (2002): Identification of unknown target genes of human transcription factors using chromatin immunoprecipitation. *Methods* **26**: 37-47.

Weiterer S, Uhle F, Lichtenstern C, Siegler BH, Bhuju S, Jarek M, Bartkuhn M & Weigand MA (2015): Sepsis induces specific changes in histone modification patterns in human monocytes. *PLoS One* **10**: e0121748.

Werner F, Jain MK, Feinberg MW, Sibinga NE, Pellacani A, Wiesel P, Chin MT, Topper JN, Perrella MA & Lee ME (2000): Transforming growth factor-beta 1 inhibition of macrophage activation is mediated via Smad3. *J Biol Chem* **275**: 36653-36658.

Wheeler DS, Lahni PM, Denenberg AG, Poynter SE, Wong HR, Cook JA & Zingarelli B (2008): Induction of endotoxin tolerance enhances bacterial clearance and survival in murine polymicrobial sepsis. *Shock* **30**: 267-273.

Witsell AL & Schook LB (1992): Tumor necrosis factor alpha is an autocrine growth regulator during macrophage differentiation. *Proc Natl Acad Sci U S A* **89**: 4754-4758.

Wotton D, Knoepfler PS, Laherty CD, Eisenman RN & Massague J (2001): The Smad transcriptional corepressor TGIF recruits mSin3. *Cell Growth Differ* **12**: 457-463.

Wotton D, Lo RS, Lee S & Massague J (1999a): A Smad transcriptional corepressor. *Cell* **97**: 29-39.

Wotton D, Lo RS, Swaby LA & Massague J (1999b): Multiple modes of repression by the Smad transcriptional corepressor TGIF. *J Biol Chem* **274**: 37105-37110.

Wright SD, Ramos RA, Tobias PS, Ulevitch RJ & Mathison JC (1990): CD14, a receptor for complexes of lipopolysaccharide (LPS) and LPS binding protein. *Science* **249**: 1431-1433.

Xu S, Grullon S, Ge K & Peng W (2014): Spatial clustering for identification of ChIP-enriched regions (SICER) to map regions of histone methylation patterns in embryonic stem cells. *Methods Mol Biol* **1150**: 97-111.

Xue J, Schmidt SV, Sander J, Draffehn A, Krebs W, Quester I, De Nardo D, Gohel TD, Emde M, Schmidleithner L *et al.* (2014): Transcriptome-based network analysis reveals a spectrum model of human macrophage activation. *Immunity* **40**: 274-288.

Yan Q, Carmody RJ, Qu Z, Ruan Q, Jager J, Mullican SE, Lazar MA & Chen YH (2012): Nuclear factor-kappaB binding motifs specify Toll-like receptor-induced gene repression through an inducible repressosome. *Proc Natl Acad Sci U S A* **109**: 14140-14145.

Young HA & Hardy KJ (1995): Role of interferon-gamma in immune cell regulation. *J Leukoc Biol* **58**: 373-381.

Yoza BK, Hu JY, Cousart SL & McCall CE (2000): Endotoxin inducible transcription is repressed in endotoxin tolerant cells. *Shock* **13**: 236-243.

Yu G, Wang LG & He QY (2015): ChIPseeker: an R/Bioconductor package for ChIP peak annotation, comparison and visualization. *Bioinformatics*.

Zang C, Schones DE, Zeng C, Cui K, Zhao K & Peng W (2009): A clustering approach for identification of enriched domains from histone modification ChIP-Seq data. *Bioinformatics* **25**: 1952-1958.

Zanoni I & Granucci F (2013): Role of CD14 in host protection against infections and in metabolism regulation. *Front Cell Infect Microbiol* **3**: 32.

Zanoni I, Ostuni R, Marek LR, Barresi S, Barbalat R, Barton GM, Granucci F & Kagan JC (2011): CD14 controls the LPS-induced endocytosis of Toll-like receptor 4. *Cell* **147**: 868-880.

Ziegler-Heitbrock HW, Wedel A, Schraut W, Strobel M, Wendelgass P, Sternsdorf T, Bauerle PA, Haas JG & Riethmuller G (1994): Tolerance to lipopolysaccharide involves mobilization of nuclear factor kappa B with predominance of p50 homodimers. *J Biol Chem* **269**: 17001-17004.

7. Contributions of Third Parties to the Present Work

PD Dr. Gerald Grütz (Institut für Medizinische Immunologie, Charité Berlin, Germany) has supervised the present work, contributed conceptionally and assisted in experimental design. Prof. Dr. Hans-Dieter Volk (Institut für Medizinische Immunologie, Charité Berlin, Germany) supported the project and contributed concepts to the present work.

Dr. Daniel Ibrahim (MPI für Molekulare Genetik, Germany) assisted in establishment of ChIP assays and helped with the bioinformatical alignment of ChIP-Seq data.

Carolin Walter (Institut für Medizinische Informatik, Westfälische Wilhelms-Universität (WWU) Münster, Germany) and Josephine Fischer (Institut für Molekulare Tumorbiologie, Westfälische Wilhelms-Universität (WWU) Münster, Germany) contributed concepts for interpretation of ChIP-Seq data. Carolin Walter performed downstream analyses of aligned ChIP-Seq data (peak calling and filtering of peaks, gene annotation, TFBS discovery by HOMER).

Peter Hansen (Computational Biology Group, Charité, Germany) and Dr. Jochen Hecht (now Centre for Genomic Regulation, Barcelona, Spain) provided general help in bioinformatical analyses and interpretation of data. Peter Hansen assisted with programming and carried out the quality control, adapter trimming and alignment of BS-Seq data.

Dr. Karsten Jürchott (BCRT, Charité Berlin, Germany) provided the pipeline for evaluation of MethylCap-Seq data and assisted in data analysis.

Dr. Stephan Schlickeiser (Institut für Medizinische Immunologie, Charité Berlin, Germany) assisted in R analysis and helped with the generation of heat maps.

High-throughput sequencing of DNA (ChIP-Seq, MethylCap-Seq and BS-Seq) was carried out at the core facility of the Berlin-Brandenburg Center for Regenerative Therapies (BCRT, Charité Berlin, Germany) under the guidance of Dr. Jochen Hecht (until 2014) and Ulrike Krüger, respectively.

High-throughput sequencing of mRNA was carried out at the genomics core facility of the Center of Excellence for Fluorescent Bioanalytics (KFB, University of Regensburg, Germany) under the guidance of Dr. Thomas Stempfl.

Curriculum Vitae

Der Lebenslauf ist aus Gründen des Datenschutzes nicht enthalten.

Danksagung

Die Arbeit wurde durch das DFG Graduiertenkolleg *„Genetic and Immunologic Determinants of Pathogen-Host-Interactions“* (GRK1121) im Rahmen der Graduiertenschule des Zentrums für Infektionsbiologie und Immunität (ZIBI) unterstützt und angefertigt.

Ich möchte mich zunächst bei Herrn Prof. Dr. Hans-Dieter Volk bedanken, dass er mir die Möglichkeit eröffnet hat, meine Doktorarbeit bei Ihm im Institut für Medizinische Immunologie (Charité Berlin) innerhalb des Graduiertenkollegs zu erarbeiten und für seine Betreuung als Doktorvater. Ebenso gilt ein besonderer Dank Herrn PD Dr. Gerald Grütz für seine direkte Betreuung und für die absolute Freiheit, die er mir bei der Erarbeitung meiner Doktorarbeit gewährt hat. Ich habe in dieser Zeit enorm viel gelernt und wertvolle Erfahrungen gesammelt.
Mein Dank geht außerdem an die *ZIBI Graduate School*, welche neben der finanziellen insbesondere eine moralische Unterstützung während der Doktorarbeit war. Hier möchte ich mich besonders bei Juliane Kofer, Susanne Pocai und Andreas Schmidt für die tolle Zeit bedanken.
Ich möchte diese Seite auch nutzen, um mich bei Herrn Prof. Dr. Alf Hamann und Herrn Prof. Dr. Robert Jack zu bedanken, welche sich als weitere Gutachter bereit erklärt haben.

Ganz besonders möchte ich mich bei meinen lieben Arbeitskollegen für ihre Unterstützung – in wissenschaftlicher und privater Hinsicht – und für eine tolle gemeinsame Zeit bedanken: Andreas, Anja, Christina, Christine, Claudia, David, Ivo, Julia, Katarina, Katrin, Kim, Levent, Simone, Steffi, Stephan und Ulrike. Insbesondere bedanke ich mich bei der AG Sawitzki, die mich als „assoziiertes“ Mitglied schnell in ihre Mitte aufgenommen hat. Eure warme Atmosphäre ist bezeichnend für Euch! Hier, möchte ich mich auch herzlich bei Prof. Dr. Birgit Sawitzki für Ihre Kritik und Anregungen bedanken.
Ein weiterer Dank geht an das gesamte Institut für Medizinische Immunologie für die freundschaftliche und hilfsbereite Atmosphäre, Bereitstellung von Materialien und Beratung. Zudem möchte ich mich bei Katarina, Laura und Lisa für die gemeinsame Zeit während der Doktorarbeit und die tollen Janeway-Stunden bedanken. Nun wissen wir, dass wir nichts wissen!

In gleicher Weise gilt ein besonderer Dank meinen vielen Helfern, ohne deren Unterstützung diese Arbeit nicht möglich gewesen wäre!
Ich bedanke mich insbesondere bei Dr. Daniel Ibrahim (MPI für molekulare Genetik, Berlin) und Dr. Jochen Hecht (Centre for Genomic Regulation, Barcelona) für die Etablierung und Durchführung der ChIP-Technik. Hier möchte ich mich auch bei der NGS Core Facility des Berlin-Brandenburg Zentrums für Regenerative Therapien (BCRT, Charité Berlin) für die Erarbeitung der Sequenzierungen bedanken (Dr. Jochen Hecht bzw. Ulrike Krüger, Catrin

und Gundula). Bei Carolin Walter und Josephine Fischer (Universität Münster) möchte ich mich besonders für die bioinformatische Auswertung, Hilfe und Interpretation der ChIP-Daten bedanken. Hier gilt mein besonderer Dank Carolin Walter, welche alle Server in Bewegung gesetzt hat, um Licht ins Dunkeln der ChIP-Daten zu bringen. Außerdem möchte ich mich bei Peter Hansen (Computational Biology Group, Charité Berlin) und Dr. Karsten Jürchott (BCRT, Charité Berlin) für Ihre bioinformatische Unterstützung und wertvollen Ratschläge bedanken. Ich habe aufgehört zu zählen, wie oft ich bei Euch Rat eingeholt habe.

Am allermeisten möchte ich mich bei meiner Familie und meinen Freunden für Ihre Geduld bedanken. Ihr habt mich durch alle Hochs und Tiefs der Arbeit begleitet und immer an mich geglaubt. Ich danke Euch!

Eidesstattliche Erklärung

Hiermit versichere ich, Claudia Reschke, dass ich die vorliegende Arbeit selbstständig und ohne Benutzung anderer als der angegebenen Hilfsmittel und Quellen angefertigt habe. Ergebnisse, die in Zusammenarbeit mit anderen Personen entstanden sind, wurden entsprechend gekennzeichnet.

Ich erkläre weiterhin, dass diese Arbeit nie in dieser oder anderer Form Gegenstand eines früheren Promotionsverfahrens war. Ich habe mich nicht anderwärtig um den akademischen Doktorgrad „Doctor rerum naturalium“ beworben und besitze keinen entsprechenden Titel. Der Inhalt der Promotionsordnung der Mathematisch-Naturwissenschaftlichen Fakultät I der Humboldt Universität zu Berlin (Stand: 6. Juli 2009) ist mir bekannt.

Berlin, den

(Claudia Reschke)